

Copyright  
by  
Byung Joon Lim  
2017

**The Dissertation Committee for Byung Joon Lim Certifies that this is the approved  
version of the following dissertation:**

**Synthesis and Application of Electrochemically Active Oligonucleotides**

**Committee:**

---

Jonathan L. Sessler, Co-Supervisor

---

Andrew. D. Ellington, Co-Supervisor

---

Eric. V. Anslyn

---

Hung-wen Liu

---

Rick Russell

# **Synthesis and Application of Electrochemically Active Oligonucleotides**

**by**

**Byung Joon Lim, B.S. Chem.; M.S.**

## **Dissertation**

Presented to the Faculty of the Graduate School of

The University of Texas at Austin

in Partial Fulfillment

of the Requirements

for the Degree of

**Doctor of Philosophy**

**The University of Texas at Austin**

**May 2017**

Isn't it a pleasure to study and practice what you have learned?

- The Analects of Confucius, Chapter 1

## **Acknowledgements**

First of all, I would like to thank my co-advisors, Professors Jonathan L. Sessler and Andrew D. Ellington. They give me an opportunity to study and great advice on the scientific knowledge as well as on attitude as a scientist. I am honored to be a joint student under two wonderful supervisors.

I also would like to thank all members of Sessler and Ellington group members for past and present. In particular, I feel grateful to Drs. Bingling Li and Yan du for their teaching and advice all about electrochemical analyses. Dr. Gretchen Marie Peters, Aaron Lammer, and James Brewster helped me to prepare this dissertation. I also thank to Dr. Cheulhee Jung, Dr. Sung Kuk Kim, Dr. Dong Sub Kim, Dr. Yerim Yeon, Dr. Yoo-jin Ghang, Juhoon Lee, and Inhong Hwang for their guidance and friendship. I would like to give thanks to my collaborators Professor Nanshu Lu and Ruchika Mitbender for their effort to design and fabricate new devices.

Finally, I would like to give special thanks to my better half, Yeonjin and to my son, Sean. I greatly appreciate the strong support by my parents on the other side of the earth.

# **Synthesis and Application of Electrochemically Active Oligonucleotides**

Byung Joon Lim, Ph.D.

The University of Texas at Austin, 2017

Co-Supervisor: Jonathan L. Sessler

Co-Supervisor: Andrew D. Ellington

Modified oligonucleotides with redox-active functional groups could emerge as attractive tools for sensor development. In principle, changes in oligonucleotide hybridization or conformation may be read out as a change in an electrochemical signal. Monitoring this signal might allow for a direct interface between biology and electronics. This dissertation describes efforts devoted to creating redox active oligonucleotide derivatives designed to allow these application goals to be pursued. The focus is primarily on the synthesis, characterization, and application of oligonucleotides bearing on of two electroactive moieties, namely ferrocene and methylene blue.

Chapter 1 provides a brief overview of electrochemically modified oligonucleotides and is designed to provide an historical perspective. Synthetic methodology, fabrication of electrode system, and current applications are introduced. Chapter 2 describes the synthesis of a ferrocene-modified oligonucleotide and its use as a multiplexing signal probe. Included in this chapter are syntheses of a ferrocene subunit bearing alkynes, as well as modified nucleoside phosphoramidites and the oligonucleotide syntheses they permit. A synopsis of electrochemical studies are also provided. Chapter 3 describes a ratiometric electrochemical DNA sensor (a so-called E-Sensor) based on the ferrocene-modified oligonucleotide described in Chapter 2 and its used in the detection of

specific genes with greatly improved reproducibility. Oligonucleotide syntheses achieved through enzyme ligation, the fabrication of an E-sensor, and the results of electrochemical assays are provided in this chapter. Chapter 4 describes the design and fabrication of possible wearable devices with the modified electrochemically active oligonucleotides toward real diagnostic applications. This work is being done in collaboration with Dr. Nanshu Lu's group in the Dept. of Aerospace Engineering and Engineering Mechanics at the University of Texas at Austin. Chapter 5 details the synthetic procedures, provides characterization of all new products, and contains electrochemical analytical data discussed in this dissertation.

## Table of Contents

List of Tables .....	xii
List of Figures .....	xiii
List of Schemes.....	xxii
Chapter 1: General Introduction to Electrochemically Active Oligonucleotides ....	1
1.1 Modified oligonucleotides .....	1
1.1.1 Introduction.....	1
1.1.2 Chemical synthesis of modified oligonucleotides .....	8
1.1.3 Enzymatic synthesis of modified oligonucleotides.....	13
1.1.4 Post-synthetic modification .....	16
1.2 Electrochemically active oligonucleotides as sensing tools .....	19
1.2.1 Introduction.....	19
1.2.2 Redox-active functional groups .....	22
1.2.2.1 Ferrocene.....	22
1.2.2.2 Methylene blue.....	26
1.2.3 Applications .....	30
1.2.3.1 Covalently modified electroactive oligonucleotide .....	30
.....	36
1.2.3.2 Electrochemically active oligonucleotide with intercalating probes.....	37
1.3 Summary and Outline .....	40
1.4 References.....	43
Chapter 2: Synthesis of multiplexing electrochemical DNA sensors based on a combination of various ferrocene derivatives.....	62
2.1 Introduction.....	62
2.2 Result and discussion.....	65
2.2.1 Design of Ferrocene derivatives with terminal alkynes.....	65
2.2.2 Synthesis of ferrocene derivatives with terminal alkynes.....	68
2.2.3 Electrochemistry of ferrocene derivatives with terminal alkynes	71



2.2.4 Linear correlation between redox potential and Hammett constant .....	72
2.2.5 Synthesis and electrochemical property of the ferrocene modified thymidine .....	74
2.2.6 Synthesis of the ferrocene modified thymidine phosphoramidites	76
2.2.7 Solid-phase oligonucleotide synthesis and self-assembled monolayer formation on gold.....	78
2.2.8 Electrochemical analysis of the ferrocene modified oligonucleotides .....	80
2.3 Current and future works .....	81
2.3.1 Synthesis of oligonucleotides with ferrocene derivatives.....	81
2.3.2 Post-synthetic modification of oligonucleotides with ferrocene	82
2.4 Conclusion .....	84
2.5 References.....	84
Chapter 3: Construction and Application of Ratiometric electrochemical DNA sensor .....	88
3.1 Introduction.....	88
3.2 Result and discussion.....	90
3.2.1 Synthesis and characterization of the ratiometric E-DNA Sensor	90
3.2.2 Electrochemical characteristics of the ratiometric E-sensor .....	93
3.2.3 Detection of a target oligonucleotide .....	94
3.2.4 Detection of mismatched oligonucleotides .....	98
3.3 Current and future works .....	99
3.3.1 Simple dual-labeling of MB and Fc by post-synthetic modifications .....	99
3.4 Conclusion .....	100
3.5 References.....	101
Chapter 4: Development of wearable devices based on E-sensor technologies for the detection of small molecules in sweat .....	105
4.1 Introduction.....	105
4.2 Result and discussion.....	107
4.2.1 Device fabrication.....	107

4.2.2 Sensing of oligonucleotide sequence .....	110
4.3 Current and future works .....	113
4.3.1 Sensing of cocaine with aptamer based E-sensor .....	113
4.3.2. Sensing of aminoglycoside antibiotics.....	114
4.4 Conclusion .....	115
4.5 References.....	116
Chapter 5: Experimental Procedures .....	119
5.1 Materials .....	119
5.2 Instruments.....	119
5.3 Synthetic procedures and characterization.....	120
Synthesis of compound 2.1 .....	120
Synthesis of compound 2.2 .....	121
Synthesis of compound 2.3 .....	121
Synthesis of compound 2.4 .....	122
Synthesis of compound 2.5 .....	123
Synthesis of compound 2.6 .....	124
Synthesis of compound 2.7 .....	124
Synthesis of compound 2.8 .....	125
Synthesis of DMT-protected 5-iodo-2'-deoxyuridine, 2.16.....	125
Synthesis of ferrocene-thymidines, 2.17 – 2.24.....	126
Synthesis of thymidine phosphoramidites 2.23 – 2.30 .....	128
Synthesis of modified oligonucleotides 2.31, 2.32, and HS-Fc-P .....	129
Synthesis of ratiometric E-sensor oligonucleotide Probe P .....	129
Preparation of oligonucleotides with free thiol for SAM formation..	130
5.4 Procedures of electrochemical analyses.....	130
Cyclic voltammetry for ferrocene bearing alkynes.....	130
Square wave voltammetry for oligonucleotides .....	131
Alternating current voltammetry for wearable devices .....	132

Appendix A Cyclic voltammograms of compounds.....	133
References.....	138

## List of Tables

<b>Table 2.1</b> Eight ferrocene derivatives considered for study. The structure, corresponding functional group used to apply the Hammett constants ( $\sigma_m$ and $\sigma_p$ ), measured oxidation potential ( $E_{1/2} = (E_{pc} + E_{pa})/2$ ), and the difference between the two peak potentials ( $\Delta E_p =  E_{pc} - E_{pa} $ ) are also included in this table. ....	67
<b>Table 2.2</b> Synthesized oligonucleotide sequences .....	78
<b>Table 3.1</b> Sequence of oligonucleotides used in this work. X: <b>2.23</b> (Ferrocene-modified thymidine phosphoramidite).....	92
<b>Table 4.1</b> Sequence of oligonucleotides used in this work (MB: methylene blue, SH: thiol modifier, X: random base).....	111

## List of Figures

<b>Figure 1.1</b> Structures of A) DNA and B) RNA.....	1
<b>Figure 1.2</b> Four nucleobases and their canonical Watson-Crick base pairing interactions. Sugar and phosphate groups are omitted for clarity.....	3
<b>Figure 1.3</b> A) 2-D and B) 3-D DNA origami. Adapted from refs. 5 and 6.....	4
<b>Figure 1.4</b> Strand displacement of a DNA complex. Complex L is thermodynamically more stable than complex S because it allows for a greater number of base pairing interactions. ....	4
<b>Figure 1.5</b> A) Positions for possible modification of nucleobases and B) specific examples. Sugar and phosphate groups are omitted for clarity. ....	6
<b>Figure 1.6</b> Unnatural base pairs. The base pairing is based on hydrogen bonding (A and B) <sup>20</sup> or hydrophobic interactions (C and D). <sup>21-22</sup> Sugar and phosphate groups are omitted for clarity. ....	6
<b>Figure 1.7</b> Structures of several XNAs. A) Therosene nucleic acid (TNA), <sup>28</sup> B) locked nucleic acid, <sup>29</sup> C) glycol nucleic acid, <sup>30</sup> D) cyclohexene nucleic acid (CeNA), <sup>31</sup> and DNA (in the box). ....	7
<b>Figure 1.8</b> Structures of A) phosphorothioate bonded oligonucleotide, B) PNA, and DNA (in the box). ....	8
<b>Figure 1.9</b> Chemical modification of nucleotides with non-base or non-sugar functional groups, such as A) alkyne for click chemistry, B) amine for amide coupling, C) bipicoline for metal chelation, D) biotin for labeling, E) fluorescein for fluorescent labeling, and F) cross-linking branching elements. ....	9

<b>Figure 1.10</b> Nucleoside phosphoramidite. 5' hydroxyl group is protected by DMT group (red) and 3' one is activated by phosphoramidite .....	10
<b>Figure 1.11</b> 2'-O-Protected nucleotide phosphoramidite for RNA synthesis.....	13
<b>Figure 1.12</b> Nucleotide triphosphate (NTP and dNTP) .....	13
<b>Figure 1.13</b> The Sanger DNA sequencing method. A) A primer is hybridized with the target sequence. B) DNA polymerase, dNTPs, fluorophore-labeled dideoxy-nucleotides (ddNTPs) are mixed. The random insertion of a ddNTP terminates synthesis of the polymerized chain. Each sequence is characterized by the fluorescence of the terminal ddNTP. (3) The products are separated on the basis of length by capillary gel chromatography and the fluorescence from each sequence is determined. (4) The sequence is then constructed using a computational program. This figure was adapted from ref. 59 with modifications being made by the author. <sup>59</sup> .....	15
<b>Figure 1.14</b> Examples of chemically or enzymatically synthesized modified oligonucleotides for further post-synthetic modifications. Each molecule has a linker for bio-conjugation on A) the 5' end, B) the 3' end, C) at an internal nucleobase, and D) an internal backbone site of oligonucleotides. ....	16
<b>Figure 1.15</b> A) Electrocatalytic oxidation of an oligonucleotide with $\text{Ru}(\text{bpy})_3^{2+}$ as a redox mediator. If this scenario, the $\text{Ru}(\text{bpy})_3^{3+}$ is reduced to $\text{Ru}(\text{bpy})_3^{2+}$ by guanines and regenerated by the electrode. B) Electron transfer to the electrode is measured as a change in the current signal. The elements in this figure were adapted from refs. 79 and 83, respectively. ....	21

- Figure 1.16** A) Schematic overview of the electrocatalytic oxidation of glucose by glucose oxidase (GOx) using ferrocene as a redox mediator. Glucose is oxidized by GOx and the electrons from the glucose are transferred to the electrode via a FAD (co-factor) with the assistance of ferrocene, which acts as a redox mediator. The electron transfer is measured by amperometry. Adapted from ref. 109. B) Schematic illustration of the assembled layer of GOx (in the red circle) and ferrocene embedded within a polymer matrix (highlighted by a blue circle) on a gold electrode. The sulfate-thiol on the gold electrode (contained within a green circle, negatively charged), ferrocene polymer (ferrocenium form, positively charged), and GOx (negatively charged) are assembled as the layer through simple electrostatic interactions. This part of this figure was adapted from ref. 108.....25
- Figure 1.17** A) Structure of  $\beta$ -Cyclodextrin (left) and cucurbit[7]uril (CB7, right). B) Supramolecular complex of CB7 and Fc. Adapted from ref. 118. ...26
- Figure 1.18** A) Mechanism of the blue bottle reaction and B) photograph of the color change before, 3 min, 3.3 min and 4.3 min of the experiment, respectively. Adapted from ref. 124. ....29
- Figure 1.19** The first genetic sensing system involving an electrochemically active oligonucleotide as reported by Maeda's group in 1997. Shown in A) is the oligonucleotide used in the study, whereas B) shows the genetic sensing scheme. Adapted from ref. 132.....31

<b>Figure 1.20</b> The first E-DNA sensor as reported by Plaxco et al. A) Schematic representation of the sensor. B) Plot of the current decrease seen upon addition of an appropriately chosen target sequence. Adapted from ref. 80.....	32
<b>Figure 1.21</b> Electrochemical detection based on use of CHR. A) The requisite catalytic amplification is initiated by the addition of C1. The resulting assembled construct, H1-E-H2, the binds to an electrode as the result of hybridization to the immobilized sequence S. B) The current signal is increased after the addition of the target for the amplification while C) the signal intensity varies with different concentrations of C1. Adapted from ref. 137. ....	33
<b>Figure 1.22</b> Electrochemical real-time PCR. A) Surface-immobilized primers are elongated with Fc-incorporated thymidine, which increase the electrochemical signal. B) The signal increases with each reaction cycle with the template sequence (red) but not in its absence (black). Adapted from ref. 138. ....	34
<b>Figure 1.23</b> Genetic sensing using the Fc- $\beta$ CD interaction. A) Structure of the molecule. B) Scheme of the system. The exposure of the ferrocene out of the $\beta$ CD gives increased electrochemical signal. Adapted from ref. 139.....	35
<b>Figure 1.24</b> A) Thrombin (signal-off) and B) cocaine (signal-on) E-AB sensors. Adapted from ref 140 and 141.....	36



<b>Figure 1.25</b> Real-time measurement of specific molecules in blood by Soh's group. (A) Sampling of blood by microfluidic techniques. (B) The E-AB sensor used in the study. (C) The continuous-flow diffusion filter (CDF) for filtering and detection of the target molecule. (D) Monitoring of the target concentration through either a signal-on (red) or a signal-off (blue) approach. Adapted from ref. 142.....	37
<b>Figure 1.26</b> A) Ethidium bromide and B) Hoechst 33342 dye. ....	38
<b>Figure 1.27</b> A) Schematic illustration of the intercalation of MB (black bars) on an electrode-immobilized oligonucleotide. B) Increased electrochemical signals elicited by concentration increase. Adapted from ref. 149. ...	39
<b>Figure 1.28</b> Electrocatalytic detection of mismatched oligonucleotide with MB (as a signal probe) and $\text{Fe}(\text{CN})_6^{3-}$ (as a redox mediator). Electron transfer from electrode to $\text{Fe}(\text{CN})_6^{3-}$ is blocked by mismatched base-pairing. As a result, the signal from MB is decreased. Adapted from ref. 79. ....	40
<b>Figure 1.29</b> Electrochemically active diviologen compound developed by Hvastkov's group. ....	40
<b>Figure 2.1</b> Schematic illustration of E-Sensor. ....	63
<b>Figure 2.2</b> Modulation of redox potential of ferrocene via the incorporation of EDGs and EWGs .....	64
<b>Figure 2.3</b> Design of the ferrocene probes and pathway leading to modified oligonucleotides. A) Chemical synthesis, B) enzymatic synthesis, and C) post-synthetic modification strategies for the incorporation of a ferrocene subunit into oligonucleotide.....	66

<b>Figure 2.4</b> Cyclic voltammetry of synthesized ferrocene probes in CH <sub>2</sub> Cl <sub>2</sub> . (Normalized values for clear comparison of the $E_p$ ) (0.2 M tetrabutylammonium hexafluorophosphate (TBAPF <sub>6</sub> ) in CH <sub>2</sub> Cl <sub>2</sub> , working electrode (WE) – glassy carbon (GCE); counter electrode (CE) – platinum wire (Pt); reference electrode (RE) – Ag/AgCl).....	71
<b>Figure 2.5</b> The linear plot of the Hammett constants vs. the measured redox potentials for compounds 2.1 – 2.8. The Red square in each plot corresponds to unmodified ferrocene. A) Potential vs. $\sigma_m$ and B) vs. $\sigma_p$ . .....	73
<b>Figure 2.6</b> Comparison between <b>2.1</b> ( $E_{1/2}$ = 660 mV, line) and <b>2.17</b> ( $E_{1/2}$ = 630 mV, dots) in CV (0.2 M TBAPF <sub>6</sub> in CH <sub>2</sub> Cl <sub>2</sub> , WE – GCE; CE – PT, RE – Ag/AgCl).....	76
<b>Figure 2.7</b> <sup>31</sup> P NMR spectra of a representative phosphoramidite target <b>2.23</b> . ....	78
<b>Figure 2.8</b> SWV curves of the SAM prepared from <b>2.31</b> and <b>2.32</b> on gold electrode surface in PBS. A) Signals produced by the individual oligonucleotide <b>2.31</b> (red) and <b>2.32</b> (black) (Overnight incubation with 10 $\mu$ M of each oligonucleotide in PBS for surface immobilization, WE – gold disk electrode (GE); CE – Pt; RE – Ag/AgCl). B) Signals produced by a the 1:1 mixture of the probes used for A. (5 $\mu$ M of each oligonucleotide under the same condition).....	80
<b>Figure 3.1</b> Scheme of sensing process and predicted signal by electron transfer.	90
<b>Figure 3.2</b> PAGE gel characterization and purification of the ligation process. Because both the ligation product (Probe P) and the MB-P contain MB, these bands have a blue tinge.....	92

**Figure 3.3** Comparison between non-ratiometric and ratiometric E-sensors. A)

Typical SWV curves scanned prior to target binding on three different sensing electrodes. B) Reproducibility of the nonratiometric E-sensor.

C) Reproducibility of the ratiometric E-sensor. Throughout,  $(I_{MB})^{\circ}$  refers to the initial background response of MB prior to target binding.

$(I_{MB}/I_{Fc})^{\circ}$  refers to the initial background ratio of MB and Fc signals prior to target binding. The black histograms represent the background responses of 50 individual measurements over eight electrodes. Average values are represented by the red bars. The error bars in the red

histograms represent the SD for 50 individual measurements. ....93

**Figure 3.4** Typical SWV curves as obtained before and after target binding. The peak current from Fc is normalized for each curve. ....95

**Figure 3.5** Gel electrophoresis of E-sensor conformational transitions. Samples were developed on a 12% native PAGE. **A)** Unlabeled Probe P, lane 1:  $[T] = 100$  nM; lanes 2 and 4:  $[P] = [T] = 100$  nM; lane 3:  $[P] = 2[T] = 100$  nM; lane 5:  $[P] = 100$  nM. **B)** HS- and Fc- and MB-labeled Probe P, lane 6:  $[P] = 200$  nM; lane 7:  $[T] = 200$  nM; lanes 8 and 9:  $[P] = [T] = 200$  nM. The mobilities of the different conformers are indicated at the sides of the gels. The arrow indicates a faint band, as described in the text. .96

**Figure 3.6** Concentration dependence of Target T as observed using ratiometric E-sensors and non-ratiometric E-sensors. **A)** Concentration dependence of Target T based on the ratio  $I_{MB}/I_{Fc}$ . **B)** Concentration dependence of Target T represented by a log–linear plot of  $I_{MB}/I_{Fc}$ . **C)** Concentration dependence of Target T based on  $I_{MB}$ . **D)** Concentration dependence of Target T represented by log–linear plot of  $I_{MB}$ . The error bars are standard deviations of measurements based on three independent experiments. ....97

**Figure 3.7** Selectivity of the ratiometric E-sensor. **A)** Transduction by Probe P with a series matched and mismatched targets at 25 °C. Buffer only (1), 1  $\mu$ M Non-T (2), 1  $\mu$ M T-SNP4 (4 mismatches) (3), 1  $\mu$ M T-SNP3 (3 mismatches) (4), 1  $\mu$ M T-SNP2 (2 mismatches) (5), 1  $\mu$ M T-SNP1 (1 mismatch) (6), and correctly paired Target T (7). **B)** Selectivity at different temperatures. T-SNP1 and T-SNP2 contain 1 and 2 mismatches relative to Target T, respectively. ....98

**Figure 4.1** Schematic process for the fabrication of wearable sensor. Adopted from ref. 20. ....106

**Figure 4.2** Schematic design (A) and the first prototype (B) of the epidermal wearable device fabricated by Lu’s group. ....107

**Figure 4.3** (A) Linear sweep voltammetry of the first prototype device with  $Fe(CN)_6^{3-}/Fe(CN)_6^{4-}$  in PBS. The arrow shows a collapsing of the electrodes. (B) The electrodes were peeled off the device after the experiment.....108

**Figure 4.4** The second-generation of the device fabricated by Lu’s group. ....109

**Figure 4.5** CV of the device with  $\text{Fe}(\text{CN})_6^{3-}/\text{Fe}(\text{CN})_6^{4-}$  in PBS. Each arrow shows the direction of potential sweep A) positive and B) negative, respectively.

.....110

**Figure 4.6** Construction process of wearable device with E-sensor .....111

**Figure 4.7** ACV of the device for oligonucleotide detection.....112

**Figure 4.8** ACV of the device for benzoylecgonine detection.....114

## List of Schemes

<b>Scheme 1.1</b> Summary of the phosphoramidate-based synthetic cycle used to prepare oligonucleotides. ....	11
<b>Scheme 1.2</b> Cleavage of nucleotides from solid supports after the solid-phase synthesis with concomitant deprotection of A) the cyanoethyl group on the phosphate ester and B) other protecting groups present on the nucleobases. ....	12
<b>Scheme 1.3</b> Representative bio-conjugation reactions involving oligonucleotides. A) Amide coupling reaction between an amino-functionalized oligonucleotide and an NHS-activated functional molecule. B) Click reaction between an alkyne-oligo and an azide-bearing molecule. C) Michael addition reaction between a thiol-oligonucleotide and maleimide-molecule.....	18
<b>Scheme 1.4</b> Enzymatic modification of oligonucleotides using A) polynucleotide kinase and phosphatase, as well B) DNA ligase.....	19
<b>Scheme 1.5</b> Redox conversion between ferrocene (left) and the ferrocenium ion (right). The standard reduction potential of the ferrocenium ion is 0.64 V (vs. SHE).....	22
<b>Scheme 1.6</b> Synthesis of ferrocene derivatives. ....	23
<b>Scheme 1.7</b> Methylene blue (left) and leucomethylene blue (right). The standard reduction potential of methylene blue is 0.01 V (vs. SHE). ....	26
<b>Scheme 1.8</b> Synthesis of A) MB, B) its derivatives, and C) mono-substituted thionines. ....	28
<b>Scheme 2.1</b> Synthesis of the ferrocene probes <b>2.1 – 2.4</b> .....	69

<b>Scheme 2.2</b> Synthesis of the ferrocene probes <b>2.5 – 2.8</b> .....	70
<b>Scheme 2.3</b> Synthesis of DMT-protected modified thymidines with the ferrocene probes on 5 position .....	75
<b>Scheme 2.4</b> Synthesis of thymidine phosphoramidites bearing the ferrocene probes. ....	77
<b>Scheme 2.5</b> Schematic representation of a SAM produced using a generalized modified oligonucleotide in combinations with 6-mercaptohexanol (MCH). ....	79
<b>Scheme 2.6</b> Post-synthetic modification of an azide-functionalized oligonucleotide to obtain <b>2.33</b> (Sequence: 5'- <b>N<sub>3</sub>-TTACTCTC GATCGGCGTTTTA GAGAGG-SH-3'</b> ) .....	83
<b>Scheme 3.1</b> Construction of Probe P from MB-P and HS-Fc-P. After hybridization to a complementary strand, Ligation-P, the phosphorylated HS-Fc-P and MB-P were ligated together by T4 DNA ligase. ....	91
<b>Scheme 3.2</b> Duel-labeling of the ratiometric E-sensor via post-synthetic modification. ....	100

# Chapter 1: General Introduction to Electrochemically Active Oligonucleotides

## 1.1 MODIFIED OLIGONUCLEOTIDES

### 1.1.1 Introduction

Nucleic acids are some of the most important biomolecules in living organisms. They are biopolymers consisting of repeating monomers called nucleotide, which include a nucleobase, a 5-carbon sugar, and phosphates (Figure 1.1).<sup>1-2</sup> Each base is attached at the 1' position of the sugar via a covalent *N*-glycosidic bond, while the phosphate serves to link the 5' position of one nucleobase-functionalized sugar and the 3' hydroxyl of the next nucleotide in sequence as a phosphodiester bond. Two main classes of nucleic acids, ribonucleic acid (RNA) and deoxyribonucleic acid (DNA), are known; they are differentiated by the presence or absence of a 2' hydroxyl group, respectively.

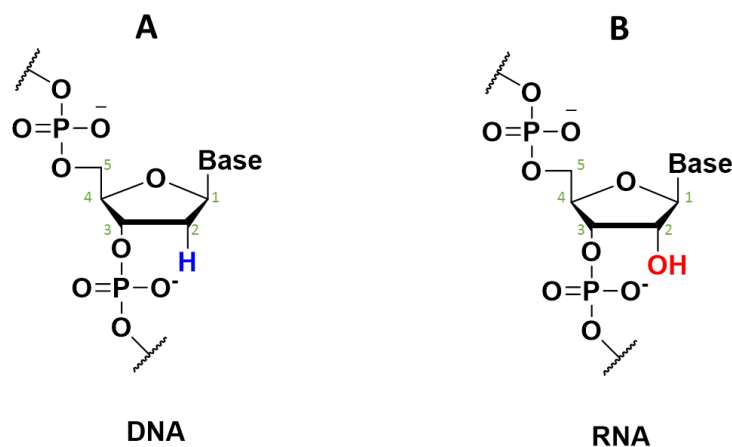


**Figure 1.1** Structures of A) DNA and B) RNA.

DNA plays a pivotal role in biology by storing the genetic information of each and every organism. It is composed of four different bases, adenine (A), guanine (G), cytosine (C), and thymine (T), and the complementary hydrogen bonding of A-T and G-C forms a



special interaction called base pairing (Figure 1.2). Through this base pairing interaction, a DNA strand can associate with another strand that has a complementary sequence to form a double helical structure. The stability of this structure enables DNA to maintain the fidelity of genetic information. RNA is characterized by a few functional and structural distinctions compared to DNA. For instance, while DNA is quite robust, RNA is a less stable. It is also a more dynamic polymer due to a presence of hydroxyl group at the 2' position.<sup>3</sup> Additionally, thymine (T) is replaced by its demethylated analogue, uracil (U), in RNA. While the main function of RNA is translation of genetic information from DNA to a protein as a phenotype, RNA also performs several other functions in cells. Thus, in addition to messenger RNA (mRNA), there are other types of RNAs in cells, such as transfer RNA (tRNA), ribosomal RNA (rRNA), micro RNA (miRNA). Additionally, some viruses store their genetic information in RNA rather than in DNA. Nevertheless, they are able to encode functional proteins.<sup>1</sup> Inspired by the discovery of this latter function, researchers have hypothesized the concept of the “RNA world”, which is predicated on the argument that RNA molecules were the precursors of all current biomolecules, such as DNAs, RNAs, and proteins. This ground-breaking suggestion challenged the so-called “central dogma” of molecular biology, which states DNA makes RNA and RNA makes protein.<sup>4</sup>

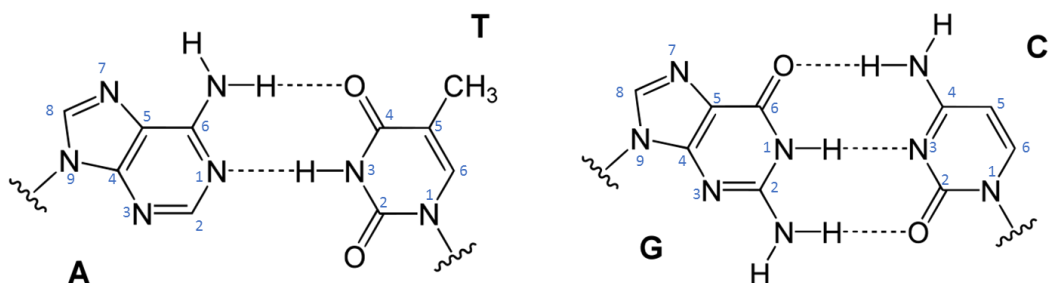


**Figure 1.2** Four nucleobases and their canonical Watson-Crick base pairing interactions. Sugar and phosphate groups are omitted for clarity.

In addition to their biological roles in organisms, fragments of nucleic acids, or oligonucleotides, have features that make them attractive as materials in various fields. First, they are easy to synthesize by chemical or enzymatic methods. The details of both synthetic routes will be described later. Oligonucleotides are also some of the most easily controlled macromolecules in nature. The secondary structure of synthesized oligonucleotides can be controlled by varying the number and position of the base pairing interactions, which in turn, determines the energy level of the molecules. One example of this tuning involves nanoscale self-assemblies called “DNA origami”.<sup>5-6</sup> The Rothmund, Seeman, and Yin groups designed and shaped various 2-D or even 3-D structures using only oligonucleotide sequences (Figure 1.3). Another attractive characteristic of oligonucleotide assemblies is the reversible nature of the base pairing. This can be exploited to permit a variety of strand displacement and amplification reactions.<sup>7-9</sup> The addition of an oligonucleotide strand can perturb the equilibrium of a system and induce further conformational change resulting from the displacement of the previous strand and a formation of the new assembly (Figure 1.4). These reactions have been applied in myriad of studies for signal detection and amplifications. Finally, some oligonucleotides show distinct affinity to specific targets, such as molecular receptors or antibodies.<sup>10-11</sup> These oligonucleotides, called aptamers, are typically obtained via the systematic evolution of

ligands by exponential enrichment (SELEX). To date, they have been used in the detection of a number of molecules, large and small.<sup>12</sup>

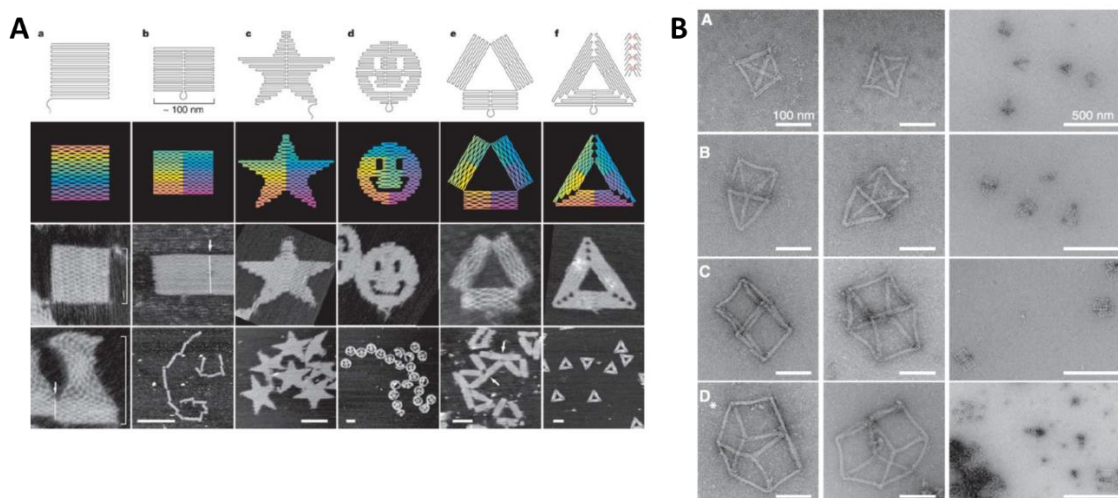


**Figure 1.3** A) 2-D and B) 3-D DNA origami. Adapted from refs. 5 and 6.

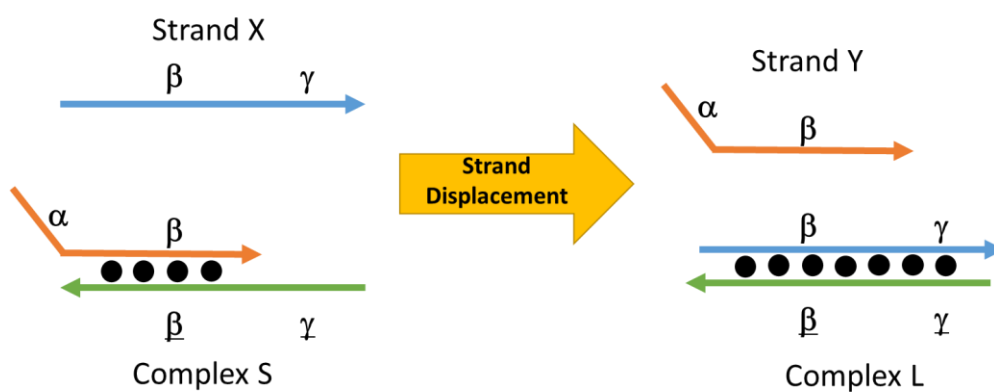


**Figure 1.4** Strand displacement of a DNA complex. Complex L is thermodynamically more stable than complex S because it allows for a greater number of base pairing interactions.

Natural oligonucleotides without any modification have many limitations in terms of their applications-related utility. In particular, the lack of specific functional groups on

the oligonucleotides causes difficulties in terms detection, both of the oligonucleotides themselves and of any target molecule. It also makes it difficult to connect the oligonucleotides in question to other molecules or supports.

Typically, oligonucleotides are detected using UV spectroscopy by measuring the absorbance at 260 nm, a wavelength that corresponds to an absorption feature associated with the aromatic nucleobases.<sup>1, 13</sup> Since many aromatic compounds absorb at 260 nm, this method is limited to studying only pure oligonucleotide solutions. Furthermore, as all the nucleobases absorb in this region, UV spectroscopy typically does not allow the base composition or order of the oligonucleotide to be determined.

To overcome the above deficiencies, various modifications have been made to oligonucleotides.<sup>14-17</sup> These modifications are categorized according to the position of the modification. First, nucleobase modification is a well-known method to add specific functional groups to the oligonucleotide (Figure 1.5). Various linkers have been used to add additional conjugation, attach fluorophores, or tether electrochemical probes or other functional motifs to oligonucleotides.<sup>17-18</sup> Since the nucleobases are essential components for base pairing and a key to maintaining the secondary conformation of oligonucleotides, only a limited number of the positions on the bases may be modified without loss of function. At present, it is known that substitution at the C5 position of pyrimidines and the N7 or C8 positions of purines does not affect substantially the double helical structure of the resulting DNA.<sup>16, 19</sup> Base modification has the advantage of site-specificity, because the position of modification is controlled by chemical synthesis. Recently, the Benner and Romesburg groups individually synthesized oligonucleotides containing new nucleobase analogues called “unnatural base pairs”, which have orthogonal interactions analogous to A-T and G-C base pairs (Figure 1.6).<sup>20-22</sup> These studies served to demonstrate the potential of an expanded genetic coding system which uses six bases rather than four.

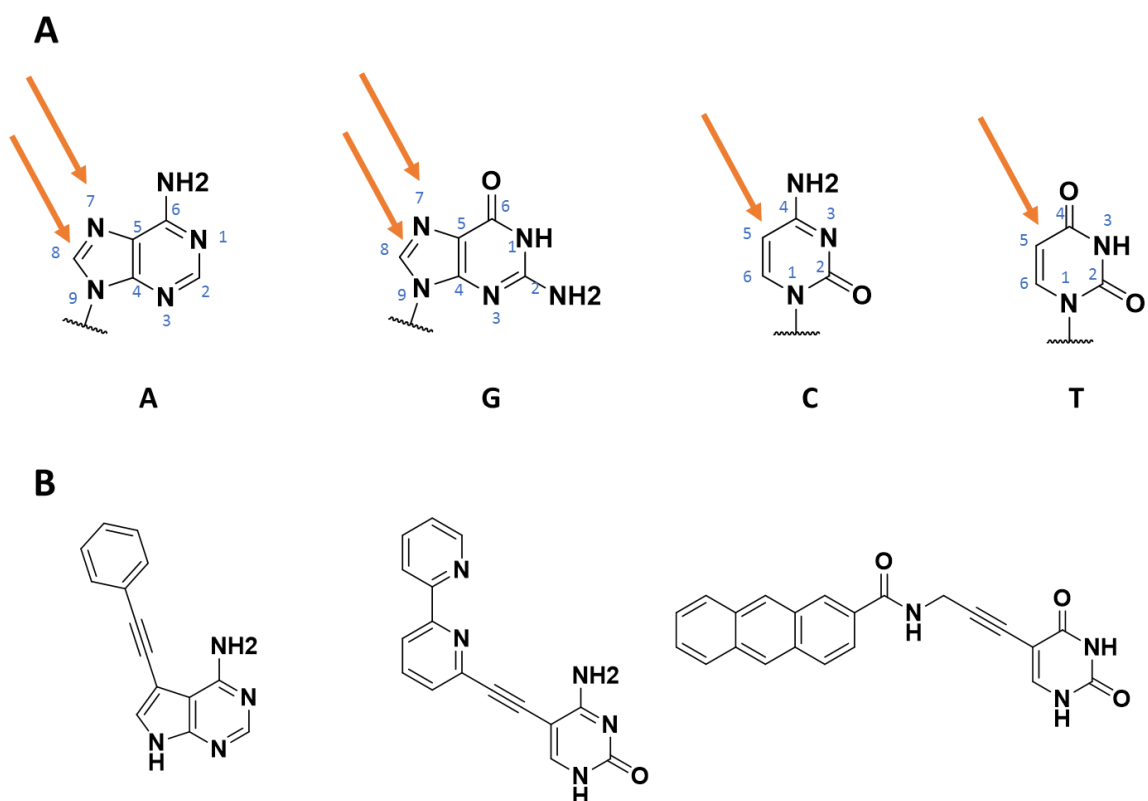


**Figure 1.5** A) Positions for possible modification of nucleobases and B) specific examples. Sugar and phosphate groups are omitted for clarity.

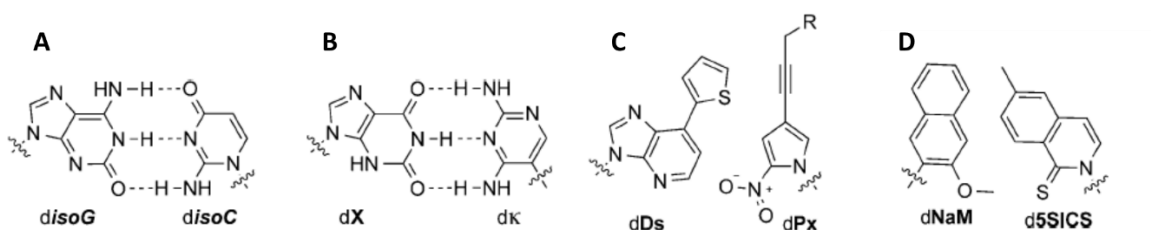


**Figure 1.6** Unnatural base pairs. The base pairing is based on hydrogen bonding (A and B)<sup>20</sup> or hydrophobic interactions (C and D).<sup>21-22</sup> Sugar and phosphate groups are omitted for clarity.

The 5-membered ribose ring is also a candidate for modification. The 2' hydroxyl group on RNA can be easily modified by substitution reactions while exploiting reactivity differences relative to other hydroxyl groups on the ribose.<sup>16, 23-27</sup> This modification not only permits the attachment of new functional groups, it also increases the stability of the RNA against hydrolysis and cleavage of the phosphodiester backbone.<sup>26-27</sup> Recently, researchers, including the Eschenmoser and Imanishi groups, developed modified oligonucleotides, so-called xeno nucleic acid (XNA) (Figure 1.7), which include non-ribose sugar backbones.<sup>28-31</sup> These new modified oligonucleotides showed highly improved stability under physiological conditions due to resistance against nucleases.<sup>28</sup> Thus, they have been widely used in clinical applications.<sup>32-34</sup>

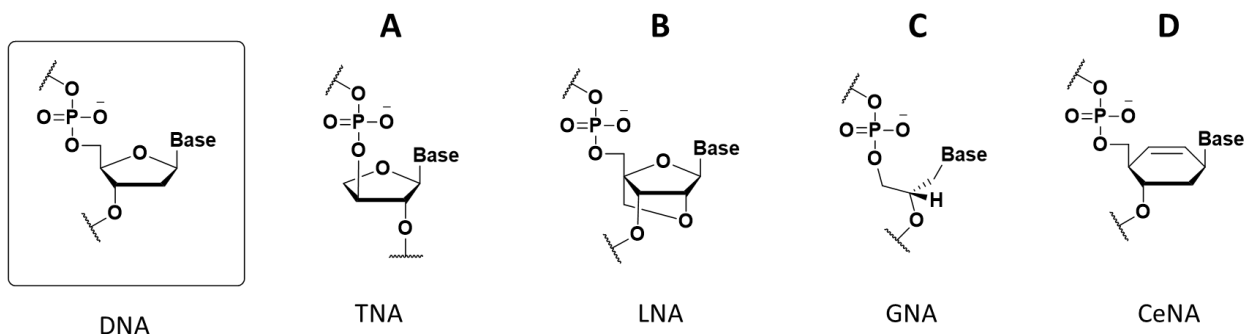


**Figure 1.7** Structures of several XNAs. A) Therose nucleic acid (TNA),<sup>28</sup> B) locked nucleic acid,<sup>29</sup> C) glycol nucleic acid,<sup>30</sup> D) cyclohexene nucleic acid (CeNA),<sup>31</sup> and DNA (in the box).

Finally, modification of the phosphodiester backbones is also possible. Typically, backbone modification is carried out to strengthen the oligonucleotide structure and protect it from enzymatic or nucleophilic attack.<sup>16</sup> The most common examples involve the use of phosphorothioate bonds, a change that provides resistance against nucleases (Figure 1.8A).<sup>35-36</sup> It is also known that this modified backbone destabilizes hybridization

complexes formed by interactions with oligonucleotides having natural phosphodiester backbones.<sup>37</sup> Therefore, such modifications are often used in nucleic acid amplification where it is useful to perturb the hybridization energy.<sup>38</sup>

Another example of backbone modification is peptide nucleic acid (PNA) (Figure 1.8B). This class of oligonucleotide is composed of recurring units of amino acids rather than ribose and phosphate backbones.<sup>39-40</sup> PNA is synthesized easily by well-established peptide synthetic methods; however, except for its base pairing function, its chemical and physical properties are distinct from those of natural oligonucleotides.<sup>41-42</sup>

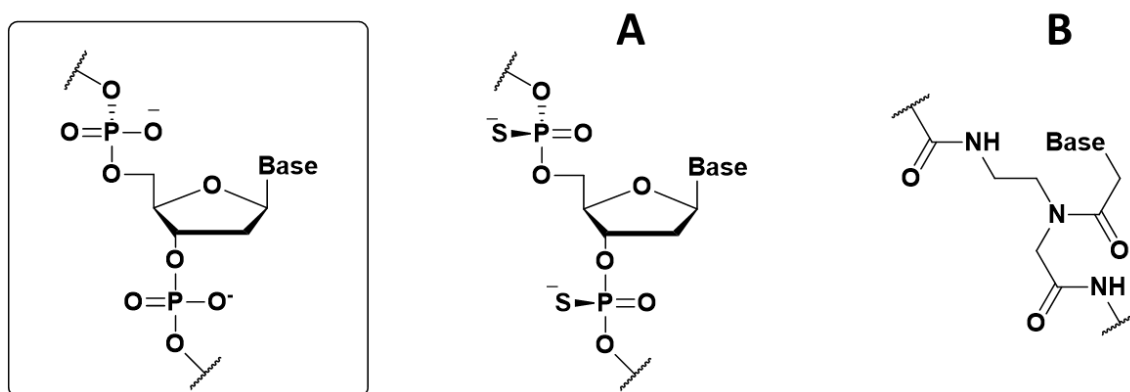


**Figure 1.8** Structures of A) phosphorothioate bonded oligonucleotide, B) PNA, and DNA (in the box).

### 1.1.2 Chemical synthesis of modified oligonucleotides

Including modified oligonucleotides, most nucleic acids are synthesized by two major methods: chemical synthesis and enzymatic synthesis. Of these, chemical syntheses have many advantages for oligonucleotide modification: 1) the sequence and length of oligonucleotide can be easily controlled; 2) point modifications are straightforward on certain bases; 3) template oligonucleotides and primers are not required; and 4) the synthesis may often be performed in an automated synthesizer. On the other hand,

modifications are limited to functional groups that are robust enough to endure the harsh reaction condition in each step of the synthesis, and the efficiency of the reaction is lower than analogous enzymatic reactions, especially for long oligonucleotides. For these reasons, relatively short oligonucleotides (up to 200 base pairs) are usually synthesized by chemical means.<sup>16, 43</sup> Most unnatural bases and backbones are incorporated into the oligonucleotide using chemical approaches, unless orthogonal polymerases for the bases are not developed yet.<sup>34</sup> Non-base or non-sugar functional groups, as well as modified nucleotides, can also be incorporated into the sequence, a modification that provides a great deal of diversity in the resulting oligonucleotides. For example, linkers, fluorophores, and even branches that serve to link multiple strands may be inserted into the oligonucleotide chains (Figure 1.9).<sup>44</sup>

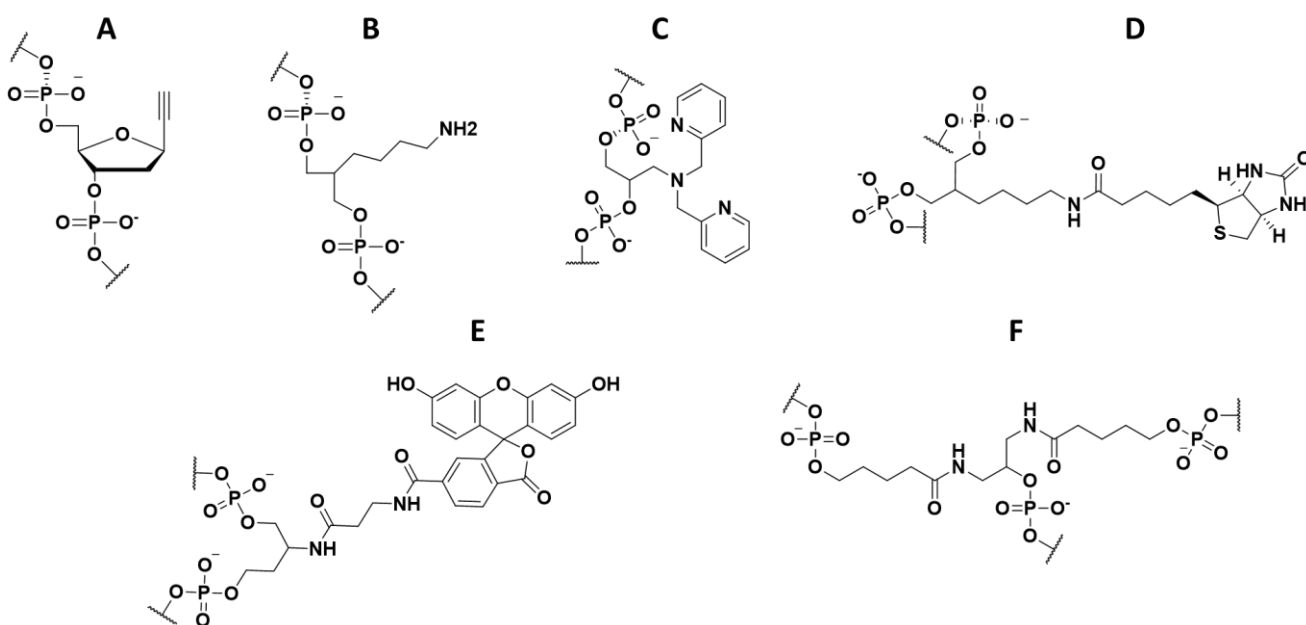


**Figure 1.9** Chemical modification of nucleotides with non-base or non-sugar functional groups, such as A) alkyne for click chemistry, B) amine for amide coupling, C) bipicoline for metal chelation, D) biotin for labeling, E) fluorescein for fluorescent labeling, and F) cross-linking branching elements.



The chemical synthesis of oligonucleotides was first reported by Alexander Todd's group in the early of 1950s.<sup>45</sup> This group synthesized oligonucleotides using intermediates called H-phosphonate and phosphate triesters. Since the methods was first developed, many other approaches were attempted, including those based on phosphodiester,<sup>46</sup> phosphotriesters,<sup>47</sup> and phosphite triesters.<sup>48</sup> Today phosphoramidate methods remain the most commonly used.<sup>49</sup>

The building blocks required for the phosphoramidite-based involves, as the name implies, a nucleoside phosphoramidite (Figure 1.10). Using these intermediates oligonucleotides are synthesized on a solid-phase setup in accord with standard automated procedures. The 5' hydroxyl groups are protected with 4,4'-dimethoxytrityl (DMT) groups and the hydroxyl groups on the 3' position are activated in the form of a 2-cyanoethyl-*N,N*-diisopropyl phosphoramidite.<sup>16</sup> This latter reactive phosphoramidite group is prone to attack by nucleophiles. Due to the position of the

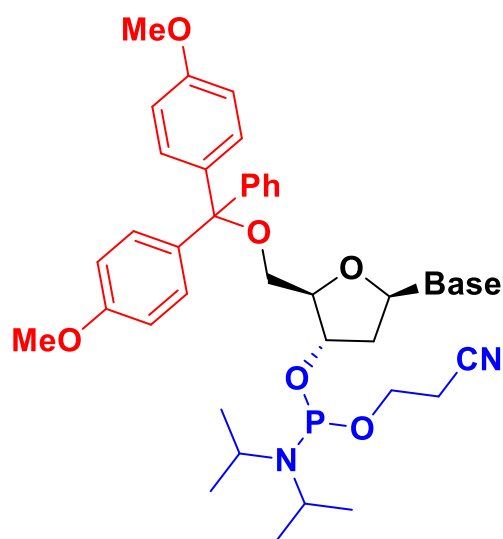
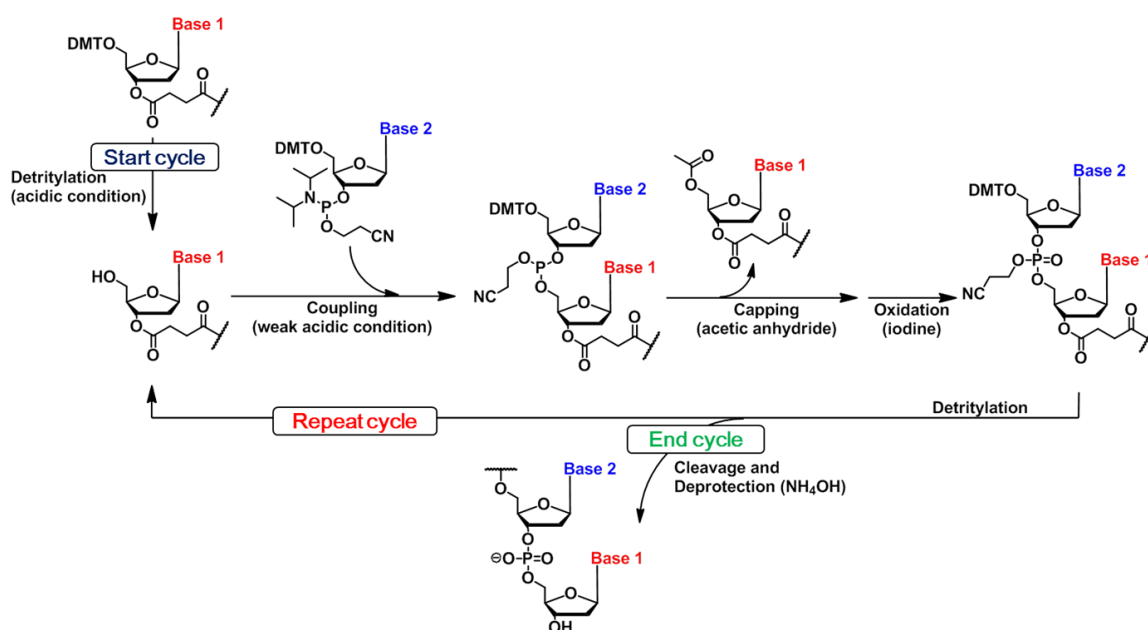


**Figure 1.10** Nucleoside phosphoramidite. 5' hydroxyl group is

protecting and activating groups, the direction of the synthesis is 3' to 5', i.e., the reverse of enzymatic synthesis. The first base incorporated during synthesis is attached to a solid-phase support with an ester linker and cleaved in the final step. The detailed synthetic cycle of a deoxyoligonucleotide is described in the following paragraph and shown in Scheme 1.1.

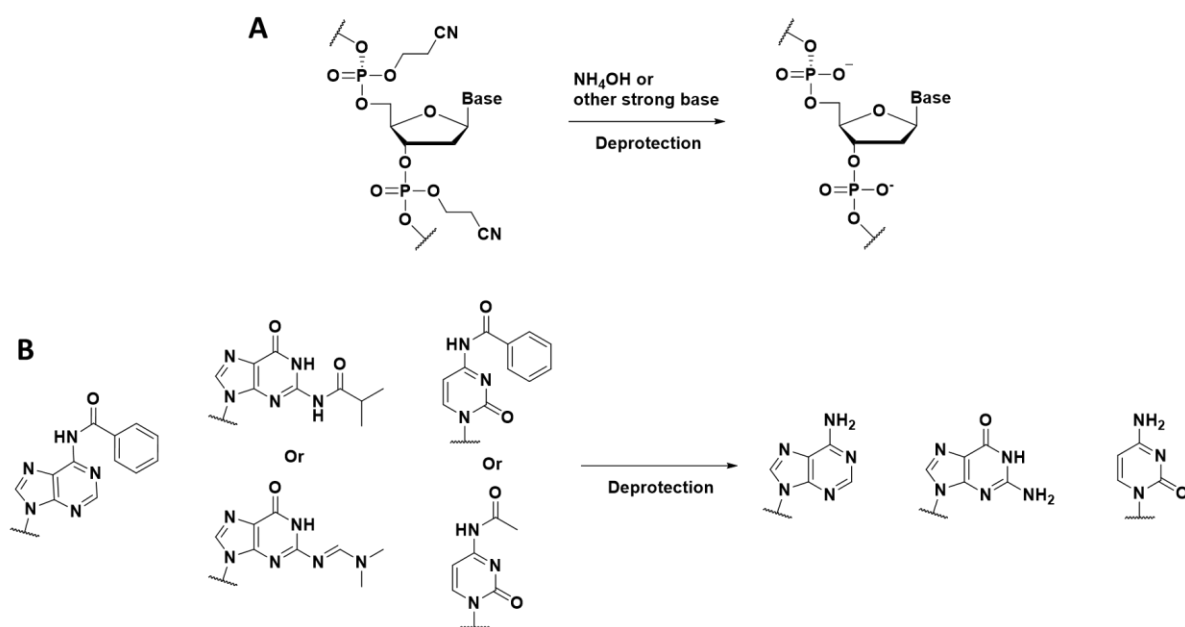


**Scheme 1.1** Summary of the phosphoramidate-based synthetic cycle used to prepare oligonucleotides.

First, the DMT protection group on 5' is 'de-blocked' to expose a nucleophilic hydroxyl group on the terminal nucleotide. Weak acids, such as dilute solutions of trichloroacetic acid (TCA) or dichloroacetic acid (DCA), are widely used to effect this deprotection. A nucleoside phosphoramidite is then added under anhydrous conditions, which couples with the exposed hydroxyl group. The diisopropylamine moiety on the phosphorous adds to the 5' hydroxyl group to form a phosphite ester. After the coupling reaction, any unreacted free hydroxyl groups are capped by treatment with acetic anhydride and 1-methylimidazole to prevent further elongations. Finally, an aqueous iodine solution is added. This oxidizes the phosphite ester to the natural and more stable phosphate ester, which completes the synthetic cycle.

After the solid-phase synthesis of the oligonucleotide is complete, the solid support is treated with a strongly basic solution, such as 40% aqueous sodium hydroxide. This basic treatment leads to cleavage from the solid support, as well as deprotection of the 2-

cyanoethyl group on the phosphate and various other protecting groups on the nucleobases (Scheme 1.2). This liberates the target oligonucleotide containing native phosphodiester linkages and in a form suitable for hybridization via base-pairing.



**Scheme 1.2** Cleavage of nucleotides from solid supports after the solid-phase synthesis with concomitant deprotection of A) the cyanoethyl group on the phosphate ester and B) other protecting groups present on the nucleobases.

The chemical synthesis of RNA is almost identical to that of DNA. However, additional protection of the 2' hydroxyl group is required (Figure 1.11) so as to inhibit its reaction as a nucleophile during the synthesis. Silyl protection groups, such as *t*-butyldimethylsilyl (TBDMS)<sup>50</sup> or tri-isopropylsilyloxymethyl (TOM),<sup>51</sup> are generally used. They are deprotected by treatment with fluoride solutions after the synthesis.

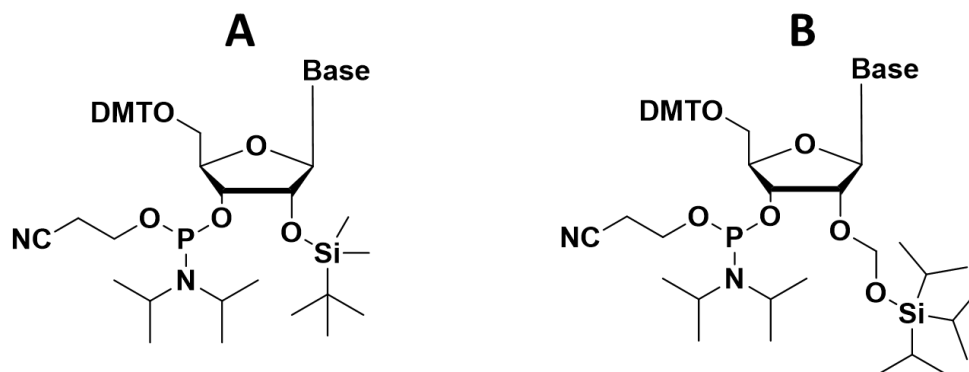


**Figure 1.11** 2'-O-Protected nucleotide phosphoramidite for RNA synthesis.

### 1.1.3 Enzymatic synthesis of modified oligonucleotides

All natural oligonucleotides found in living organisms are synthesized by enzymes. One key class of enzymes involved in these syntheses are polymerases. These enzymes synthesize DNA or RNA polymers using a complementary sequence of the target oligonucleotide as a template. There are three main classes of polymerase: DNA polymerase (from DNA to DNA), RNA polymerase (from DNA to RNA), and reverse transcriptase (from RNA to DNA). They commonly need a

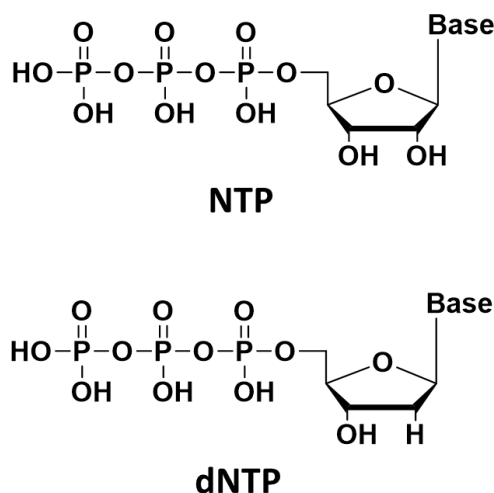


**Figure 1.12** Nucleotide triphosphate (NTP and dNTP)

complementary sequence as a template and consume nucleotide triphosphates or deoxynucleotide triphosphates (NTPs or dNTPs) (Figure 1.12) as building blocks for the synthesis. Thus, the direction of polymerization is from the 5' to 3' positions of the ribose in accord with the nature of the nucleophile (3' hydroxyl) and leaving group (pyrophosphate

on a 5' hydroxyl). DNA polymerases and reverse transcriptases additionally require small fragments of oligonucleotides called primers to initiate the polymerization.<sup>1, 3</sup>

In principle, modified oligonucleotides can be obtained by enzymatic methods. In this case, the requisite modified nucleotide triphosphates must be prepared prior to initiating the enzymatic synthesis.<sup>17, 52-53</sup> One key issue associated the enzymatic method is the compatibility of the modified substrate with polymerases. As mentioned earlier, functional groups attached to the C5 position of pyrimidines and the N7 or C8 positions of purines are relatively compatible with DNA polymerases. One of the most common applications of enzymatic modified oligonucleotide synthesis is the Sanger DNA sequencing method. Recognizing dideoxynucleotides (ddNTPs) modified with four-colored fluorophores as terminating building blocks (Figure 1.12), DNA polymerase synthesizes a series of terminated fragment sequences that have different fluorescence according to the terminating group.<sup>54-55</sup>

Unlike simple base modification, unnatural bases and XNAs are not compatible to natural polymerases. Therefore, researchers have developed artificial polymerases by direct evolution and protein engineering of enzymes. For example, Romesberg's group designed a DNA polymerase that duplicates an oligonucleotide sequence with three base pairs including an artificial one they invented.<sup>56</sup> Polymerases for locked nucleic acids (LNA)<sup>57</sup> and threose nucleic acids (TNA)<sup>58</sup> have also been developed.

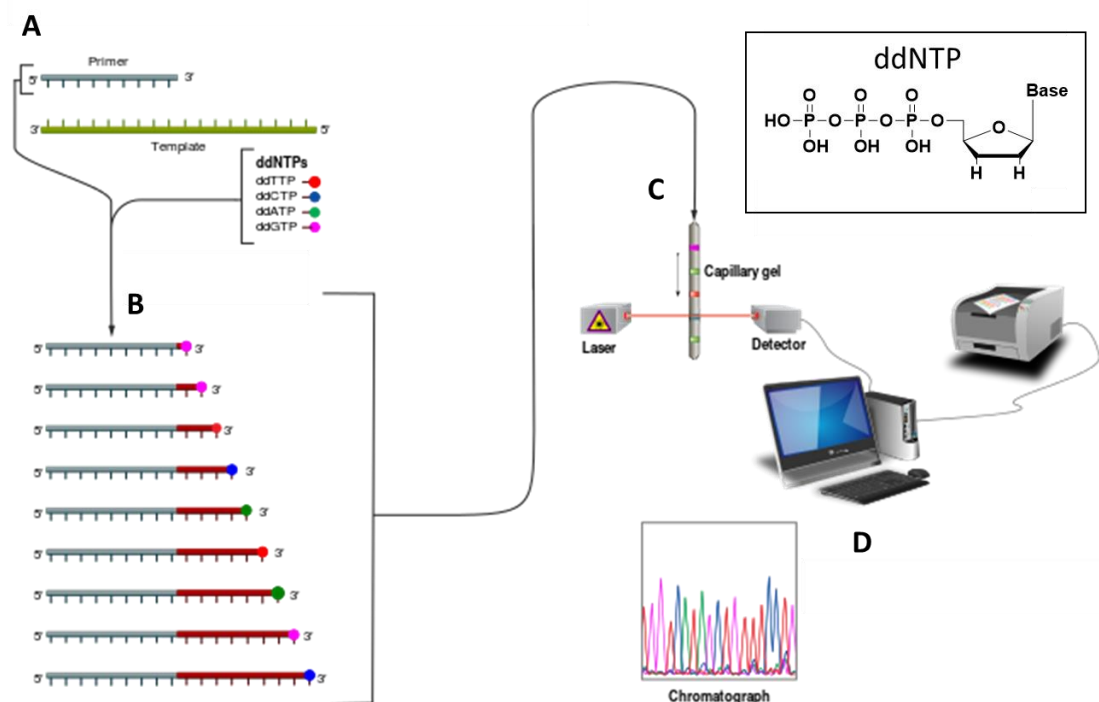


**Figure 1.13** The Sanger DNA sequencing method. A) A primer is hybridized with the target sequence. B) DNA polymerase, dNTPs, fluorophore-labeled dideoxynucleotides (ddNTPs) are mixed. The random insertion of a ddNTP terminates synthesis of the polymerized chain. Each sequence is characterized by the fluorescence of the terminal ddNTP. (3) The products are separated on the basis of length by capillary gel chromatography and the fluorescence from each sequence is determined. (4) The sequence is then constructed using a computational program. This figure was adapted from ref. 59 with modifications being made by the author.<sup>59</sup>

The main advantage of the enzymatic modified oligonucleotide synthesis is the outstanding efficiency. Compared to chemical syntheses, the natural enzyme systems enable the production of far longer nucleic acids sequences and with much higher fidelity.<sup>1</sup> Furthermore, when enzymes are used it is not necessary to carry out sequences involving what are inherently complex synthetic steps. However, under enzymatic conditions modifications at a specific point are almost impossible to achieve. This is because

polymerases recognize both modified and unmodified NTPs or dNTPs as a substrate. It is also hard to pause the polymerization to complete the reaction so as to introduce selective modifications in the middle of the sequence.

#### 1.1.4 Post-synthetic modification

In addition to modifying an oligonucleotide via dedicated synthesis, alterations can also be made after the synthesis.<sup>16, 60</sup> As mentioned above, chemical or enzymatic syntheses of modified oligonucleotides are limited to functional groups that are compatible with each synthetic method. On the other hand, post-synthetic modifications allow for the attachment of more diverse set of functional groups. Figure 1.14 shows numerous examples of linker-bearing oligonucleotides that allow for post-synthetic modifications.

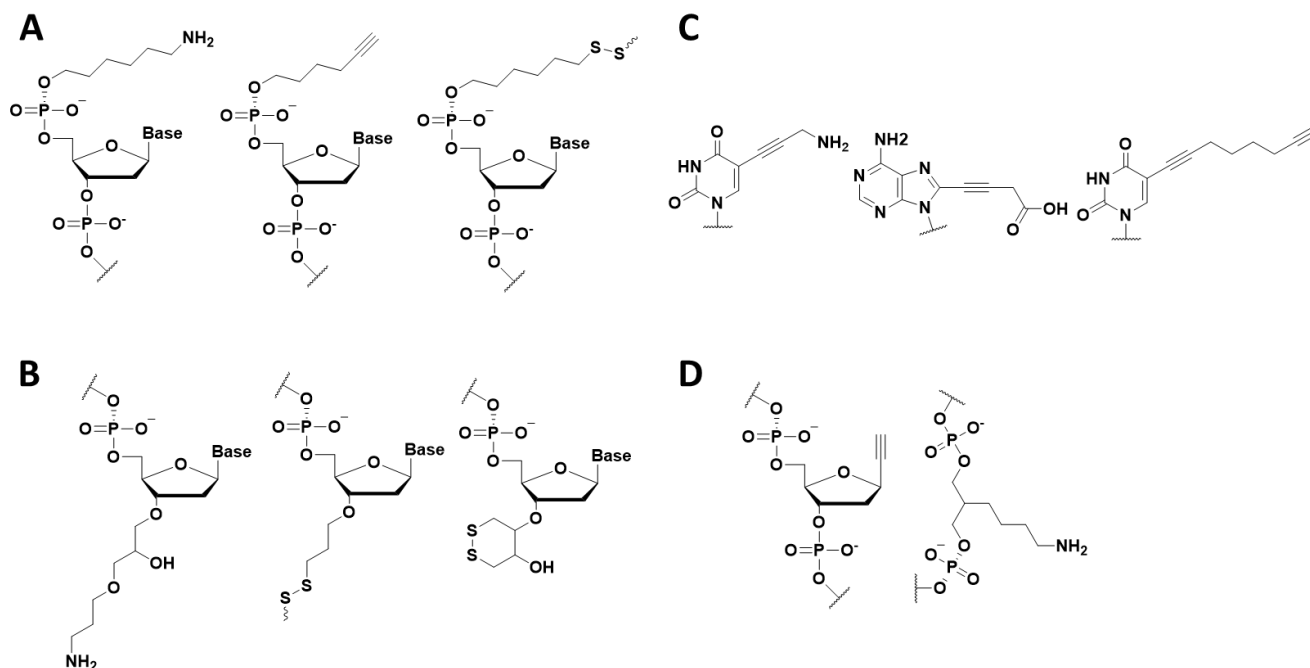
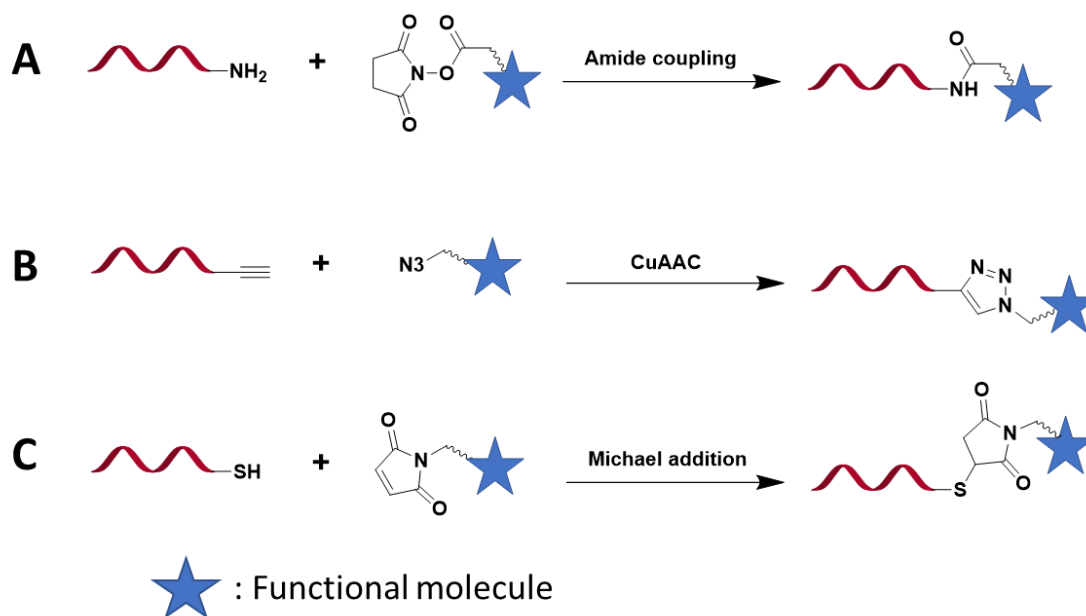


**Figure 1.14** Examples of chemically or enzymatically synthesized modified oligonucleotides for further post-synthetic modifications. Each molecule has a linker for bio-conjugation on A) the 5' end, B) the 3' end, C) at an internal nucleobase, and D) an internal backbone site of oligonucleotides.

For post-synthetic modification, it is convenient to use oligonucleotide targets that have specific functional groups that allow for conjugation. These functional groups are used as components for covalent linking reactions called bio-conjugations (Scheme 1.3).<sup>61-</sup>  
<sup>62</sup> The most common reaction is an amide coupling reaction, which connects an amine group on an oligonucleotide to an activated-carboxylic acid, such as *N*-hydroxysuccinimide ester (NHS-ester) on the modifying molecule.<sup>16, 61</sup> Azide-alkyne Huisgen cycloaddition, also referred to as a copper(I)-catalyzed azide-alkyne cycloaddition (CuAAC), is another common conjugation reaction.<sup>62</sup> Azide and alkyne species are rarely found in nature, so this reaction is widely used as a bio-orthogonal conjugation *in vitro* and *in vivo*. Thiols and  $\alpha,\beta$ -unsaturated carbonyl compounds can also be introduced and linked via Michael addition reactions. For synthetic convenience, these couplings are generally carried out using oligonucleotides containing a thiol and a modifying target containing a maleimide unit.<sup>63</sup> Thiols on oligonucleotides are also utilized in the modification of metal surfaces because of their strong affinity for metallic gold and silver surfaces.



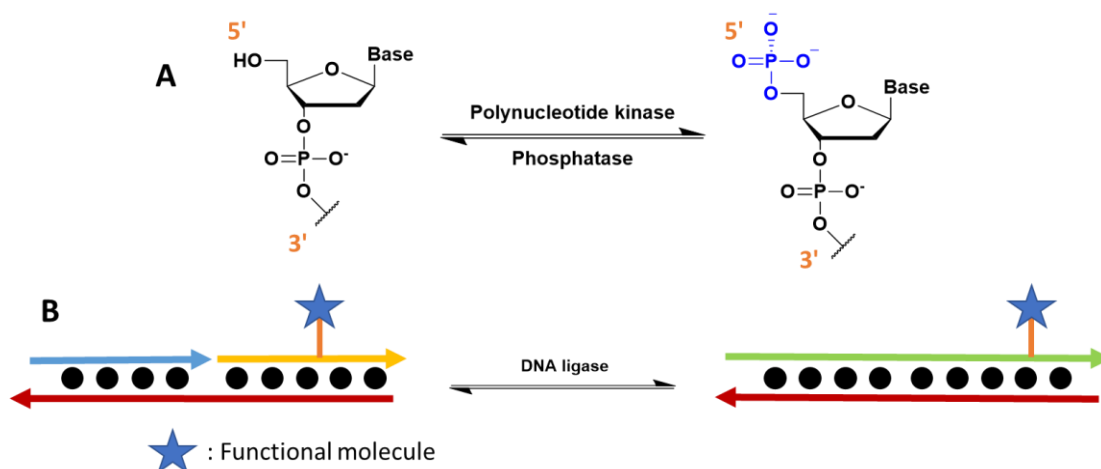


**Scheme 1.3** Representative bio-conjugation reactions involving oligonucleotides. A) Amide coupling reaction between an amino-functionalized oligonucleotide and an NHS-activated functional molecule. B) Click reaction between an alkyne-oligo and an azide-bearing molecule. C) Michael addition reaction between a thiol-oligonucleotide and maleimide-molecule.

Since a proper linker is required to permit post-synthetic conjugation chemistry, the underlying modification is commonly performed on the 3', 5', or nucleobase positions of the oligonucleotide. These positions are easy to functionalize with various linkers. On the other hand, linkers are not commonly attached to either the sugar or phosphate backbones because these positions affect the structure and function of the oligonucleotide.<sup>14, 16</sup>

Enzymatic modification of previously synthesized oligonucleotides is also possible (Figure 1.15). Polynucleotide kinases phosphorylate the 5' hydroxyl group of oligonucleotides.<sup>66</sup> For instance, by using ATP composed of <sup>32</sup>P-containing phosphates, oligonucleotides can be radioactively labeled by treating with this enzyme. On the other

hand, some phosphatases, such as alkaline phosphatase, hydrolyze the terminal phosphate group to a free hydroxyl group.<sup>67</sup> Another set of enzymes used for post-synthetic modification are the DNA ligases. These enzymes connect two pieces of DNA with the guidance of a complementary template.<sup>68</sup> Using these enzymes, modified oligonucleotides can be attached to other unmodified or modified oligonucleotides. Lastly, polymerases can be genetically engineered to incorporate linker-containing nucleobases directly into oligonucleotides, which in turn permits further conjugation to other molecules.<sup>69-70</sup>



**Scheme 1.4** Enzymatic modification of oligonucleotides using A) polynucleotide kinase and phosphatase, as well B) DNA ligase.

## 1.2 ELECTROCHEMICALLY ACTIVE OLIGONUCLEOTIDES AS SENSING TOOLS

### 1.2.1 Introduction

Oligonucleotides have many advantages for sensing applications compared to other organic or inorganic materials. In particular, oligonucleotides are the most efficient molecules for the detection of a specific DNA sequence, which is one of the most important targets in molecular biology.<sup>71-72</sup> Numerous methodologies have been reported for

detecting the hybridization of oligonucleotides on the basis of radioactivity,<sup>73</sup> fluorescence,<sup>71, 74</sup> surface plasmon resonance (SPR),<sup>75</sup> nanoparticle aggregation,<sup>76</sup> electronics,<sup>77</sup> and electrochemical readouts.

Among the diverse signal outputs, electrochemical sensing provides remarkable sensitivity and selectivity.<sup>78</sup> Furthermore, this technique is much less expensive than other methods.<sup>79-80</sup> These advantages are critical for miniaturizing the sensing system for *in vitro* or *in vivo* diagnostics, especially for point-of-care (POC) diagnostics.<sup>81</sup> With this goal in mind, many groups have synthesized electroactive oligonucleotides and have utilized them for genetic sensing as well as macromolecule detection.

Natural oligonucleotides present no additional functional groups. Moreover, they undergo irreversible oxidation at relatively high positive potentials. In 1988, the Palecek group reported that purines on oligonucleotides can be directly oxidized electrochemically.<sup>82</sup> However, this direct oxidation occurs only if the oligonucleotides are thoroughly immobilized or adsorbed on the electrodes for easy electron transfer. To overcome this limitation, the Thorp group developed an electrocatalytic system using tris(bipyridine)ruthenium(II) ( $\text{Ru}(\text{bpy})_3^{2+}$ ) as a mediator; this permits the oxidation of guanine units within oligonucleotides (Figure 1.15).<sup>83</sup> The organometallic ruthenium species transfers electrons from the electrode to the guanine by diffusion. Adopting this system, Marchal's group developed a system capable of effecting the electrochemical real-time monitoring of polymerase chain reactions (real-time PCR).<sup>84</sup>

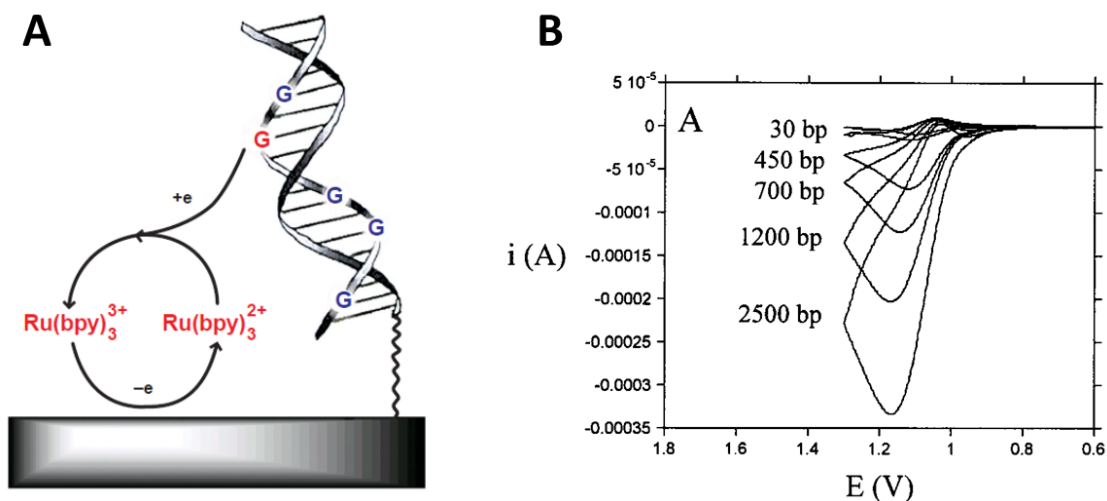


**Figure 1.15** **A)** Electrocatalytic oxidation of an oligonucleotide with  $\text{Ru}(\text{bpy})_3^{2+}$  as a redox mediator. If this scenario, the  $\text{Ru}(\text{bpy})_3^{3+}$  is reduced to  $\text{Ru}(\text{bpy})_3^{2+}$  by guanines and regenerated by the electrode. **B)** Electron transfer to the electrode is measured as a change in the current signal. The elements in this figure were adapted from refs. 79 and 83, respectively.

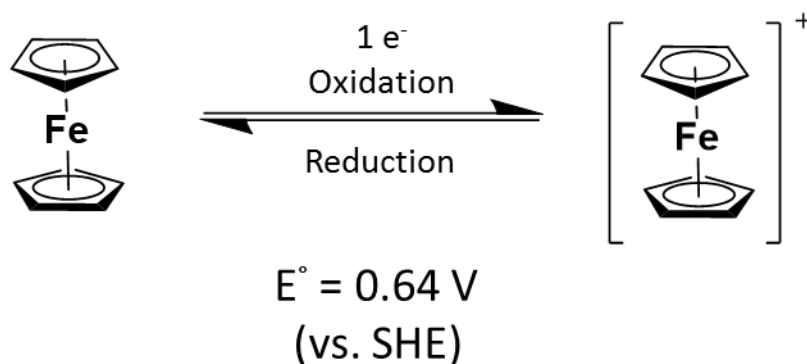
Unfortunately, both direct and indirect electron transfer from nucleobases is subject to many limitations when utilized in more complex sensing systems. Firstly, such electron transfer processes provide only quantitative information regarding the number of oligonucleotides and no details about the identity or organization of the nucleobases within an oligonucleotide. Secondly, the approach is limited in that it is not sensitive enough to detect small amount of targets.<sup>79</sup> To overcome these limitations, most oligonucleotide-based sensing systems use other electrochemically active molecules, such as redox-active small molecules, enzymes, nanoparticles, or nanostructured carbons (i.e., carbon nanotube or graphene) as adjuvants.<sup>79, 85-86</sup> This dissertation will be limited to the use of specific redox-active small molecules.

### 1.2.2 Redox-active functional groups

There are several redox-active functional groups reported as electrochemical tags for the modification of oligonucleotides.<sup>87</sup> The most common molecular tags are ferrocene and methylene blue.

#### 1.2.2.1 Ferrocene

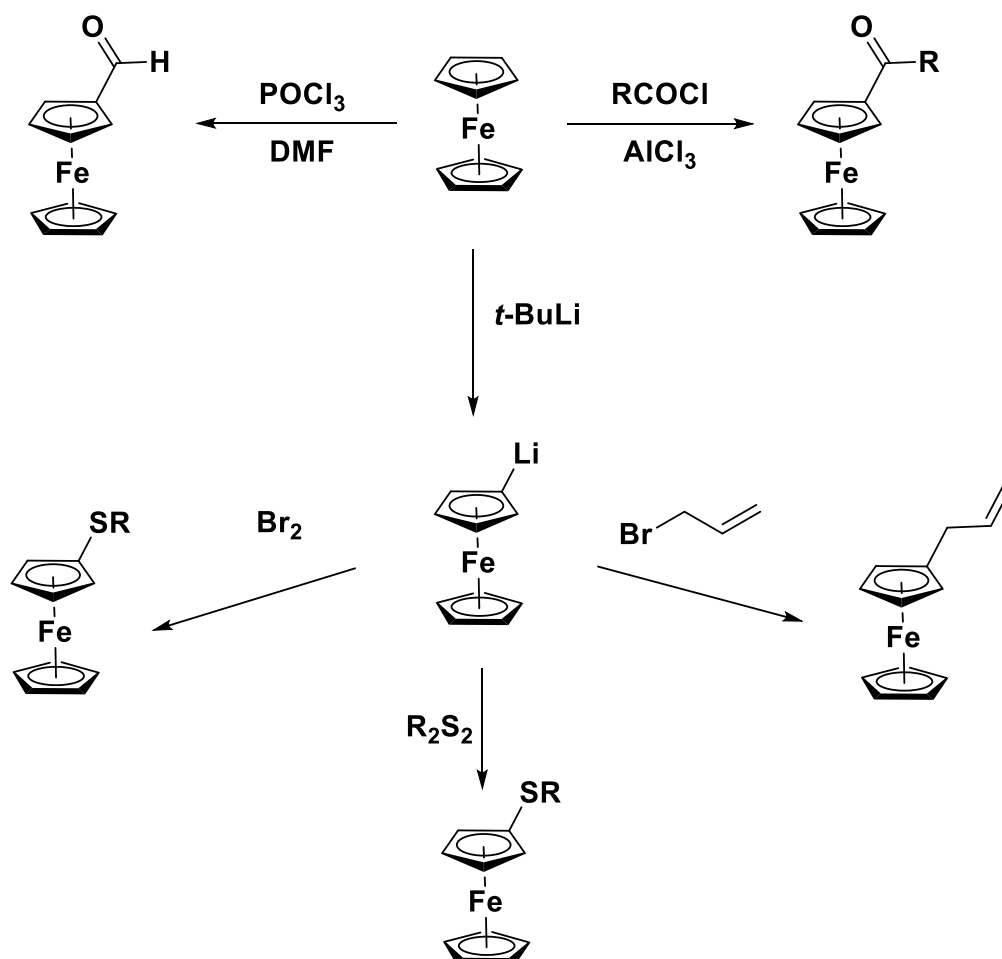
Ferrocene (Fc) is an orange-colored organometallic compound composed of two cyclopentadienyl rings (Cp) and a Fe(II) ion at the middle of the two rings (Scheme 1.5).<sup>88-</sup><sup>89</sup> The total charge of the molecule is zero due to the sum of the two negative charges from the Cp rings and the divalent  $\text{Fe}^{2+}$  cation. This sandwich structure stabilizes the whole molecule because both the  $4n + 2$  Hückel aromaticity and 18-electron rules for transition metal complex are satisfied.<sup>88, 90</sup>



**Scheme 1.5** Redox conversion between ferrocene (left) and the ferrocenium ion (right). The standard reduction potential of the ferrocenium ion is 0.64 V (vs. SHE).

The reactivity of the Cp ring in ferrocene is similar to that of typical aromatic compounds. It is relatively stable under most chemical conditions. However, this subunit is reactive under electrophilic aromatic substitution (EAS) conditions, including those associated with Friedel-Craft acylation<sup>91-93</sup> or Vilsmeier–Haack formylation<sup>94</sup> (Scheme

1.6). One exception to this is nitration. This is because the electrophilic nitronium ion ( $\text{NO}^{2+}$ ) oxidizes the ferrocene to the corresponding ferrocenium ion.<sup>95</sup> Lithiation of ferrocene with *t*-butyllithium produces a stronger ferrocene nucleophile,  $\text{FcLi}$ .<sup>96-97</sup> This precursor can be converted to halogenated,<sup>98</sup> alkylated,<sup>99</sup> or other hetero-atom linked ferrocene<sup>100-102</sup> derivatives by nucleophilic reactions.



**Scheme 1.6** Synthesis of ferrocene derivatives.

Another salient feature of ferrocene is its electrochemical activity. It undergoes reversible one-electron transfer, an effect ascribed to the two Cp rings stabilizing the

oxidized Fe(III) center through charge distribution.<sup>103-104</sup> The relatively stable ferrocenium ( $\text{Fc}^+$ ) ion is deep blue in color and is easily reduced back to the ferrocene form. This occurs reversibly. The redox potential ( $E^0_{1/2}$ ) of  $\text{Fc}^+/\text{Fc}$  is around 0.64 V vs. SHE.

Because it undergoes reversible electron transfer, ferrocene is frequently used as an electrochemical marker in a range of chemical constructs. It is also used as a reference in electrochemical assays.<sup>105</sup> Often reference electrodes in non-aqueous solutions are calibrated relative to the ferrocene/ferrocenium couple, which is used as an internal standard.

Ferrocene is also used as a redox-mediator in a large number of electrochemical reactions. In particular, heterogeneous interfaces between an electron donor and acceptor require reversible  $\text{Fc}/\text{Fc}^+$  couples to transfer the electron by diffusion.<sup>106</sup> For instance, glucose sensors use a ferrocene/ferrocenium redox couple to transfer an electron from glucose oxidase to the electrodes (Figure 1.16).<sup>107-109</sup> Since the active site of glucose oxidase is hindered by bulky and insulating side chains, direct electron transfer to a conventional electrode is not facile. Having ferrocene in solution or in the assembled layer with the enzymes helps transfer an electron to and from the electrode. This amount of electron transfer is proportional to the amount of glucose in solution. Ferrocene has also been used to create solar cells; it helps transfer high energy electrons from an activated photosensitizer molecules to an electrode.<sup>110-111</sup>

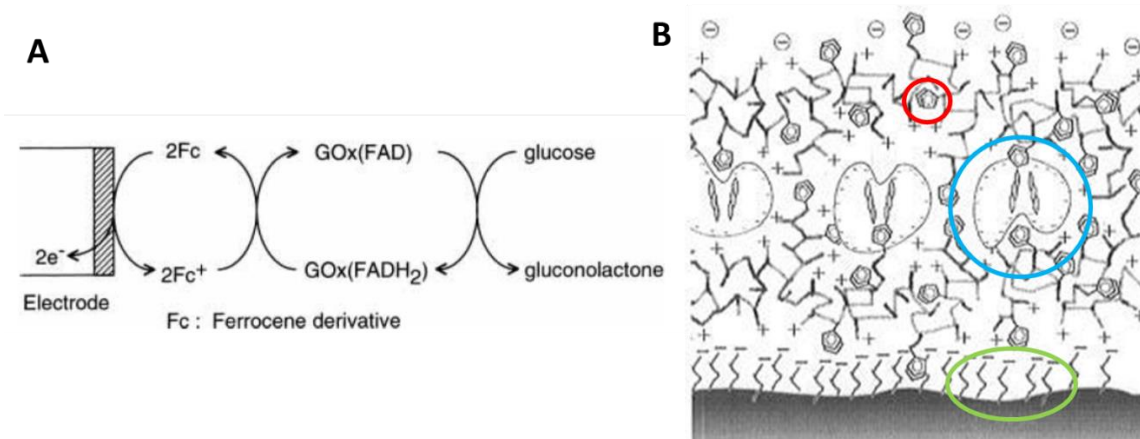


**Figure 1.16** A) Schematic overview of the electrocatalytic oxidation of glucose by glucose oxidase (GOx) using ferrocene as a redox mediator. Glucose is oxidized by GOx and the electrons from the glucose are transferred to the electrode via a FAD (co-factor) with the assistance of ferrocene, which acts as a redox mediator. The electron transfer is measured by amperometry. Adapted from ref. 109. B) Schematic illustration of the assembled layer of GOx (in the red circle) and ferrocene embedded within a polymer matrix (highlighted by a blue circle) on a gold electrode. The sulfate-thiol on the gold electrode (contained within a green circle, negatively charged), ferrocene polymer (ferrocenium form, positively charged), and GOx (negatively charged) are assembled as the layer through simple electrostatic interactions. This part of this figure was adapted from ref. 108.

Finally, ferrocene derivatives form supramolecular complexes with various organic host molecules in aqueous solution. The ferrocene derivatives are typically bound within the hydrophobic binding sites of the encapsulating host molecule, an effect driven presumably by a need to avoid exposure to bulk water molecules. The best studied ferrocene hosts are  $\beta$ -cyclodextrin ( $\beta$ -CD)<sup>104, 112</sup> and cucurbit[7]uril (CB[7]).<sup>113</sup> (Figure 1.17). Both molecules contain a hydrophobic cavity and a hydrophilic boundary that is solvated in aqueous solution. A key feature of the resulting  $\beta$ -CD-Fc complex is its redox responsive features.<sup>112, 114</sup> Once a ferrocene is oxidized to a ferrocenium ion, it is expelled from the cavity due electrostatic repulsion. Exploiting this property, researchers developed



redox-responsive polymers that can form nanofibers,<sup>115</sup> hydrogels,<sup>116</sup> and self-healing materials.<sup>117</sup>

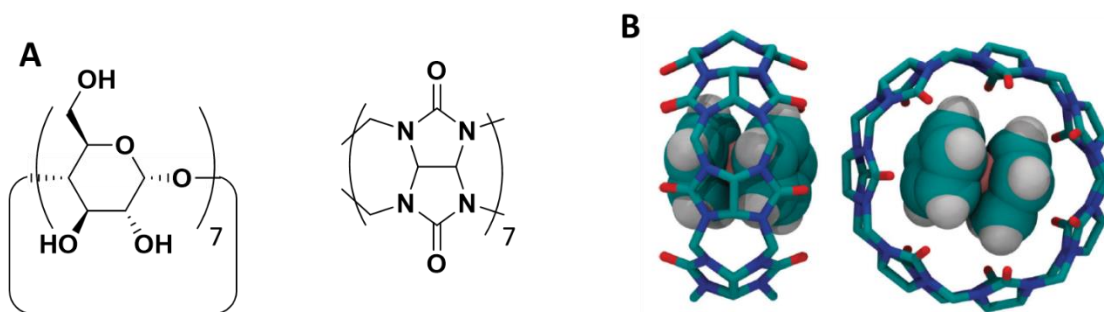
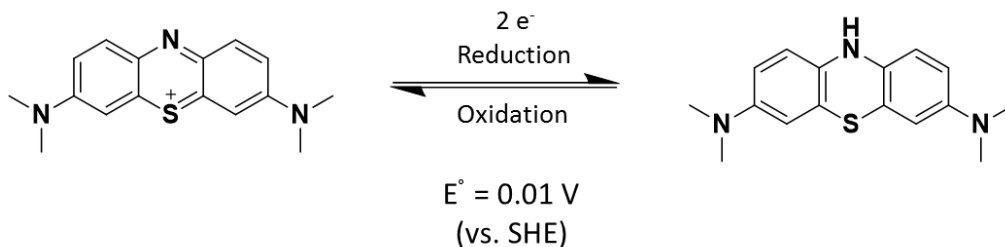


**Figure 1.17** A) Structure of  $\beta$ -Cyclodextrin (left) and cucurbit[7]uril (CB7, right). B) Supramolecular complex of CB7 and Fc. Adapted from ref. 118.

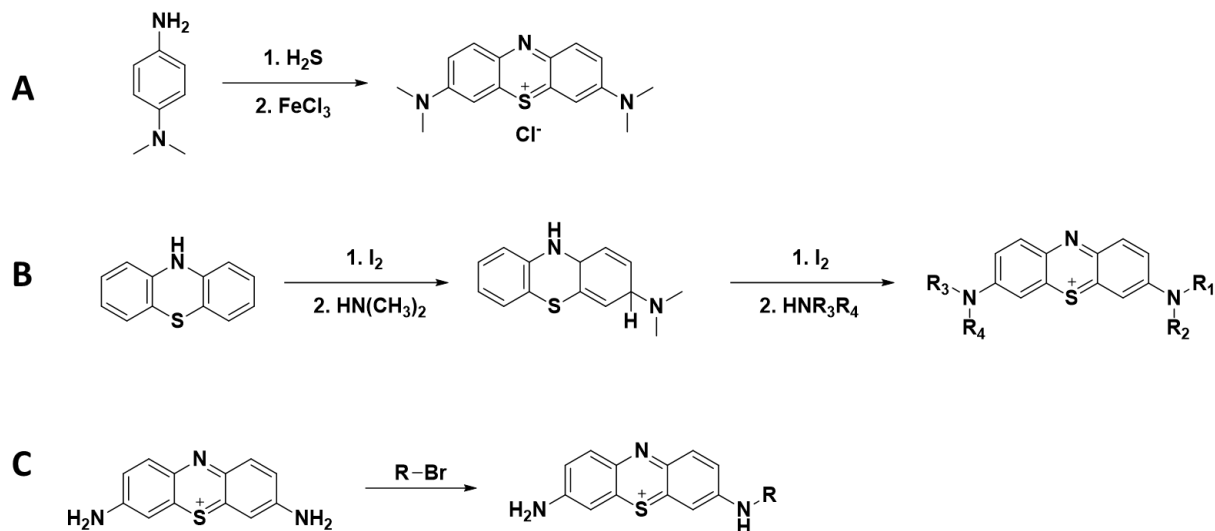
#### 1.2.2.2 Methylene blue

Methylene blue (MB) is a phenothiazine derivative with two dimethylamino groups on each side of the annulated benzene rings (Scheme 1.7). It is deep blue in solution as its name evokes. The molecule has a positive charge that is distributed over both dimethylamino groups and the phenothiazine nitrogen. MB accepts two electrons to form the reduced neutral form called leucomethylene blue (LB).<sup>119</sup> When MB is reduced to LB, the color of the solution changes from blue to colorless.



**Scheme 1.7** Methylene blue (left) and leucomethylene blue (right). The standard reduction potential of methylene blue is 0.01 V (vs. SHE).

MB is synthesized by reacting dimethyl-4-phenylenediamine and hydrogen sulfide in hydrochloric acid and subsequently oxidizing with ferric chloride (Scheme 1.8A).<sup>120</sup> Since the two dimethylamino groups are already present in the precursors before the phenothiazine ring is formed, MB is difficult to modify with other functional groups under the standard conditions associated with its direct synthesis. For this reason, asymmetric MB derivatives are typically synthesized using other synthetic routes (Scheme 1.8B).<sup>121-122</sup> For instance, the starting phenothiazine may first be oxidized by treating with iodine. Then, a secondary amine can be used to attack the 3-position; this gives a mono-substituted phenothiazine via nucleophilic aromatic substitution. After isolation from the starting material and the di-substituted byproduct, the mono-substituted intermediate can be reacted with another amine nucleophile to produce an asymmetric MB. Using this method, various MB derivatives can be prepared, including an *N*-hydroxysuccinimide-activated MB (NHS-MB).<sup>123</sup> Thionine can also be converted into MB analogues by monoalkylation of an aniline nitrogen. However, the syntheses are typically inefficient and the resulting products display electrochemical features that differ from those of MB (Scheme 1.8C).<sup>87</sup>



**Scheme 1.8** Synthesis of A) MB, B) its derivatives, and C) mono-substituted thionines.

MB is used in a number of chemical applications. First, it is one of the better studied redox indicators.<sup>78</sup> When exposed to reducing species in solution, MB undergoes a distinct color change from deep blue to colorless. One example is the so-called “blue bottle” experiment commonly used in classic general chemistry demonstrations. Here, MB reacts with sugar and serves as a probe for the redox reaction that occurs when these two species react with one another (Figure 1.18).<sup>124</sup> Second, MB generates singlet oxygen species when exposed to oxygen and light. It thus acts as a photosensitizer.<sup>125</sup> The singlet oxygen produced in this way may be used in photodynamic therapy, the synthesis of organic peroxides,<sup>126</sup> and water purification,<sup>127</sup> to name a few lead applications.

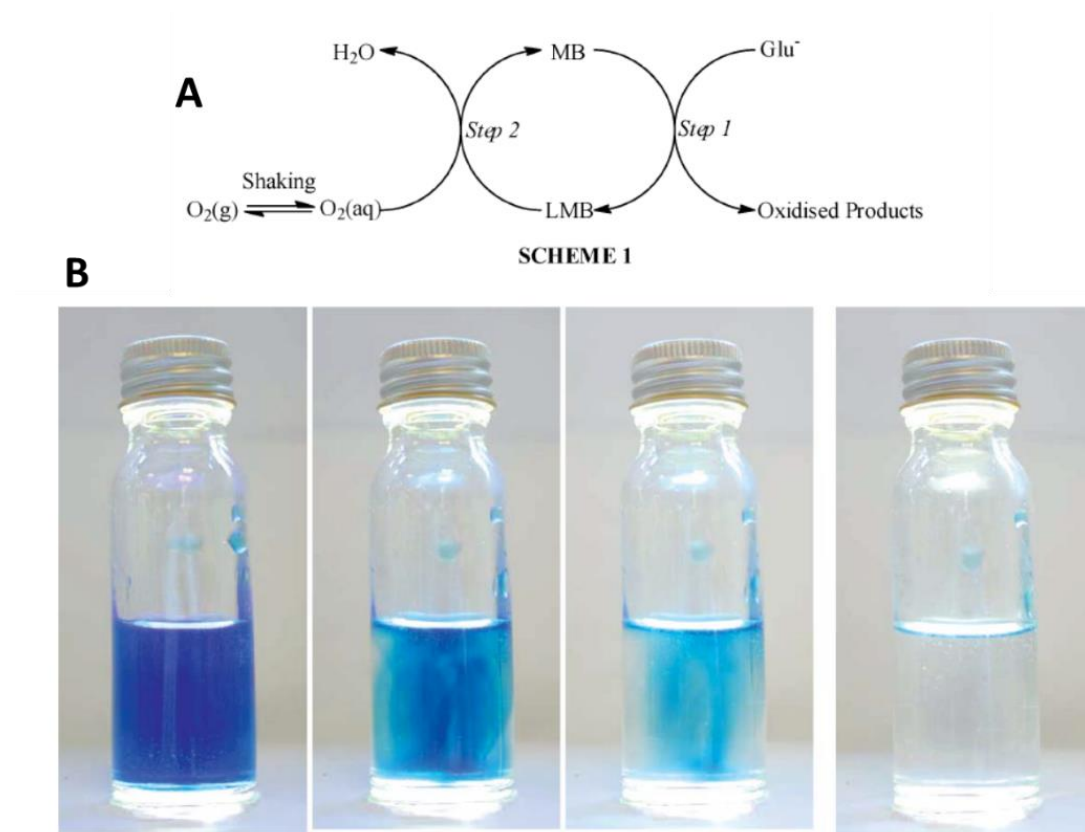


**Figure 1.18** A) Mechanism of the blue bottle reaction and B) photograph of the color change before, 3 min, 3.3 min and 4.3 min of the experiment, respectively. Adapted from ref. 124.

MB has also seen widespread use in the areas of biochemistry and medical sciences. Its flat structure and strong absorbance in the visible region allows it to stain tissues for endoscopies and surgeries.<sup>128-129</sup> Moreover, the combination of MB and light has led to it being exploited as a treatment for several diseases. On the other hand, it has been proposed that MB may cause DNA damage in cells.<sup>130-131</sup>

### 1.2.3 Applications

#### *1.2.3.1 Covalently modified electroactive oligonucleotide*

As mentioned earlier, a major application for electrochemically active modified oligonucleotides is the detection of specific target molecules, particularly sequences of nucleic acids. Hybridization between the modified oligonucleotide and the target sequence can lead to a huge conformational change. In the case of electrochemically active modified oligonucleotides this change in conformation can produce a modulated electrochemical output.

Ferrocene has been used for some time as an electrochemical tag in the context of preparing covalently modified oligonucleotides for sensing applications. In 1997, the Maeda group reported the first genetic sensing system with a ferrocene-modified oligonucleotide (Figure 1.19).<sup>132</sup> They attached a ferrocene subunit to the 5' position of an oligonucleotide using a post-synthetic modification strategy involving amide coupling. In this study, the target oligonucleotide has a sequence that is partially complementary to both that of the ferrocene-bearing oligonucleotide probe and an immobilized strand of DNA attached to a gold electrode. When the target sequence is added to the solution hybridization takes place between all three oligonucleotide fragments. As a result, the ferrocene tag is brought into the vicinity of the electrode surface. This permits enhanced electronic communication between the electrode surface and the ferrocene probe thus providing a voltammetric assay.

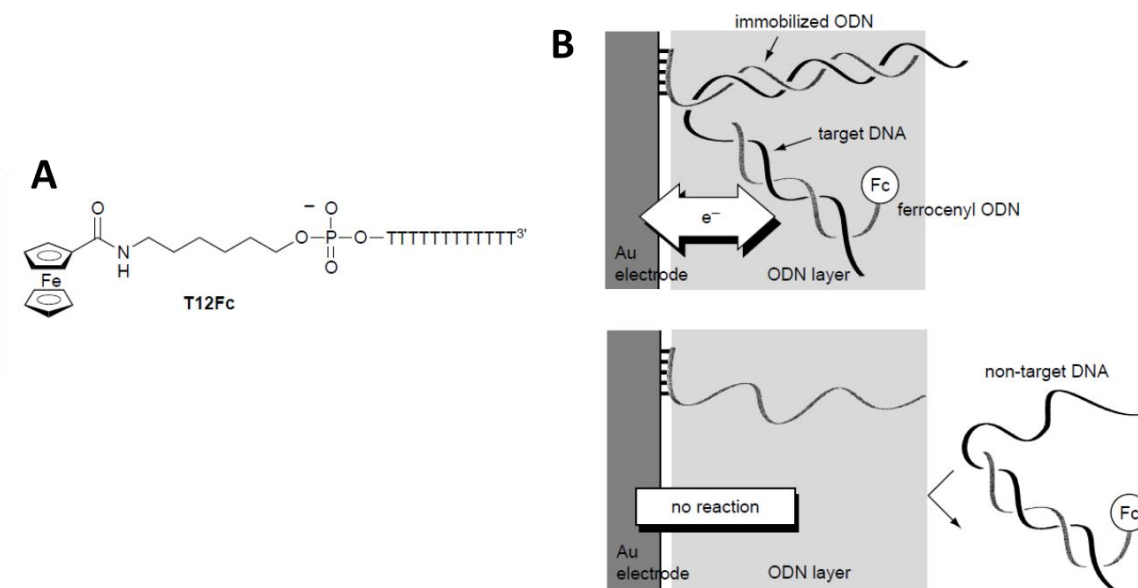


**Figure 1.19** The first genetic sensing system involving an electrochemically active oligonucleotide as reported by Maeda's group in 1997. Shown in A) is the oligonucleotide used in the study, whereas B) shows the genetic sensing scheme. Adapted from ref. 132.

Systems now known as electrochemical DNA sensors, or E-DNA sensors for short, represent modifications of an approach introduced by Plaxco's group in 2003 (Figure 1.20).<sup>80</sup> These researchers synthesized by chemical means a stem-loop-structured DNA with a hexyl thiol at the 5' end and a ferrocene moiety at the 3' end. Both chemical functionalities were added via post-synthetic modification. This functionalized oligonucleotide was then immobilized on a gold electrode surface through thiol-gold interactions, which was then treated with 6-mercaptohexanols to form a monolayer interface. When a complementary sequence to the stem region present in the functionalized oligonucleotide is added, break up the hairpin structure occurs. This leads to reduction in the current as a consequence of the ferrocene tag having moved away from the electrode. The original Plaxco system displayed good sensitivity and could be reused without having to add any additional reagents. In recent studies, the Plaxco group has used MB rather than

ferrocene as the electrochemical tag their E-DNA sensors. They found that MB gave rise to improved stability and markedly better reusability in aqueous media.<sup>133-134</sup> Nevertheless, ferrocene remains widely used and can be found in a variety of electroactive modified oligonucleotides; likely, this reflects its synthetic versatility.<sup>135-136</sup>

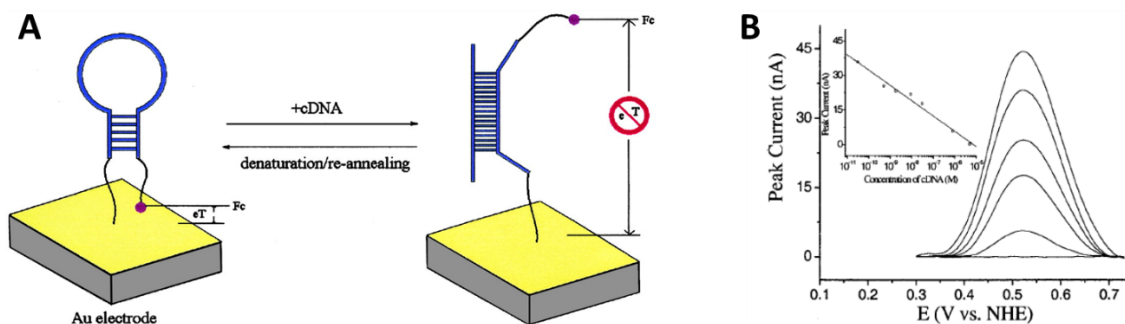


**Figure 1.20** The first E-DNA sensor as reported by Plaxco et al. A) Schematic representation of the sensor. B) Plot of the current decrease seen upon addition of an appropriately chosen target sequence. Adapted from ref. 80.

The combination of DNA amplification techniques and electrochemical detection can give rise to useful tools for genetic sensing. For example, the Ellington group designed a catalytic chain reaction (CHR) system that relies on a MB-based signal as the output (Figure 1.21).<sup>137</sup> In the presence of a catalytic sequence C1, any H1-E:H2 complex that forms becomes amplified by CHR. This causes the terminal MB to approach the electrode due to the hybridization between the complex and the surface-immobilized sequence S1 producing a change in the electrochemical signature. This system showed detection limits as low as 10 pM for the target sequence (C1).

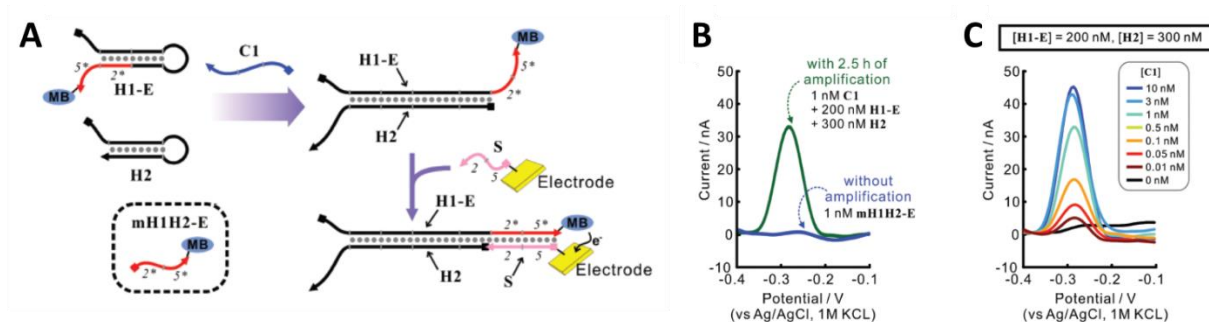


**Figure 1.21** Electrochemical detection based on use of CHR. A) The requisite catalytic amplification is initiated by the addition of C1. The resulting assembled construct, H1-E-H2, the binds to an electrode as the result of hybridization to the immobilized sequence S. B) The current signal is increased after the addition of the target for the amplification while C) the signal intensity varies with different concentrations of C1. Adapted from ref. 137.

Hsing's group also developed a real-time PCR with a ferrocene modified thymidine triphosphate (TTP) as the monomer for use in the polymerase reaction.<sup>138</sup> They found the ferrocene-derived electrochemical signal gradually increases as the number of recurring reaction cycles increases (Figure 1.22).



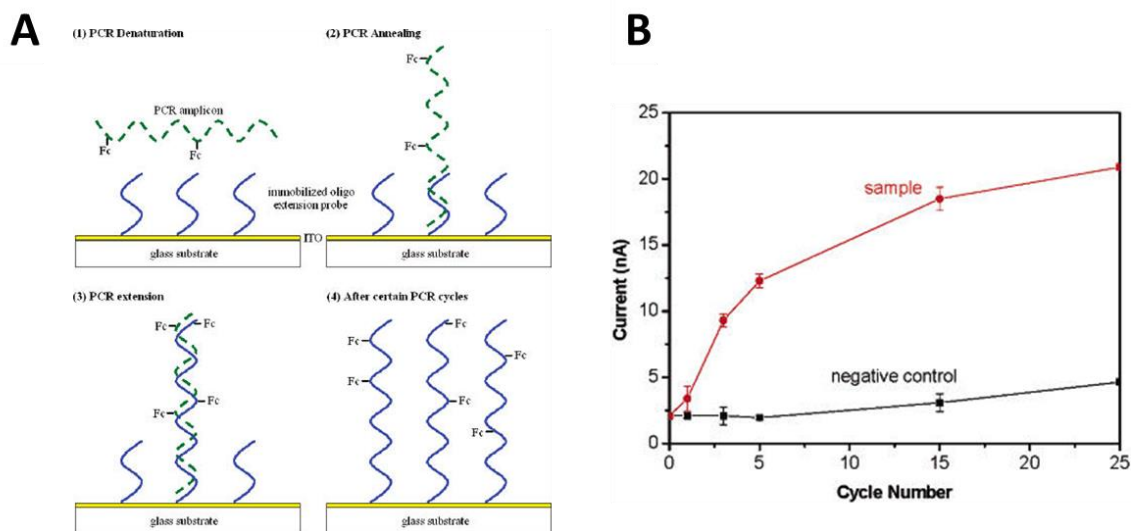


**Figure 1.22** Electrochemical real-time PCR. A) Surface-immobilized primers are elongated with Fc-incorporated thymidine, which increase the electrochemical signal. B) The signal increases with each reaction cycle with the template sequence (red) but not in its absence (black). Adapted from ref. 138.

Another example of nucleic acid hybridization detection involves utilizes the  $\beta$ -CD-Fc interactions for sensing. Tao's group synthesized an oligonucleotide modified with a  $\beta$ -CD and a Fc at each terminus to induce the formation of an intramolecular supramolecular complex (Figure 1.23).<sup>139</sup> Addition of the complementary sequence of the oligonucleotide dissociates the complex and exposes the ferrocene to the solution to facilitate the electron transfer to electrodes.

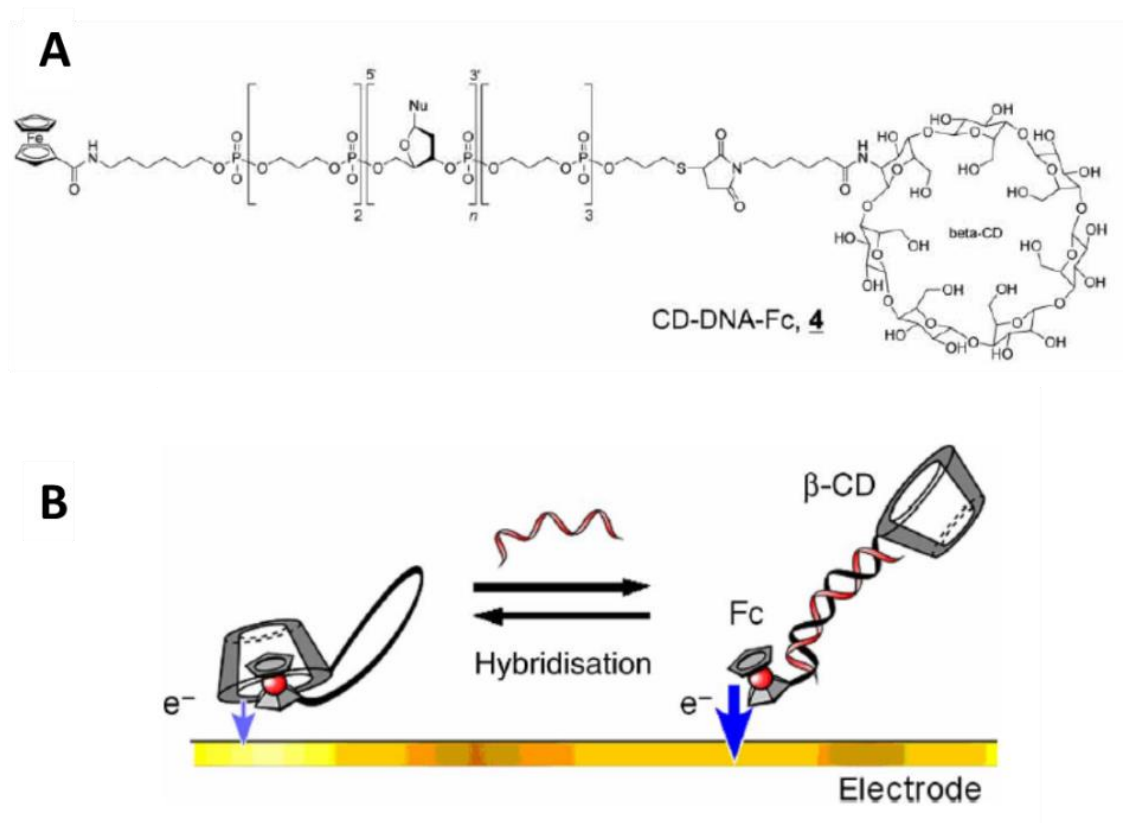


**Figure 1.23** Genetic sensing using the Fc- $\beta$ CD interaction. A) Structure of the molecule. B) Scheme of the system. The exposure of the ferrocene out of the  $\beta$ CD gives increased electrochemical signal. Adapted from ref. 139.

Electrochemically active oligonucleotides also can be applied to small molecule and macromolecule detection. Attachment of redox-active tag to the aptamer for the targets is necessary, just as in genetic sensing. In 2005, the Plaxco group, who invented the E-DNA sensors, also developed an electrochemical aptamer-based sensor, so-called E-AB sensor, in order to detect thrombin in blood serum (Figure 1.24A).<sup>140</sup> The conformational change of aptamer was induced upon binding with thrombin, resulting in a change in distance between MB and the electrode. Small molecule aptamers have been applied in the same manner. Cocaine (Figure 1.24B),<sup>141</sup> doxorubicin,<sup>142</sup> and aminoglycoside species detection<sup>143</sup> has been reported with MB functionalized E-AB sensors. In particular, the Soh

group developed a real-time detection system for doxorubicin and kanamycin using microfluidic techniques and a continuous diffusion filter to monitor the circulating drugs in the blood stream of living animals (Figure 1.25).<sup>142</sup>

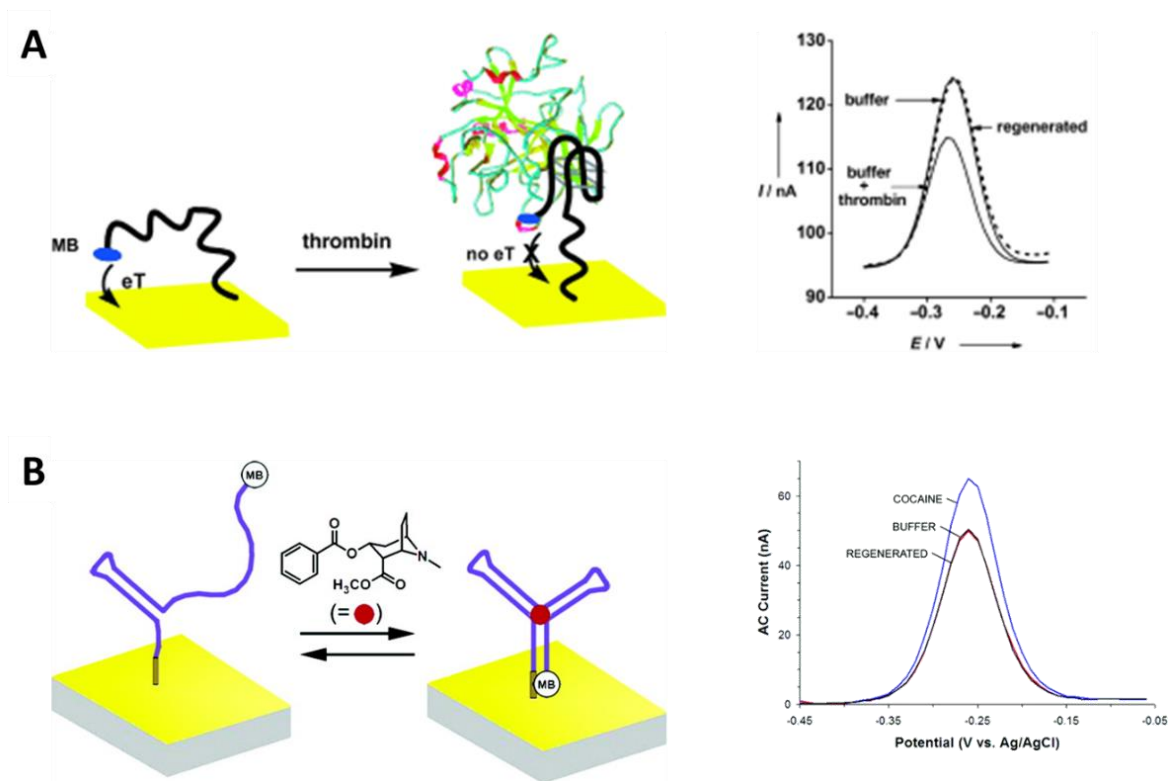


**Figure 1.24** A) Thrombin (signal-off) and B) cocaine (signal-on) E-AB sensors. Adapted from ref 140 and 141.

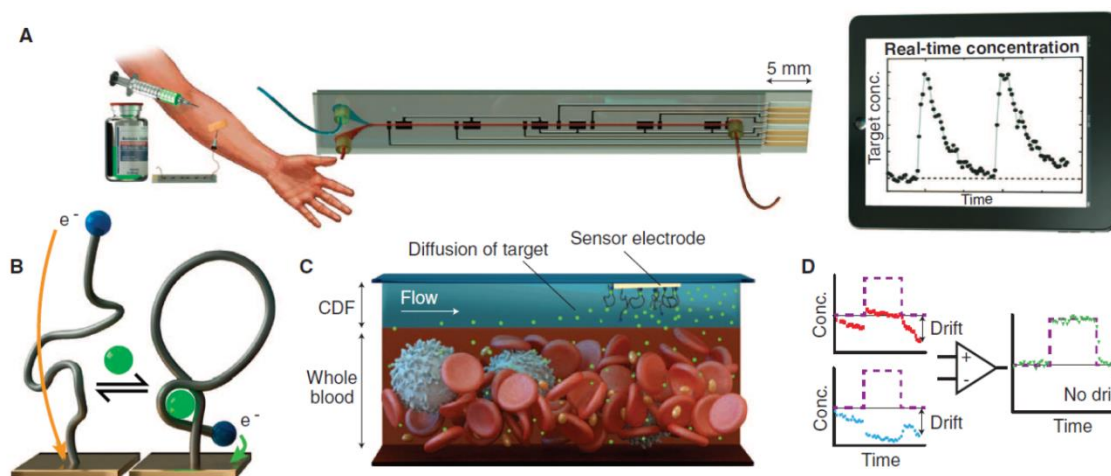


**Figure 1.25** Real-time measurement of specific molecules in blood by Soh's group. (A) Sampling of blood by microfluidic techniques. (B) The E-AB sensor used in the study. (C) The continuous-flow diffusion filter (CDF) for filtering and detection of the target molecule. (D) Monitoring of the target concentration through either a signal-on (red) or a signal-off (blue) approach. Adapted from ref. 142.

### 1.2.3.2 Electrochemically active oligonucleotide with intercalating probes

Electrochemically active oligonucleotides can be constructed not only by covalent modification, but also through non-covalent interactions between oligonucleotides and redox-active small molecules. Most commonly, these non-covalent interactions arise from the intercalation of the small molecule into oligonucleotide.<sup>144-145</sup> These intercalation interactions are promoted and stabilized by  $\pi$ - $\pi$  interactions between the intercalated, aromatic small molecules and the nucleobases. Most of the redox active small molecules used in this capacity are planar. This allows them to fit into the gap between two adjacent base pairs. Thus, the intercalators are easily embedded in double helix dsDNAs, but bind less tightly or not at all with single stranded DNAs (ssDNAs). These features are similar to those of fluorescent dyes selective for dsDNAs and the nucleus, such as ethidium bromide<sup>146</sup> and Hoechst dyes (Figure 1.26).<sup>147</sup> In addition to acting as stains, many

intercalators displays cytotoxicity. This is because they block the transcription of dsDNA.<sup>143</sup>

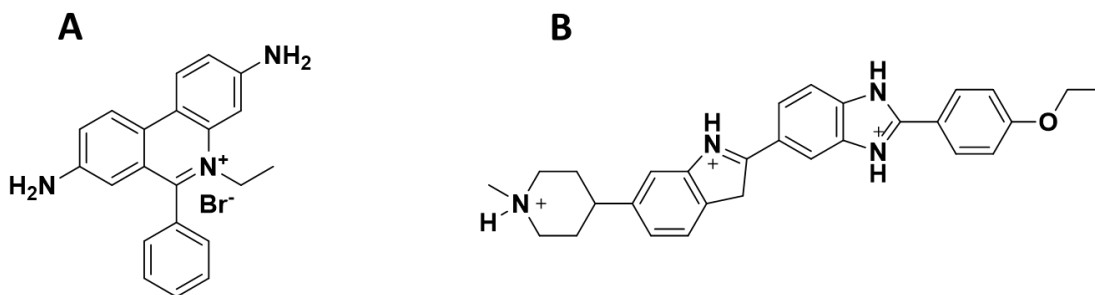


**Figure 1.26** A) Ethidium bromide and B) Hoechst 33342 dye.

MB is also a good intercalator due to its planar and aromatic structure, as well as its favorable electrostatic interactions with the negatively charged phosphate backbones.<sup>148</sup> Barton's group reported the combination of MB with dsDNA showed an electrochemical current upon hybridization on the surface of the electrode in 1997 (Figure 1.27).<sup>149</sup> Likewise, researchers reported anthraquinone species<sup>150</sup> and Ir(III) organometallic compounds<sup>151-152</sup> bound to dsDNA that can be utilized as reporters for hybridization.

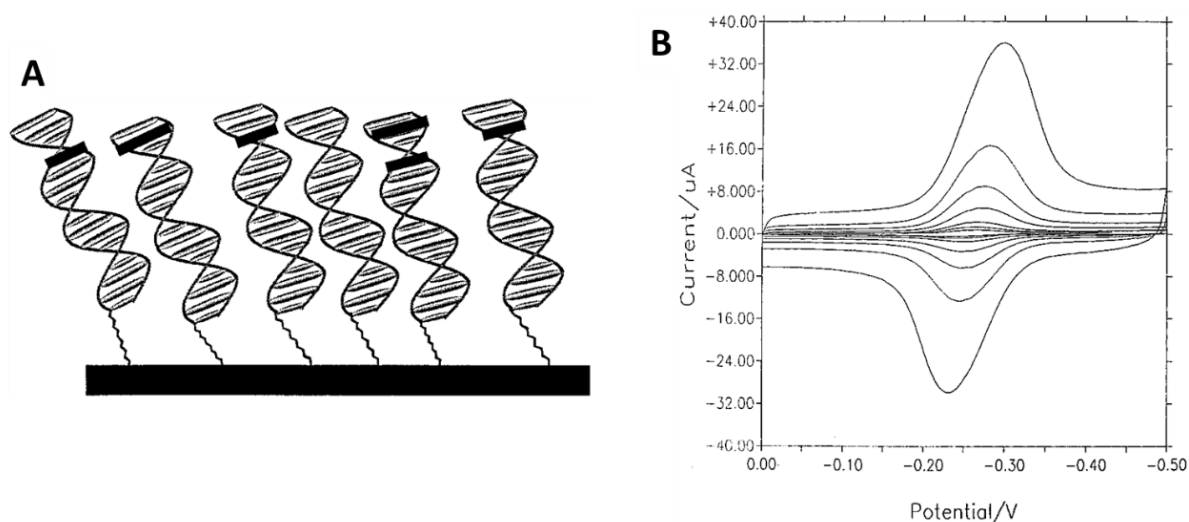


**Figure 1.27** A) Schematic illustration of the intercalation of MB (black bars) on an electrode-immobilized oligonucleotide. B) Increased electrochemical signals elicited by concentration increase. Adapted from ref. 149.

In later studies, it was shown that mismatched DNA or single nucleotide polymorphism (SNP) can be monitored with intercalators. For example, Barton's group amplified the MB signal with an electrocatalytic reaction using potassium cyanide ( $\text{K}_3\text{Fe}(\text{CN})_6$ ) as a mediator to detect a single mismatched oligonucleotide (Figure 1.28).<sup>119</sup> Hvastkovs' group also developed electrochemically active diviologen derivatives for SNP applications (Figure 1.29).<sup>153</sup>

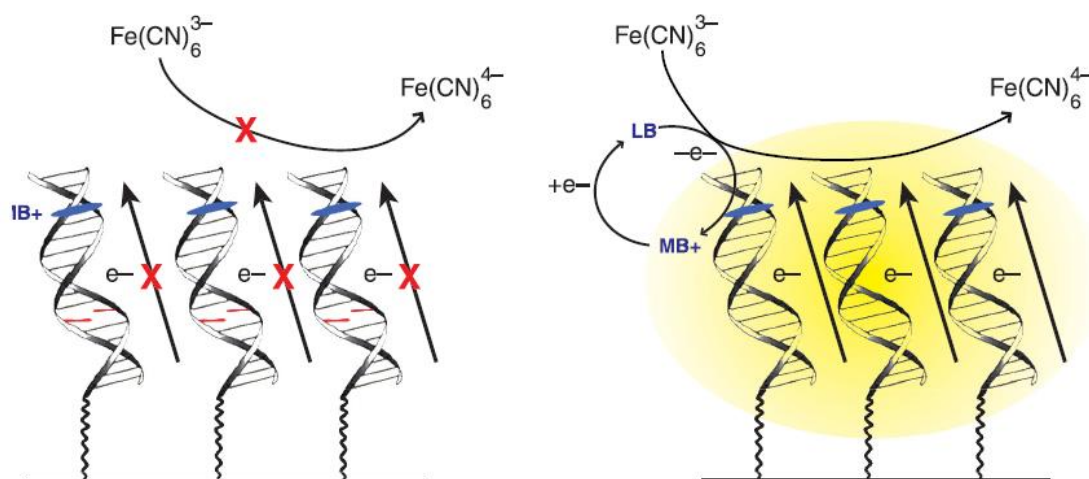


**Figure 1.28** Electrocatalytic detection of mismatched oligonucleotide with MB (as a signal probe) and  $\text{Fe}(\text{CN})_6^{3-}$  (as a redox mediator). Electron transfer from electrode to  $\text{Fe}(\text{CN})_6^{3-}$  is blocked by mismatched base-pairing. As a result, the signal from MB is decreased. Adapted from ref. 79.

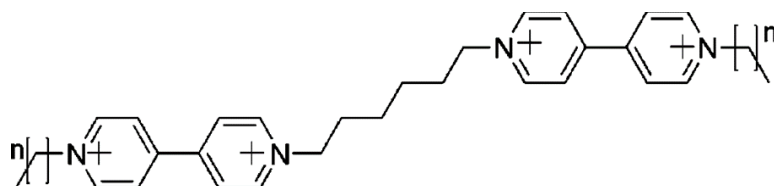


**Figure 1.29** Electrochemically active diviologen compound developed by Hvastkov's group.

### 1.3 SUMMARY AND OUTLINE

In this chapter, the author provides a brief introduction to oligonucleotides for sensing applications. Oligonucleotides, including DNAs and RNAs, have potential as the building blocks for the creation of electrochemical sensing platforms, especially when they are modified with proper functional groups. The goal in this summary was to introduce the

structural components of oligonucleotides and describe how nucleobases, riboses, and phosphodiester backbones can be modified. Approaches to creating modified systems has been organized into three categories: chemical synthesis, enzymatic synthesis, and post-synthetic modification. Detailed pros and cons of each method were also discussed. A brief summary of electrochemically active oligonucleotides in terms of modifications and resulting applications was also included in this chapter. Additionally, the applications and inherent limitations of electrochemical reactions of unmodified oligonucleotides were reviewed. Subsequently, the two major electrochemically active small molecule probes (ferrocene and MB) were discussed in the context of their chemical properties and practical applications. Modified oligonucleotides using these probes were then applied in myriad studies of electrochemical sensing applications. Lastly, the applications of covalently modified oligonucleotides and oligonucleotides with non-covalent intercalators were introduced.

From this background, the author presents studies related to electrochemically active oligonucleotides. The two main goals of these studies are to improve the versatility of electrochemical probes for multiplex sensing and to develop more reliable and practical diagnostic system based on electrochemical analysis.

Chapter 2 describes the synthesis of ferrocene-modified oligonucleotides and their use as multiplexing signal probes. By introducing various functional groups, the author studied the variation of the oxidation potentials of ferrocene derivatives. To achieve this, ferrocene subunits bearing alkynes, modified nucleoside phosphoramidites, and the oligonucleotides were synthesized. The synthesized derivatives were also analyzed by electrochemical assays. The author was responsible for the synthesis, purification, characterization, and electrochemical analyses for the study.



Chapter 3 describes the development of a ratiometric electrochemical DNA sensor using one of the ferrocene-modified oligonucleotides described in Chapter 2 in combination with MB. The modified oligonucleotide was prepared through chemical oligonucleotide synthesis and enzyme ligation. Subsequent electrochemical analysis showed remarkable improvement in terms of reproducibility and sensitivity compared with traditional E-sensors. This work was included in the article published in *Analytical Chemistry*.<sup>154</sup> The author is a co-first author of the publication and was responsible for the synthesis, purification, and characterization of the oligonucleotides used in the study and for a part of the electrochemical analyses.

Chapter 4 describes the design and fabrication of possible wearable devices with the modified electrochemically active oligonucleotides toward real diagnostic applications. The device array on a wearable patch was fabricated and modified with an E-DNA sensor with the goal of detecting specific genes and small molecules. The author was responsible for the modification of a prototype device with the oligonucleotides and the following electrochemical analyses. This work is being done in collaboration with Dr. Nanshu Lu's group in the Dept. of Aerospace Engineering and Engineering Mechanics at the University of Texas at Austin.

Chapter 5 details the synthetic procedures, provides characterization of all new products, and contains electrochemical analytical data discussed in this dissertation. proton,  $^{13}\text{C}$ , and  $^{31}\text{P}$  NMR spectroscopy data, ESI and MALDI mass spectrometry data, HPLC traces, PAGE images, cyclic voltammograms, ACV, and SWV are also included.

## 1.4 REFERENCES

1. Berg, J. M.; Tymoczko, J. L.; Stryer, L.; Stryer, L., *Biochemistry*. 6th ed.; W. H. Freeman: New York, 2007; p 1 v.
2. Watson, J. D.; Crick, F. H. C., Molecular Structure of Nucleic Acids - a Structure for Deoxyribose Nucleic Acid. *Nature* **1953**, *171* (4356), 737-738.
3. Lehninger, A. L.; Nelson, D. L.; Cox, M. M., *Lehninger principles of biochemistry*. 4th ed.; W.H. Freeman: New York, 2005; p 1 v.
4. Gilbert, W., ORIGIN OF LIFE - THE RNA WORLD. *Nature* **1986**, *319* (6055), 618-618.
5. Rothemund, P. W. K., Folding DNA to create nanoscale shapes and patterns. *Nature* **2006**, *440* (7082), 297-302.
6. Inuma, R.; Ke, Y.; Jungmann, R.; Schlichthaerle, T.; Woehrstein, J. B.; Yin, P., Polyhedra Self-Assembled from DNA Tripods and Characterized with 3D DNA-PAINT. *Science* **2014**, *344* (6179), 65-69.
7. Zhang, D. Y.; Winfree, E., Control of DNA Strand Displacement Kinetics Using Toehold Exchange. *J Am Chem Soc* **2009**, *131* (47), 17303-17314.
8. Zhang, D. Y.; Seelig, G., Dynamic DNA nanotechnology using strand-displacement reactions. *Nat Chem* **2011**, *3* (2), 103-113.
9. Asiello, P. J.; Baeumner, A. J., Miniaturized isothermal nucleic acid amplification, a review. *Lab on a Chip* **2011**, *11* (8), 1420-1430.
10. Oliphant, A. R.; Brandl, C. J.; Struhl, K., Defining the sequence specificity of DNA-binding proteins by selecting binding sites from random-sequence oligonucleotides: analysis of yeast GCN4 protein. *Molecular and Cellular Biology* **1989**, *9* (7), 2944-2949.

11. Ellington, A. D.; Szostak, J. W., In vitro selection of RNA molecules that bind specific ligands. *Nature* **1990**, *346* (6287), 818-822.
12. Stoltenburg, R.; Reinemann, C.; Strehlitz, B., SELEX—A (r)evolutionary method to generate high-affinity nucleic acid ligands. *Biomolecular Engineering* **2007**, *24* (4), 381-403.
13. Tataurov, A. V.; You, Y.; Owczarzy, R., Predicting ultraviolet spectrum of single stranded and double stranded deoxyribonucleic acids. *Biophysical Chemistry* **2008**, *133* (1–3), 66-70.
14. Goodchild, J., Conjugates of oligonucleotides and modified oligonucleotides: a review of their synthesis and properties. *Bioconjugate Chemistry* **1990**, *1* (3), 165-187.
15. Thuong, N. T.; Hélène, C., Sequence-Specific Recognition and Modification of Double-Helical DNA by Oligonucleotides. *Angewandte Chemie International Edition in English* **1993**, *32* (5), 666-690.
16. Verma, S.; Eckstein, F., Modified oligonucleotides: Synthesis and strategy for users. *Annu. Rev. Biochem.* **1998**, *67*, 99-134.
17. Sinkeldam, R. W.; Greco, N. J.; Tor, Y., Fluorescent Analogs of Biomolecular Building Blocks: Design, Properties, and Applications. *Chem Rev* **2010**, *110* (5), 2579-2619.
18. Bucci, E.; De Napoli, L.; Di Fabio, G.; Messere, A.; Montesarchio, D.; Romanelli, A.; Piccialli, G.; Varra, M., A new ferrocenemethyl-thymidine nucleoside: Synthesis, incorporation into oligonucleotides and optical spectroscopic studies on the resulting single strand, duplex and triplex structures. *Tetrahedron* **1999**, *55* (50), 14435-14450.

19. Sági, J.; Szemző, A.; Ébinger, K.; Szabolcs, A.; Sági, G.; Ruff, É.; Ötvös, L., Base-modified oligodeoxynucleotides. I. effect of 5-alkyl, 5-(1-alkenyl) and 5-(1-alkynyl) substitution of the pyrimidines on duplex stability and hydrophobicity. *Tetrahedron Letters* **1993**, *34* (13), 2191-2194.
20. Piccirilli, J. A.; Benner, S. A.; Krauch, T.; Moroney, S. E.; Benner, S. A., Enzymatic incorporation of a new base pair into DNA and RNA extends the genetic alphabet. *Nature* **1990**, *343* (6253), 33-37.
21. Hirao, I.; Kimoto, M.; Mitsui, T.; Fujiwara, T.; Kawai, R.; Sato, A.; Harada, Y.; Yokoyama, S., An unnatural hydrophobic base pair system: site-specific incorporation of nucleotide analogs into DNA and RNA. *Nat Meth* **2006**, *3* (9), 729-735.
22. Malyshev, D. A.; Romesberg, F. E., The Expanded Genetic Alphabet. *Angewandte Chemie International Edition* **2015**, *54* (41), 11930-11944.
23. Manoharan, M., 2'-Carbohydrate modifications in antisense oligonucleotide therapy: importance of conformation, configuration and conjugation. *Biochimica et Biophysica Acta (BBA) - Gene Structure and Expression* **1999**, *1489* (1), 117-130.
24. Yamana, K.; Iwase, R.; Furutani, S.; Tsuchida, H.; Zako, H.; Yamaoka, T.; Murakami, A., 2'-Pyrene modified oligonucleotide provides a highly sensitive fluorescent probe of RNA. *Nucleic Acids Res* **1999**, *27* (11), 2387-2392.
25. Fauster, K.; Hartl, M.; Santner, T.; Aigner, M.; Kreutz, C.; Bister, K.; Ennifar, E.; Micura, R., 2'-Azido RNA, a Versatile Tool for Chemical Biology: Synthesis, X-ray Structure, siRNA Applications, Click Labeling. *ACS Chemical Biology* **2012**, *7* (3), 581-589.
26. Wilson, C.; Keefe, A. D., Building oligonucleotide therapeutics using non-natural chemistries. *Current Opinion in Chemical Biology* **2006**, *10* (6), 607-614.

27. Lamond, A. I.; Sproat, B. S., Antisense oligonucleotides made of 2'-O-alkylRNA: their properties and applications in RNA biochemistry. *FEBS Letters* **1993**, *325* (1-2), 123-127.
28. Schöning, K.-U.; Scholz, P.; Guntha, S.; Wu, X.; Krishnamurthy, R.; Eschenmoser, A., Chemical Etiology of Nucleic Acid Structure: The  $\alpha$ -Threofuranosyl-(3'→2') Oligonucleotide System. *Science* **2000**, *290* (5495), 1347-1351.
29. Obika, S.; Nanbu, D.; Hari, Y.; Morio, K.-i.; In, Y.; Ishida, T.; Imanishi, T., Synthesis of 2'-O,4'-C-methyleneuridine and -cytidine. Novel bicyclic nucleosides having a fixed C3, -endo sugar puckering. *Tetrahedron Letters* **1997**, *38* (50), 8735-8738.
30. Zhang, L.; Peritz, A.; Meggers, E., A Simple Glycol Nucleic Acid. *J Am Chem Soc* **2005**, *127* (12), 4174-4175.
31. Wang, J.; Verbeure, B.; Luyten, I.; Lescrinier, E.; Froeyen, M.; Hendrix, C.; Rosemeyer, H.; Seela, F.; Van Aerschot, A.; Herdewijn, P., Cyclohexene Nucleic Acids (CeNA): Serum Stable Oligonucleotides that Activate RNase H and Increase Duplex Stability with Complementary RNA. *J Am Chem Soc* **2000**, *122* (36), 8595-8602.
32. Petersen, M.; Wengel, J., LNA: a versatile tool for therapeutics and genomics. *Trends in Biotechnology* **2003**, *21* (2), 74-81.
33. Fattal, E.; Barratt, G., Nanotechnologies and controlled release systems for the delivery of antisense oligonucleotides and small interfering RNA. *British Journal of Pharmacology* **2009**, *157* (2), 179-194.
34. Pinheiro, V. B.; Holliger, P., Towards XNA nanotechnology: new materials from synthetic genetic polymers. *Trends in Biotechnology* **2014**, *32* (6), 321-328.
35. Stec, W. J.; Zon, G.; Egan, W., Automated solid-phase synthesis, separation, and stereochemistry of phosphorothioate analogs of oligodeoxyribonucleotides. *J Am Chem Soc* **1984**, *106* (20), 6077-6079.

36. Agrawal, S.; Goodchild, J.; Civeira, M. P.; Thornton, A. H.; Sarin, P. S.; Zamecnik, P. C., Oligodeoxynucleoside phosphoramidates and phosphorothioates as inhibitors of human immunodeficiency virus. *Proceedings of the National Academy of Sciences* **1988**, *85* (19), 7079-7083.
37. Boczkowska, M.; Guga, P.; Stec, W. J., Stereodefined Phosphorothioate Analogues of DNA: Relative Thermodynamic Stability of the Model PS-DNA/DNA and PS-DNA/RNA Complexes. *Biochemistry* **2002**, *41* (41), 12483-12487.
38. Jung, C.; Ellington, A. D., A primerless molecular diagnostic: phosphorothioated-terminal hairpin formation and self-priming extension (PS-THSP). *Analytical and Bioanalytical Chemistry* **2016**, 1-9.
39. Nielsen, P. E.; Egholm, M.; Buchardt, O., Peptide nucleic acid (PNA). A DNA mimic with a peptide backbone. *Bioconjugate Chemistry* **1994**, *5* (1), 3-7.
40. Nielsen, P. E., Peptide Nucleic Acids (PNA) in Chemical Biology and Drug Discovery. *Chemistry & Biodiversity* **2010**, *7* (4), 786-804.
41. Totsingan, F.; Jain, V.; Bracken, W. C.; Faccini, A.; Tedeschi, T.; Marchelli, R.; Corradini, R.; Kallenbach, N. R.; Green, M. M., Conformational Heterogeneity in PNA:PNA Duplexes. *Macromolecules* **2010**, *43* (6), 2692-2703.
42. Yeh, J. I.; Shivachev, B.; Rapireddy, S.; Crawford, M. J.; Gil, R. R.; Du, S.; Madrid, M.; Ly, D. H., Crystal Structure of Chiral  $\gamma$ PNA with Complementary DNA Strand: Insights into the Stability and Specificity of Recognition and Conformational Preorganization. *J Am Chem Soc* **2010**, *132* (31), 10717-10727.
43. Beaucage, S. L.; Iyer, R. P., Advances in the Synthesis of Oligonucleotides by the Phosphoramidite Approach. *Tetrahedron* **1992**, *48* (12), 2223-2311.

44. Zatsepin, T.; Stetsenko D. A.; Gait, M. J.; Oretskaya, T. S. Use of Carbonyl Group Addition–Elimination Reactions for Synthesis of Nucleic Acid Conjugates. *Bioconjugate Chem.*, **2005**, *16* (3), pp 471–489.
45. Michelson, A. M.; Todd, A. R., Nucleotides part XXXII. Synthesis of a dithymidine dinucleotide containing a 3': 5'-internucleotidic linkage. *Journal of the Chemical Society* **1955**, (0), 2632-2638.
46. Gilham, P. T.; Khorana, H. G., Studies on Polynucleotides. I. A New and General Method for the Chemical Synthesis of the C5''-C3'' Internucleotidic Linkage. Syntheses of Deoxyribo-dinucleotides1. *J Am Chem Soc* **1958**, *80* (23), 6212-6222.
47. Letsinger, R. L.; Ogilvie, K. K., Nucleotide chemistry. XIII. Synthesis of oligothymidylates via phosphotriester intermediates. *J Am Chem Soc* **1969**, *91* (12), 3350-3355.
48. Letsinger, R. L.; Finnan, J. L.; Heavner, G. A.; Lunsford, W. B., Nucleotide chemistry. XX. Phosphite coupling procedure for generating internucleotide links. *J Am Chem Soc* **1975**, *97* (11), 3278-3279.
49. Beaucage, S. L.; Caruthers, M. H., Deoxynucleoside phosphoramidites—A new class of key intermediates for deoxypolynucleotide synthesis. *Tetrahedron Letters* **1981**, *22* (20), 1859-1862.
50. Ogilvie, K. K.; Theriault, N.; Sadana, K. L., Synthesis of oligoribonucleotides. *J Am Chem Soc* **1977**, *99* (23), 7741-7743.
51. Pitsch, S.; Weiss, P. A.; Xu, X. L.; Ackermann, D.; Honegger, T., Fast and reliable automated synthesis of RNA and partially 2'-O-protected precursors ('caged RNA') based on two novel, orthogonal 2'-O-protecting groups. *Helv Chim Acta* **1999**, *82* (10), 1753-1761.

52. Burgess, K.; Cook, D., Syntheses of Nucleoside Triphosphates. *Chem Rev* **2000**, *100* (6), 2047-2060.
53. Borsenberger, V.; Kukwikila, M.; Howorka, S., Synthesis and enzymatic incorporation of modified deoxyuridine triphosphates. *Organic & Biomolecular Chemistry* **2009**, *7* (18), 3826-3835.
54. Smith, L. M.; Sanders, J. Z.; Kaiser, R. J.; Hughes, P.; Dodd, C.; Connell, C. R.; Heiner, C.; Kent, S. B. H.; Hood, L. E., Fluorescence detection in automated DNA sequence analysis. *Nature* **1986**, *321* (6071), 674-679.
55. Sanger, F.; Nicklen, S.; Coulson, A. R., DNA sequencing with chain-terminating inhibitors. *Proceedings of the National Academy of Sciences* **1977**, *74* (12), 5463-5467.
56. Malyshev, D. A.; Dhami, K.; Lavergne, T.; Chen, T.; Dai, N.; Foster, J. M.; Correa, I. R.; Romesberg, F. E., A semi-synthetic organism with an expanded genetic alphabet. *Nature* **2014**, *509* (7500), 385-388.
57. Veedu, R. N.; Vester, B.; Wengel, J., Polymerase directed incorporation studies of LNA-G nucleoside 5[prime or minute]-triphosphate and primer extension involving all four LNA nucleotides. *New Journal of Chemistry* **2010**, *34* (5), 877-879.
58. Yu, H.; Zhang, S.; Chaput, J. C., Darwinian evolution of an alternative genetic system provides support for TNA as an RNA progenitor. *Nat Chem* **2012**, *4* (3), 183-187.
59. Image from Wikipedia.
60. Jäger, S.; Rasched, G.; Kornreich-Leshem, H.; Engeser, M.; Thum, O.; Famulok, M., A Versatile Toolbox for Variable DNA Functionalization at High Density. *J Am Chem Soc* **2005**, *127* (43), 15071-15082.



61. Ono, A.; Haginoya, N.; Kiyokawa, M.; Minakawa, N.; Matsuda, A., Nucleosides and nucleotides. 127. A novel and convenient post-synthetic modification method for the synthesis of oligodeoxyribonucleotides carrying amino linkers at the 5-position of 2'-deoxyuridine. *Bioorganic & Medicinal Chemistry Letters* **1994**, *4* (2), 361-366.
62. Gramlich, P. M. E.; Wirges, C. T.; Manetto, A.; Carell, T., Postsynthetic DNA Modification through the Copper-Catalyzed Azide-Alkyne Cycloaddition Reaction. *Angewandte Chemie International Edition* **2008**, *47* (44), 8350-8358.
63. Ghosh, S. S.; Kao, P. M.; McCue, A. W.; Chappelle, H. L., Use of maleimide-thiol coupling chemistry for efficient syntheses of oligonucleotide-enzyme conjugate hybridization probes. *Bioconjugate Chemistry* **1990**, *1* (1), 71-76.
64. Herne, T. M.; Tarlov, M. J., Characterization of DNA Probes Immobilized on Gold Surfaces. *J Am Chem Soc* **1997**, *119* (38), 8916-8920.
65. Zhang, Y.; Zhang, K.; Ma, H., Electrochemical DNA biosensor based on silver nanoparticles/poly(3-(3-pyridyl) acrylic acid)/carbon nanotubes modified electrode. *Analytical Biochemistry* **2009**, *387* (1), 13-19.
66. Richardson, C. C., Phosphorylation of nucleic acid by an enzyme from T4 bacteriophage-infected Escherichia coli. *P Natl Acad Sci USA* **1965**, *54* (1), 158-165.
67. Kim, E. E.; Wyckoff, H. W., Reaction mechanism of alkaline phosphatase based on crystal structures. *J Mol Biol* **1991**, *218* (2), 449-464.
68. Pascal, J. M.; O'Brien, P. J.; Tomkinson, A. E.; Ellenberger, T., Human DNA ligase I completely encircles and partially unwinds nicked DNA. *Nature* **2004**, *432* (7016), 473-478.
69. Paredes, E.; Evans, M.; Das, S. R., RNA labeling, conjugation and ligation. *Methods* **2011**, *54* (2), 251-259.

70. Hili, R.; Niu, J.; Liu, D. R., DNA Ligase-Mediated Translation of DNA Into Densely Functionalized Nucleic Acid Polymers. *J Am Chem Soc* **2013**, *135* (1), 98-101.
71. Schena, M.; Shalon, D.; Davis, R. W.; Brown, P. O., Quantitative Monitoring of Gene Expression Patterns with a Complementary DNA Microarray. *Science* **1995**, *270* (5235), 467-470.
72. Cosnier, S.; Mailley, P., Recent advances in DNA sensors. *Analyst* **2008**, *133* (8), 984-991.
73. Neuhaus-Url, G.; Neuhaus, G., The use of the nonradioactive digoxigenin chemiluminescent technology for plant genomic Southern blot hybridization: A comparison with radioactivity. *Transgenic Research* **1993**, *2* (2), 115-120.
74. Tyagi, S.; Kramer, F. R., Molecular Beacons: Probes that Fluoresce upon Hybridization. *Nat Biotech* **1996**, *14* (3), 303-308.
75. Nelson, B. P.; Grimsrud, T. E.; Liles, M. R.; Goodman, R. M.; Corn, R. M., Surface Plasmon Resonance Imaging Measurements of DNA and RNA Hybridization Adsorption onto DNA Microarrays. *Anal Chem* **2001**, *73* (1), 1-7.
76. Elghanian, R.; Storhoff, J. J.; Mucic, R. C.; Letsinger, R. L.; Mirkin, C. A., Selective Colorimetric Detection of Polynucleotides Based on the Distance-Dependent Optical Properties of Gold Nanoparticles. *Science* **1997**, *277* (5329), 1078-1081.
77. Gao, Z.; Agarwal, A.; Trigg, A. D.; Singh, N.; Fang, C.; Tung, C.-H.; Fan, Y.; Buddharaju, K. D.; Kong, J., Silicon Nanowire Arrays for Label-Free Detection of DNA. *Anal Chem* **2007**, *79* (9), 3291-3297.
78. Harris, D. C., *Quantitative chemical analysis*. 7th ed.; W.H. Freeman and Co.: New York, NY, 2007; p 1 v.
79. Drummond, T. G.; Hill, M. G.; Barton, J. K., Electrochemical DNA sensors. *Nat Biotechnol* **2003**, *21* (10), 1192-1199.

80. Fan, C.; Plaxco, K. W.; Heeger, A. J., Electrochemical interrogation of conformational changes as a reagentless method for the sequence-specific detection of DNA. *Proceedings of the National Academy of Sciences* **2003**, *100* (16), 9134-9137.
81. Jia, X.; Dong, S.; Wang, E., Engineering the bioelectrochemical interface using functional nanomaterials and microchip technique toward sensitive and portable electrochemical biosensors. *Biosensors and Bioelectronics* **2016**, *76*, 80-90.
82. Palecek, E., Adsorptive Transfer Stripping Voltammetry - Determination of Nanogram Quantities of DNA Immobilized at the Electrode Surface. *Analytical Biochemistry* **1988**, *170* (2), 421-431.
83. Yang, I. V.; Thorp, H. H., Modification of Indium Tin Oxide Electrodes with Repeat Polynucleotides: Electrochemical Detection of Trinucleotide Repeat Expansion. *Anal Chem* **2001**, *73* (21), 5316-5322.
84. Deféver, T.; Druet, M.; Rochelet-Dequaire, M.; Joannes, M.; Grossiord, C.; Limoges, B.; Marchal, D., Real-Time Electrochemical Monitoring of the Polymerase Chain Reaction by Mediated Redox Catalysis. *J Am Chem Soc* **2009**, *131* (32), 11433-11441.
85. Sassolas, A.; Leca-Bouvier, B. D.; Blum, L. J., DNA Biosensors and Microarrays. *Chem Rev* **2008**, *108* (1), 109-139.
86. Wang, J., Carbon-Nanotube Based Electrochemical Biosensors: A Review. *Electroanalysis* **2005**, *17* (1), 7-14.
87. Williams, T. T.; Dohno, C.; Stemp, E. D. A.; Barton, J. K., Effects of the Photooxidant on DNA-Mediated Charge Transport. *J Am Chem Soc* **2004**, *126* (26), 8148-8158.

88. Wilkinson, G.; Rosenblum, M.; Whiting, M. C.; Woodward, R. B., THE STRUCTURE OF IRON BIS-CYCLOPENTADIENYL. *J Am Chem Soc* **1952**, *74* (8), 2125-2126.
89. Yu, C. J.; Yowanto, H.; Wan, Y.; Meade, T. J.; Chong, Y.; Strong, M.; Donilon, L. H.; Kayyem, J. F.; Gozin, M.; Blackburn, G. F., Uridine-Conjugated Ferrocene DNA Oligonucleotides: Unexpected Cyclization Reaction of the Uridine Base. *J Am Chem Soc* **2000**, *122* (28), 6767-6768.
90. Tolman, C. A., The 16 and 18 electron rule in organometallic chemistry and homogeneous catalysis. *Chemical Society Reviews* **1972**, *1* (3), 337-353.
91. Rinehart, K. L.; Motz, K. L.; Moon, S., Organic Chemistry of Ferrocene. I. The Acetylation of Dialkylferrocenes<sup>1</sup>. *J Am Chem Soc* **1957**, *79* (11), 2749-2754.
92. Cunningham, A. F., Friedel-Crafts acetylation of bis(trimethylsilyl)- and bis(tributylstannyl)ferrocene: implications on the mechanisms of acylation and proton exchange of ferrocene derivatives. *J Am Chem Soc* **1991**, *113* (13), 4864-4870.
93. Rosenblum, M.; Santer, J. O.; Howells, W. G., The Chemistry and Structure of Ferrocene. VIII. Interannular Resonance and the Mechanism of Electrophilic Substitution. *J. Am. Chem. Soc.*, **1963**, *85* (10), 1450–1458.
94. Masaru, S.; Hiromichi, K.; Mikio, S.; Izumi, M.; Kazuo, H., A Simple Modification of Vilsmeier Method for the Preparation of Formylferrocene. *B Chem Soc Jpn* **1968**, *41* (1), 252-252.
95. Grubert, H.; Rinehart, K. L., Nitroferrocene. *Tetrahedron Letters* **1959**, *1* (12), 16-17.
96. Rebiere, F.; Samuel, O.; Kagan, H. B., A convenient method for the preparation of monolithioferrocene. *Tetrahedron Letters* **1990**, *31* (22), 3121-3124.

97. Atkinson, R. C. J.; Gibson, V. C.; Long, N. J., The syntheses and catalytic applications of unsymmetrical ferrocene ligands. *Chemical Society Reviews* **2004**, 33 (5), 313-328.
98. Nieto, D.; Bruña, S.; González-Vadillo, A. M.; Perles, J.; Carrillo-Hermosilla, F.; Antiñolo, A.; Padrón, J. M.; Plata, G. B.; Cuadrado, I., Catalytically Generated Ferrocene-Containing Guanidines as Efficient Precursors for New Redox-Active Heterometallic Platinum(II) Complexes with Anticancer Activity. *Organometallics* **2015**, 34 (22), 5407-5417.
99. Wedeking, K.; Mu, Z.; Kehr, G.; Cano Sierra, J.; Mück Lichtenfeld, C.; Grimme, S.; Erker, G.; Fröhlich, R.; Chi, L.; Wang, W.; Zhong, D.; Fuchs, H., Oligoethylene Chains Terminated by Ferrocenyl End Groups: Synthesis, Structural Properties, and Two-Dimensional Self-Assembly on Surfaces. *Chemistry – A European Journal* **2006**, 12 (6), 1618-1628.
100. McCulloch, B.; Ward, D. L.; Woollins, J. D.; Brubaker, C. H., Ferrocenyl sulfides. Preparation and reactivity as bidentate chelating ligands. *Organometallics* **1985**, 4 (8), 1425-1432.
101. Lenze, N.; Neumann, B.; Salmon, A.; Stammer, A.; Stammer, H.-G.; Jutzi, P., Multiply trimethylstannyl substituted ferrocenes synthesis, NMR studies, X-ray structural analysis and electrochemistry. *Journal of Organometallic Chemistry* **2001**, 619 (1-2), 74-87.
102. Sadeh, S.; Bhattacharjee, H.; Khozeimeh Sarbisheh, E.; Quail, J. W.; Müller, J., Chiral Bora[1]ferrocenophanes: Syntheses, Mechanistic Insights, and Ring-Opening Polymerizations. *Chemistry – A European Journal* **2014**, 20 (49), 16320-16330.
103. Connelly, N. G.; Geiger, W. E., Chemical Redox Agents for Organometallic Chemistry. *Chem Rev* **1996**, 96 (2), 877-910.

104. Coutouli-Argyropoulou, E.; Kelaidopoulou, A.; Sideris, C.; Kokkinidis, G., Electrochemical studies of ferrocene derivatives and their complexation by  $\beta$ -cyclodextrin. *Journal of Electroanalytical Chemistry* **1999**, 477 (2), 130-139.
105. Gritzner, G.; Kuta, J., Recommendations on Reporting Electrode-Potentials in Nonaqueous Solvents (Recommendations 1983). *Pure Appl Chem* **1984**, 56 (4), 461-466.
106. Löffler, U.; Wiemhöfer, H. D.; Göpel, W., Amperometric biosensors: characterization of dispersed mediator systems. *Biosensors and Bioelectronics* **1991**, 6 (4), 343-352.
107. Chen, C. J.; Liu, C. C.; Savinell, R. F., Polymeric redox mediator enzyme electrodes for anaerobic glucose monitoring. *Journal of Electroanalytical Chemistry* **1993**, 348 (1), 317-338.
108. Hodak, J.; Etchenique, R.; Calvo, E. J.; Singhal, K.; Bartlett, P. N., Layer-by-Layer Self-Assembly of Glucose Oxidase with a Poly(allylamine)ferrocene Redox Mediator. *Langmuir* **1997**, 13 (10), 2708-2716.
109. Kobayashi, Y.; Hoshi, T.; Anzai, J.-i., Glucose and Lactate Biosensors Prepared by a Layer-by-Layer Deposition of Concanavalin A and Mannose-Labeled Enzymes: Electrochemical Response in the Presence of Electron Mediators. *Chemical and Pharmaceutical Bulletin* **2001**, 49 (6), 755-757.
110. Daeneke, T.; Mozer, A. J.; Kwon, T.-H.; Duffy, N. W.; Holmes, A. B.; Bach, U.; Spiccia, L., Dye regeneration and charge recombination in dye-sensitized solar cells with ferrocene derivatives as redox mediators. *Energy & Environmental Science* **2012**, 5 (5), 7090-7099.

111. Daeneke, T.; Kwon, T.-H.; Holmes, A. B.; Duffy, N. W.; Bach, U.; Spiccia, L., High-efficiency dye-sensitized solar cells with ferrocene-based electrolytes. *Nat Chem* **2011**, *3* (3), 211-215.
112. Matsue, T.; Evans, D. H.; Osa, T.; Kobayashi, N., Electron-transfer reactions associated with host-guest complexation. Oxidation of ferrocenecarboxylic acid in the presence of .beta.-cyclodextrin. *J Am Chem Soc* **1985**, *107* (12), 3411-3417.
113. Cui, L.; Gadde, S.; Li, W.; Kaifer, A. E., Electrochemistry of the Inclusion Complexes Formed Between the Cucurbit[7]uril Host and Several Cationic and Neutral Ferrocene Derivatives†Part of the “Langmuir 25th Year: Molecular and macromolecular self-assemblies” special issue. *Langmuir* **2009**, *25* (24), 13763-13769.
114. Osella, D.; Carretta, A.; Nervi, C.; Ravera, M.; Gobetto, R., Inclusion Complexes of Ferrocenes and  $\beta$ -Cyclodextrins. Critical Appraisal of the Electrochemical Evaluation of Formation Constants. *Organometallics* **2000**, *19* (14), 2791-2797.
115. Yan, Q.; Feng, A.; Zhang, H.; Yin, Y.; Yuan, J., Redox-switchable supramolecular polymers for responsive self-healing nanofibers in water. *Polymer Chemistry* **2013**, *4* (4), 1216-1220.
116. Nakahata, M.; Takashima, Y.; Hashidzume, A.; Harada, A., Redox-Generated Mechanical Motion of a Supramolecular Polymeric Actuator Based on Host–Guest Interactions. *Angewandte Chemie International Edition* **2013**, *52* (22), 5731-5735.
117. Nakahata, M.; Takashima, Y.; Yamaguchi, H.; Harada, A., Redox-responsive self-healing materials formed from host–guest polymers. *Nature Communications* **2011**, *2*, 511.
118. Assaf, K. I.; Nau, W. M., Cucurbiturils: from synthesis to high-affinity binding and catalysis. *Chemical Society Reviews* **2015**, *44* (2), 394-418.

119. Kelley, S. O.; Boon, E. M.; Barton, J. K.; Jackson, N. M.; Hill, M. G., Single-base mismatch detection based on charge transduction through DNA. *Nucleic Acids Res* **1999**, 27 (24), 4830-4837.
120. Michaelis, L.; Schubert, M. P.; Granick, S., Semiquinone Radicals of the Thiazines. *J Am Chem Soc* **1940**, 62 (1), 204-211.
121. Wainwright, M.; Giddens, R. M., Phenothiazinium photosensitisers: choices in synthesis and application. *Dyes and Pigments* **2003**, 57 (3), 245-257.
122. De Crozals, G.; Farre, C.; Sigaud, M.; Fortgang, P.; Sanglar, C.; Chaix, C., Methylene blue phosphoramidite for DNA labelling. *Chemical Communications* **2015**, 51 (21), 4458-4461.
123. Pheeney, C. G.; Barton, J. K., DNA Electrochemistry with Tethered Methylene Blue. *Langmuir* **2012**, 28 (17), 7063-7070.
124. Mills, A.; Lawrie, K.; McFarlane, M., Blue bottle light: lecture demonstrations of homogeneous and heterogeneous photo-induced electron transfer reactions. *Photochemical & Photobiological Sciences* **2009**, 8 (3), 421-425.
125. Fernandez, J. M.; Bilgin, M. D.; Grossweiner, L. I., Singlet oxygen generation by photodynamic agents. *Journal of Photochemistry and Photobiology B: Biology* **1997**, 37 (1), 131-140.
126. Smith, J. P.; Schrock, A. K.; Schuster, G. B., Chemiluminescence of organic peroxides. Thermal generation of an o-xylylene peroxide. *J Am Chem Soc* **1982**, 104 (4), 1041-1047.
127. Malik, M. A., Water Purification by Plasmas: Which Reactors are Most Energy Efficient? *Plasma Chemistry and Plasma Processing* **2010**, 30 (1), 21-31.



128. Pretlow, T. P.; Barrow, B. J.; Ashton, W. S.; O'Riordan, M. A.; Pretlow, T. G.; Jurecsek, J. A.; Stellato, T. A., Aberrant Crypts: Putative Preneoplastic Foci in Human Colonic Mucosa. *Cancer Research* **1991**, *51* (5), 1564-1567.
129. Armour, J. A.; Murphy, D. A.; Yuan, B. X.; MacDonald, S.; Hopkins, D. A., Gross and microscopic anatomy of the human intrinsic cardiac nervous system. *Anat Rec* **1997**, *247* (2), 289-298.
130. Wagner, S. J.; Skripchenko, A.; Pugh, J. C.; Suchmann, D. B.; Ijaz, M. K., Duck hepatitis B photoinactivation by dimethylmethylene blue in RBC suspensions. *Transfusion* **2001**, *41* (9), 1154-1158.
131. Papin, J. F.; Floyd, R. A.; Dittmer, D. P., Methylene blue photoinactivation abolishes West Nile virus infectivity in vivo. *Antiviral Research* **2005**, *68* (2), 84-87.
132. Ihara, T.; Nakayama, M.; Murata, M.; Nakano, K.; Maeda, M., Gene sensor using ferrocenyl oligonucleotide. *Chemical Communications* **1997**, (17), 1609-1610.
133. Kang, D.; Zuo, X.; Yang, R.; Xia, F.; Plaxco, K. W.; White, R. J., Comparing the Properties of Electrochemical-Based DNA Sensors Employing Different Redox Tags. *Anal Chem* **2009**, *81* (21), 9109-9113.
134. Lubin, A. A.; Plaxco, K. W., Folding-Based Electrochemical Biosensors: The Case for Responsive Nucleic Acid Architectures. *Accounts of Chemical Research* **2010**, *43* (4), 496-505.
135. Xuan, F.; Luo, X.; Hsing, I. M., Sensitive immobilization-free electrochemical DNA sensor based on isothermal circular strand displacement polymerization reaction. *Biosensors and Bioelectronics* **2012**, *35* (1), 230-234.
136. Qian, Y.; Tang, D.; Du, L.; Zhang, Y.; Zhang, L.; Gao, F., A novel signal-on electrochemical DNA sensor based on target catalyzed hairpin assembly strategy. *Biosensors and Bioelectronics* **2015**, *64*, 177-181.

137. Li, B.; Ellington, A. D.; Chen, X., Rational, modular adaptation of enzyme-free DNA circuits to multiple detection methods. *Nucleic Acids Res* **2011**.
138. Yeung, S. S. W.; Lee, T. M. H.; Hsing, I. M., Electrochemical Real-Time Polymerase Chain Reaction. *J Am Chem Soc* **2006**, *128* (41), 13374-13375.
139. Aoki, H.; Kitajima, A.; Tao, H., Label-free and 'signal-on' DNA detection using a probe DNA terminated with ferrocene and  $\beta$ -cyclodextrin. *Supramolecular Chemistry* **2010**, *22* (7-8), 455-460.
140. Xiao, Y.; Lubin, A. A.; Heeger, A. J.; Plaxco, K. W., Label-Free Electronic Detection of Thrombin in Blood Serum by Using an Aptamer-Based Sensor. *Angewandte Chemie International Edition* **2005**, *44* (34), 5456-5459.
141. Baker, B. R.; Lai, R. Y.; Wood, M. S.; Doctor, E. H.; Heeger, A. J.; Plaxco, K. W., An Electronic, Aptamer-Based Small-Molecule Sensor for the Rapid, Label-Free Detection of Cocaine in Adulterated Samples and Biological Fluids. *J Am Chem Soc* **2006**, *128* (10), 3138-3139.
142. Ferguson, B. S.; Hoggarth, D. A.; Maliniak, D.; Ploense, K.; White, R. J.; Woodward, N.; Hsieh, K.; Bonham, A. J.; Eisenstein, M.; Kippin, T. E.; Plaxco, K. W.; Soh, H. T., Real-Time, Aptamer-Based Tracking of Circulating Therapeutic Agents in Living Animals. *Science Translational Medicine* **2013**, *5* (213), 213ra165-213ra165.
143. Rowe, A. A.; Miller, E. A.; Plaxco, K. W., Reagentless Measurement of Aminoglycoside Antibiotics in Blood Serum via an Electrochemical, Ribonucleic Acid Aptamer-Based Biosensor. *Anal Chem* **2010**, *82* (17), 7090-7095.
144. Liu, H.-K.; Sadler, P. J., Metal Complexes as DNA Intercalators. *Accounts of Chemical Research* **2011**, *44* (5), 349-359.

145. Wang, M.; Yu, Y.; Liang, C.; Lu, A.; Zhang, G., Recent Advances in Developing Small Molecules Targeting Nucleic Acid. *International Journal of Molecular Sciences* **2016**, *17* (6), 779.
146. Waring, M. J., Complex formation between ethidium bromide and nucleic acids. *J Mol Biol* **1965**, *13* (1), 269-282.
147. Latt, S. A.; Stetten, G., Spectral studies on 33258 Hoechst and related bisbenzimidazole dyes useful for fluorescent detection of deoxyribonucleic acid synthesis. *Journal of Histochemistry & Cytochemistry* **1976**, *24* (1), 24-33.
148. Tuite, E.; Norden, B., Sequence-Specific Interactions of Methylene Blue with Polynucleotides and DNA: A Spectroscopic Study. *J Am Chem Soc* **1994**, *116* (17), 7548-7556.
149. Kelley, S. O.; Barton, J. K.; Jackson, N. M.; Hill, M. G., Electrochemistry of Methylene Blue Bound to a DNA-Modified Electrode. *Bioconjugate Chemistry* **1997**, *8* (1), 31-37.
150. Lin, Y.-J.; Wu, Y.-C.; Mani, V.; Huang, S.-T.; Huang, C.-H.; Hu, Y.-C.; Peter Shan, H.-C., Designing anthraquinone–pyrrole redox intercalating probes for electrochemical gene detection. *Biosensors and Bioelectronics* **2016**, *79*, 294-299.
151. Hall, D. B.; Barton, J. K., Sensitivity of DNA-Mediated Electron Transfer to the Intervening  $\pi$ -Stack: A Probe for the Integrity of the DNA Base Stack. *J Am Chem Soc* **1997**, *119* (21), 5045-5046.
152. Stinner, C.; Wightman, M. D.; Kelley, S. O.; Hill, M. G.; Barton, J. K., Synthesis and Spectroelectrochemistry of Ir(bpy)(phen)(phi)<sub>3</sub><sup>+</sup>, a Tris(heteroleptic) Metallointercalator. *Inorg Chem* **2001**, *40* (20), 5245-5250.
153. Hvastkovs, E. G.; Buttry, D. A., Minor Groove Binding of a Novel Tetracationic Diviologen. *Langmuir* **2006**, *22* (25), 10821-10829.

154. Du, Y.; Lim, B. J.; Li, B.; Jiang, Y. S.; Sessler, J. L.; Ellington, A. D., Reagentless, Ratiometric Electrochemical DNA Sensors with Improved Robustness and Reproducibility. *Anal Chem* **2014**, 86 (15), 8010-8016.

## **Chapter 2: Synthesis of multiplexing electrochemical DNA sensors based on a combination of various ferrocene derivatives**

### **2.1 INTRODUCTION**

Electrochemical DNA sensors, so-called “E-sensors”, have been utilized as a platform for molecular sensing due to their high sensitivity, low cost, and wide versatility (Figure 2.1).<sup>1-2</sup> A conformational change triggered by hybridization or other interactions between a target molecule and a probe DNA strand results in a change in the electrochemical signal from the covalently-linked redox-active functional groups on the modified probe DNA. In terms of sensitivity and robustness, it is necessary to choose a proper redox “tag” to incorporate in E-sensor DNA so as to induce effective electron transfer. Thus, researchers have applied many electrochemically active compounds to create modified DNA oligonucleotides, including methylene blue (MB),<sup>3</sup> ferrocene (Fc),<sup>4</sup> anthraquinone (AQ),<sup>5</sup> and tris(bipyridine)ruthenium(II) (Ru(bpy)<sub>3</sub>).<sup>6</sup> Among them, MB has been used as the major covalent tag for E-sensors, especially in recent studies conducted by Plaxco’s group.<sup>7-8</sup> It is attractive due to its reversible electrochemical characteristic, moderate redox potential, and commercial availability.<sup>3</sup> Despite these advantages, MB is not an optimal redox probe for the construction of more elaborate systems that might allow simultaneous detection of multi targets with differentiated signals. This because MB is hard to modify so as to tailor its redox potential value. Since syntheses of MB derivatives are laborious and limited to simple modification on the dimethylamino group present in the molecule,<sup>9</sup> this results the MB-modified E-sensors have fixed potentials around -200 mV (vs Ag/AgCl).<sup>3</sup> As a result, they act like a “monochromic” sensors.

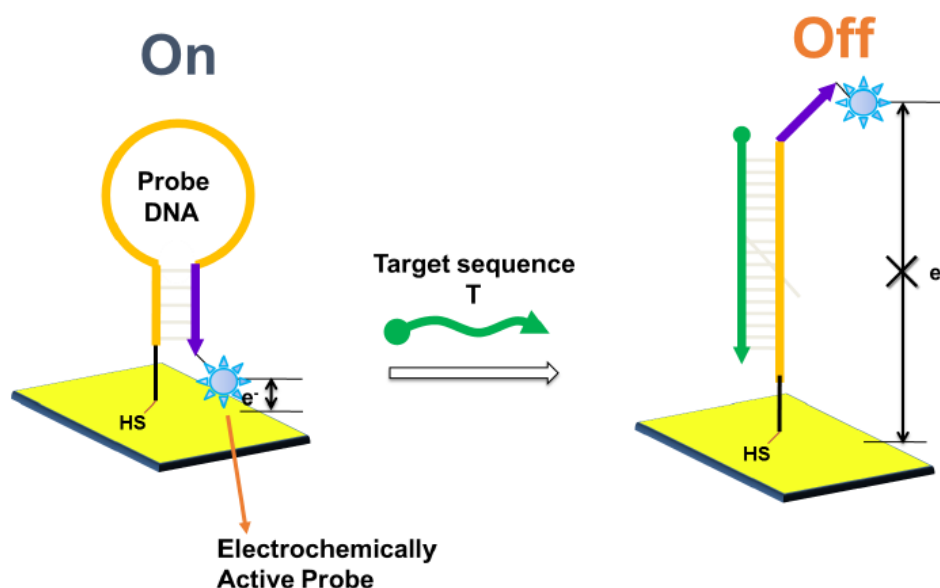


**Figure 2.1** Schematic illustration of E-Sensor.

Compared with MB, it is relatively easy to modulate the oxidation potential of ferrocene, which is another major redox probe used in electrochemical analyses. Ferrocene is a stable and robust organometallic compound that contains a Fe(II) ion sandwiched between two aromatic cyclopentadiene rings.<sup>10</sup> It is formally an 18-electron complex. Although it is stable such under ambient conditions, ferrocene also undergoes typical chemical reactions, such as conventional aromatic compounds. This allows the attachment of various functional groups via simple transformations. For example, a number of electrophilic aromatic substitutions and metalation reactions of ferrocene are reported.<sup>11-13</sup> Furthermore, the reacting synthesized ferrocene derivatives have various redox potentials as a result of the perturbation of the electron density on the ferrocene core.<sup>14</sup> This adjustment bears analogy to the variation of the emission wavelength of fluorophores via the attachment of various functional groups. To achieve the potential variations in the case of ferrocene, electron donation group (EDG) or electron withdrawing groups (EWG) can

be appended to the ferrocene core.<sup>15</sup> It is also possible to predict how much the potential of the new molecules will deviate from the standard potential of unfunctionalized ferrocene (i.e.  $E_{1/2}$  = 400 mV in DCM) (Figure 2.2).

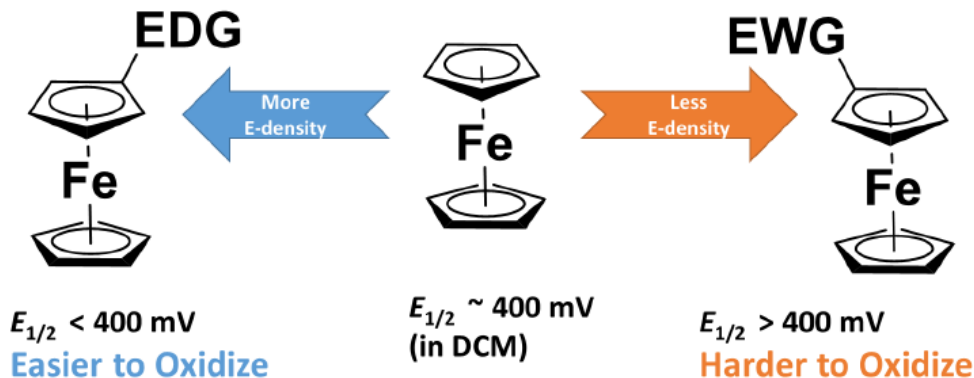


**Figure 2.2** Modulation of redox potential of ferrocene via the incorporation of EDGs and EWGs

In this chapter, the author describes synthesis of ferrocene derivatives with various redox potentials as electrochemical probes for use in E-sensors. The synthesized compounds were also incorporated in chemically synthesized oligonucleotides for multiple target under conditions of parallel detection. We also expected to apply the synthesized oligonucleotides to other applications, including single nucleotide polymorphism (SNP) and electrochemical genetic sequencing. With these objectives in mind, we synthesized several ferrocene-embedded terminal alkynes, nucleosides, and nucleoside phosphoramidites. These were then used to prepare oligonucleotides via automated solid-phase synthesis. The potential utility of the oligonucleotides was then tested by means of voltammetric assays, including cyclic voltammetry (CV) and square wave voltammetry

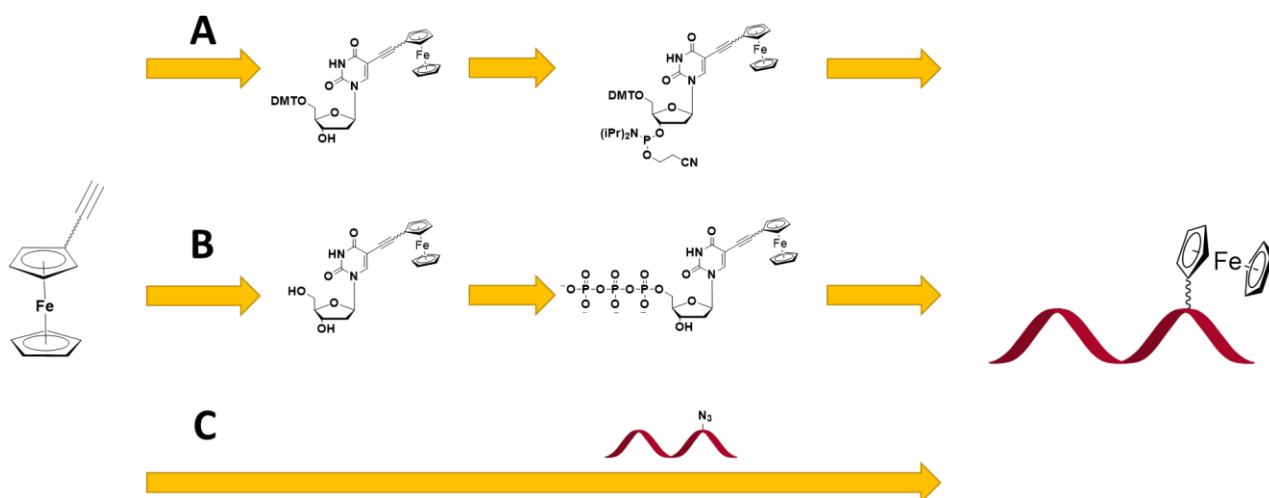
(SWV). Complementary, involving the incorporation of ferrocene probes into oligonucleotides via post-synthetic or enzymatic methods are currently in progress.

## **2.2 RESULT AND DISCUSSION**

### **2.2.1 Design of Ferrocene derivatives with terminal alkynes**

To attach the ferrocene derivatives to oligonucleotides, we chose a terminal alkyne group as a functional linker on the ferrocene (Figure 2.3). These alkynes can be utilized as a linker in two major conjugation methods, Sonogashira coupling,<sup>16</sup> and copper (I)-catalyzed azide-alkyne cycloaddition reaction (CuAAC, or click chemistry).<sup>17</sup> Using these conjugation methods, nucleotides can be modified with the ferrocene derivatives before or after preparing of the oligonucleotides. Bases with functionality attached via an alkyne linker generally enzymatically compatible.<sup>18</sup> It means they can be incorporated into oligonucleotides to create modified NTPs via enzymatic oligonucleotide synthesis. Finally, an alkyne bond is linear, minimizing any effects on the secondary structures of the desired oligonucleotides.

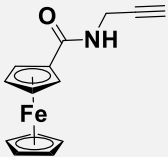
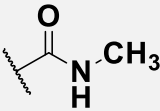
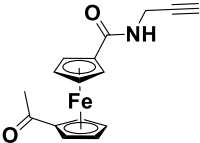
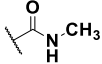
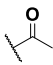
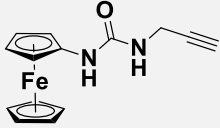
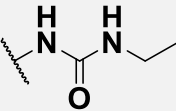
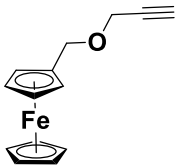
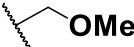




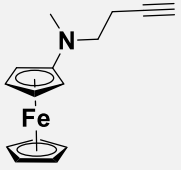
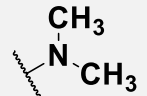
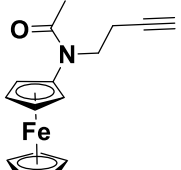
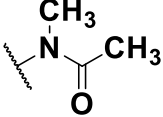
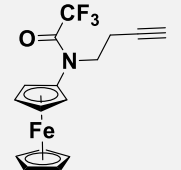
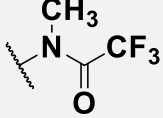
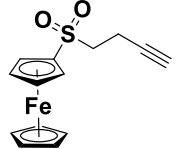
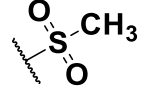
**Figure 2.3** Design of the ferrocene probes and pathway leading to modified oligonucleotides. A) Chemical synthesis, B) enzymatic synthesis, and C) post-synthetic modification strategies for the incorporation of a ferrocene subunit into oligonucleotide

At first, eight functional groups were chosen to vary the electron density of the ferrocene core. These ferrocene derivatives are shown in Table 2.1. Each functional group is also expected to be easily attached to the ferrocene core via with alkyne linker under simple reaction conditions. To predict the difference in the electrochemical potential caused by each attachment, we consulted the Hammett constants for the corresponding functional groups in the literature.<sup>19</sup> The Hammett constants used correspond to the change in the pKa values of benzoic acid bearing the functional groups of interests. However, we assumed that the basic trends are also applicable to predicting the electron density difference of ferrocenes due to the aromaticity of both molecules. On the basis of the Hammett constants, the redox potential of the ferrocene derivatives 2.1-2.8 were selected for the actual synthesis.

**Table 2.1** Eight ferrocene derivatives considered for study. The structure, corresponding functional group used to apply the Hammett constants ( $\sigma_m$  and  $\sigma_p$ ), measured oxidation potential ( $E_{1/2} = (E_{pc} + E_{pa})/2$ ), and the difference between the two peak potentials ( $\Delta E_p = |E_{pc} - E_{pa}|$ ) are also included in this table.

Compound	Structure	Functional group	$\sigma_m$	$\sigma_p$	$E_{1/2}$ (mV)	$\Delta E$ (mV)
2.1			0.35	0.36	660	91
2.2 <sup>a</sup>		 	0.73	0.86	890	100
2.3			0.04	-0.26	270	81
2.4			0.08	-0.07	470	89

(Table 2.1 Continued)

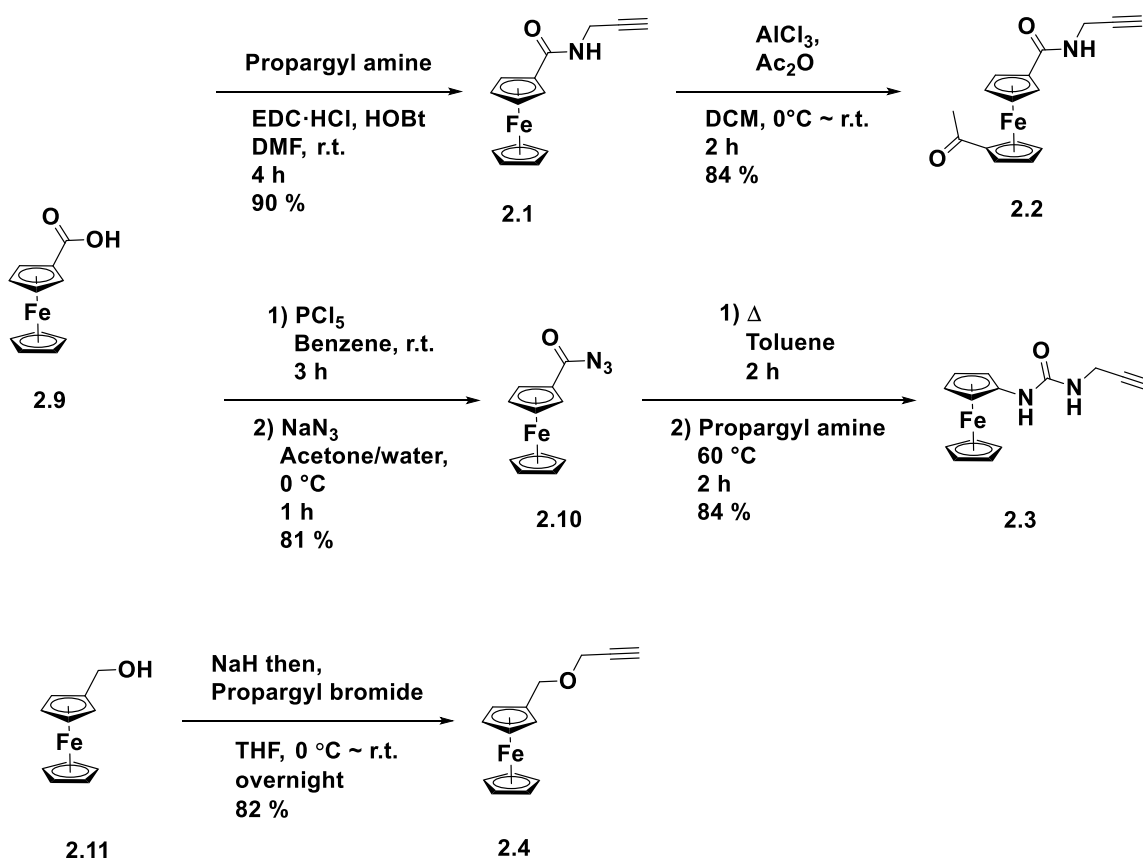
Compound	Structure	Functional group	$\sigma_m$	$\sigma_p$	$E_{1/2}$ (mV)	$\Delta E$ (mV)
2.5			-0.16	-0.83	80	83
2.6			0.21	0.00	450	97
2.7			0.41	0.39	630	86
2.8			0.60	0.72	840	146

a. The constants were derived from the sum of the two functional groups.

### 2.2.2 Synthesis of ferrocene derivatives with terminal alkynes

The ferrocene **2.1** – **2.8** derivatives were synthesized from commercially available ferrocene sources as follows (Scheme 2.1 and 2.2). At first, ferrocenecarboxylic acid **2.9** was reacted with propargyl amine under *N*-(3-dimethylaminopropyl)-*N'*-ethylcarbodiimide (EDC) amide coupling conditions to give compound **2.1**.<sup>20</sup> Then, **2.1** was reacted with

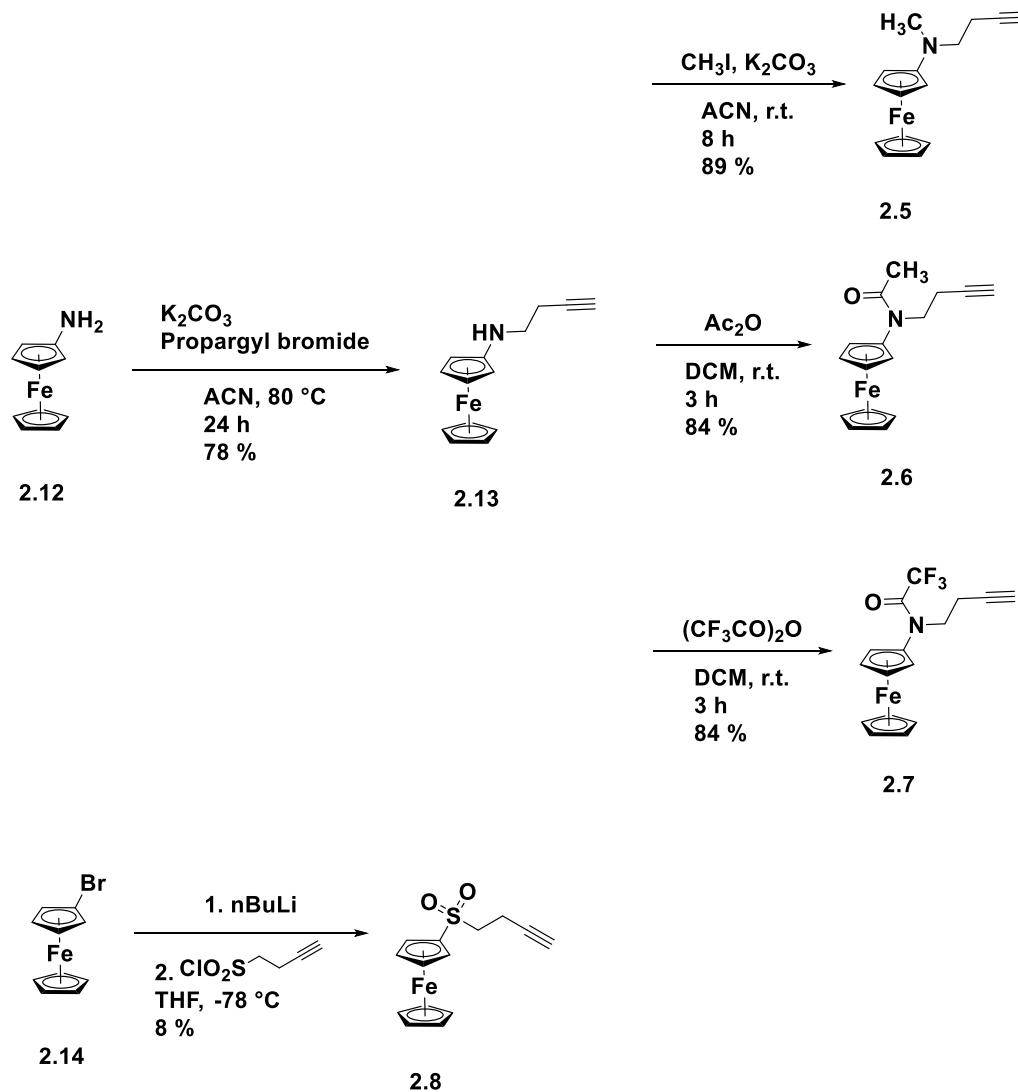
acetic anhydride and aluminum chloride under the Friedel–Crafts reaction condition to give **2.2**.<sup>11</sup> Precursor **2.9** was also converted to the acyl azide **2.10** with sodium azide via acyl chloride formation by phosphorous pentachloride. The resulting azide was then refluxed to yield urea **2.3** by the Curtius rearrangement.<sup>21</sup> Furthermore, **2.4** was obtained by means of a Williamson ether synthesis that involved coupling ferrocenemethanol **2.11** with propargyl bromide in basic conditions.<sup>22</sup>



**Scheme 2.1** Synthesis of the ferrocene probes **2.1** – **2.4**

Another precursor aminoferrocene **2.12** was converted to the corresponding mono-substituted alkyne functionalized intermediate **2.13** under  $\text{S}_{\text{N}}2$  reaction conditions (Scheme

2.2).<sup>23</sup> Subsequent methylation with methyl iodide gave **2.5**. Compounds **2.6**, and **2.7** were also synthesized from **2.12** by acetylation with acetic anhydride or trifluoroacetic anhydride, respectively. Finally, lithiation of bromoferrocene **2.14** and reaction with alkyne-containing sulfonyl chloride produced **2.8**.<sup>24</sup> This chemistry is also shown in scheme 2.2.



**Scheme 2.2** Synthesis of the ferrocene probes **2.5** – **2.8**

### 2.2.3 Electrochemistry of ferrocene derivatives with terminal alkynes

After the synthesis of the ferrocene derivatives, cyclic voltammetry (CV) was performed to check their half-wave potentials ( $E_{1/2}$ ) and electrochemical reversibility (Figure 2.4). In the most of CV spectra, the oxidation and reduction peak current were almost identical and the  $\Delta E_p$  were close to about 90 mV. This result demonstrates that electrochemical reaction from the ferrocene moieties were quasi-reversible except for **2.8**, which bears a sulfone group between the ferrocene and the alkyne.<sup>25</sup>

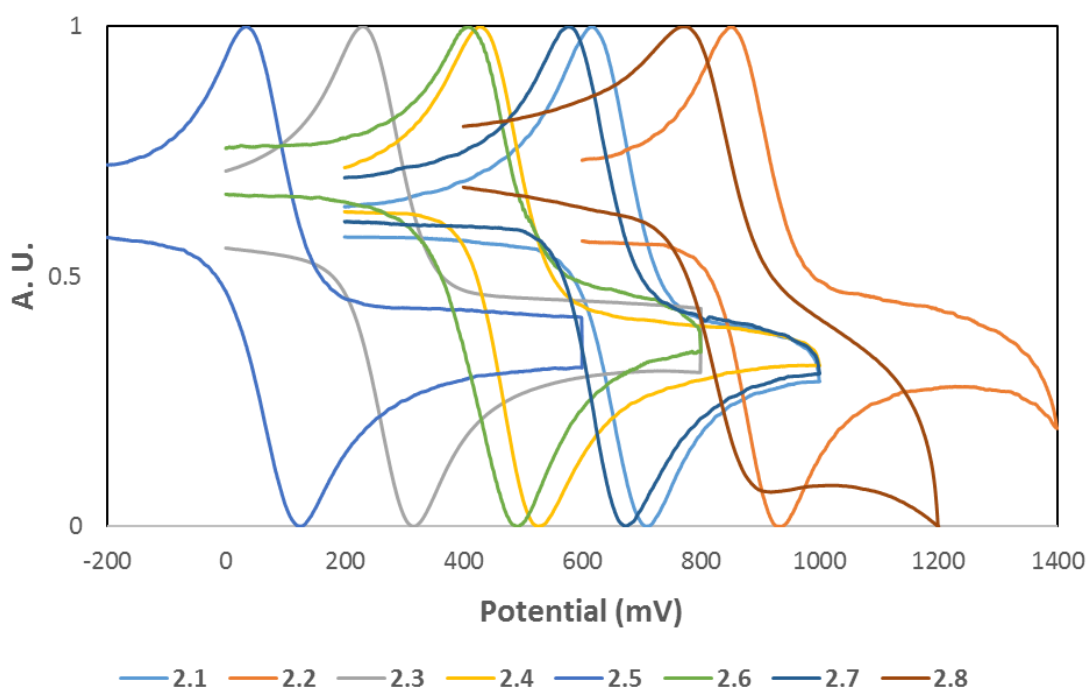


**Figure 2.4** Cyclic voltammetry of synthesized ferrocene probes in  $\text{CH}_2\text{Cl}_2$ . (Normalized values for clear comparison of the  $E_p$ ) (0.2 M tetrabutylammonium hexafluorophosphate (TBAPF<sub>6</sub>) in  $\text{CH}_2\text{Cl}_2$ , working electrode (WE) – glassy carbon (GCE); counter electrode (CE) – platinum wire (Pt); reference electrode (RE) – Ag/AgCl)

It was also found as expected that the ferrocene derivatives with electron withdrawing groups i.e., **2.1**, **2.2**, **2.6** and **2.8** displayed higher redox potentials than the derivatives with electron donating groups (**2.3** and **2.5**) as expected. Compounds bearing

groups whose electronic character was not expected to be perturbed significantly (**2.4** and **2.6**) gave  $E_{1/2}$  values in the middle of the two groups of species. Except for compounds with  $E_{1/2}$  maxima adjacent to one another (e.g. **2.1** and **2.7**, **2.4** and **2.6**, and **2.2** and **2.8**), the difference in the  $E_{1/2}$  values was around 200 mV: 1) between **2.5** and **2.3** (first two peaks in Figure 2.4) – 190 mV; 2) **2.3** and **2.4** – 200 mV; 3) **2.4** and **2.1** – 210 mV; 4) **2.1** and **2.2** – 230 mV. Based on published studies,<sup>5, 14</sup> these are peak splits that might be expected for the ferrocene derivatives. Similar values were found using linear sweep voltammetric methods such as square wave voltammetry (SWV), differential pulse voltammetry, and alternating current voltammetry (ACV), which revealed even better peak resolution than obtained using conventional CV methods (data not shown here).

#### 2.2.4 Linear correlation between redox potential and Hammett constant

We also explored the relationship between the electronic features of each functional group and the redox potential (Figure 2.5). As shown in Table 2.1, we plotted the measured redox potential values versus two Hammett constants,  $\sigma_m$  (*meta* substituent) and  $\sigma_p$  (*para* substituent), for each functional moiety. Since the constants for the exact functional group linked via an alkyne moiety as presenting the compound set were not available in literatures, the value from the most analogous substituents were introduced in the plot. For example, the  $\sigma_m$  and  $\sigma_p$  of 3-[(methylamino)carbonyl]benzoic acid and 4-[(methylamino)carbonyl]benzoic acid were plotted versus the redox potential of **2.3** (See Table 2.1).

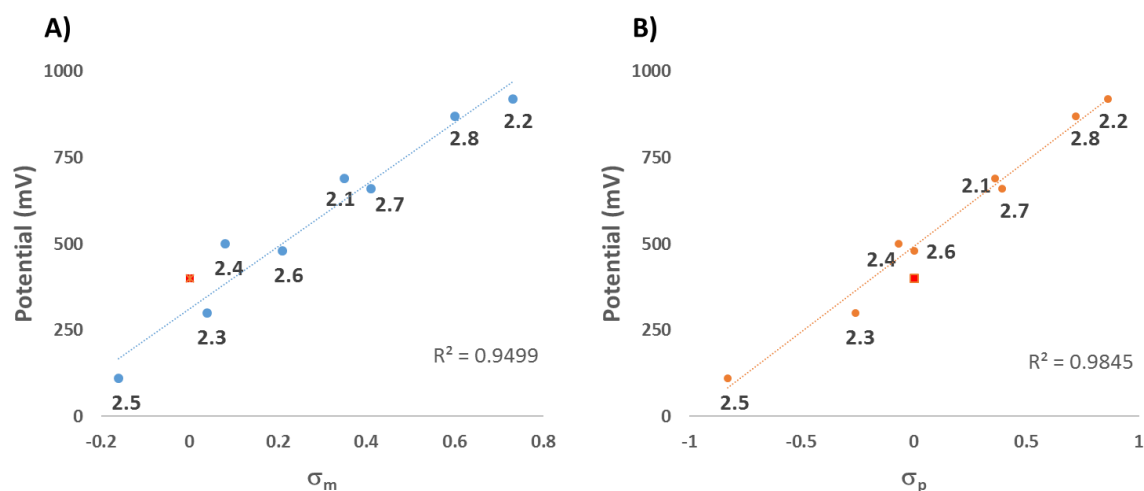


**Figure 2.5** The linear plot of the Hammett constants vs. the measured redox potentials for compounds 2.1 – 2.8. The Red square in each plot corresponds to unmodified ferrocene. A) Potential vs.  $\sigma_m$  and B) vs.  $\sigma_p$ .

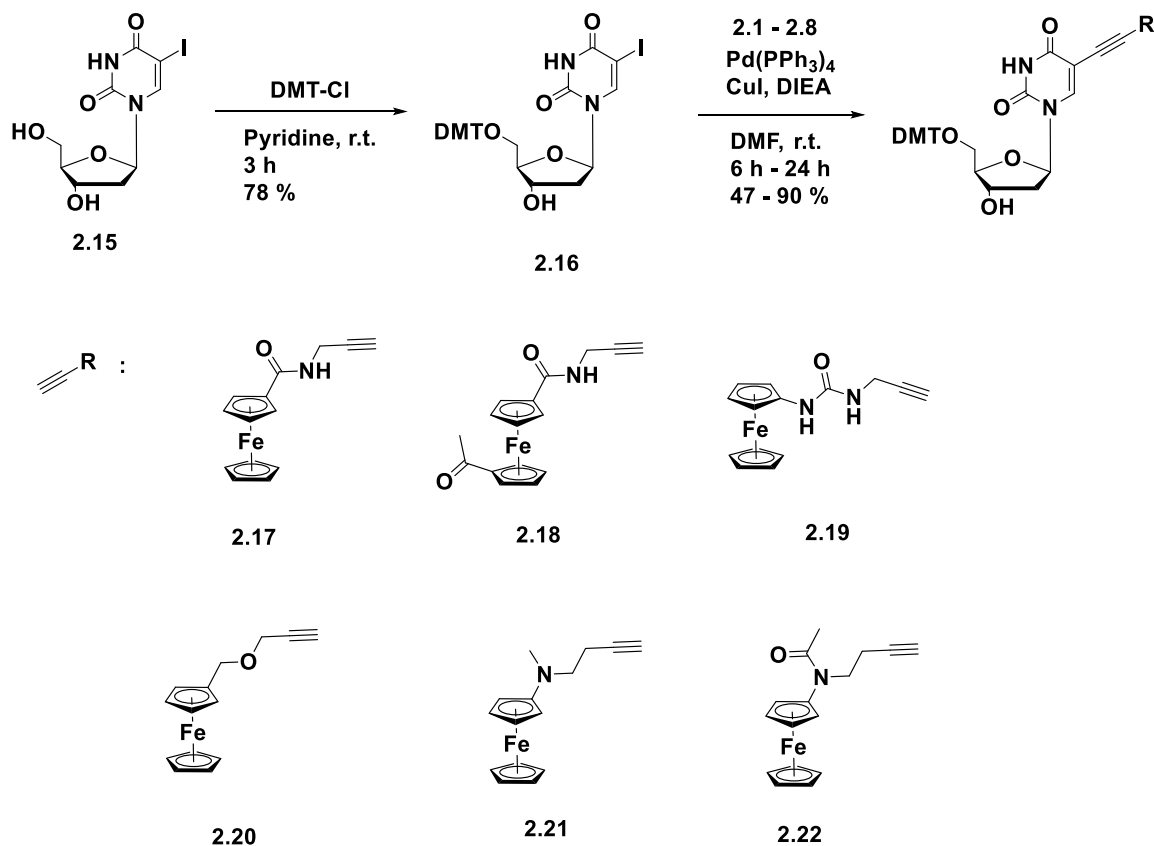
As shown in the Figure 2.5, the redox potentials were found to correlate well with the constants with good  $R^2$  values being obtained for the corresponding linear plots. Compared with  $\sigma_m$  and  $\sigma_p$  values produced a better correlation with the measured redox potentials. Although the trend was similar in the case of both Hammett constants, these findings leads us to conclude the redox potential of the ferrocene derivative are more dependent on a resonance effect of the substituent than an inductive effect. We thus propose that these correlations can be exploited in the optimal design of new derivatives since they allow predictions of redox potential. Interestingly, the di-substituted ferrocene **2.2** also showed good correlation when plotted using the sum of the Hammett constants for the two substituents. It may thus prove possible to predict the potential of multi-substituted ferrocene derivatives. However, additional studies will be needed to confirm this preliminary conclusion.



### 2.2.5 Synthesis and electrochemical property of the ferrocene modified thymidine

To incorporate the synthesized terminal alkynes into oligonucleotides, we first attempted chemical oligonucleotide synthesis. As precursors of nucleoside phosphoramidites, we synthesized modified thymidines bearing the ferrocene probes. Unlike other nucleobases, thymine does not require any additional protection or deprotection to be employed in oligonucleotide syntheses.<sup>26</sup> To conjugate the probes to thymine, a Sonogashira coupling reaction was used as mentioned in the introductory chapter.

The synthesis of the targeted modified thymidines commenced from commercially available 5-iodo-2'-deoxyuridine **2.15** as shown in Scheme 2.2. The primary 5'-hydroxyl group of thymidine was selectively protected by a dimethoxytrityl chloride (DMT-Cl) to yield the DMT protected nucleoside **2.16**. The iodide on the 5 position allows coupling with the terminal alkyne of the ferrocene derivatives **2.17** through. Unfortunately, the yields were moderate.



**Scheme 2.3** Synthesis of DMT-protected modified thymidines with the ferrocene probes on 5 position

The ferrocene-modified thymidines synthesized via this coupling procedure were subject to CV analysis to check whether they retain their redox activities. As shown in Figure 2.6, the redox features of the functionalized nucleosides mirrored those of the precursor terminal alkynes, although there was a small shift toward negative potential (about -30 mV). Presumably, this shift is due to the electron-donating property of the thymidine ring.

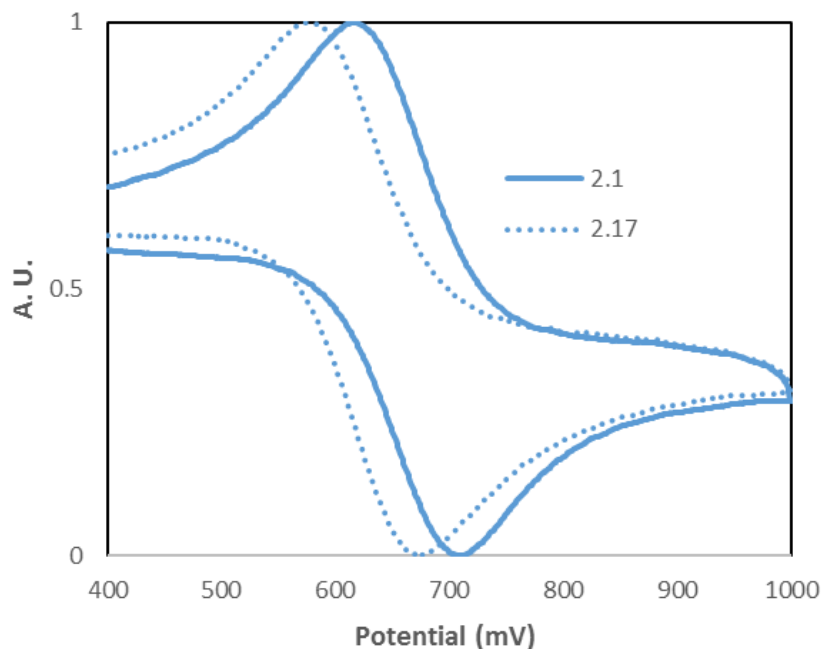
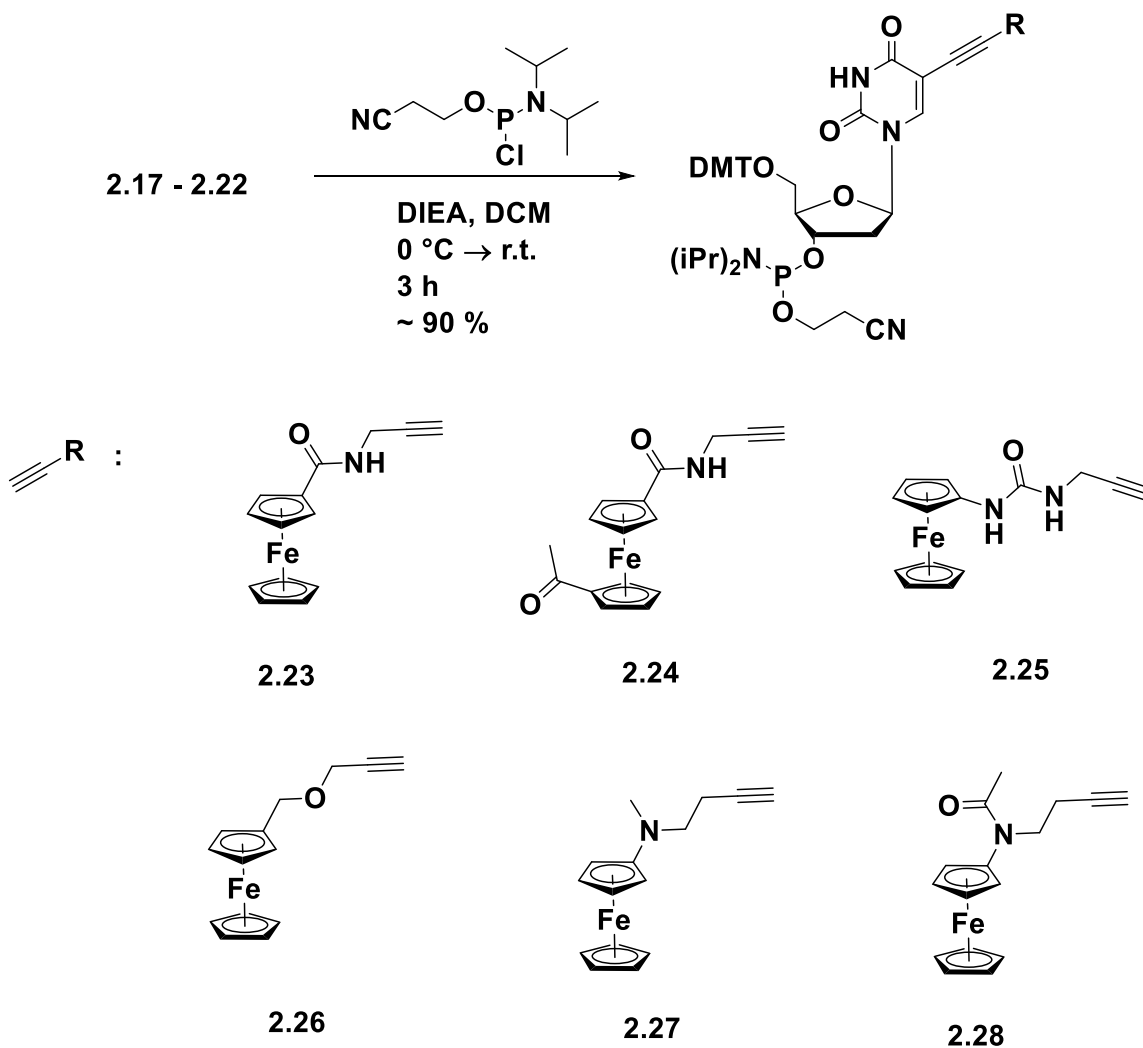


**Figure 2.6** Comparison between **2.1** ( $E_{1/2} = 660$  mV, line) and **2.17** ( $E_{1/2} = 630$  mV, dots) in CV (0.2 M TBAPF<sub>6</sub> in CH<sub>2</sub>Cl<sub>2</sub>, WE – GCE; CE – PT, RE – Ag/AgCl)

### 2.2.6 Synthesis of the ferrocene modified thymidine phosphoramidites

After obtaining the ferrocene-modified nucleosides bearing DMT protecting group on the 5' position, the following nucleoside phosphoramidites syntheses were carried out (Scheme 2.4).<sup>5, 14, 16</sup> The thymidine with the ferrocene probes **2.17** to **2.22** were reacted with 2-cyanoethyl *N,N*-diisopropylchlorophosphoramidite to yield the phosphoramidites **2.25** to **2.32**. After the reaction between the electrophilic chlorophosphoramidite and the free hydroxyl group under basic conditions, the products were purified by recrystallization in anhydrous pentane and ether mixture (8:2), followed by drying overnight *in vacuo*. The phosphoramidites obtained in this way were used immediately to avoid decomposition of the product. Because of stability concerns, no CV analyses of the phosphoramidites were attempted.



**Scheme 2.4** Synthesis of thymidine phosphoramidites bearing the ferrocene probes.

The conversion was confirmed by  $^{31}\text{P}$  NMR spectroscopy. A clear doublet peak around 150 ppm was seen that corresponds to what is expected for a phosphoramidite (Figure 2.7 and Chapter 5). The peak observed around 10 ppm is nucleoside *H*-phosphonate, which is one of the major decomposition products of the phosphoramidites.<sup>27</sup>

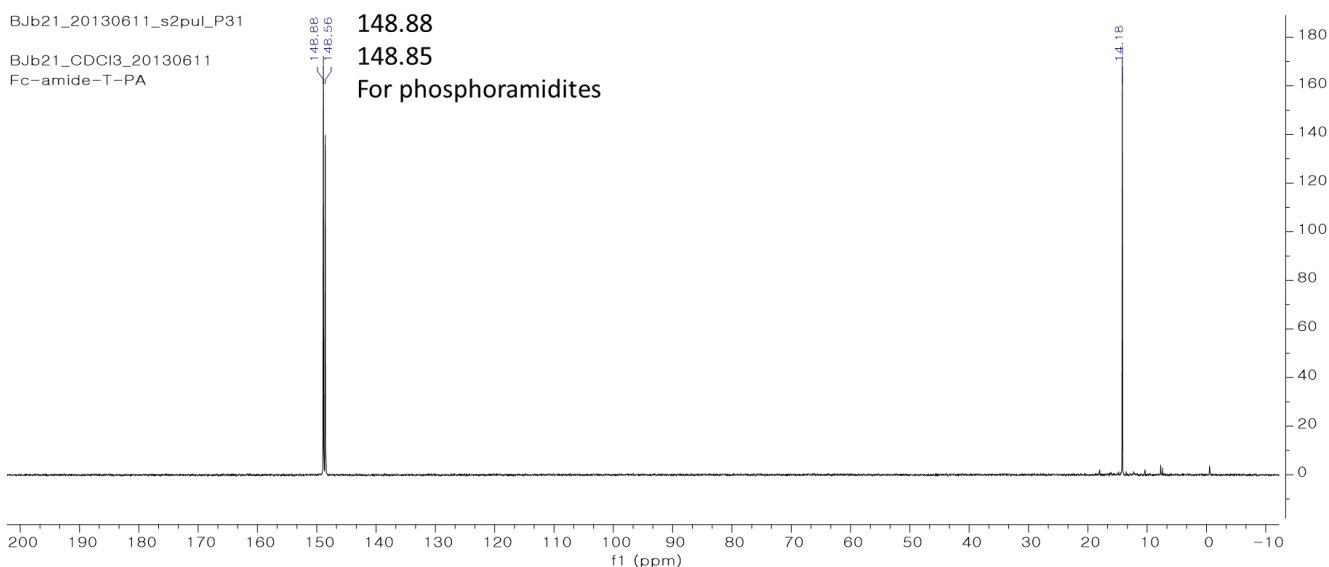


**Figure 2.7**  $^{31}\text{P}$  NMR spectra of a representative phosphoramidite target **2.23**.

### 2.2.7 Solid-phase oligonucleotide synthesis and self-assembled monolayer formation on gold

The thymidine phosphoramidites **2.23** and **2.26** were incorporated to sequences **2.31** and **2.32**, respectively (Table 2.2) so as to obtain oligonucleotides with ferrocene probes. The syntheses were performed using an automated standard solid-phase oligonucleotide strategy (see Chapter 1.1.2) in conjunction with four unmodified nucleoside phosphoramidites (A, T, G, and C).

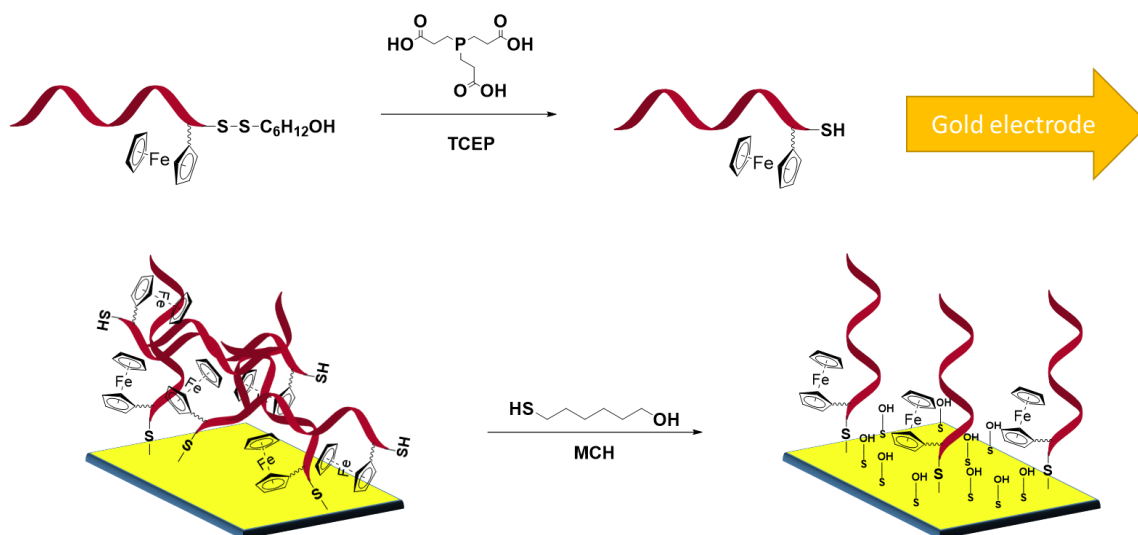
**Table 2.2** Synthesized oligonucleotide sequences

Name	Sequence (5' to 3')	X =
<b>2.31</b>	5'-CCATGCGCAAATACTCXXXXT-SH-3'	<b>2.23</b>
<b>2.32</b>		<b>2.26</b>

Due to the lower coupling efficiency seen for the modified phosphoramidites relative to those based on A, T, G, and C, it was required to carry out the incorporation with higher concentrations and longer reaction times.<sup>28</sup> After the synthesis, the sequences

were purified using a commercially available DNA purification cartridge charged with reversed-phase silica gel. This approach allowed the desired full-length oligonucleotide bearing DMT protection groups to be separated from truncated oligonucleotides produced during the synthetic process. Following deprotection of DMT group with trifluoroacetic acid (TFA) and lyophilizing of the resulting solution, the desired oligonucleotides were obtained as solids.

In addition to **2.23** and **2.26**, cleavage of disulfide bond is required if immobilization onto a gold surface is to be performed. Such attachment is desired since the goal is to construct self-assembled monolayer (SAM) using gold-thiol interactions that can serve as E-sensors (Scheme 2.5).<sup>4, 29</sup>



**Scheme 2.5** Schematic representation of a SAM produced using a generalized modified oligonucleotide in combinations with 6-mercaptohexanol (MCH).

To accomplish thiol release, tris(2-carboxyethyl)phosphine (TCEP) was added to a solution of the oligonucleotides solution in aqueous buffer. After the formation of free thiol group by reduction, the oligonucleotides were immobilized on hand-polished gold disk

electrode to check their electrochemical properties. In addition, the electrode surface was treated with 6-mercaptohexanol (MCH) solution to wash off nonspecifically bound oligonucleotides and to construct a SAM consisting of surface bound MCH and oligonucleotide subunits. Oligonucleotides **2.31** and **2.32** were used separately in these studies.

### 2.2.8 Electrochemical analysis of the ferrocene modified oligonucleotides

After immobilization on the gold surface as described above, we investigated the electrochemical properties of oligonucleotide **2.31** and **2.32** by various voltammetric methods, including DPV, SWV, and ACV. Among them, SWV was chosen as the optimal sensing method due to its outstanding signal to noise ratio.

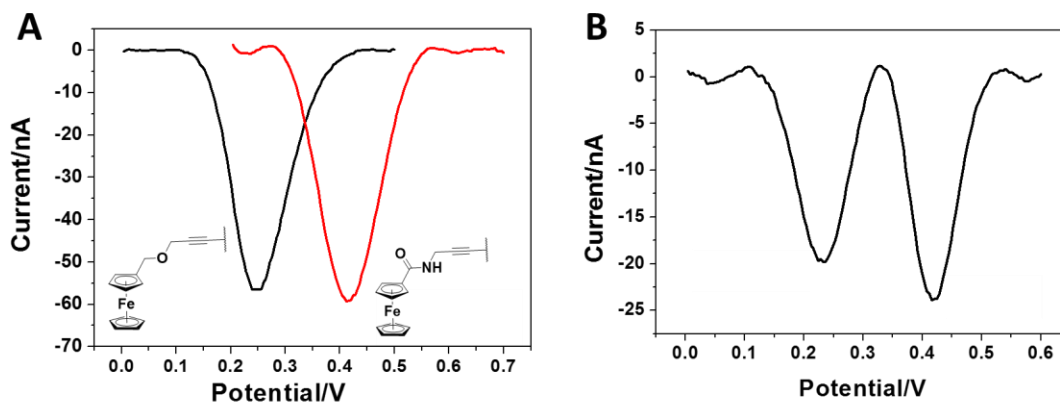


**Figure 2.8** SWV curves of the SAM prepared from **2.31** and **2.32** on gold electrode surface in PBS. A) Signals produced by the individual oligonucleotide **2.31** (red) and **2.32** (black) (Overnight incubation with 10  $\mu$ M of each oligonucleotide in PBS for surface immobilization, WE – gold disk electrode (GE): CE – Pt: RE – Ag/AgCl). B) Signals produced by a the 1:1 mixture of the probes used for A. (5  $\mu$ M of each oligonucleotide under the same condition)

As shown in Figure 2.8A, the electrode-immobilized oligonucleotides **2.31** and **2.32** showed peak currents at 250 mV and 420 mV, respectively in phosphate buffered

saline (PBS). These peak potentials ( $E_p$ ) are positioned at about 200 mV lower than the  $E_{1/2}$  of their precursor ferrocene-alkynes. We assume that this discrepancy reflects the different polarity and electrochemical environment of the organic solvent ( $\text{CH}_2\text{Cl}_2$ ) and the aqueous buffer (PBS) conditions used to study the SAMs. However, the difference between the two  $E_p$  values was still about 200 mV, just as it was in corresponding ferrocene alkynes and functionalized nucleosides. This implies that the redox potential of the synthesized oligonucleotides can be predicted by those of the precursors in advance of carrying out the actual oligonucleotide synthesis.

We also performed SWV with studies 1:1 mixture of the **2.31** and **2.32** on gold electrode surface. This was done to check the variation of redox potential of the modified oligonucleotides. As expected, the current peaks were clearly split enough to detect each signal at the same time (Figure 2.8B). Thus, it is suggested that the synthesized ferrocene derivatives can be utilized in the multiplexing sensing on the basis of the difference between each  $E_p$ , however further experiments will be required to establish the general viability of this concept by testifying other redox active oligonucleotide derivatives.

## **2.3 CURRENT AND FUTURE WORKS**

### **2.3.1 Synthesis of oligonucleotides with ferrocene derivatives**

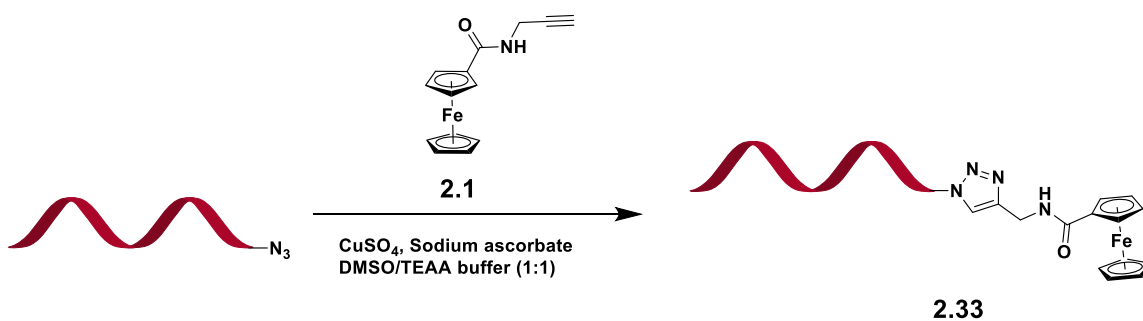
Currently, the incorporation of the other ferrocene derivatives is in progress to achieve more variable potentials. However, attempts to prepare oligonucleotides based on other modified phosphoramidites now in hand (**2.24**, **2.25**, **2.26**, and **2.28**) have not been successful. The presumed phosphoramidites were decomposed immediately in aqueous solution. After the purification of the presumed oligonucleotide, no current peak could be detected via SWV after immobilization on a gold surface.



We assume that these synthetic difficulties reflect an instability of the attached ferrocene in aqueous media.<sup>3, 30</sup> Despite the stable characteristics of ferrocene in organic solvents, it is known that halide anions in aqueous solution can react with ferrocene to give  $\text{FeX}_2$ .<sup>31-32</sup> Under the solid-phase synthetic conditions, aqueous iodine is converted to the iodide anion during the oxidation step. The iodide anion may, in turn, decompose the ferrocene complex resulting in the loss of any electrochemical properties. To avoid this putative decomposition, we plan to replace the oxidant used in the solid-phase synthesis with organic peroxide and carry out the reaction in  $\text{CH}_2\text{Cl}_2$ .<sup>33</sup> It is also appreciated that conventional storage buffers for nucleic acids, such as tris(hydroxymethyl)aminomethane hydrochloride (Tris-HCl) or phosphate buffered saline (PBS), are rich in chloride anions. Therefore, the newly synthesized oligonucleotides will be stored in 4-(2-hydroxyethyl)-1-piperazineethanesulfonic acid/sodium perchlorate (HEPES/ $\text{NaClO}_4$ ) buffer, where ferrocene derivatives have been shown to have better stability.<sup>3</sup>

### **2.3.2 Post-synthetic modification of oligonucleotides with ferrocene**

In addition to the chemical synthesis, we also performed post-synthetic modification with the ferrocene probes in an effort to bypass the aqueous oxidation step. With this goal in mind, the terminal alkyne **2.1** was incorporated into oligonucleotides by reacting with an azide-functionalized oligonucleotide under CuAAC coupling conditions (Scheme 2.5).



**Scheme 2.6** Post-synthetic modification of an azide-functionalized oligonucleotide to obtain **2.33** (Sequence: 5'-N<sub>3</sub>-TTACTCTC GATCGGCGTTTTA GAGAGG-SH-3')

The resulting oligonucleotide **2.33** was purified by HPLC and stored in HEPES/NaClO<sub>4</sub> buffer. By using the same protocol described above, a SAM were prepared from **2.33**. SWV analysis of this electrode revealed an  $E_p$  at 400 mV, which matched well what was seen for **2.1** in aqueous solution (Figure 2.8).

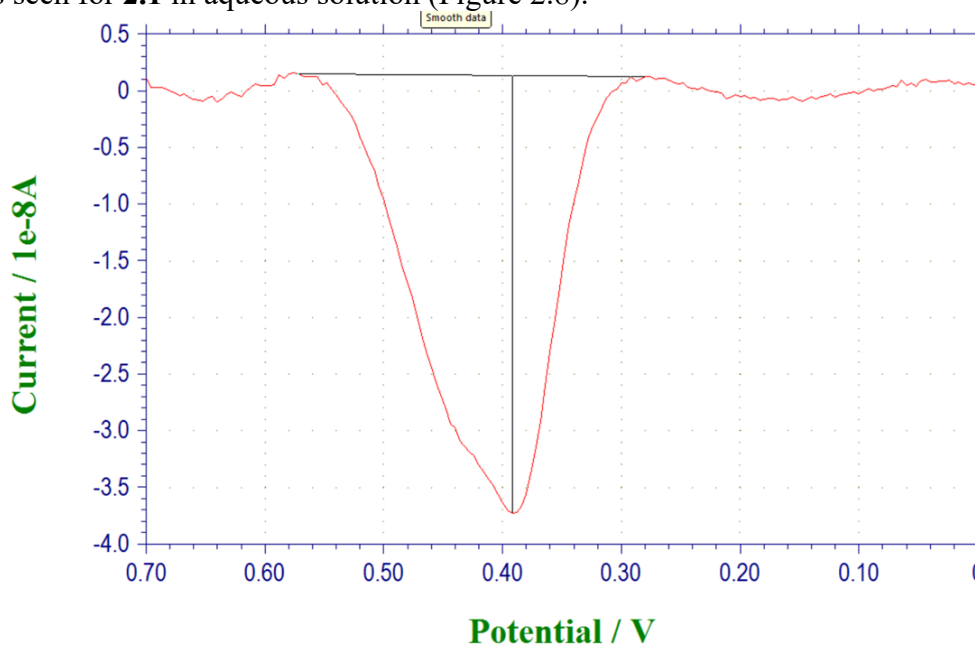


**Figure 2.8** SWV of the SAM prepared from **2.33** in HEPES/NaClO<sub>4</sub> buffer (Overnight incubation with 2  $\mu$ M in HEPES/NaClO<sub>4</sub> buffer, WE –GE; CE – Pt; RE – Ag/AgCl)

After the fabrication of the SAM, one ferrocene conjugate prepared using the so-called “click reaction” gave rise to a relatively strong peak current studied by SWV. This contrasts to the corresponding ferrocene produced by solid-phase synthesis, wherein multiple ferrocenes were required in order to produce a current strong enough for clear detection. Based on this preliminary result, it is expected that further post-synthetic modifications with other ferrocene-modified terminal alkynes such as precursors (**2.1** – **2.8**) will produce SAMs displaying a range of  $E_p$  values.

## 2.4 CONCLUSION

In conclusion, we have synthesized a series of functionalized ferrocene derivatives that provide a range of voltammetric signals, an effect ascribed perturbation of the electron density on the ferrocene cores. These ferrocene derivatives were incorporated into oligonucleotides by chemical synthesis or post-synthetic modification. Two systems differed, which is taken as being promising in terms of eventual multiplexing sensing. Currently, efforts to optimize the oligonucleotide synthesis conditions as well as construction of further SAMs for the electrochemical sensing are in progress. To the extent this work can be completed, it may permit the analysis of multiple nucleic acid analytes in parallel via the use of probes producing different electrochemical ‘colors’. The targeted system, if obtained, could prove useful as a promising platform for SNP detection and for the electrochemical sequencing for genetic materials.

## 2.5 REFERENCES

1. Drummond, T. G.; Hill, M. G.; Barton, J. K., Electrochemical DNA sensors. *Nat Biotech* **2003**, *21* (10), 1192-1199.
2. Li, D.; Song, S.; Fan, C., Target-Responsive Structural Switching for Nucleic Acid-Based Sensors. *Accounts of Chemical Research* **2010**, *43* (5), 631-641.

3. Kang, D.; Zuo, X.; Yang, R.; Xia, F.; Plaxco, K. W.; White, R. J., Comparing the Properties of Electrochemical-Based DNA Sensors Employing Different Redox Tags. *Analytical Chemistry* **2009**, *81* (21), 9109-9113.
4. Fan, C.; Plaxco, K. W.; Heeger, A. J., Electrochemical interrogation of conformational changes as a reagentless method for the sequence-specific detection of DNA. *Proceedings of the National Academy of Sciences* **2003**, *100* (16), 9134-9137.
5. Pheaney, C. G.; Barton, J. K., Intraduplex DNA-Mediated Electrochemistry of Covalently Tethered Redox-Active Reporters. *Journal of the American Chemical Society* **2013**, *135* (40), 14944-14947.
6. Hu, X.; Smith, G. D.; Sykora, M.; Lee, S. J.; Grinstaff, M. W., Automated Solid-Phase Synthesis and Photophysical Properties of Oligodeoxynucleotides Labeled at 5'-Aminothymidine with Ru(bpy)<sub>2</sub>(4-m-4'-cam-bpy)<sub>2</sub><sup>+</sup>. *Inorganic Chemistry* **2000**, *39* (12), 2500-2504.
7. Arroyo-Currás, N.; Somerson, J.; Vieira, P. A.; Ploense, K. L.; Kippin, T. E.; Plaxco, K. W., Real-time measurement of small molecules directly in awake, ambulatory animals. *Proceedings of the National Academy of Sciences* **2017**, *114* (4), 645-650.
8. Hsieh, K.; Ferguson, B. S.; Eisenstein, M.; Plaxco, K. W.; Soh, H. T., Integrated Electrochemical Microsystems for Genetic Detection of Pathogens at the Point of Care. *Accounts of Chemical Research* **2015**, *48* (4), 911-920.
9. De Crozals, G.; Farre, C.; Sigaud, M.; Fortgang, P.; Sanglar, C.; Chaix, C., Methylene blue phosphoramidite for DNA labelling. *Chemical Communications* **2015**, *51* (21), 4458-4461.
10. Wilkinson, G.; Rosenblum, M.; Whiting, M. C.; Woodward, R. B., THE STRUCTURE OF IRON BIS-CYCLOPENTADIENYL. *Journal of the American Chemical Society* **1952**, *74* (8), 2125-2126.
11. Rinehart, K. L.; Motz, K. L.; Moon, S., Organic Chemistry of Ferrocene. I. The Acetylation of Dialkylferrocenes. *Journal of the American Chemical Society* **1957**, *79* (11), 2749-2754.
12. Rosenblum, M.; Santer, J. O.; Howells, W. G., The Chemistry and Structure of Ferrocene. VIII. Interannular Resonance and the Mechanism of Electrophilic Substitution. *Journal of the American Chemical Society* **1963**, *85* (10), 1450-1458.
13. Rebiere, F.; Samuel, O.; Kagan, H. B., A convenient method for the preparation of monolithioferrocene. *Tetrahedron Letters* **1990**, *31* (22), 3121-3124.
14. Yu, C. J.; Wan, Y.; Yowanto, H.; Li, J.; Tao, C.; James, M. D.; Tan, C. L.; Blackburn, G. F.; Meade, T. J., Electronic Detection of Single-Base Mismatches in DNA with Ferrocene-Modified Probes. *Journal of the American Chemical Society* **2001**, *123* (45), 11155-11161.
15. Batterjee, S. M.; Marzouk, M. I.; Aazab, M. E.; El-Hashash, M. A., The electrochemistry of some ferrocene derivatives: redox potential and substituent effects. *Applied Organometallic Chemistry* **2003**, *17* (5), 291-297.
16. Tierney, M. T.; Grinstaff, M. W., Synthesis and Stability of Oligodeoxynucleotides Containing C8-Labeled 2'-Deoxyadenosine: Novel Redox Nucleobase Probes for DNA-Mediated Charge-Transfer Studies. *Organic Letters* **2000**, *2* (22), 3413-3416.

17. Amblard, F.; Cho, J. H.; Schinazi, R. F., Cu(I)-Catalyzed Huisgen Azide–Alkyne 1,3-Dipolar Cycloaddition Reaction in Nucleoside, Nucleotide, and Oligonucleotide Chemistry. *Chemical Reviews* **2009**, *109* (9), 4207-4220.
18. Sinkeldam, R. W.; Greco, N. J.; Tor, Y., Fluorescent Analogs of Biomolecular Building Blocks: Design, Properties, and Applications. *Chemical Reviews* **2010**, *110* (5), 2579-2619.
19. Hansch, C.; Leo, A.; Taft, R. W., A survey of Hammett substituent constants and resonance and field parameters. *Chemical Reviews* **1991**, *91* (2), 165-195.
20. Beilstein, A. E.; W. Grinstaff, M., On-column derivatization of oligodeoxynucleotides with ferrocene. *Chemical Communications* **2000**, (6), 509-510.
21. Liu, W.; Tang, Y.; Guo, Y.; Sun, B.; Zhu, H.; Xiao, Y.; Dong, D.; Yang, C., Synthesis, characterization and bioactivity determination of ferrocenyl urea derivatives. *Applied Organometallic Chemistry* **2012**, *26* (4), 189-193.
22. Thakur, A.; Adarsh, N. N.; Chakraborty, A.; Devi, M.; Ghosh, S., Synthesis of mono and doubly alkynyl substituted ferrocene and its crystal engineering using  $-C-H\cdots O$  supramolecular synthon. *Journal of Organometallic Chemistry* **2010**, *695* (7), 1059-1064.
23. Hagen, H.; Marzenell, P.; Jentzsch, E.; Wenz, F.; Veldwijk, M. R.; Mokhir, A., Aminoferrocene-Based Prodrugs Activated by Reactive Oxygen Species. *Journal of Medicinal Chemistry* **2012**, *55* (2), 924-934.
24. Khobragade, D. A.; Mahamulkar, S. G.; Pospíšil, L.; Císařová, I.; Rulíšek, L.; Jahn, U., Acceptor-Substituted Ferrocenium Salts as Strong, Single-Electron Oxidants: Synthesis, Electrochemistry, Theoretical Investigations, and Initial Synthetic Application. *Chemistry – A European Journal* **2012**, *18* (39), 12267-12277.
25. Bard, A. J.; Faulkner, L. R., *Electrochemical methods : fundamentals and applications*. 2nd ed.; Wiley: New York, 2001; p xxi.
26. Berg, J. M.; Tymoczko, J. L.; Stryer, L.; Stryer, L., *Biochemistry*. 6th ed.; W. H. Freeman: New York, 2007; p 1 v.
27. Krotz, A. H.; Rentel, C.; Gorman, D.; Olsen, P.; Gaus, H. J.; McArdle, J. V.; Scozzari, A. N., Solution Stability and Degradation Pathway of Deoxyribonucleoside Phosphoramidites in Acetonitrile. *Nucleosides, Nucleotides and Nucleic Acids* **2004**, *23* (5), 767-775.
28. Beaucage, S. L.; Iyer, R. P., The synthesis of modified oligonucleotides by the phosphoramidite approach and their applications. *Tetrahedron* **1993**, *49* (28), 6123-6194.
29. Lucarelli, F.; Marrazza, G.; Turner, A. P. F.; Mascini, M., Carbon and gold electrodes as electrochemical transducers for DNA hybridisation sensors. *Biosensors and Bioelectronics* **2004**, *19* (6), 515-530.
30. Ge, D.; Levicky, R., A comparison of five bioconjugatable ferrocenes for labeling of biomolecules. *Chemical Communications* **2010**, *46* (38), 7190-7192.
31. Prins, R.; Korswagen, A. R.; Kortbeek, A. G. T. G., Decomposition of the ferricenium cation by nucleophilic reagents. *Journal of Organometallic Chemistry* **1972**, *39* (2), 335-344.

32. Han, S. W.; Seo, H.; Chung, Y. K.; Kim, K., Electrochemical and Vibrational Spectroscopic Characterization of Self-Assembled Monolayers of 1,1'-Disubstituted Ferrocene Derivatives on Gold. *Langmuir* **2000**, *16* (24), 9493-9500.
33. Prakash, T. P.; Johnston, J. F.; Graham, M. J.; Condon, T. P.; Manoharan, M., 2'-O-[2-[(N,N-dimethylamino)oxy]ethyl]-modified oligonucleotides inhibit expression of mRNA in vitro and in vivo. *Nucleic Acids Research* **2004**, *32* (2), 828-833.

## Chapter 3: Construction and Application of Ratiometric electrochemical DNA sensor<sup>1</sup>

### 3.1 INTRODUCTION

The ability to transduce the DNA hybridization into electrochemical signals has been greatly advanced by the development of so-called electrochemical DNA sensors (E-sensors). The E-sensors have a variety of intrinsic advantages, including high sensitivity, relatively low cost, and amenability to miniaturization and multiplexing.<sup>1-3</sup> Nucleic acid analytes, including single nucleotide polymorphisms (SNPs), have been specifically detected by adapting molecular beacons<sup>4</sup> to electrochemical signalling.<sup>5</sup> An extremely robust and adaptable design for electrochemical signaling with molecular beacons has been developed by Plaxco group.<sup>6</sup> In this design the distance of a redox tag to an electrode surface was altered as a consequence of nucleic acid target-induced conformational change in the molecular beacon (see Figure 3.1). Variations on this theme have included molecular beacon E-sensors with ferrocene (Fc),<sup>7</sup> methylene blue (MB),<sup>8</sup> and other redox tags;<sup>9-10</sup> transduction to both reusable<sup>6</sup> and disposable electrodes;<sup>11</sup> and the detection of targets ranging from short DNA<sup>6, 10</sup> to RNA<sup>12-13</sup> to amplicons from isothermal amplification.<sup>14</sup> To improve the sensitivity of the E-sensor, enzyme<sup>15-16</sup> or nanomaterial<sup>17-18</sup> amplification of the initial conformational transduction has been achieved; some of these transduction methods have allowed certain DNA targets to be detected at the atto-molar level.

As with many other electrochemical biosensors, a barrier to the wider adoption of E-sensors as analytical devices are recognized problems relating to reproducibility, robustness and reliability, which in turn stem from hard-to-avoid variations in electrode

---

<sup>1</sup> Du, Y.; Lim, B. J.; Li, B.; Jiang, Y. S.; Sessler, J. L.; Ellington, A. D., Reagentless, Ratiometric Electrochemical DNA Sensors with Improved Robustness and Reproducibility. *Anal Chem* **2014**, 86 (15), 8010-8016. The author is a co-first author of the publication and was responsible for the synthesis, purification, and characterization of the oligonucleotides used in the study and for a part of the electrochemical analyses.

areas, DNA loading densities, and non-target-induced reagent degradation/dissociation. This can lead to differences in the initial background currents on different sensing electrodes. The idiosyncratic background currents observed with disparate electrodes make direct determination of target binding unreliable, ultimately requiring time-consuming background scans with each new electrode or in each new analysis. Relative signal changes before and after the addition of target can be carried out for individual electrodes;<sup>19-20</sup> however, such methods are inconvenient and considered impractical for potential point-of-care devices. Moreover, using such methods it is difficult to confirm whether the observed signal changes are due to target binding or deterioration of the sensing surface.

In this chapter, we describe a simple ratiometric method for improving the robustness and reproducibility of E-sensors, specifically, a new “ratiometric E-sensor”. As detailed below, we build on the basic Plaxco’s E-sensor approach. We have done so because such E-sensors are reagentless and thus excellent candidates for the development of point-of-care diagnostics.<sup>8, 20-21</sup> However, the inclusion of the two redox components uniquely addresses the shortcomings note above, especially in relation to variations that arise from different DNA loading densities and non-target-induced reagent degradation/dissociation. The ratiometric E-sensor we describe here is expected to be general and thus readily extrapolated to create a range of other oligonucleotide electrochemical DNA or aptamer-based biosensors that rely on the same or other conformational transduction principles.<sup>3, 22-25</sup>

The major work of this chapter was published in the journal *Analytical Chemistry*: Du, Y.; Lim, B. J.; Li, B.; Jiang, Y. S.; Sessler, J. L.; Ellington, A. D., Reagentless, Ratiometric Electrochemical DNA Sensors with Improved Robustness and Reproducibility. *Anal Chem* **2014**, 86 (15), 8010-8016.



## 3.2 RESULT AND DISCUSSION

### 3.2.1 Synthesis and characterization of the ratiometric E-DNA Sensor

The ratiometric method we describe here is based on the use of two electrochemical probes in parallel. In addition to the classic signal probe (MB) found in other E-sensors, we have included another redox probe, Fc as a control. The design principle is that during target-induced conformational transduction, only the distance between the signal probe (MB) and the electrode will be changed, while the relative distance between the control probe (Fc) and the electrode should remain constant. Therefore, the control probe is expected to serve as an internal control. (Figure 3.1)

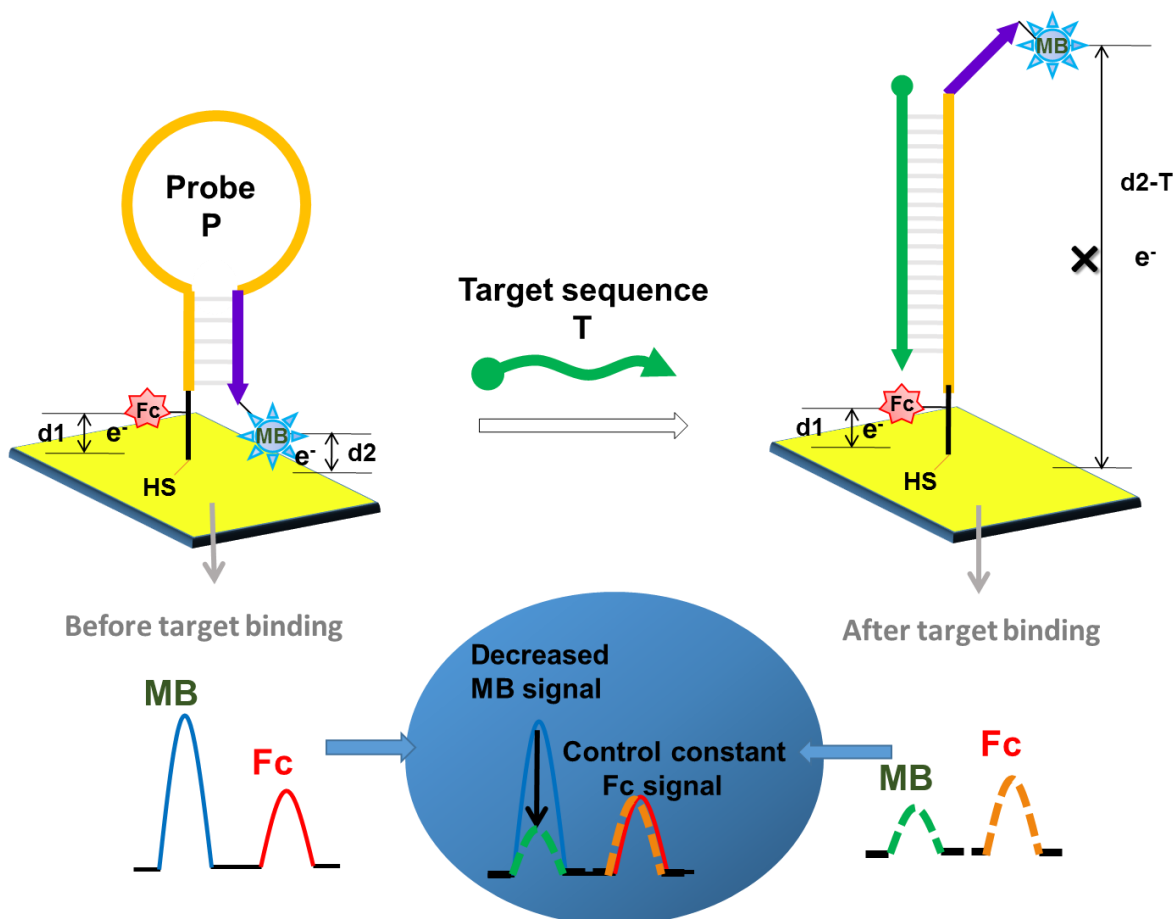
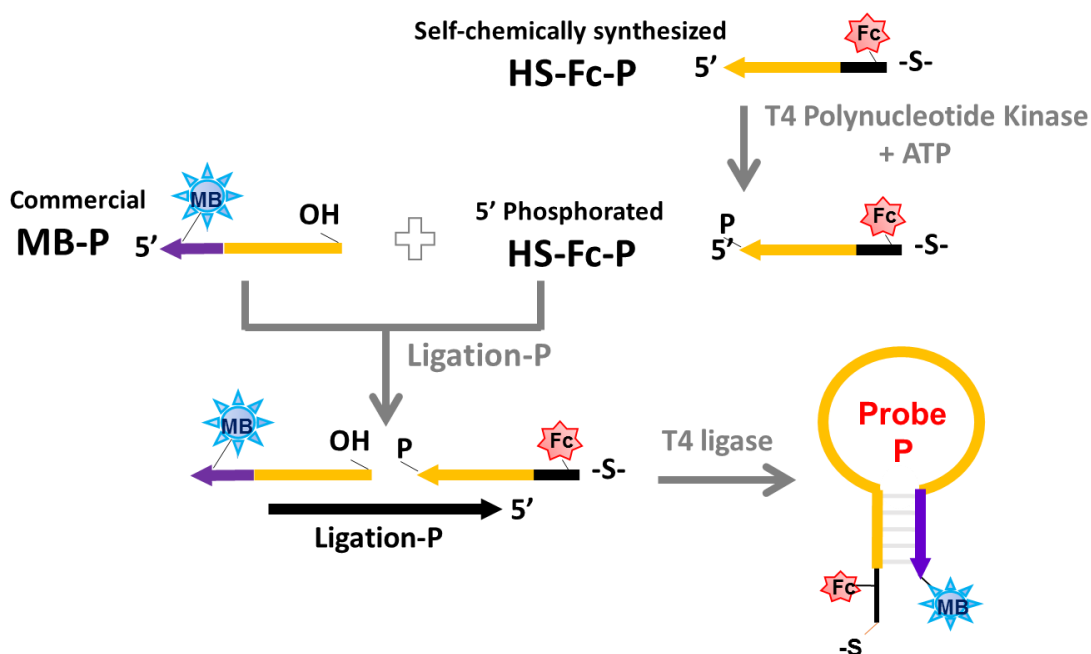


**Figure 3.1** Scheme of sensing process and predicted signal by electron transfer.

To demonstrate the utility of our ratiometric standardization, we designed a “Signal-Off” E-DNA sensor<sup>6</sup> similar to one reported previously by Plaxco and coworkers. However, in addition to adding a second redox component, we changed the target sequence so as to detect sequences present in the human T-lymphotropic virus type I gene (Target T).<sup>26</sup> As shown in figure 3.1 and table 3.1, a 37-mer molecular beacon (Probe P) was immobilized on a hand-polished gold disk electrode via a 3' thiol. Probe P was constructed by enzymatically ligation of an HS- and Fc-labeled oligonucleotide (HS-Fc-P) with a MB-labeled oligonucleotide (MB-P) and the following PAGE purification (Figure 3.2). The HS-Fc-P was synthesized using a commercial 3'-thiol modifier solid phase column and a Fc-modified thymidine (T) phosphoramidite (**2.23**) (Scheme 3.1). MB-P was obtained from a commercial supplier.



**Scheme 3.1** Construction of Probe P from MB-P and HS-Fc-P. After hybridization to a complementary strand, Ligation-P, the phosphorylated HS-Fc-P and MB-P were ligated together by T4 DNA ligase.

**Table 3.1** Sequence of oligonucleotides used in this work. X: **2.23** (Ferrocene-modified thymidine phosphoramidite)

Name	Sequence (5' to 3')	5' modification	3' modification
Unlabeled Probe P	TTTGAGTATTCCTCCAGGCCATGCGCAAATACTCTTTT		
MB-P	TTTGAGTATTCCTCCAGG	MB	
HS-Fc-P	CCATGCGCAAATACTCXXXXT		C3 - SH
Ligation-P	ATTTGCGCATGGCCTGGAGGAATAC		
Target T	GAGTATTTGCGCATGGCCTGGAGGA		
T-SNP1	GAGTATTTGCGCATGGCCTGTAGGA		
T-SNP2	GAGTATTTCCGCATGGCCTGTAGGA		
T-SNP3	GAGTATTTCCGCATGGCCAGTAGGA		
T-SNP4	GAGTATTTCCGCTTGCCAGTAGGA		
Non-T	AACCAGCCAGTGAGCCAATTCATGA		

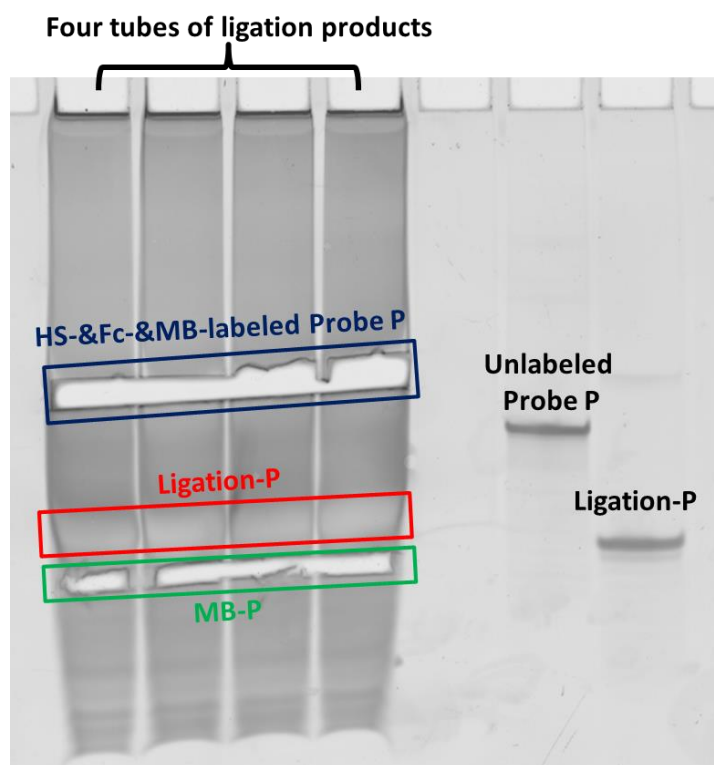


**Figure 3.2** PAGE gel characterization and purification of the ligation process. Because both the ligation product (Probe P) and the MB-P contain MB, these bands have a blue tinge.

### 3.2.2 Electrochemical characteristics of the ratiometric E-sensor

As shown in Figure 3.1 and Figure 3.3, in the absence of the target, both the Fc and MB tags are held in proximity to the electrode and yield effective electron transfer signals at 0.440 V and -0.265 V (vs Ag/AgCl, 2 M NaCl), respectively. The Fc probe was chosen because its  $E^\circ$  is well-separated from that of MB. Figure 3.3 shows square wave voltammetry (SWV) curves from three different electrodes. As hypothesized, under standard experimental operation, irrespective of differences in electrode areas, probe densities, or idiosyncrasies of cleaning, the background current ratio between MB and Fc was generally the same on each sensing surface.

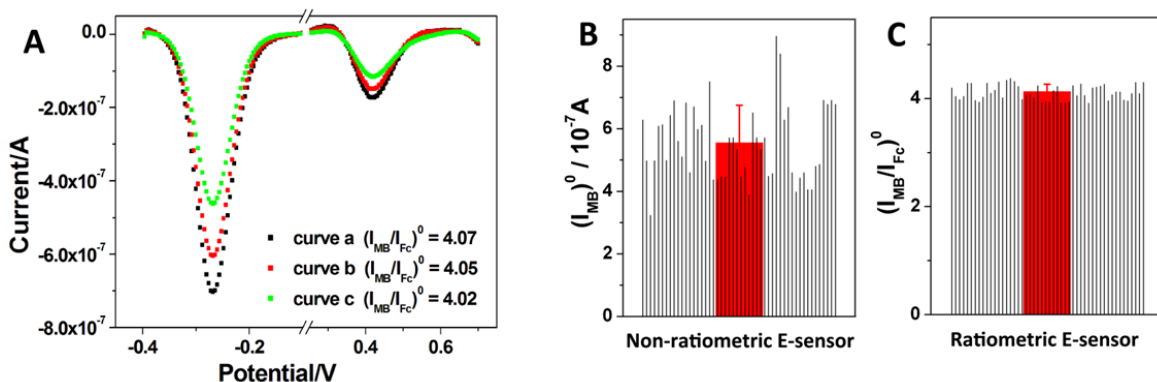


**Figure 3.3** Comparison between non-ratiometric and ratiometric E-sensors. A) Typical SWV curves scanned prior to target binding on three different sensing electrodes. B) Reproducibility of the nonratiometric E-sensor. C) Reproducibility of the ratiometric E-sensor. Throughout,  $(I_{MB})^0$  refers to the initial background response of MB prior to target binding.  $(I_{MB}/I_{Fc})^0$  refers to the initial background ratio of MB and Fc signals prior to target binding. The black histograms represent the background responses of 50 individual measurements over eight electrodes. Average values are represented by the red bars. The error bars in the red histograms represent the SD for 50 individual measurements.

To confirm that the ratiometric E-sensor (containing both MB and Fc) is highly reproducible relative to the non-ratiometric E-sensor (containing only MB), the initial

background SWV peak currents of MB ( $(I_{MB})^\circ$ ) and Fc ( $(I_{Fc})^\circ$ ) and the initial background current ratios of ( $(I_{MB}/I_{Fc})^\circ$ ) before target detection were collected over fifty individual measurements (Figure 3.3B and 3.3C). These data were obtained using eight electrodes, including the same electrodes on different days and different electrodes on the same day. Similar to the classic E-sensor, the background ( $(I_{MB})^\circ$ ) response in these fifty tests showed wide variation (Figure 3.3B) with an average (standard deviation, SD) of  $5.54 \times 10^{-7}$  A and a variance of 1.21. However, in our ratiometric E-sensor the variation in background signal was significantly reduced ( $(I_{MB}/I_{Fc})^\circ$ ; Figure 3.3C) with an average background ratio response of 4.13 and a variance of 0.14. The ratiometric approach was far more robust, reliable, and reproducible than the previous approach that relied on electrochemical “absolute values”.

### **3.2.3 Detection of a target oligonucleotide**

In response to the target sequence (Target T, at e.g., 500 nM), the Probe P undergoes a conformational change due to formation of a P-T duplex. While the Faradic current from the 3' Fc tag was almost unchanged (presumably since its distance to the electrode, d1 remained unchanged), the 5' MB tag showed a sharp decrease in current, consistent with it being further away from the electrode (d2 goes to d2-T) (Figure 3.1 and Figure 3.4).

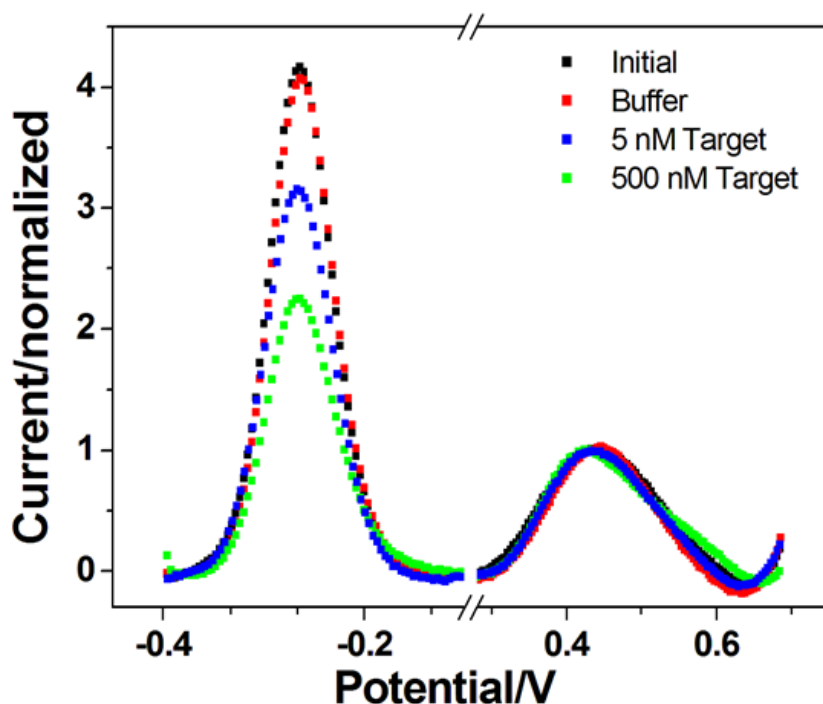


**Figure 3.4** Typical SWV curves as obtained before and after target binding. The peak current from Fc is normalized for each curve.

In order to confirm that electrochemical signals were due to nucleic acid hybridization and conformational changes rather than other unattributed effects, the behavior of Probe P was analyzed using native polyacrylamide gel electrophoresis (PAGE) (Figure 3.5). As can be seen from inspection of Figures 3.5A (using unlabeled Probe P and Target T) and 3.5B (using MB- and Fc-labeled Probe P and Target T), a higher band was observed only in the presence of Target T (lanes 2-4, 8-9). Moreover, the density of this band was in direct proportion to the target added. Interestingly, the presence of one or both electrochemical tags on Probe P reduced SYBR Gold staining fluorescence (blue arrow in Figure 3.5B, lane 6). Nevertheless, evidence for hybridization between Probe P and Target T was observed (Figure 3.5B, lanes 8-9).

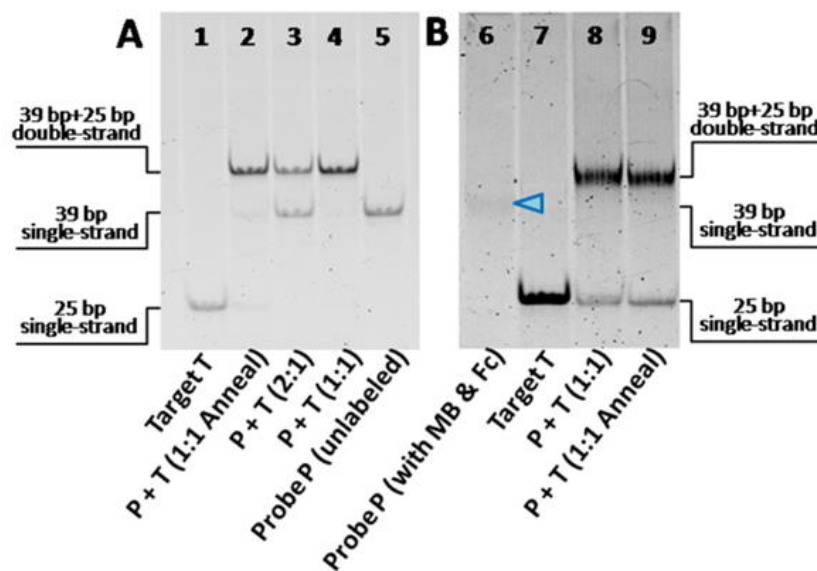


**Figure 3.5** Gel electrophoresis of E-sensor conformational transitions. Samples were developed on a 12% native PAGE. **A)** Unlabeled Probe P, lane 1: [T] = 100 nM; lanes 2 and 4: [P] = [T] = 100 nM; lane 3: [P] = 2[T] = 100 nM; lane 5: [P] = 100 nM. **B)** HS- and Fc- and MB-labeled Probe P, lane 6: [P] = 200 nM; lane 7: [T] = 200 nM; lanes 8 and 9: [P] = [T] = 200 nM. The mobilities of the different conformers are indicated at the sides of the gels. The arrow indicates a faint band, as described in the text.

A dose-response curve was prepared for the ratiometric E-sensor by monitoring the SWV peak current ratio between the MB current and the Fc current ( $I_{MB}/I_{Fc}$ ) after Target T detection. Such analyses provide a complement to measurements of the absolute MB current value ( $I_{MB}$ ) or the relative current ( $I_{MB}/(I_{MB})^{\circ}$ ). They are attractive because they are potentially more reproducible. To construct these curves, data were collected using different electrodes. As can be seen from an inspection of Figures 3.6A and 3.6B, the response varied in a log-linear fashion with the target concentration, as expected. Target T concentrations from 50 pM to 1  $\mu$ M could be measured, with the highest ratio signal suppression being around 50% from the background and an overall  $R^2 = 0.997$ . The detection limit (LOD) at a signal-to-noise ratio of 3 was calculated to be 25.1 pM,

comparable with the non-ratiometric or classic E-DNA sensor.<sup>6</sup> However, in contrast to this latter classic approach, control studies carried out using just the signal probe MB ( $I_{MB}$ ) revealed relatively large standard deviations and an overall  $R^2$  of 0.958, although peak current suppression with increasing target concentration was seen (Figures 3.6C and 3.6D). The lower reliability observed with the control system is ascribed to the variance in the background signal ( $I_{MB}$ )<sup>o</sup> discussed above (cf. Figure 3.3B).

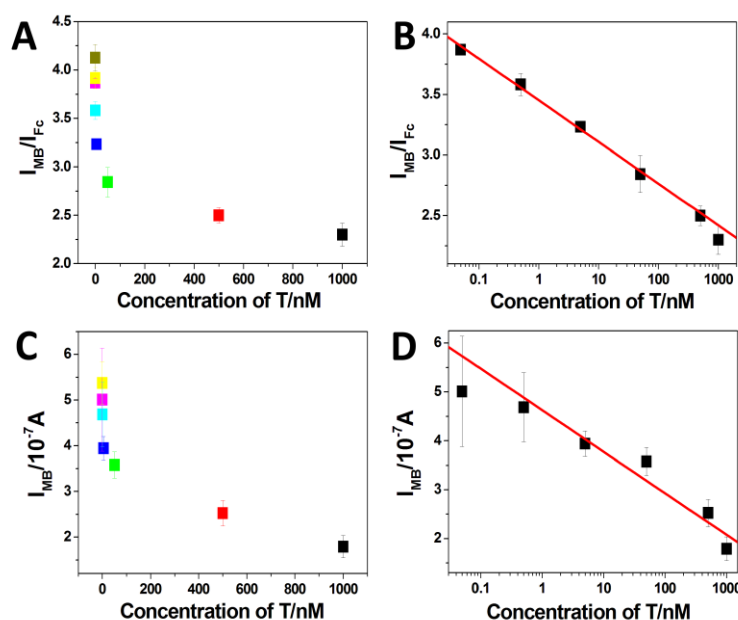


**Figure 3.6** Concentration dependence of Target T as observed using ratiometric E-sensors and non-ratiometric E-sensors. **A)** Concentration dependence of Target T based on the ratio  $I_{MB}/I_{Fc}$ . **B)** Concentration dependence of Target T represented by a log-linear plot of  $I_{MB}/I_{Fc}$ . **C)** Concentration dependence of Target T based on  $I_{MB}$ . **D)** Concentration dependence of Target T represented by log-linear plot of  $I_{MB}$ . The error bars are standard deviations of measurements based on three independent experiments.



### 3.2.4 Detection of mismatched oligonucleotides

In order to ensure that the signals observed were due to the specific hybridization of Target T to the probe sequence (Probe P), a series of control experiments were carried out with non-complementary DNA (Non-T), and with targets containing 1 to 4 mismatches (T-SNP1, T-SNP2, T-SNP3, and T-SNP4). The targets that contained three or more mismatches produced no observable interactions with Probe P, while single and double mismatches gave signals smaller than the completely matched target (Figure 3.7A). As with non-ratiometric E-sensors, it is anticipated that long targets will yield larger signal changes than shorter targets, but that the specificity of long targets will be poorer than that of shorter targets.<sup>27</sup>

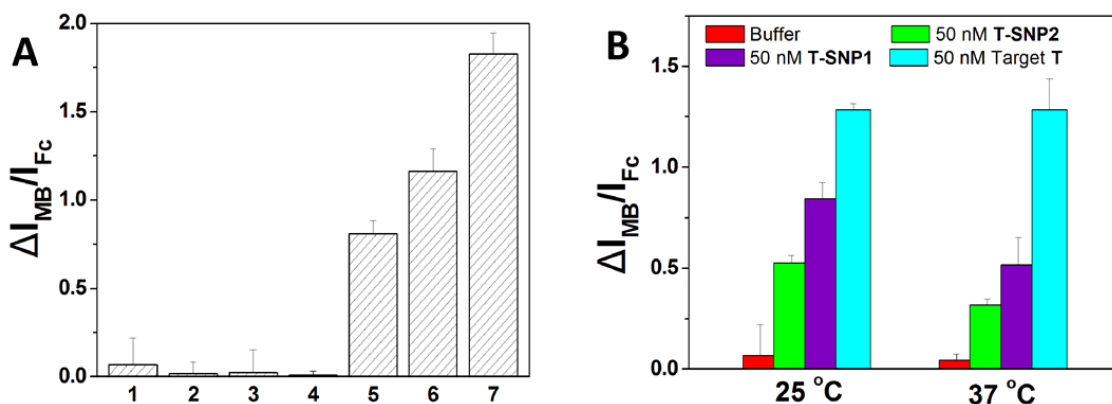


**Figure 3.7** Selectivity of the ratiometric E-sensor. **A)** Transduction by Probe P with a series of matched and mismatched targets at 25 °C. Buffer only (1), 1  $\mu$ M Non-T (2), 1  $\mu$ M T-SNP4 (4 mismatches) (3), 1  $\mu$ M T-SNP3 (3 mismatches) (4), 1  $\mu$ M T-SNP2 (2 mismatches) (5), 1  $\mu$ M T-SNP1 (1 mismatch) (6), and correctly paired Target T (7). **B)** Selectivity at different temperatures. T-SNP1 and T-SNP2 contain 1 and 2 mismatches relative to Target T, respectively.

More quantitatively, the single-base mismatch discrimination factor can be defined as the ratio of the decrease in signal with a perfectly paired target ( $\Delta I_{MB}/I_{Fc}$ ) versus that seen with a mismatched target. The larger the discrimination factor is, the better the

specificity for single-base mismatch will be. The discrimination factor, for the single-base mismatched sequence T-SNP1 was 1.60 at 25 °C. Increasing the temperature should increase the level of discrimination.<sup>28-29</sup> In the present instance, increasing the temperature to 37 °C, resulted in a discrimination value of 2.50 (Figure 3.7B). These latter values are comparable to those obtained with E-sensors,<sup>7</sup> where a discrimination factor of 2.33 was noted. However, our internally controlled, double redox sensor shows mismatch discrimination comparable to fluorescence methods (discrimination factor of 2.18),<sup>30</sup> and somewhat better than similar experiments that have been reported in the context of electrochemistry (1.67),<sup>31</sup> colorimetry (1.33),<sup>32</sup> surface plasmon resonance (1.67),<sup>33</sup> quartz crystal microbalance (1.22),<sup>33</sup> or surface-enhanced Raman scattering (1.33) sensing.<sup>34</sup> Based on prior studies, it is anticipated that additional mutation discrimination could likely be obtained by manipulating salt concentrations and other buffer components.<sup>35</sup> Optimization efforts along these latter lines are in progress.

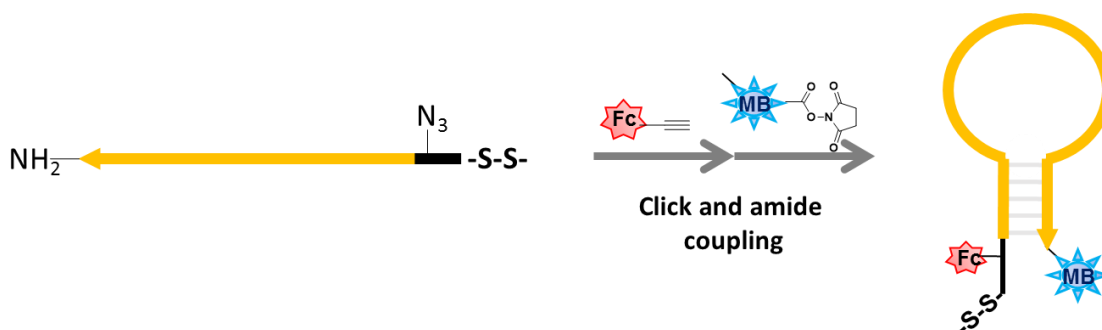
### **3.3 CURRENT AND FUTURE WORKS**

#### **3.3.1 Simple dual-labeling of MB and Fc by post-synthetic modifications**

We have performed the both of oligonucleotide synthesis and enzymatic ligation to synthesize the E-sensor probe with both of MB and Fc. This methodology requires laborious multi-step synthesis and purification even though the MB-attached oligonucleotide was obtained from commercial source (see scheme 3.1). This disadvantage may be troublesome in application to practical devices with the E-sensor despite the improved reproducibility and sensitivity. Another issue is the performance of the Fcs for reference probes, which was multi-incorporated on the E-sensor oligonucleotide in order to provide clear signal to detect as described in Chapter 2. This also reduces the efficiency

of the solid-phase oligonucleotide synthesis with more time and cost due to synthesis of Fc-modified phosphoramidite (**2.23**).

To overcome this, we designed new E-sensor oligonucleotide synthesized by two post-synthetic modifications with a dual-functionalized oligonucleotide (Scheme 3.2). First, the oligonucleotide with two functional groups for conjugation reactions, amine and amide coupling, will be prepared by oligonucleotide synthesis or commercial source. The following sequential conjugation with a Fc-alkyne (i.e. **2.1** - **2.8**) and MB-NHS will yield the desired E-sensor oligonucleotide. As mentioned in Chapter 2.3.2, one Fc is expected to show clear current peak to function as a reference probe. We expect this synthetic way will effectively reduce the time and cost for the double modifications and enzyme ligation.



**Scheme 3.2** Duel-labeling of the ratiometric E-sensor via post-synthetic modification.

### 3.4 CONCLUSION

In conclusion, we have developed a novel ratiometric method that greatly improves the performance of E-sensors. By importing an internal control redox probe into the sensing platform, we have overcome a disadvantage of electrochemical DNA sensors, namely irreproducibility, and have done so without loss of sensitivity or selectivity. An additional potential advantage of the MB/Fc approach detailed here is that the current ratio prior to

target binding can be used as a positive control to validate electrode function. This is useful since drastic variations in the baseline ratio over time can be indicative of a faulty electrode.

It is likely that this advance can also be applied to other types of E-sensors, including those based on aptamer refolding in the presence of a ligand.<sup>3, 22-23, 25, 36-40</sup> Efforts are currently being made to extrapolate the present approach in such directions. The key point is that in any configuration, the analyte-dependent signal can be read out directly by simply calculating the current ratio between MB and Fc (or some other appropriate redox probe). In other words, even if the change in the relative current response cannot be readily predicted (or correlated accurately with target concentration), the change in the current ratio will be indicative of target binding. We thus deem the approach described here as useful and attractive as a potentially generalizable approach to oligonucleotide sensor development.

### 3.5 REFERENCES

1. Drummond, T. G.; Hill, M. G.; Barton, J. K., Electrochemical DNA sensors. *Nat Biotechnol* **2003**, *21* (10), 1192-1199.
2. Willner, I.; Zayats, M., Electronic aptamer-based sensors. *Angew Chem Int Edit* **2007**, *46* (34), 6408-6418.
3. Li, D.; Song, S. P.; Fan, C. H., Target-Responsive Structural Switching for Nucleic Acid-Based Sensors. *Accounts of Chemical Research* **2010**, *43* (5), 631-641.
4. Tyagi, S.; Landegren, U.; Tazi, M.; Lizardi, P. M.; Kramer, F. R., Extremely sensitive, background-free gene detection using binary probes and Q beta replicase. *P Natl Acad Sci USA* **1996**, *93* (11), 5395-5400.
5. Huang, T. J.; Liu, M. S.; Knight, L. D.; Grody, W. W.; Miller, J. F.; Ho, C. M., An electrochemical detection scheme for identification of single nucleotide polymorphisms using hairpin-forming probes. *Nucleic Acids Res* **2002**, *30* (12).
6. Fan, C. H.; Plaxco, K. W.; Heeger, A. J., Electrochemical interrogation of conformational changes as a reagentless method for the sequence-specific detection of DNA. *P Natl Acad Sci USA* **2003**, *100* (16), 9134-9137.
7. Immoos, C. E.; Lee, S. J.; Grinstaff, M. W., Conformationally gated electrochemical gene detection. *ChemBiochem* **2004**, *5* (8), 1100-1103.

8. Xiao, Y.; Lubin, A. A.; Baker, B. R.; Plaxco, K. W.; Heeger, A. J., Single-step electronic detection of femtomolar DNA by target-induced strand displacement in an electrode-bound duplex. *P Natl Acad Sci USA* **2006**, *103* (45), 16677-16680.
9. Wu, J. K.; Huang, C. H.; Cheng, G. F.; Zhang, F.; He, P. G.; Fang, Y. Z., Electrochemically active-inactive switching molecular beacon for direct detection of DNA in homogenous solution. *Electrochem Commun* **2009**, *11* (1), 177-180.
10. Liu, G.; Wan, Y.; Gau, V.; Zhang, J.; Wang, L. H.; Song, S. P.; Fan, C. H., An enzyme-based E-DNA sensor for sequence-specific detection of femtomolar DNA targets. *J Am Chem Soc* **2008**, *130* (21), 6820-6825.
11. Jenkins, D. M.; Chami, B.; Kreuzer, M.; Presting, G.; Alvarez, A. M.; Liaw, B. Y., Hybridization probe for femtomolar quantification of selected nucleic acid sequences on a disposable electrode. *Anal Chem* **2006**, *78* (7), 2314-2318.
12. Yin, H. S.; Zhou, Y. L.; Zhang, H. X.; Meng, X. M.; Ai, S. Y., Electrochemical determination of microRNA-21 based on graphene, LNA integrated molecular beacon, AuNPs and biotin multifunctional bio bar codes and enzymatic assay system. *Biosens Bioelectron* **2012**, *33* (1), 247-253.
13. Liu, C.; Zeng, G. M.; Tang, L.; Zhang, Y.; Li, Y. P.; Liu, Y. Y.; Li, Z.; Wu, M. S.; Luo, J., Electrochemical detection of *Pseudomonas aeruginosa* 16S rRNA using a biosensor based on immobilized stem-loop structured probe. *Enzyme Microb Tech* **2011**, *49* (3), 266-271.
14. Hsieh, K. W.; Patterson, A. S.; Ferguson, B. S.; Plaxco, K. W.; Soh, H. T., Rapid, Sensitive, and Quantitative Detection of Pathogenic DNA at the Point of Care through Microfluidic Electrochemical Quantitative Loop-Mediated Isothermal Amplification. *Angew Chem Int Edit* **2012**, *51* (20), 4896-4900.
15. Xuan, F.; Luo, X. T.; Hsing, I. M., Ultrasensitive Solution-Phase Electrochemical Molecular Beacon-Based DNA Detection with Signal Amplification by Exonuclease III-Assisted Target Recycling. *Anal Chem* **2012**, *84* (12), 5216-5220.
16. Miranda-Castro, R.; De-Los-Santos-Alvarez, P.; Lobo-Castanon, M. J.; Miranda-Ordieres, A. J.; Tunon-Blanco, P., Hairpin-DNA probe for enzyme-amplified electrochemical detection of *Legionella pneumophila*. *Anal Chem* **2007**, *79* (11), 4050-4055.
17. Gao, W. C.; Dong, H. F.; Lei, J. P.; Ji, H. X.; Ju, H. X., Signal amplification of streptavidin-horseradish peroxidase functionalized carbon nanotubes for amperometric detection of attomolar DNA. *Chemical Communications* **2011**, *47* (18), 5220-5222.
18. Fang, X.; Jiang, W.; Han, X. W.; Zhang, Y. Z., Molecular beacon based biosensor for the sequence-specific detection of DNA using DNA-capped gold nanoparticles-streptavidin conjugates for signal amplification. *Microchim Acta* **2013**, *180* (13-14), 1271-1277.
19. Bonham, A. J.; Hsieh, K.; Ferguson, B. S.; Vallee-Belisle, A.; Ricci, F.; Soh, H. T.; Plaxco, K. W., Quantification of Transcription Factor Binding in Cell Extracts Using an Electrochemical, Structure-Switching Biosensor. *J Am Chem Soc* **2012**, *134* (7), 3346-3348.

20. Xiao, Y.; Lai, R. Y.; Plaxco, K. W., Preparation of electrode-immobilized, redox-modified oligonucleotides for electrochemical DNA and aptamer-based sensing. *Nat Protoc* **2007**, *2* (11), 2875-2880.
21. Lubin, A. A.; Plaxco, K. W., Folding-Based Electrochemical Biosensors: The Case for Responsive Nucleic Acid Architectures. *Accounts of Chemical Research* **2010**, *43* (4), 496-505.
22. Baker, B. R.; Lai, R. Y.; Wood, M. S.; Doctor, E. H.; Heeger, A. J.; Plaxco, K. W., An electronic, aptamer-based small-molecule sensor for the rapid, label-free detection of cocaine in adulterated samples and biological fluids. *J Am Chem Soc* **2006**, *128* (10), 3138-3139.
23. Mir, M.; Jenkins, A. T. A.; Katakis, I., Ultrasensitive detection based on an aptamer beacon electron transfer chain. *Electrochem Commun* **2008**, *10* (10), 1533-1536.
24. Gong, H.; Zhong, T. Y.; Gao, L.; Li, X. H.; Bi, L. J.; Kraatz, H. B., Unlabeled Hairpin DNA Probe for Electrochemical Detection of Single-Nucleotide Mismatches Based on MutS-DNA Interactions. *Anal Chem* **2009**, *81* (20), 8639-8643.
25. Wu, D. H.; Zhang, Q.; Chu, X.; Wang, H. B.; Shen, G. L.; Yu, R. Q., Ultrasensitive electrochemical sensor for mercury (II) based on target-induced structure-switching DNA. *Biosens Bioelectron* **2010**, *25* (5), 1025-1031.
26. Yang, X.; Du, Y.; Li, D.; Lv, Z. Z.; Wang, E. K., One-step synthesized silver micro-dendrites used as novel separation mediums and their applications in multi-DNA analysis. *Chemical Communications* **2011**, *47* (38), 10581-10583.
27. Lubin, A. A.; Hunt, B. V. S.; White, R. J.; Plaxco, K. W., Effects of Probe Length, Probe Geometry, and Redox-Tag Placement on the Performance of the Electrochemical E-DNA Sensor. *Anal Chem* **2009**, *81* (6), 2150-2158.
28. Breslauer, K. J.; Frank, R.; Blocker, H.; Marky, L. A., Predicting DNA Duplex Stability from the Base Sequence. *P Natl Acad Sci USA* **1986**, *83* (11), 3746-3750.
29. Rychlik, W.; Spencer, W. J.; Rhoads, R. E., Optimization of the Annealing Temperature for DNA Amplification In vitro. *Nucleic Acids Res* **1990**, *18* (21), 6409-6412.
30. Lu, X. C.; Dong, X.; Zhang, K. Y.; Han, X. W.; Fang, X.; Zhang, Y. Z., A gold nanorods-based fluorescent biosensor for the detection of hepatitis B virus DNA based on fluorescence resonance energy transfer. *Analyst* **2013**, *138* (2), 642-650.
31. Bonanni, A.; Chua, C. K.; Zhao, G. J.; Sofer, Z.; Pumera, M., Inherently Electroactive Graphene Oxide Nanoplatelets As Labels for Single Nucleotide Polymorphism Detection. *Acs Nano* **2012**, *6* (10), 8546-8551.
32. Pylaev, T. E.; Khanadeev, V. A.; Khlebtsov, B. N.; Dykman, L. A.; Bogatyrev, V. A.; Khlebtsov, N. G., Colorimetric and dynamic light scattering detection of DNA sequences by using positively charged gold nanospheres: a comparative study with gold nanorods. *Nanotechnology* **2011**, *22* (28).
33. Altintas, Z.; Tothill, I. E., DNA-based biosensor platforms for the detection of TP53 mutation. *Sensor Actuat B-Chem* **2012**, *169*, 188-194.
34. Ganbold, E. O.; Kang, T.; Lee, K.; Lee, S. Y.; Joo, S. W., Aggregation effects of gold nanoparticles for single-base mismatch detection in influenza A (H1N1) DNA

sequences using fluorescence and Raman measurements. *Colloid Surface B* **2012**, *93*, 148-153.

35. Dirks, R. M.; Bois, J. S.; Schaeffer, J. M.; Winfree, E.; Pierce, N. A., Thermodynamic analysis of interacting nucleic acid strands. *Siam Rev* **2007**, *49* (1), 65-88.

36. Lu, Y.; Li, X. C.; Zhang, L. M.; Yu, P.; Su, L.; Mao, L. Q., Aptamer-based electrochemical sensors with aptamer-complementary DNA oligonucleotides as probe. *Anal Chem* **2008**, *80* (6), 1883-1890.

37. Radi, A. E.; O'Sullivan, C. K., Aptamer conformational switch as sensitive electrochemical biosensor for potassium ion recognition. *Chemical Communications* **2006**, (32), 3432-3434.

38. Zhang, Y. L.; Huang, Y.; Jiang, J. H.; Shen, G. L.; Yu, R. Q., Electrochemical aptasensor based on proximity-dependent surface hybridization assay for single-step, reusable, sensitive protein detection. *J Am Chem Soc* **2007**, *129* (50), 15448-+.

39. Zuo, X. L.; Song, S. P.; Zhang, J.; Pan, D.; Wang, L. H.; Fan, C. H., A target-responsive electrochemical aptamer switch (TREAS) for reagentless detection of nanomolar ATP. *J Am Chem Soc* **2007**, *129* (5), 1042-1043.

40. Hayashi, E.; Takada, T.; Nakamura, M.; Yamana, K., Electronic Aptamer-based Biosensor for Multiprotein Analytes on a Single Platform. *Chem Lett* **2010**, *39* (5), 454-455.

## **Chapter 4: Development of wearable devices based on E-sensor technologies for the detection of small molecules in sweat**

### **4.1 INTRODUCTION**

Sweat comprises one of the major fluids excreted by the human body with its main role acting as a method for regulating body temperature by evaporation of water. Interestingly, in recent years, sweat has been exploited in diagnostics.<sup>1-2</sup> For example, ions,<sup>3-6</sup> carbohydrates,<sup>7</sup> steroids,<sup>8</sup> and even peptides<sup>9</sup> have been detected to provide patient's health status. Moreover, sweat can contain residual drugs or metabolite<sup>10</sup>s due to passive diffusion of the molecules from blood to sweat gland.<sup>10-11</sup> These sweat diagnostics allow researchers or regulatory agencies to bypass invasive sampling to obtain patient's or subject's blood. As mentioned in chapter 1, electrochemical sensing has the advantage as a sensing platform due to high sensitivity, simplicity, and low cost. Furthermore, the miniaturization of the devices can perform 'real-time' monitoring of a target analyte via the combination with improved electronics, while the old-fashioned sweat diagnostics were based on collecting and extracting sweat samples for 'end-point' analysis.<sup>12-13</sup> Significant work has also been put towards developing wearable sensors for real-time monitoring of multiple analytes in one device.<sup>14-15</sup>

The current standard for existing wearable sensors are based upon ion-selective electrodes or enzyme reactions and the fabrication of the device requires high costs and efforts. Moreover, the target analytes have been limited to several ions (e.g. sodium,<sup>16</sup> potassium,<sup>15</sup> chloride<sup>17</sup> ions) and few organic compounds (e.g. glucose<sup>15</sup> and lactate<sup>18</sup>). To overcome these challenges, adoption of E-sensor based on DNA aptamer can be an excellent sensing platform for detection of a specific analyte. Many aptamers have already been developed to detect various target molecules, especially complex small and large molecules, which might prove difficult in attempting to find the corresponding enzyme or



selective electrode.<sup>19</sup> Another advantage is simple fabrication process for multiple sensing platform. Unlike the conventional sensors demand each manufacturing step for each analyte, all E-sensors are able to share the same steps for fabrications.

In this chapter, we describe the design and fabrication of a prototype wearable device based on E-sensors. To perform electrochemical analysis on the device, the three electrodes (i.e. working, counter, and reference electrode) were fabricated<sup>20</sup> on flexible solid support as shown in Figure 4.1: A) gold film on polyethylene terephthalate and thermal release tape (Au-PET-TRT, or APT) was laminated on the cutting mat; B) The designed patterns are carved by automated cutting machine; C) APT is peeled off from the cutting mat; D) Extra Au-PET layer was removed after deactivation the TRT for release of the film; E) The designed patterns were printed on target support. All fabrication works have been performed by Nanshu Lu's group in of Dept. of Aerospace Engineering and Engineering Mechanics at UT Austin.

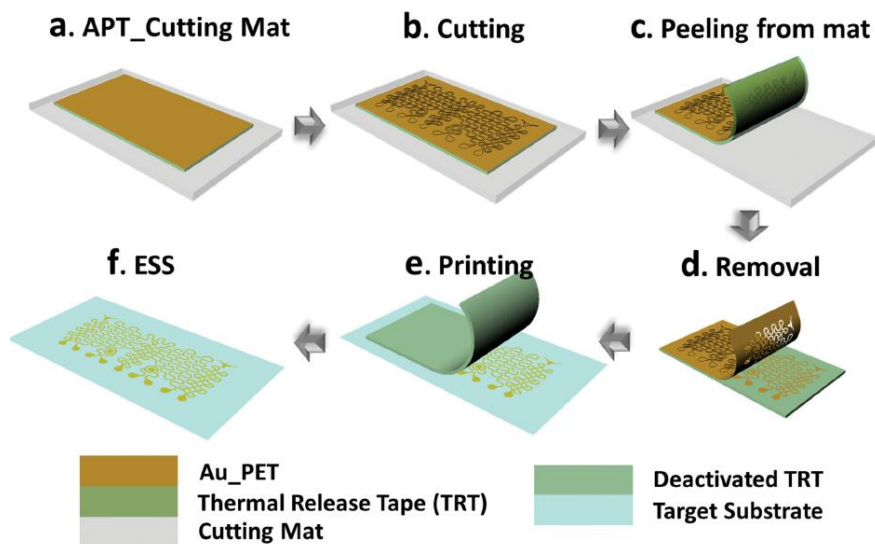


**Figure 4.1** Schematic process for the fabrication of wearable sensor. Adopted from ref. 20.

## 4.2 RESULT AND DISCUSSION

### 4.2.1 Device fabrication

To apply an E-sensor system to the wearable devices, we designed a prototype of the device with three electrodes on a wearable support to perform conventional electrochemical analysis (Figure 4.2). All design of the devices was performed by the author and the actual fabrications were carried out by Lu's group. The solid support was prepared from a commercially available sticky tape (3M removal silicone tape, KRST), which is sticky and flexible enough to stick and stay on the epidermal surface.<sup>20</sup> At first, a working electrode (WE) was patterned by gold film for immobilization of E-sensor oligonucleotide per a usual E-sensor system. A counter electrode (CE) was fabricated with the working electrode at the same time for easy process and chemical inertness of gold. Silver metal film was pasted on the support as a pseudo-reference electrode (PRE), which does not provide a thermodynamically constant reference potential but is predictable in specific conditions.<sup>21</sup> The first prototype design can be found in Figure 4.2B. In this system, the electrodes had an arrow shape with a circle tip at the functioning area as an electrode and a larger horseshoe-shaped interface area at the other end as an interface between the device and potentiostat.

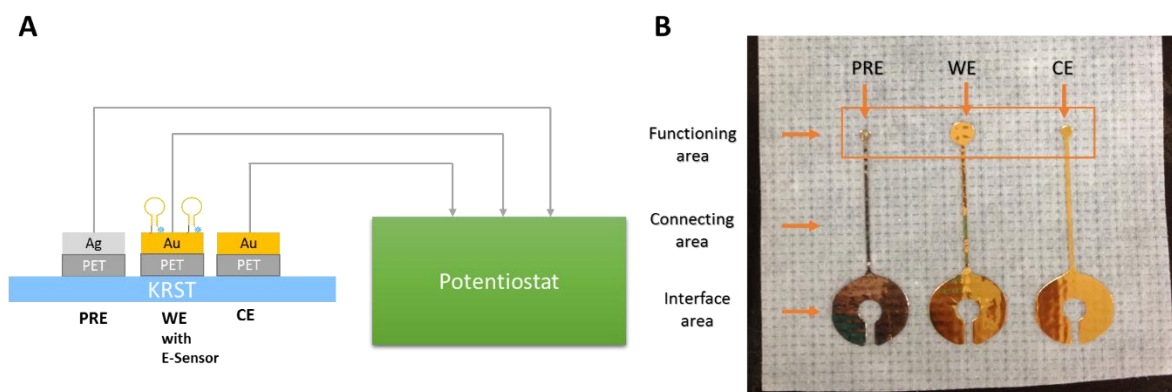


**Figure 4.2** Schematic design (A) and the first prototype (B) of the epidermal wearable device fabricated by Lu's group.

After the fabrication of the device, the connecting and functioning area were immersed in  $\text{K}_2\text{Fe}(\text{CN})_6/\text{K}_3\text{Fe}(\text{CN})_6$  in PBS solution and linear sweep voltammetry was carried out in order to test whether the pasted metal electrodes work properly. However, the device did not function over the potential of 0.6 V in positive sweep, as shown in figure 4.3A. We also found the metal film of the working and counter electrodes were peeled off and dissociated into the buffer solution (Figure 4.3B).

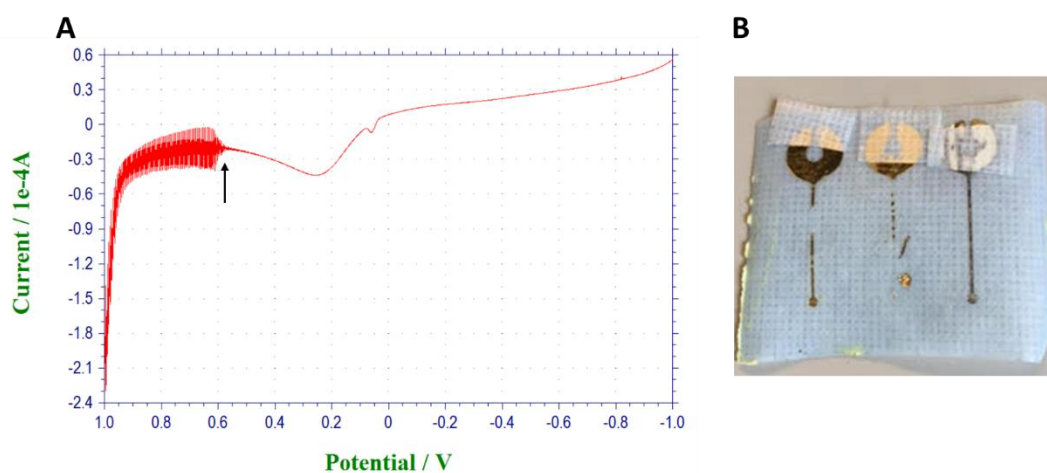


**Figure 4.3** (A) Linear sweep voltammetry of the first prototype device with  $\text{Fe}(\text{CN})_6^{3-}/\text{Fe}(\text{CN})_6^{4-}$  in PBS. The arrow shows a collapsing of the electrodes. (B) The electrodes were peeled off the device after the experiment

We thus designed and fabricated a second-generation model to solve the problems (Figure 4.4). At first, we covered a silicone rubber film on the connecting area to attach the area on the support more tightly<sup>22</sup> as well as to insulate the metal films from the conducting buffer solution except for the functioning areas. In addition, the functioning and connecting areas were broadened to make them more robust from electric current.



**Figure 4.4** The second-generation of the device fabricated by Lu's group.

The new device was then tested by CV at the same solution (Figure 4.5). The redox coupling of  $\text{Fe}(\text{CN})^{3-}/\text{Fe}(\text{CN})^{4-}$  were clearly detected with peak currents with  $E_{1/2}$  around 150 mV. By utilizing silver metal as a pseudo-reference, this value is slightly decreased when compared to measurement with Ag/AgCl reference electrode (around 300 mV, data not shown here).<sup>21</sup> We also tested the available potential range of device by the varied scanning in the positive and negative direction. As shown in figure 4.5, the device shows similar pattern with a conventional gold-disk electrode, which provides available range from 0.8 V to -0.8 V.<sup>23</sup> Thus, we concluded that the device has a potential use for the platform wherein the conventional electrochemical analyses have been performed.

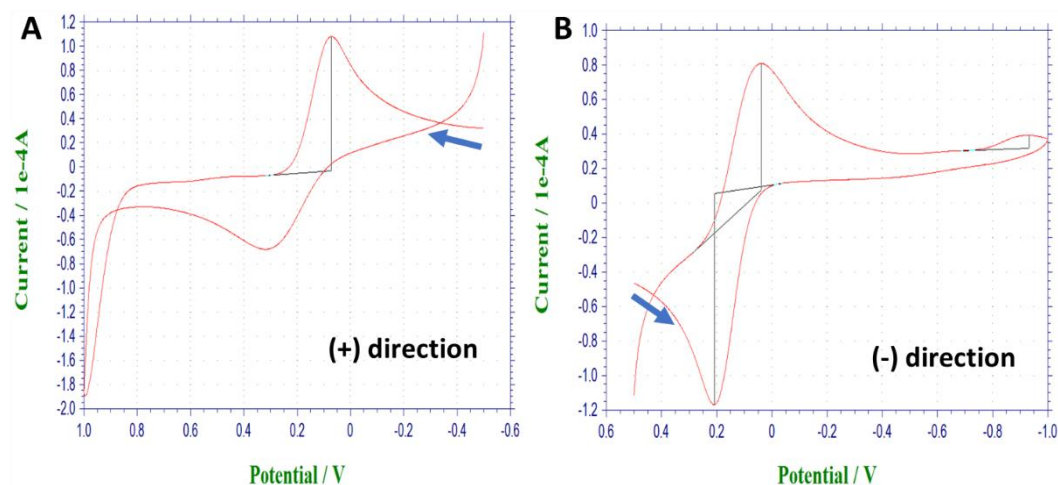


**Figure 4.5** CV of the device with  $\text{Fe(CN)}_6^{3-}/\text{Fe(CN)}_6^{4-}$  in PBS. Each arrow shows the direction of potential sweep A) positive and B) negative, respectively.

#### 4.2.2 Sensing of oligonucleotide sequence

Initial experiments in oligonucleotide sensing was put towards the detection of a complementary DNA sequence. Following the E-sensor construction procedure in Chapter 2 and 3, the E-sensor sequence with MB probe was immobilized on the gold working electrode using a thiol-gold interaction (Figure 4.6A). Upon incubating in the dark overnight (Figure 4.6B), the working electrode was treated with 6-mercaptohexanol to construct a SAM. The device was then wrapped around a conical tube submerged in a target solution diluted in PBS for hybridization between the E-sensor DNA and the target DNA (Figure 4.6C). After the reaction, the device was connected with a potentiostat for electrochemical measurements (Figure 4.6D). The sequences used in the work are shown in table 4.1.

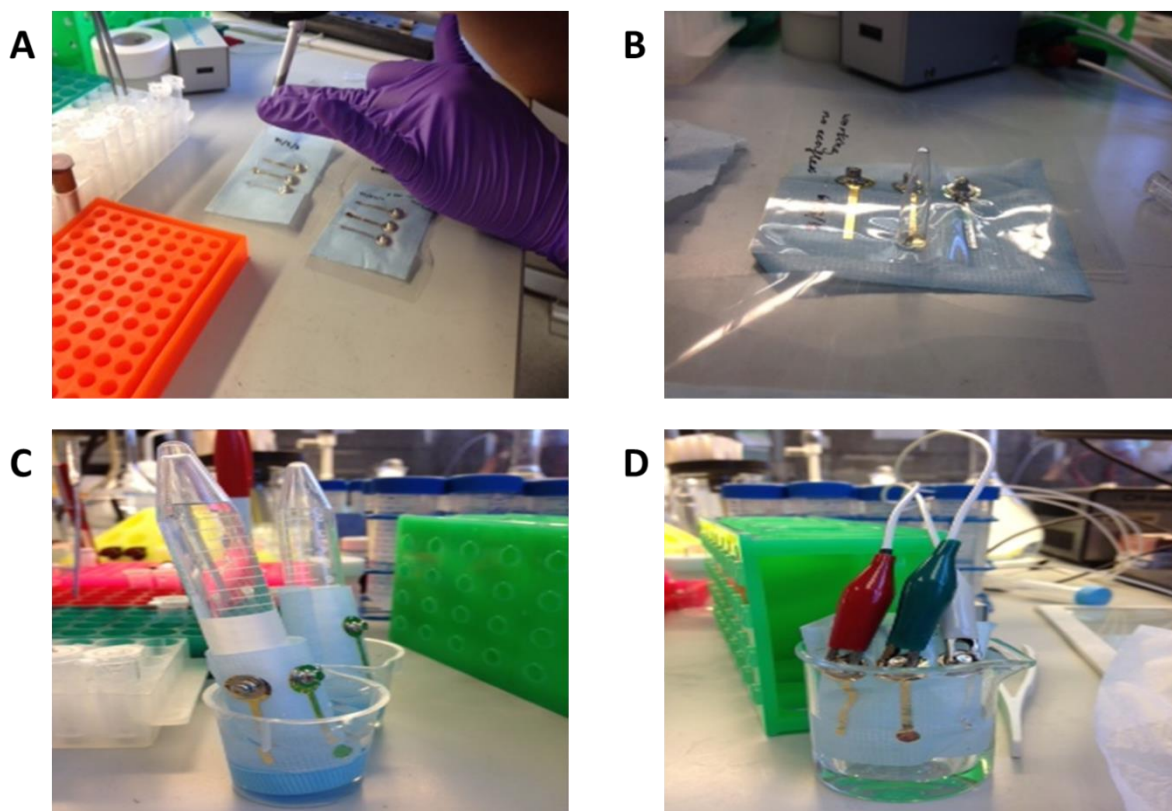


**Figure 4.6** Construction process of wearable device with E-sensor

**Table 4.1** Sequence of oligonucleotides used in this work (MB: methylene blue, SH: thiol modifier, X: random base)

Name	Sequence (5' to 3')
<b>E-sensor sequence</b>	<b>SH- TTACTCTC GATCGGCGTTTGA GAGAGG -MB</b>
<b>Target sequence</b>	TAAACGCCGATC
<b>Random sequence</b>	XXXXXXXXXXXXXX
<b>Cocaine E-sensor</b>	<b>SH- AGACAAGGAAAATCCTTCAATGAAGTGGGTCG - MB</b>

As expected, the E-sensor adopted device showed good performance for DNA sequence detection. Since ACV showed the highest current peak among several voltammetric analysis (data not shown here), we obtained the ACV curve from the device after the E-sensor construction (Figure 4.7, blue line). The peak current was  $4.57 \times 10^{-7}$  A at around -0.35 V, which is comparable to conventional gold disk electrode (see Chapter



3).<sup>24</sup> This work serves to demonstrate the utility of immobilizing the E-sensor DNA on the working electrode.

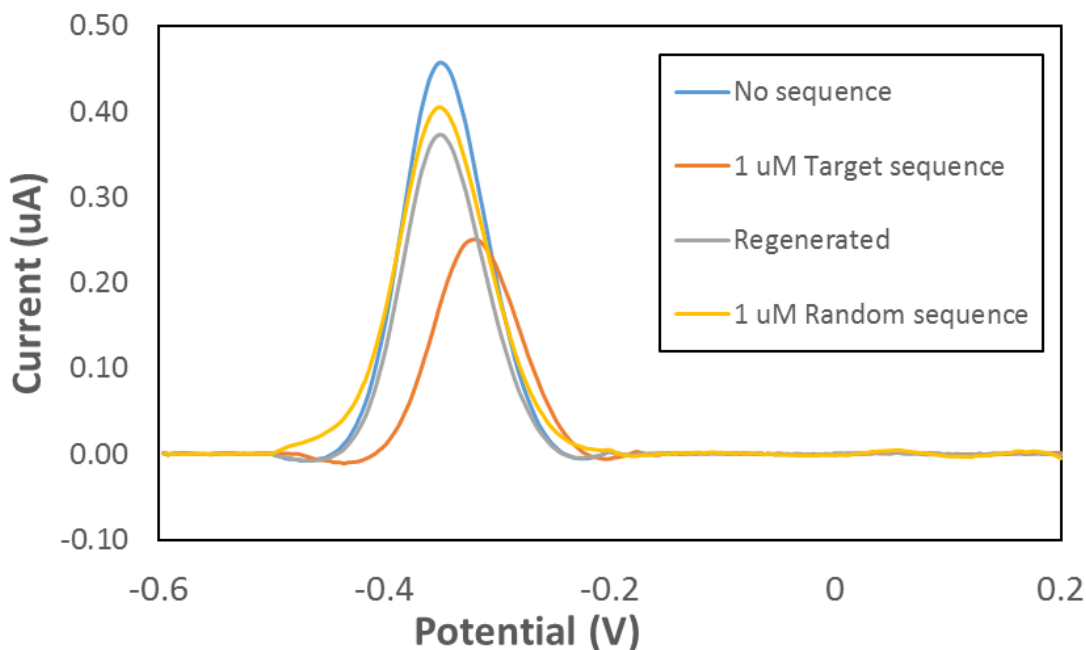


**Figure 4.7** ACV of the device for oligonucleotide detection.

The complementary target sequence was then added to the device. As conventional E-sensors using a gold disk electrode, the signal decreased 47 % (from  $4.57$  to  $2.50 \times 10^{-7}$  A), and shows a concomitant conformational change of the E-sensor sequence on the device. As a control study, we thus tested the measurement with random sequence DNA (yellow line in Figure 4.7) to confirm the signal decrease with target sequence caused by the hybridization between the target and E-sensor sequences. The device was regenerated by washing the target sequence for the application to reusable sensor and real-time monitoring. The peak current was returned close to baseline (gray line in Figure 4.7). We attribute this incomplete recovery to the destruction of E-sensor on the working electrode

in the washing step because the boundary of the electrode is not completely defined like as conventional electrode surrounded by insulating polymer.

### **4.3 CURRENT AND FUTURE WORKS**

#### **4.3.1 Sensing of cocaine with aptamer based E-sensor**

In an attempt to expand upon previous work, we are trying to develop a device based on DNA-aptamer technologies for the real-world applications to physiological target detection. Owing to its simplicity and readily available aptamers, we chose a commonly used psychotropic drug, cocaine, as a sensing target for a first attempt due to its importance in clinical and forensic analysis.

We adopted the cocaine E-sensor reported by Plaxco et al. (see table 4.1)<sup>25</sup> and fabricated the E-sensor with our device. Since handling cocaine requires a license from Federal Drug Enforcement Agency (DEA), a benzoylecgonine solution, which showed slightly less binding affinity to the aptamer, was used as target sample. The cocaine E-sensor was immobilized on the fabricated device as following the same procedure for the DNA sequence detection. The device was then immersed in benzoylecgonine solution (Figure 4.8).



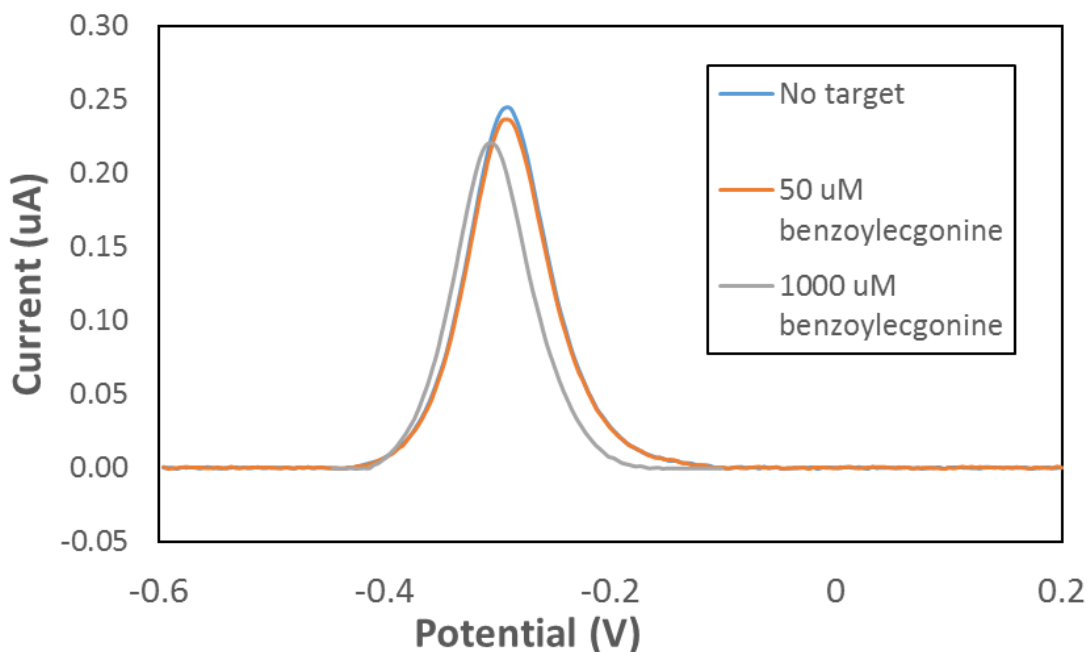


**Figure 4.8** ACV of the device for benzoylecgonine detection.

In line with previous reports, the peak current was expected to increase with the ligand due to conformational change of the DNA aptamer. However, in our system, there was no significant change in the peak current. In fact, it was even shown to decrease upon incubation with a more concentrated solution. We propose the concentration of the target molecule was not high enough to increase the signal based on the high dissociation constant ( $K_d = \sim 100$  uM) of the aptamer towards cocaine and even lower for benzoylecgonine.<sup>26-27</sup> Due to the lack of Schedule 1 DEA license, we could not perform the experiment with higher concentration.

#### 4.3.2. Sensing of aminoglycoside antibiotics

In addition, we are aiming to apply our device to detection of aminoglycoside species such as kanamycin and tobramycin in perspiration. These drugs have been widely

administered to patients in hospitals, however this has not been without adverse effects. In spite of the excellent antibacterial properties, it is always a concern that over use of the drugs may cause severe side-effects as well as produce drug-resistant pathogens.<sup>28</sup> To prevent these issues, researchers have tried to investigate the minimum dose of the drugs and optimize the administration. Monitoring the concentration and any metabolites is essential in the optimization dosing any medication.<sup>28-30</sup> However, to date, common monitoring procedure for the drugs requires invasive blood sampling from the patients.<sup>31-32</sup>

Excretions of some antibiotics from sweat glands is already reported.<sup>33,34</sup> Interestingly, the excreted drugs have been suspected one of culprits of development of antibiotic resistance in hospitals.<sup>33</sup> For these reasons, it is expected that monitoring of the aminoglycosides in sweat is potentially able to substitute blood test, as well as elucidate the mechanism of the hospital acquired infections.

To construct the sensing device, we are currently in fabrication of a wearable device detecting aminoglycosides. Since the aptamers for the drugs were already reported<sup>31-32</sup>, we are currently testing the aptamer-based E-sensor using conventional three electrodes system and the device fabrication will follow.

#### **4.4 CONCLUSION**

In conclusion, we have designed and fabricated wearable devices for electrochemical detection of biological analytes. As a prototype platform for the device, the three electrodes system was constructed on a polymer support with gold and silver metals and the E-sensor DNA was immobilized on the working electrode. The disclosed device showed promising results in oligonucleotide detection, thus warranting further studies in potential E-sensor applications. Currently, we are applying the device for

detection of aminoglycoside antibiotics using the corresponding aptamer E-sensor. It is expected the device will enable the construction of platforms to diagnose various analytes in sweat via non-invasive sampling.

#### 4.5 REFERENCES

1. Heikenfeld, J., Non-invasive Analyte Access and Sensing through Eccrine Sweat: Challenges and Outlook circa 2016. *Electroanalysis* **2016**, 28 (6), 1242-1249.
2. Jadoon, S.; Karim, S.; Akram, M. R.; Kalsoom Khan, A.; Zia, M. A.; Siddiqi, A. R.; Murtaza, G., Recent Developments in Sweat Analysis and Its Applications. *International Journal of Analytical Chemistry* **2015**, 2015, 7.
3. Rosenstein, B. J.; Cutting, G. R., The diagnosis of cystic fibrosis: A consensus statement. *The Journal of Pediatrics* **1998**, 132 (4), 589-595.
4. Das, A. K.; Chakraborty, R.; Luisa Cervera, M.; de la Guardia, M., Metal speciation in biological fluids — a review. *Microchimica Acta* **1996**, 122 (3), 209-246.
5. Souza, A. P. R. d.; Lima, A. S.; Salles, M. O.; Nascimento, A. N.; Bertotti, M., The use of a gold disc microelectrode for the determination of copper in human sweat. *Talanta* **2010**, 83 (1), 167-170.
6. Velez, A. M. A.; Warfvinge, G.; Herrera, W. L.; Velez, C. E. A.; Montoya, F. M.; Hardy, D. M.; Bollag, W. B.; Hashimoto, K., Detection of mercury and other undetermined materials in skin biopsies of endemic pemphigus foliaceus. *Am J Dermatopath* **2003**, 25 (5), 384-391.
7. Srinivasan, V.; Pamula, V. K.; Fair, R. B., An integrated digital microfluidic lab-on-a-chip for clinical diagnostics on human physiological fluids. *Lab on a Chip* **2004**, 4 (4), 310-315.
8. Jia, M.; Chew, W. M.; Feinstein, Y.; Skeath, P.; Sternberg, E. M., Quantification of cortisol in human eccrine sweat by liquid chromatography - tandem mass spectrometry. *Analyst* **2016**, 141 (6), 2053-2060.
9. Schitteck, B.; Hipfel, R.; Sauer, B.; Bauer, J.; Kalbacher, H.; Stevanovic, S.; Schirle, M.; Schroeder, K.; Blin, N.; Meier, F.; Rassner, G.; Garbe, C., Dermcidin: a novel human antibiotic peptide secreted by sweat glands. *Nat Immunol* **2001**, 2 (12), 1133-1137.
10. Kidwell, D. A.; Holland, J. C.; Athanaselis, S., Testing for drugs of abuse in saliva and sweat. *Journal of Chromatography B: Biomedical Sciences and Applications* **1998**, 713 (1), 111-135.
11. Preston, K. L.; Huestis, M. A.; Wong, C. J.; Umbricht, A.; Goldberger, B. A.; Cone, E. J., Monitoring Cocaine Use in Substance-Abuse-Treatment Patients by Sweat and Urine Testing. *Journal of Analytical Toxicology* **1999**, 23 (5), 313-322.
12. Bandodkar, A. J.; Jeerapan, I.; Wang, J., Wearable Chemical Sensors: Present Challenges and Future Prospects. *ACS Sensors* **2016**, 1 (5), 464-482.

13. Bandodkar, A. J.; Wang, J., Non-invasive wearable electrochemical sensors: a review. *Trends in Biotechnology* **2014**, *32* (7), 363-371.
14. Lee, H.; Choi, T. K.; Lee, Y. B.; Cho, H. R.; Ghaffari, R.; Wang, L.; Choi, H. J.; Chung, T. D.; Lu, N.; Hyeon, T.; Choi, S. H.; Kim, D.-H., A graphene-based electrochemical device with thermoresponsive microneedles for diabetes monitoring and therapy. *Nat Nano* **2016**, *11* (6), 566-572.
15. Gao, W.; Emaminejad, S.; Nyein, H. Y. Y.; Challa, S.; Chen, K.; Peck, A.; Fahad, H. M.; Ota, H.; Shiraki, H.; Kiriya, D.; Lien, D.-H.; Brooks, G. A.; Davis, R. W.; Javey, A., Fully integrated wearable sensor arrays for multiplexed in situ perspiration analysis. *Nature* **2016**, *529* (7587), 509-514.
16. Schazmann, B.; Morris, D.; Slater, C.; Beirne, S.; Fay, C.; Reuveny, R.; Moyna, N.; Diamond, D., A wearable electrochemical sensor for the real-time measurement of sweat sodium concentration. *Analytical Methods* **2010**, *2* (4), 342-348.
17. Gonzalo-Ruiz, J.; Mas, R.; de Haro, C.; Cabruja, E.; Camero, R.; Alonso-Lomillo, M. A.; Muñoz, F. J., Early determination of cystic fibrosis by electrochemical chloride quantification in sweat. *Biosensors and Bioelectronics* **2009**, *24* (6), 1788-1791.
18. Khodagholy, D.; Curto, V. F.; Fraser, K. J.; Gurfinkel, M.; Byrne, R.; Diamond, D.; Malliaras, G. G.; Benito-Lopez, F.; Owens, R. M., Organic electrochemical transistor incorporating an ionogel as a solid state electrolyte for lactate sensing. *Journal of Materials Chemistry* **2012**, *22* (10), 4440-4443.
19. Kim, D.; Pushkarsky, I.; Tay, A.; Di Carlo, D., Research highlights: aptamers on a chip. *Lab on a Chip* **2015**, *15* (7), 1630-1633.
20. Yang, S.; Chen, Y.-C.; Nicolini, L.; Pasupathy, P.; Sacks, J.; Su, B.; Yang, R.; Sanchez, D.; Chang, Y.-F.; Wang, P.; Schnyer, D.; Neikirk, D.; Lu, N., "Cut-and-Paste" Manufacture of Multiparametric Epidermal Sensor Systems. *Advanced Materials* **2015**, *27* (41), 6423-6430.
21. Bard, A. J.; Faulkner, L. R., *Electrochemical methods : fundamentals and applications*. 2nd ed.; Wiley: New York, 2001; p xxi.
22. Kim, D.-H.; Lu, N.; Ma, R.; Kim, Y.-S.; Kim, R.-H.; Wang, S.; Wu, J.; Won, S. M.; Tao, H.; Islam, A.; Yu, K. J.; Kim, T.-i.; Chowdhury, R.; Ying, M.; Xu, L.; Li, M.; Chung, H.-J.; Keum, H.; McCormick, M.; Liu, P.; Zhang, Y.-W.; Omenetto, F. G.; Huang, Y.; Coleman, T.; Rogers, J. A., Epidermal Electronics. *Science* **2011**, *333* (6044), 838.
23. Trasatti, S.; Petrii, O. A., Real surface area measurements in electrochemistry. *Journal of Electroanalytical Chemistry* **1992**, *327* (1-2), 353-376.
24. Kang, D.; Zuo, X.; Yang, R.; Xia, F.; Plaxco, K. W.; White, R. J., Comparing the Properties of Electrochemical-Based DNA Sensors Employing Different Redox Tags. *Analytical chemistry* **2009**, *81* (21), 9109-9113.
25. Baker, B. R.; Lai, R. Y.; Wood, M. S.; Doctor, E. H.; Heeger, A. J.; Plaxco, K. W., An Electronic, Aptamer-Based Small-Molecule Sensor for the Rapid, Label-Free Detection of Cocaine in Adulterated Samples and Biological Fluids. *Journal of the American Chemical Society* **2006**, *128* (10), 3138-3139.

26. Stojanovic, M. N.; de Prada, P.; Landry, D. W., Aptamer-Based Folding Fluorescent Sensor for Cocaine. *Journal of the American Chemical Society* **2001**, *123* (21), 4928-4931.
27. Swensen, J. S.; Xiao, Y.; Ferguson, B. S.; Lubin, A. A.; Lai, R. Y.; Heeger, A. J.; Plaxco, K. W.; Soh, H. T., Continuous, Real-Time Monitoring of Cocaine in Undiluted Blood Serum via a Microfluidic, Electrochemical Aptamer-Based Sensor. *Journal of the American Chemical Society* **2009**, *131* (12), 4262-4266.
28. Hammett-Stabler, C. A.; Johns, T., Laboratory guidelines for monitoring of antimicrobial drugs. *Clinical Chemistry* **1998**, *44* (5), 1129.
29. Prescott, W. A.; Nagel, J. L., Extended-Interval Once-Daily Dosing of Aminoglycosides in Adult and Pediatric Patients with Cystic Fibrosis. *Pharmacotherapy: The Journal of Human Pharmacology and Drug Therapy* **2010**, *30* (1), 95-108.
30. Hilmer, S. N.; Tran, K.; Rubie, P.; Wright, J.; Gnjjidic, D.; Mitchell, S. J.; Matthews, S.; Carroll, P. R., Gentamicin pharmacokinetics in old age and frailty. *British Journal of Clinical Pharmacology* **2011**, *71* (2), 224-231.
31. Ferguson, B. S.; Hoggarth, D. A.; Maliniak, D.; Ploense, K.; White, R. J.; Woodward, N.; Hsieh, K.; Bonham, A. J.; Eisenstein, M.; Kippin, T. E.; Plaxco, K. W.; Soh, H. T., Real-Time, Aptamer-Based Tracking of Circulating Therapeutic Agents in Living Animals. *Science Translational Medicine* **2013**, *5* (213), 213ra165.
32. Rowe, A. A.; Miller, E. A.; Plaxco, K. W., Reagentless Measurement of Aminoglycoside Antibiotics in Blood Serum via an Electrochemical, Ribonucleic Acid Aptamer-Based Biosensor. *Analytical Chemistry* **2010**, *82* (17), 7090-7095.
33. Hiby, N.; Johansen, H. K.; Copenhagen Study Group on Antibiotics in, S.; Jarlv, J. O.; Westh, H.; Prag, J. B.; Bangsborg, J. M.; Moser, C.; Kemp, M.; Hornsleth, A. K.; Hansen, H., Ciprofloxacin in sweat and antibiotic resistance. *The Lancet* **1995**, *346* (8984), 1235.
34. Sonner, Z.; Wilder, E.; Heikenfeld, J.; Kasting, G.; Beyette, F.; Swaile, D.; Sherman, F.; Joyce, J.; Hagen, J.; Kelley-Loughnane, N.; Naik, R. The microfluidics of the eccrine sweat gland, including biomarker partitioning, transport, and biosensing implications *Biomicrofluidics*, **2015**, p. 031301.

## **Chapter 5: Experimental Procedures**

### **5.1 MATERIALS**

All reagents and solvents were purchased from Sigma-Aldrich (St. Louis, MO) and Acros Organics (Morris Plains, NJ) and used without further purification unless otherwise noted. NMR solvents were purchased from Cambridge Isotope Laboratories (Tewksbury, MA). Column chromatography was performed on Sorbent Technologies silica gel 60 (40–63  $\mu\text{m}$ ). TLC analyses were carried out using Sorbent Technologies silica gel (200  $\mu\text{m}$ ) sheets. All unmodified phosphoramidites and materials used for solid phase oligonucleotide synthesis were purchased from Glen Research (Sterling, VA). The methylene-blue-labeled probe (MB-P) was ordered from Biosearch Technologies (Novato, CA). All other unmodified nucleotides were ordered from Integrated DNA Technology (Coralville, IA). T4 polynucleotide kinase (T4 PNK) and T4 DNA ligase were ordered from New England BioLabs Inc. (Ipswich, MA). SYBR Gold was purchased from Life Technologies (Grand Island, NY). All DNA samples and 6-mercaptohexanol (MCH) were dissolved in phosphate buffered saline (10 mM PBS, 500 mM NaCl, 2.7 mM KCl, pH 7.4) or 4-(2-hydroxyethyl)-1-piperazineethanesulfonic acid/sodium perchlorate (HEPES/ $\text{NaClO}_4$ ) buffer, and stored at 4 °C before use. Removal silicone tape (KRST) as solid support for wearable device was purchased from 3M (St. Paul, MN).

### **5.2 INSTRUMENTS**

NMR spectra were recorded on Varian Direct Drive 400 MHz and Varian MR 400 MHz instruments. High resolution electrospray ionization (ESI) mass spectra were recorded on an Agilent Technologies 6530 Accurate Mass QToF/MS apparatus. Modified oligonucleotides were synthesized by Expedite 8909 automated solid-phase

nucleic acid synthesizer. Determination of concentration of the oligonucleotides was performed by Nanodrop ND-1000 spectrophotometer (Wilmington, DE, USA). Cyclic voltammetry of compounds was performed on a CV-50W Voltammetric Analyzer (Bioanalytical Systems Inc., West Lafayette, IN). Square wave voltammetry and alternative current voltammetry of oligonucleotides were performed on a model CH Instrument 660E electrochemical workstation (CH Instruments, Inc., Austin, TX). Au electrode (1.2 mm in diameter) as the working electrode, a Ag/AgCl electrode as the reference electrode, and a platinum wire as the counter electrode were purchased from CH instruments, Inc. and used for conventional three electrode system unless otherwise noted. PAGE image was obtained using a Storm Scanner 840 instrument (GE Healthcare Life Science, Pittsburgh, PA).

### 5.3 SYNTHETIC PROCEDURES AND CHARACTERIZATION

#### Synthesis of compound **2.1**

To a suspension of ferrocenecarboxylic acid **2.9** (250 mg, 1.09 mmol) in anhydrous *N,N*-dimethylformamide (10 mL) was added propargyl amine (72 mg, 1.31 mmol) and 3-(ethyliminomethyleneamino)-*N,N*-dimethylpropan-1-amine (EDC·HCl) (418 mg, 2.18 mmol). After stirring for four hours at ambient temperature, the mixture was diluted with ethyl acetate (50 mL) and washed with equal volumes of water (three times) and brine (once). The organic layer was then dried over anhydrous MgSO<sub>4</sub> and the solvent was evaporated in vacuo. Silica gel flash column chromatography (eluent: EA/hexane (1:3 to 1:1)), followed by evaporation in vacuo, gave **2.1** (262 mg) as an orange solid (90%). <sup>1</sup>H NMR (400 MHz, CDCl<sub>3</sub>): δ 5.88 (s, 1H), 4.70 (t, *J*=1.3 Hz, 2H), 4.37 (t, *J*=1.3Hz, 2H), 4.23 (s, 5H), 4.19-4.17 (m, 2H), 2.28 (t, *J*=1.7 Hz, 1H). <sup>13</sup>C NMR (101 MHz, CDCl<sub>3</sub>): δ

170.3, 80.4, 75.1, 71.6, 70.8, 69.9, 68.3, 29.3. HR-ESI-MS:  $m/z$  268.0425 ( $M + H$ )<sup>+</sup> calcd for C<sub>14</sub>H<sub>14</sub>OFeN, found 268.0419.

### Synthesis of compound 2.2

To a suspension of **2.1** (959 mg, 3.59 mmol) in anhydrous dichloromethane (40 mL) was added aluminum chloride (AlCl<sub>3</sub>) (958 mg, 7.18 mmol). Acetic anhydride (332  $\mu$ L, 3.59 mmol) was then added to solution dropwise. After stirring for two hours at 0 °C to ambient temperature, the mixture was diluted with dichloromethane (100 mL) and washed with equal volumes of water (three times) and brine (once). The organic layer was then dried over anhydrous MgSO<sub>4</sub> and the solvent was evaporated in vacuo. Silica gel flash column chromatography (eluent: EA/hexane (1:2 to 2:1)), followed by evaporation in vacuo, gave **2.2** (749 mg) as a red-orange solid (68%). <sup>1</sup>H NMR (400 MHz, CDCl<sub>3</sub>):  $\delta$  6.67 (t,  $J$  = 5.0 Hz, 1H), 4.81 – 4.72 (m, 2H), 4.72 – 4.64 (m, 2H), 4.56 – 4.49 (m, 2H), 4.38 – 4.32 (m, 2H), 4.15 (dd,  $J$  = 5.5, 2.5 Hz, 2H), 2.38 (s, 3H), 2.26 (t,  $J$  = 2.5 Hz, 1H). <sup>13</sup>C NMR (101 MHz, acetone):  $\delta$  202.73, 168.97, 90.64, 80.16, 79.98, 73.75, 71.84, 71.34, 71.27, 70.18, 29.19, 27.82.

### Synthesis of compound 2.3

To a suspension of ferrocenecarboxylic acid **2.9** (5 g, 21.7 mmol) in benzene (100 mL) was added phosphorous pentachloride (PCl<sub>5</sub>) (4.98 g, 23.9 mmol). After stirring for three hours at ambient temperature, the solution was evaporated *in vacuo* and the mixture was dissolved in acetone. Sodium azide (NaN<sub>3</sub>) (2.83 g, 43.5 mmol) in water (5 mL) was then added to the solution at 0 °C. After stirring for three hours at the temperature, the



mixture was poured into cold water to and filtered by Buchner filter to obtain **2.10** (4.50 g) as a red solid. (81%)

Without further purification, **2.10** (500 mg, 1.96 mmol) was dissolved in dry toluene and the solution was heated to reflux under nitrogen gas. The solution was then cooled down to 60 °C and propargyl amine (251  $\mu$ L, 3.92 mmol) was added to the solution. After stirring for two hours at the temperature, the mixture poured into cold toluene to and filtered by Buchner filter to obtain **2.3** (466 mg) as an orange solid (84%).  $^1\text{H}$  NMR (400 MHz,  $\text{CDCl}_3$ ):  $\delta$  5.22 (s, 4H), 4.69 (s, 6H), 4.07 (dd,  $J$  = 5.4, 2.5 Hz, 2H), 2.21 (t,  $J$  = 2.5 Hz, 1H).  $^{13}\text{C}$  NMR (101 MHz, acetone):  $\delta$  81.51, 81.50, 70.76, 68.74, 63.60, 60.66, 60.58. HR-ESI-MS:  $m/z$  282.04500  $\text{M}^+$  calcd for  $\text{C}_{14}\text{H}_{14}\text{FeN}_2\text{O}$ , found 282.04520.

#### Synthesis of compound 2.4

To a suspension of ferrocenemethanol **2.11** (3 g, 14.3 mmol) in anhydrous tetrahydrofuran (THF) (150 mL) was added sodium hydride (NaH) (1.14 g, 28.6 mmol) and propargyl bromide (3.10 mL, 28.6 mmol). After stirring overnight at ambient temperature, the mixture was diluted with ethyl acetate (250 mL) and washed with equal volumes of water (three times) and brine (once). The organic layer was then dried over anhydrous  $\text{MgSO}_4$  and the solvent was evaporated in vacuo. Silica gel flash column chromatography (eluent: EA/hexane (1:10 with 1% TEA)), followed by evaporation in vacuo, gave **2.2** (749 mg) as a yellow solid (81%).  $^1\text{H}$  NMR (400 MHz,  $\text{CDCl}_3$ ):  $\delta$  4.39 (s, 2H), 4.26 (t,  $J$ =1.9 Hz, 2H), 4.18 – 4.16 (m, 2H), 4.15 (s, 5H), 4.12 (d,  $J$ =2.4 Hz, 2H), 2.45 (t,  $J$ =2.4 Hz, 1H).  $^{13}\text{C}$  NMR (101 MHz,  $\text{CDCl}_3$ ):  $\delta$  82.26, 79.95, 74.39, 69.54, 68.64, 68.50, 68.48, 68.46, 67.59, 56.44.

## Synthesis of compound **2.5**

To a suspension of aminoferrocene **2.12** (700 mg, 2.61 mmol) in anhydrous acetonitrile (ACN) (18 mL) was added 4-bromo-1-butyne (490  $\mu$ L, 5.22 mmol) and potassium carbonate ( $K_2CO_3$ ) (962 mg, 6.96 mmol). After stirring 24 hours at 85 °C, the mixture was diluted with ethyl acetate (50 mL) and washed with equal volumes of sodium bicarbonate ( $NaHCO_3$ ) solution (three times) and brine (once). The organic layer was then dried over anhydrous  $MgSO_4$  and the solvent was evaporated in vacuo. Silica gel flash column chromatography (eluent: EA/hexane (1:20 to 1:10)), followed by evaporation in vacuo, gave **2.13** (686 mg) as a brown-red solid (78%).  $^1H$  NMR (400 MHz,  $CDCl_3$ ):  $\delta$  4.16 (s, 5H), 3.92 (s, 2H), 3.90 (s, 2H), 3.14 (s, 2H), 2.63 (s, 1H), 2.53 (td,  $J$  = 6.5, 2.6 Hz, 2H), 2.10 (t,  $J$  = 2.6 Hz, 1H).  $^{13}C$  NMR (101 MHz,  $CDCl_3$ ):  $\delta$  82.16, 70.13, 68.14, 63.19, 55.83, 45.70, 19.58.

To a suspension of mono-substituted aminoferrocene **2.13** (170 mg, 0.67 mmol) in dimethyl sulfoxide (DMSO) (15 mL) was added methyl iodide (69  $\mu$ L, 0.74 mmol) and potassium carbonate ( $K_2CO_3$ ) (93 mg, 67.2 mmol). After stirring 8 hours at ambient temperature, the mixture was diluted with ethyl acetate (25 mL) and washed with equal volumes of sodium bicarbonate ( $NaHCO_3$ ) solution (three times) and brine (once). The organic layer was then dried over anhydrous  $MgSO_4$  and the solvent was evaporated in vacuo. Silica gel flash column chromatography (eluent: EA/hexane (1:10)), followed by evaporation in vacuo, gave **2.5** (159 mg) as a red solid (89%).  $^1H$  NMR (400 MHz,  $CDCl_3$ ):  $\delta$  4.20 (s, 5H), 4.01 – 3.84 (m, 2H), 3.79 (t,  $J$  = 2.0 Hz, 2H), 3.09 (t,  $J$  = 7.4 Hz, 2H), 2.67 (s, 3H), 2.53 (td,  $J$  = 7.4, 2.7 Hz, 2H), 2.04 (t,  $J$  = 2.6 Hz, 1H).  $^{13}C$  NMR (101 MHz,  $CDCl_3$ ):  $\delta$  113.79, 82.62, 69.53, 67.41, 63.44, 54.63, 53.57, 39.59, 17.04.

### Synthesis of compound 2.6

To a suspension of mono-substituted aminoferrocene **2.13** (686 mg, 2.71 mmol) in dichloromethane (DCM) (25 mL) was added acetic anhydride (326  $\mu$ L, 3.52 mmol). After stirring 2 hours at ambient temperature, the mixture was diluted with ethyl acetate (50 mL) and washed with equal volumes of sodium bicarbonate ( $\text{NaHCO}_3$ ) solution (three times) and brine (once). The organic layer was then dried over anhydrous  $\text{MgSO}_4$  and the solvent was evaporated in vacuo. Silica gel flash column chromatography (eluent: EA/hexane (1:5 to 1:2)), followed by evaporation in vacuo, gave **2.6** (670 mg) as a orange solid (84%).  $^1\text{H}$  NMR (400 MHz,  $\text{CDCl}_3$ ):  $\delta$  4.27 (s, 5H), 4.15 (s, 4H), 4.08 (t,  $J = 7.7$  Hz, 2H), 2.68 (td,  $J = 7.7, 2.7$  Hz, 2H), 2.03 (t,  $J = 2.7$  Hz, 1H), 1.76 (s, 3H).  $^{13}\text{C}$  NMR (101 MHz,  $\text{CDCl}_3$ ):  $\delta$  171.74, 102.56, 81.63, 69.90, 69.38, 66.18, 65.61, 51.59, 22.47, 18.17.

### Synthesis of compound 2.7

To a suspension of mono-substituted aminoferrocene **2.13** (269 mg, 1.06 mmol) in dichloromethane (DCM) (10 mL) was added trifluoroacetic anhydride (177  $\mu$ L, 1.28 mmol). After stirring 2 hours at ambient temperature, the mixture was diluted with ethyl acetate (25 mL) and washed with equal volumes of sodium bicarbonate ( $\text{NaHCO}_3$ ) solution (three times) and brine (once). The organic layer was then dried over anhydrous  $\text{MgSO}_4$  and the solvent was evaporated in vacuo. Silica gel flash column chromatography (eluent: EA/hexane (1:10)), followed by evaporation in vacuo, gave **2.7** (341 mg) as a orange solid (92%).  $^1\text{H}$  NMR (400 MHz,  $\text{CDCl}_3$ ):  $\delta$  4.32 (s, 5H), 4.24 (d,  $J = 7.7$  Hz, 2H), 4.23 – 4.15 (m, 4H), 2.77 (td,  $J = 7.7, 2.7$  Hz, 2H), 2.09 (t,  $J = 2.7$  Hz, 1H).  $^{13}\text{C}$  NMR (101 MHz,  $\text{CDCl}_3$ ):  $\delta$  140.29, 69.60, 67.18, 65.86, 54.95, 17.55.

## Synthesis of compound **2.8**

To a suspension of bromoferrocene **2.14** (mg, mmol) in anhydrous diethylether (10 mL) was added *n*-butyllithium (2.5 M sol. in hexane, 177  $\mu$ L, 1.28 mmol) dropwise. After stirring 1 hour at -78 °C, 3-butyne-1-sulfonyl chloride (177  $\mu$ L, 1.28 mmol) was added to the solution. After stirring another 1 hour at ambient temperature, the mixture was diluted with ethyl acetate (50 mL) and washed with equal volumes of sodium bicarbonate (NaHCO<sub>3</sub>) solution (three times) and brine (once). The organic layer was then dried over anhydrous MgSO<sub>4</sub> and the solvent was evaporated in vacuo. Silica gel flash column chromatography (eluent: EA/hexane (1:5)), followed by evaporation in vacuo, gave **2.8** (41 mg) as a brown red solid (8%). <sup>1</sup>H NMR (400 MHz, CDCl<sub>3</sub>):  $\delta$  4.64 (t, *J* = 2.0 Hz, 2H), 4.47 – 4.45 (m, 2H), 4.44 (s, 4H), 3.22 – 3.17 (m, 2H), 2.61 – 2.55 (m, 2H), 1.97 (t, *J* = 2.7 Hz, 1H). <sup>13</sup>C NMR (101 MHz, CDCl<sub>3</sub>):  $\delta$  109.99, 86.01, 79.73, 71.40, 70.67, 69.85, 54.88, 13.48. HR-ESI-MS: *m/z* 324.99560 (M + Na)<sup>+</sup> calcd for C<sub>14</sub>H<sub>14</sub>FeO<sub>2</sub>SNa, found 324.99540.

## Synthesis of DMT-protected 5-iodo-2'-deoxyuridine, **2.16**

To a suspension of 5-iodo-2'-deoxyuridine **2.15** (3.0 g, 8.47 mmol) in dry pyridine (50 mL) was added 4,4'-dimethoxytrityl chloride (3.25 g, 10.2 mmol). The mixture was stirred for three hours at ambient temperature. The reaction was quenched with methanol (50 mL) and the solvent was removed under reduced pressure. The residue was diluted with ethyl acetate (250 mL) and washed with equal volumes of saturated aqueous sodium bicarbonate (twice) and brine (once). The organic layer was then dried over anhydrous MgSO<sub>4</sub> and the solvent was evaporated in vacuo. Silica gel flash column chromatography (eluent: EA/hexane (1:2 to 3:1)), followed by evaporation in vacuo, yielded **2.16** (4.34 g) as a pale yellow solid (78%). <sup>1</sup>H NMR (400 MHz, CDCl<sub>3</sub>):  $\delta$  10.00 (s, 1H), 8.16 (s, 1H),

7.43-7.18 (m, 9H), 6.84 (d,  $J=8.8$  Hz, 4H), 6.34 (dd,  $J_1=3.8$  Hz,  $J_2=3.0$  Hz, 1H), 4.57 (t,  $J=4.0$  Hz, 1H), 4.15 (t,  $J=4$  Hz, 1H), 3.76 (s, 6H), 3.47 (s, 1H) 3.41-3.34 (m, 2H), 2.57-2.52 (m, 1H), 2.30 (q,  $J=5.5$  Hz, 1H).  $^{13}\text{C}$  NMR (101 MHz,  $\text{CDCl}_3$ ):  $\delta$  160.6, 158.7, 150.5, 144.5, 144.5, 135.6, 135.5, 130.2, 128.1, 127.1, 113.5, 87.1, 86.8, 85.8, 72.6, 69.0, 63.7, 55.4, 41.5. HR-ESI-MS:  $m/z$  679.0917 ( $\text{M} + \text{Na}$ ) $^+$  calcd for  $\text{C}_{30}\text{H}_{29}\text{O}_7\text{IN}_2\text{Na}$ , found 679.0911.

### Synthesis of ferrocene-thymidines, **2.17** – **2.24**

General procedure: To a solution of **2.15** (500 mg, 0.762 mmol) in anhydrous *N,N*-dimethylformamide (10 mL) was added Fc-alkynes **2.1** - **2.8** (0.914 mmol, 1.2 equivalent), tetrakis(triphenylphosphine)palladium(0) (132 mg, 0.114 mmol), copper (I) iodide (36.3 mg, 0.190 mmol), and *N,N*-diisopropylethylamine (260  $\mu\text{L}$ , 1.90 mmol). After stirring for six hours at ambient temperature, the mixture was diluted with ethyl acetate and washed with equal volumes of water (three times) and brine (once). The organic layer was then dried over anhydrous  $\text{MgSO}_4$  and the solvent was evaporated in vacuo. Silica gel flash column chromatography (eluent: EA/hexane (2:1) with 10% MeOH), followed by evaporation in vacuo, gave **2.17** – **2.24**.

**2.17**: An orange solid (74 %).  $^1\text{H}$  NMR (400 MHz,  $\text{CDCl}_3$ ):  $\delta$  9.36 (s, 1H), 8.07 (s, 1H), 7.33-7.18 (m, 9H), 6.83 (d,  $J=9.2$  Hz, 4H), 6.29 (t,  $J=4.4$  Hz, 1H), 6.09 (t,  $J=3.3$  Hz, 1H), 4.60-4.50 (m, 3H), 4.27 (t,  $J=0.8$  Hz, 2H), 4.14 (s, 5H), 4.11-4.06 (m, 2H), 4.03 (d,  $J=4.8$  Hz, 1H), 3.75 (s, 6H), 3.34 (d,  $J=3.2$  Hz, 2H), 3.22 (s, 1H), 2.53-2.48 (m, 1H), 2.26 (q,  $J=5.4$  Hz, 1H).  $^{13}\text{C}$  NMR (100 MHz,  $\text{CDCl}_3$ )  $\delta$  170.5, 162.7, 158.5, 149.5, 144.6, 143.2, 135.6, 135.6, 130.1, 128.1, 127.0, 113.4, 99.4, 90.1, 86.9, 86.7, 86.0, 75.1, 74.1, 72.1, 70.6,

69.8, 68.4, 63.7, 55.3, 41.5, 30.2. HR-ESI-MS:  $m/z$  818.2141 ( $M + Na$ )<sup>+</sup> calcd for  $C_{44}H_{41}O_8FeN_3Na$ , found 818.2135.

**2.18:** An orange-red solid (90%).  $^1H$  NMR (400 MHz,  $CDCl_3$ ):  $\delta$  9.79 (s, 1H), 8.06 (s, 1H), 7.44 – 7.17 (m, 9H), 6.83 (d,  $J$  = 8.9 Hz, 4H), 6.60 (s, 1H), 6.28 (t,  $J$  = 6.5 Hz, 1H), 4.77 – 4.72 (m, 2H), 4.72 – 4.67 (m, 2H), 4.50 (d,  $J$  = 9.1 Hz, 3H), 4.32 – 4.28 (m, 2H), 4.09 (qd,  $J$  = 18.2, 4.9 Hz, 4H), 3.75 (s, 6H), 3.56 (s, 1H), 3.34 (d,  $J$  = 3.6 Hz, 2H), 2.58 – 2.51 (m, 1H), 2.33 (m, 4H).  $^{13}C$  NMR (101 MHz,  $CDCl_3$ )  $\delta$  202.75, 168.56, 162.25, 158.52, 158.50, 149.39, 144.50, 143.19, 135.54, 135.46, 129.99, 129.97, 128.03, 127.87, 126.97, 113.33, 113.12, 99.32, 89.82, 86.91, 86.62, 86.04, 80.05, 74.12, 73.90, 73.87, 72.20, 71.97, 71.16, 71.09, 69.96, 69.90, 63.63, 55.26, 53.42, 41.45, 30.13, 29.68, 27.68.

**2.19:** An orange solid (69%)  $^1H$  NMR (400 MHz,  $CDCl_3$ ):  $\delta$  10.03 (s, 1H), 7.99 (s, 1H), 7.44 – 7.11 (m, 9H), 6.88 – 6.74 (m, 4H), 6.23 (t,  $J$  = 6.6 Hz, 1H), 6.14 (s, 1H), 5.20 (s, 1H), 4.44 (s, 2H), 4.23 (s, 5H), 4.15 (s, 1H), 4.06 (p,  $J$  = 3.2 Hz, 2H), 3.90 (t,  $J$  = 3.9 Hz, 2H), 3.74 (s, 6H), 3.23 – 3.26 (m, 2H), 2.52 – 2.39 (m, 1H), 2.25 – 2.18 (m, 1H).  $^{13}C$  NMR: HR-ESI-MS:  $m/z$  833.22450 ( $M + Na$ )<sup>+</sup> calcd for  $C_{44}H_{42}FeN_4O_8Na$ , found 833.22390.

**2.20:** A yellow solid (64%).  $^1H$  NMR (400 MHz,  $CDCl_3$ ):  $\delta$  9.64 (s, 1H), 8.02 (s, 1H), 7.45 – 7.17 (m, 9H), 6.84 (dd,  $J$  = 8.9, 1.6 Hz, 4H), 6.30 – 6.25 (m, 1H), 4.49 (s, 1H), 4.28 – 4.08 (m, 8H), 4.01 (d,  $J$  = 3.7 Hz, 2H), 3.76 (d,  $J$  = 1.2 Hz, 6H), 3.35.  $^{13}C$  NMR (101 MHz,  $CDCl_3$ ):  $\delta$  161.82, 158.63, 149.60, 144.61, 142.97, 135.62, 135.46, 130.08, 128.12, 127.95, 127.03, 113.42, 99.91, 90.33, 87.06, 86.64, 86.01, 72.42, 70.13, 69.06, 67.76, 63.70, 60.56, 57.08, 55.34, 41.49.

**2.21:** An orange-red solid (47%).

**2.22:** A yellow solid.  $^1H$  NMR (400 MHz,  $CDCl_3$ ):  $\delta$  9.24 (s, 1H), 7.92 (s, 1H), 7.48 – 7.17 (m, 9H), 6.84 (d,  $J$  = 8.7 Hz, 4H), 6.29 (s, 1H), 4.48 (s, 1H), 4.31 – 4.04 (m, 10H),

3.96 (d,  $J = 15.8$  Hz, 2H), 3.77 (s, 6H), 3.35 (s, 2H), 3.10 (s, 1H), 2.68 (s, 2H), 2.49 (d,  $J = 9.5$  Hz, 1H), 2.30 – 2.21 (m, 1H), 1.78 (s, 3H).  $^{13}\text{C}$  NMR:  $\delta$  161.68, 158.53, 149.35, 144.53, 141.81, 135.55, 135.46, 129.98, 128.02, 127.90, 126.94, 113.30, 102.46, 86.91, 85.63, 72.29, 69.43, 66.02, 65.57, 63.61, 55.23, 51.40, 41.21, 22.55, 19.22.

### Synthesis of thymidine phosphoramidites **2.23** – **2.30**

General procedure: To a suspension of **2.17** – **2.22** (0.250 mmol) in anhydrous dichloromethane (5 mL) was added *N,N*-diisopropylethylamine (88  $\mu\text{L}$ , 0.500 mmol) and 2-cyanoethyl *N,N*-diisopropylchlorophosphoramidite (112 mL, 0.500 mmol) at 0°C. The mixture was then allowed to warm to ambient temperature over the course of three hours. Most of the solvent was removed under reduced pressure and purification of the resulting mass by silica gel flash column chromatography (eluent: EA/hexane (1:1) with 0.1% pyridine), followed by concentration of the desired fraction in vacuo, gave **2.25** – **2.32**.

**2.23:** An orange solid.  $^{31}\text{P}$  NMR (162 MHz,  $\text{CD}_3\text{CN}$ ):  $\delta$  148.88, 148.85. HR-ESI-MS:  $m/z$  995.3322  $\text{M}^+$  calcd for  $\text{C}_{53}\text{H}_{58}\text{O}_9\text{FeN}_5\text{P}$ , found 995.3314.

**2.24:** An orange-red solid.  $^{31}\text{P}$  NMR (162 MHz,  $\text{CD}_3\text{CN}$ )  $\delta$  147.99, 147.95. HR-ESI-MS:  $m/z$  1060.33210  $(\text{M} + \text{Na})^+$  calcd for  $\text{C}_{55}\text{H}_{60}\text{FeN}_5\text{O}_{10}\text{PNa}$ , found 1060.33070.

**2.25:** An orange solid.  $^{31}\text{P}$  NMR (162 MHz,  $\text{CD}_3\text{CN}$ ):  $\delta$  147.94, 147.89. HR-ESI-MS: 1033.33283  $m/z$   $(\text{M} + \text{Na})^+$  calcd for  $\text{C}_{53}\text{H}_{59}\text{FeN}_6\text{O}_9\text{PNa}$ , found 1033.33250.

**2.26:** A yellow solid.  $^{31}\text{P}$  NMR (162 MHz,  $\text{CD}_3\text{CN}$ ):  $\delta$  147.27, 146.93. HR-ESI-MS:  $m/z$  1005.3263  $(\text{M} + \text{Na})^+$  calcd for  $\text{C}_{53}\text{H}_{59}\text{FeN}_4\text{O}_9\text{PNa}$ , found 1005.3260.

**2.27:** An orange-red solid.  $^{31}\text{P}$  NMR (162 MHz,  $\text{CD}_3\text{CN}$ ):  $\delta$  148.83, 148.37.

**2.28:** A yellow solid.  $^{31}\text{P}$  NMR (162 MHz,  $\text{CD}_3\text{CN}$ ):  $\delta$  148.60, 148.59. HR-ESI-MS: 1046.35280  $m/z$  ( $\text{M} + \text{Na}$ ) $^+$  calcd for  $\text{C}_{55}\text{H}_{62}\text{FeN}_5\text{O}_9\text{PNa}$ , found 1046.35090.

### **Synthesis of modified oligonucleotides 2.31, 2.32, and HS-Fc-P**

Synthesis of modified oligonucleotide was performed on a nucleic acid synthesizer with a 0.2  $\mu\text{mol}$  3'-thiol-modifier C3 S-S CPG support column. A standard oligodeoxynucleotide synthesis protocol was used except that coupling times were extended (to 15 min) and a more concentrated phosphoramidite solution (0.2 M) was employed with compound 1. The product was deprotected and purified using a Glen-Pak DNA Purification Cartridge, and the detailed procedure provided by the Glen Research Company ([http://www.glenresearch.com/Technical/GlenPak\\_UserGuide.pdf](http://www.glenresearch.com/Technical/GlenPak_UserGuide.pdf)).

### **Synthesis of ratiometric E-sensor oligonucleotide Probe P**

The phosphorylation of HS-Fc-P was performed in 1 mL of T4 ligase buffer (50 mM Tris-HCl, 10 mM  $\text{MgCl}_2$ , 1 mM ATP, 10 mM DTT, pH 7.5) solution containing 100  $\mu\text{M}$  HS-Fc-P and 50  $\mu\text{L}$  of T4 PNK (10 000 units/mL). The mixture was incubated at 37  $^\circ\text{C}$  for 3 h. The solution was then incubated at 65  $^\circ\text{C}$  for 20 min to denature the enzyme. After precipitation with ethanol, the DNA was dissolved in 90  $\mu\text{L}$  of DI water. A G25 column was used to remove residual salts, and 90  $\mu\text{L}$  of 558  $\mu\text{M}$  5'-phosphorylated HS-Fc-P was obtained for subsequent ligation reactions.

The MB-P and 5'-phosphorylated HS-Fc-P was ligated together with T4 DNA Ligase. Four tubes were prepared with that contained 80  $\mu\text{M}$  phosphorylated HS-Fc-P, 30  $\mu\text{M}$  MB-P, 30  $\mu\text{M}$  Ligation-P, and 1 $\times$  ligation buffer for a total of 100  $\mu\text{L}$  per tube. These samples were incubated for 5 min at 80  $^\circ\text{C}$  and cooled down to 25  $^\circ\text{C}$  at a rate of 0.1  $^\circ\text{C}/\text{s}$ .



After this first incubation was deemed complete, 20  $\mu\text{L}$  of 120 000 units of T4 DNA ligase in 1 $\times$  ligation buffer was added to each tube for a total of 120  $\mu\text{L}$  per tube. The reaction mixture was further incubated at 16  $^{\circ}\text{C}$  for 16 h, followed by incubation at 65  $^{\circ}\text{C}$  for 20 min. After incubation, Probe P was purified on a 12% denaturing PAGE gel (7 M urea, 1 $\times$  TBE), and its final concentration was confirmed by absorption determinations with a Nanodrop.

### **Preparation of oligonucleotides with free thiol for SAM formation**

To cleave the disulfide bond on the modified oligonucleotide, the 3  $\mu\text{L}$  of oligonucleotide solution in PBS or HEPES/ $\text{NaClO}_4$  buffer was mixed with 4.8  $\mu\text{L}$  of 100 mM tris(2-carboxyethyl)phosphine (TCEP), and this solution was incubated in the dark at room temperature for 1 h. Then, 12  $\mu\text{L}$  of 2 $\times$  PBS buffer and 4.2  $\mu\text{L}$  of deionized water (DI water) were added to that solution and stored at 4  $^{\circ}\text{C}$  for further use.

## **5.4 PROCEDURES OF ELECTROCHEMICAL ANALYSES**

### **Cyclic voltammetry for ferrocene bearing alkynes**

Cyclic voltammograms of compounds **2.1** – **2.8** (1 mM in dichloromethane) were measured with tetrabutylammonium hexafluorophosphate (0.2 M) as the supporting electrolyte. Glassy carbon and Pt used as the working and counter electrodes, respectively. Potentials were measured against a Ag/AgCl reference electrode with a scan rate of 25 mV/s. All CV curves are attached in Appendix A.

### Square wave voltammetry for oligonucleotides

The Au electrode was polished with 1.0, 0.3, and 0.05  $\mu\text{m}$   $\gamma\text{-Al}_2\text{O}_3$  and then washed ultrasonically with water for three cycles, followed by potential scanning in 0.1 M  $\text{H}_2\text{SO}_4$  between  $-0.2$  and  $1.6$  V until a reproducible cyclic voltammogram was obtained. The electrode was rinsed with a copious amount of water and blown dry with nitrogen before assembly.

The sensing platform was prepared by placing 4  $\mu\text{L}$  of freshly prepared the oligonucleotides (2  $\mu\text{M}$ ) solution on the Au electrode and then covering the end of the electrode with a plastic cap to prevent the solution from evaporating. The assembly was kept 1.5 h at room temperature in the dark and then rinsed with PBS buffer several times.

The interface was then covered with 5  $\mu\text{L}$  of 1 mM MCH (in PBS) and kept at room temperature for 30 min. After rinsing with PBS buffer, the sensing platform was stored in PBS buffer for at least 20 min prior to experimental measurements. Initial SWV signals from the MB and Fc reporters on the oligonucleotides were measured in PBS. Signals were then taken after 30 min of incubation with 50  $\mu\text{L}$  aliquots of different concentrations of target oligonucleotides and other sequences, as described in the text. The SWV parameters adopted were as follows: Increment potential was 4 mV, amplitude was 25 mV, frequency was 50 Hz, and voltage range was from  $-0.4$  to  $0.7$  V.

SWV procedure for oligonucleotide **2.33**, which is synthesized by post-synthetic modification, was exactly same with the general procedure except for the use of HEPES/ $\text{NaClO}_4$  buffer in storing, incubation, and analysis of the oligonucleotide instead of PBS.

### **Alternating current voltammetry for wearable devices**

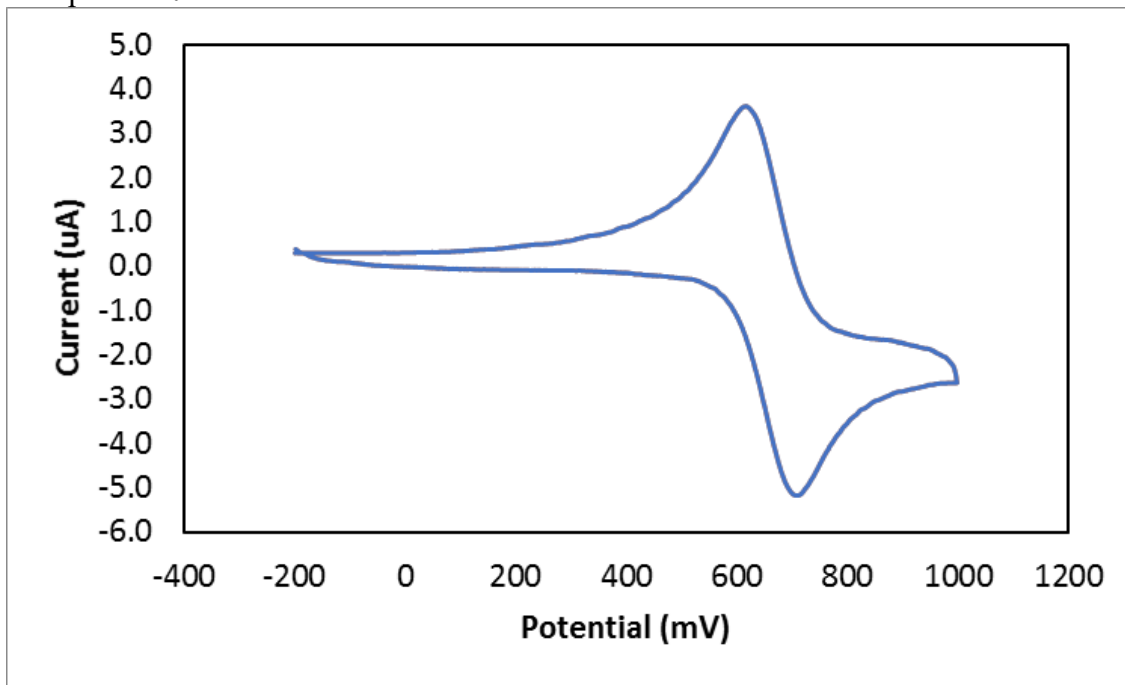
The functioning area of the device (fabricated from Dr. Lu's group) was rinsed with a copious amount of water and ethyl alcohol, and blown dry with nitrogen before assembly. Cyclic voltammetry or linear sweep voltammetry were performed in 5 mM  $\text{K}_3\text{Fe}(\text{CN})_6/\text{K}_4\text{Fe}(\text{CN})_6$  in PBS to test the electrode fabrication on the device.

The sensing platform was prepared by placing 20  $\mu\text{L}$  of freshly prepared thiol-oligonucleotides (2  $\mu\text{M}$ ) solution on central Au working electrode area and then storing in conventional petri dish with high humidity to prevent the solution from evaporating. The petri dish was kept overnight at room temperature in the dark and then rinsed with DI water. The interface was then covered with 20  $\mu\text{L}$  of 1 mM MCH (in PBS) and kept at room temperature for 4 h.

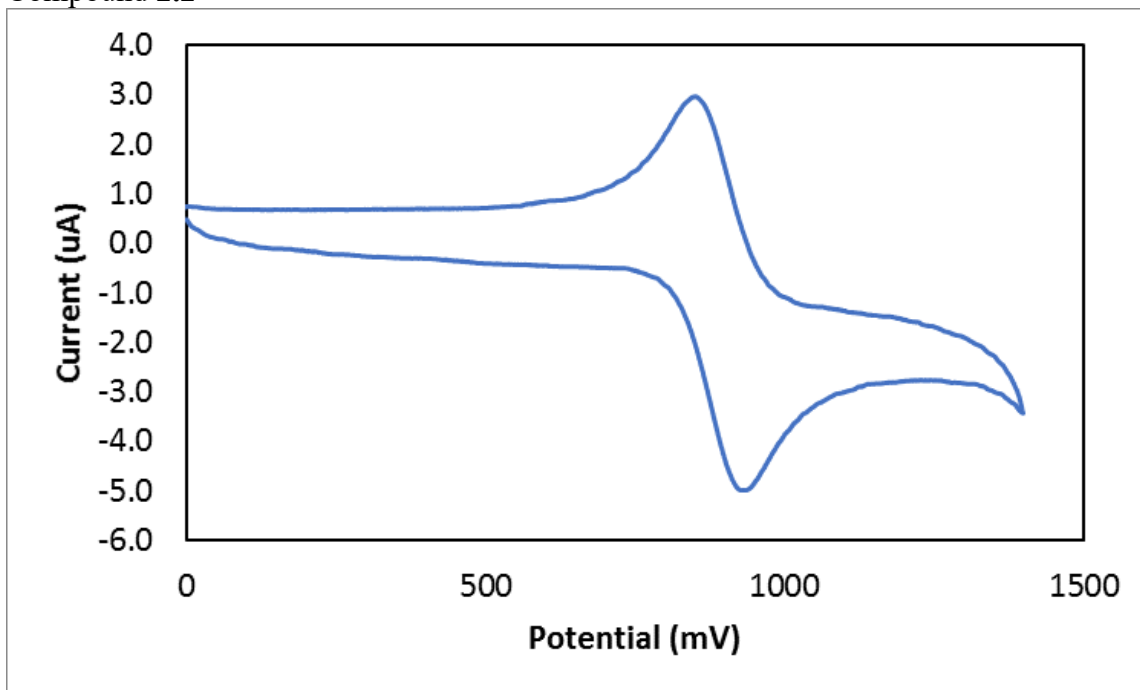
After rinsing with DI water, about a half of the device, including all functioning area, was then immersed in PBS for 20 min prior to experimental measurements. After the device was connected to potentiostat via interface area, ACV signals from the MB on the oligonucleotides were measured. Signals from analytes were taken after 30 min of partial immersing in 5 mL aliquots of different concentrations of oligonucleotides or cocaine, as described in the text. Regeneration of the device is done by rinsing with copious amount of DI water for 1 min and further 20 min incubation in PBS. The ACV parameters adopted were as follows: Increment potential of 4 mV, amplitude of 25 mV, frequency of 100 Hz, and voltage range of  $-0.6$  to  $0.2$  V.

## Appendix A Cyclic voltammograms of compounds

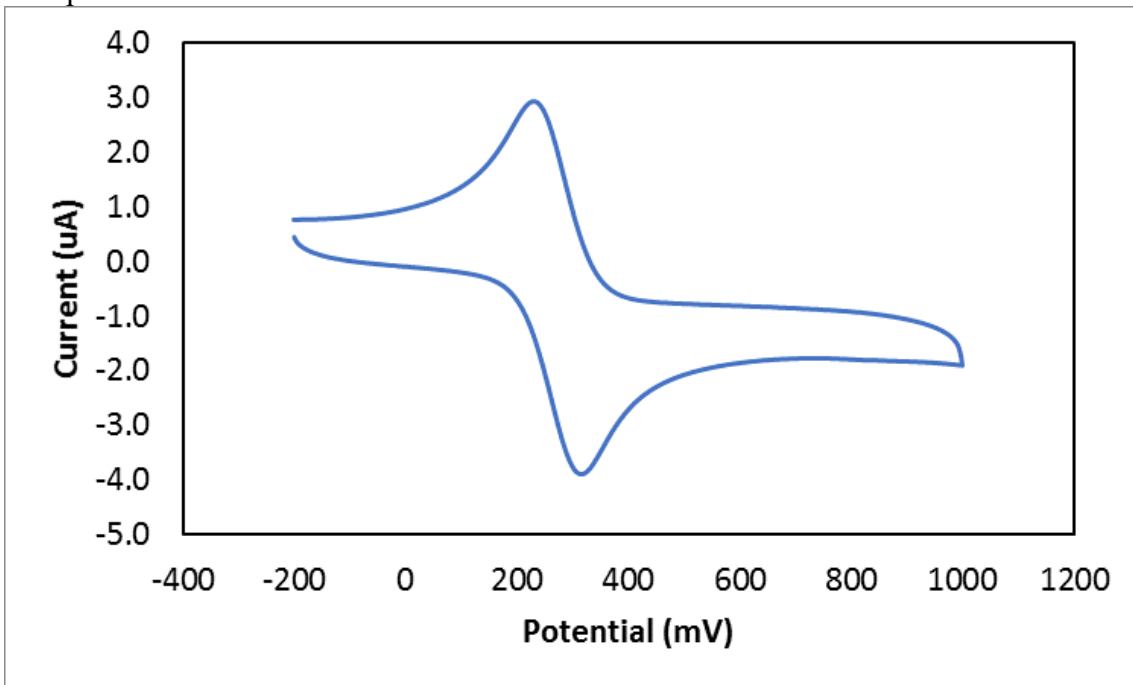
Compound 2.1



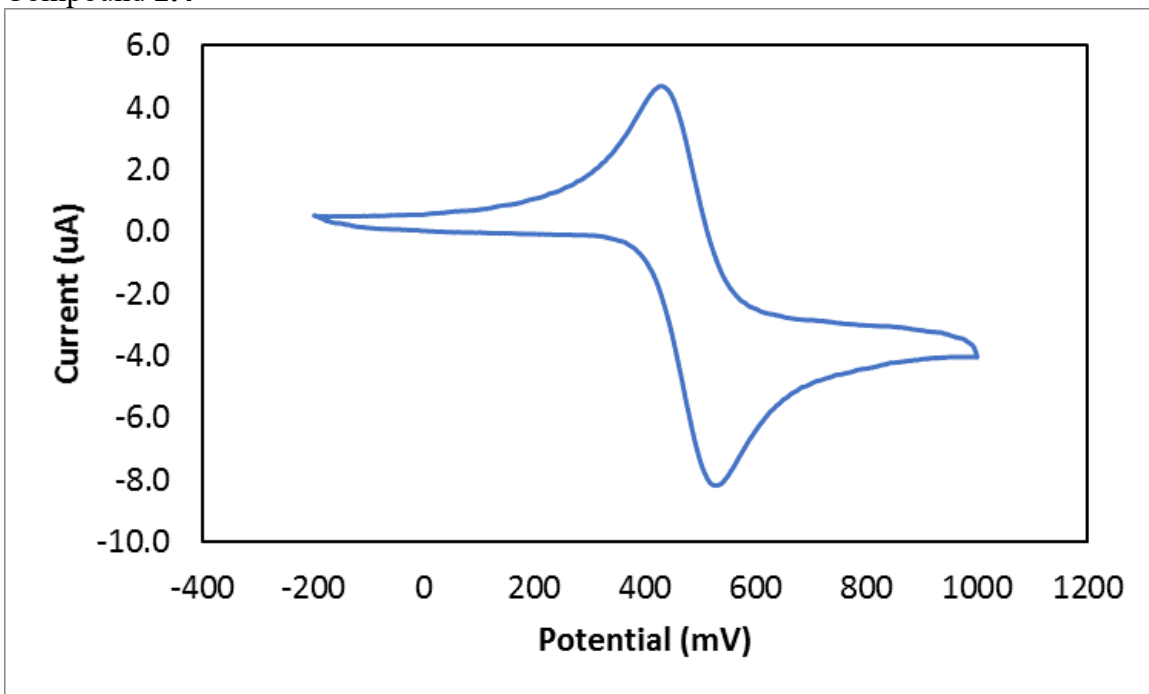
Compound 2.2



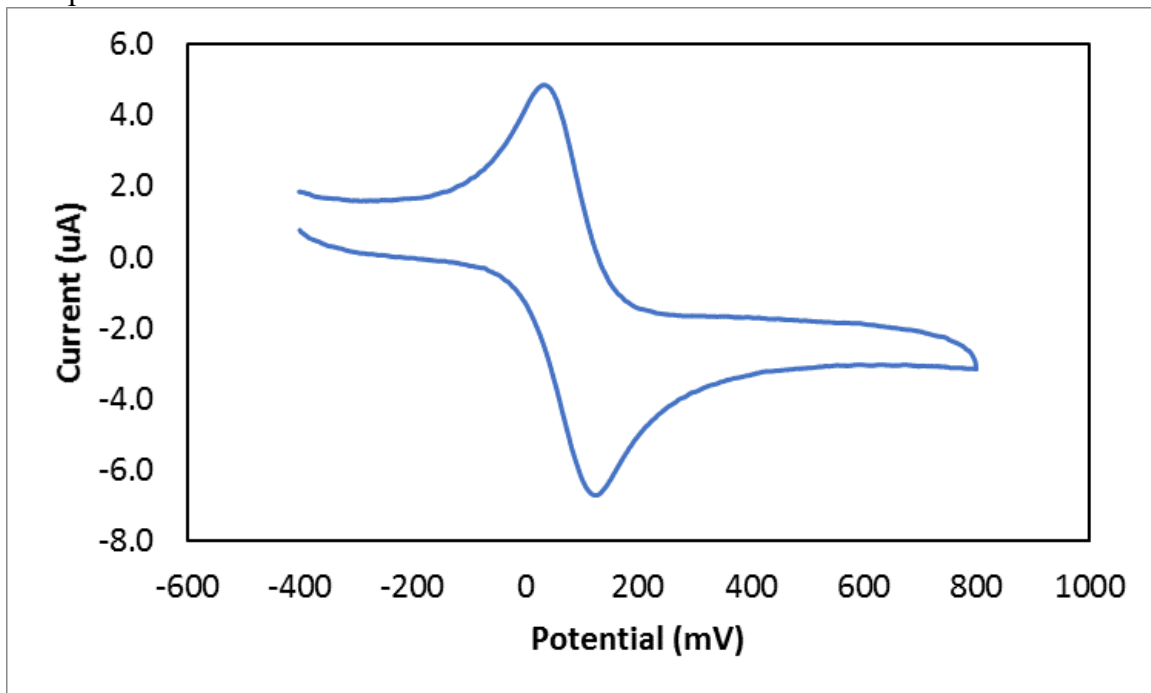
Compound 2.3



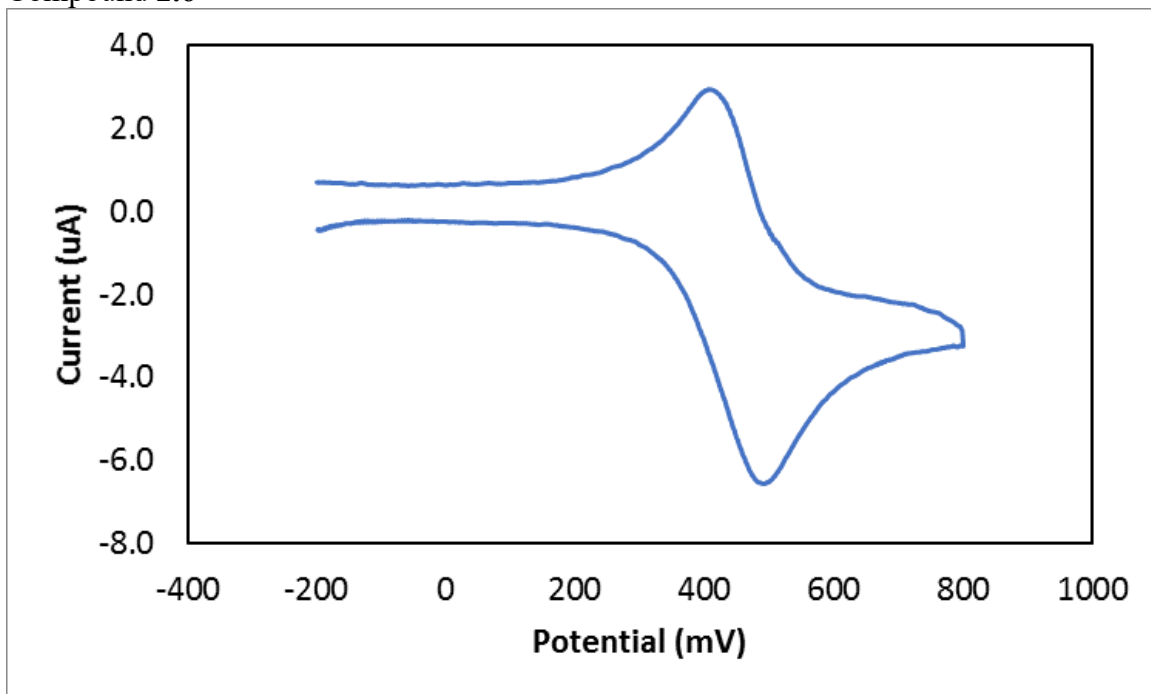
Compound 2.4



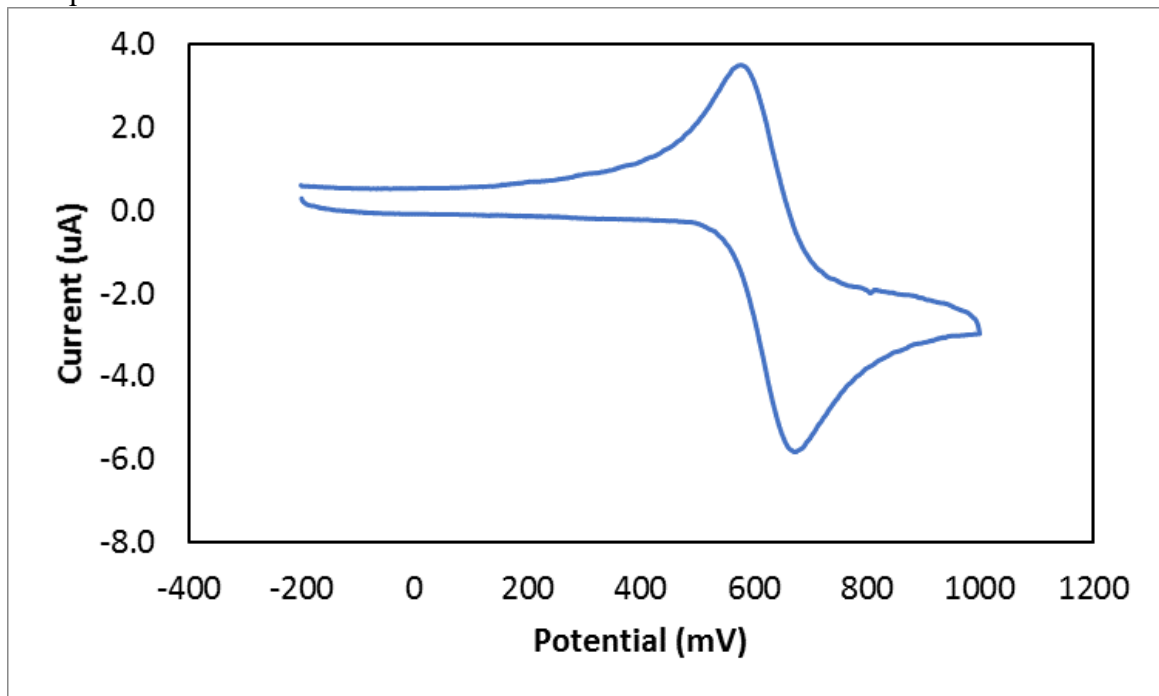
Compound 2.5



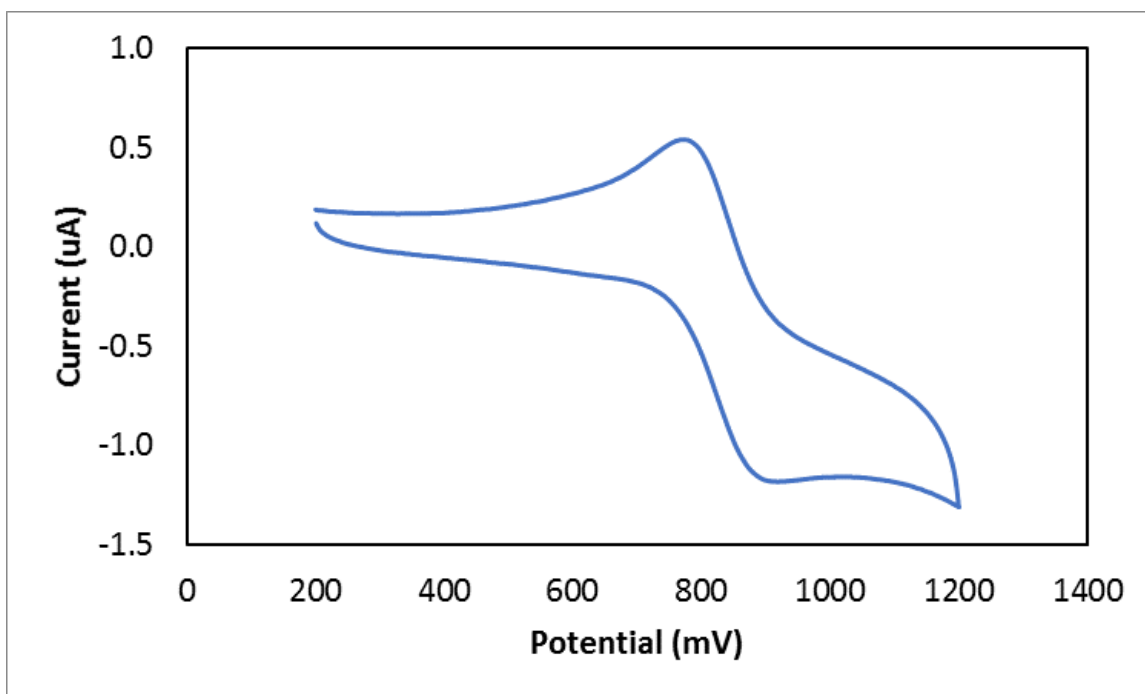
Compound 2.6



Compound 2.7

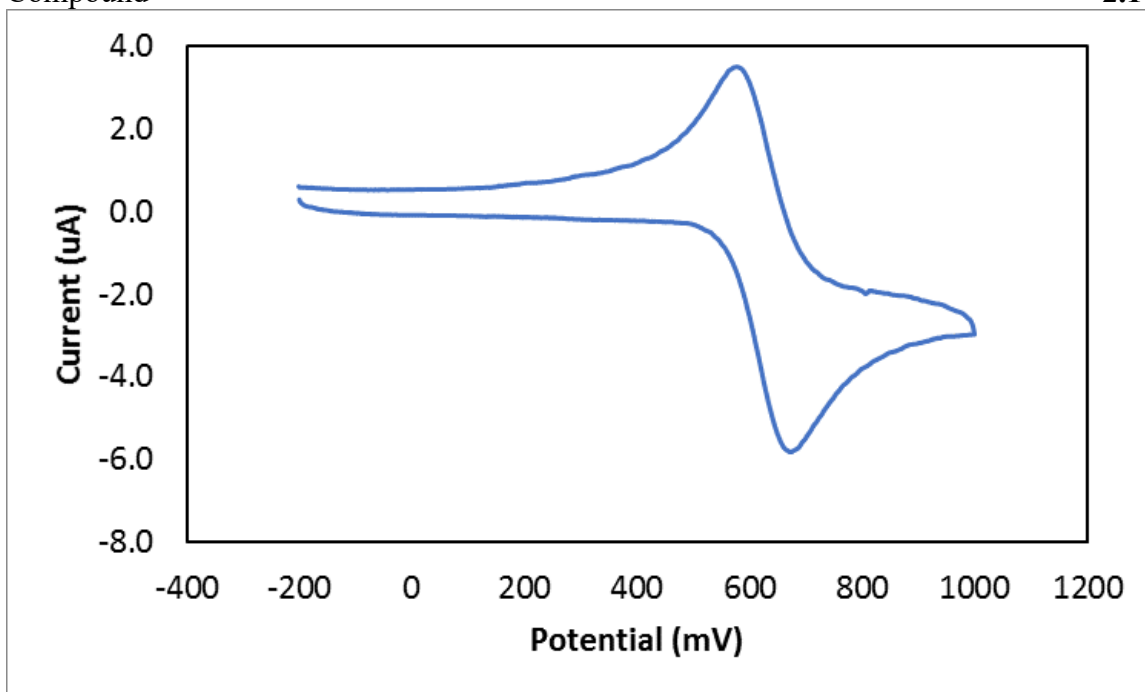


Compound 2.8



Compound

2.17





## References

- Agrawal, S.; Goodchild, J.; Civeira, M. P.; Thornton, A. H.; Sarin, P. S.; Zamecnik, P. C., Oligodeoxynucleoside phosphoramidates and phosphorothioates as inhibitors of human immunodeficiency virus. *Proceedings of the National Academy of Sciences* 1988, 85 (19), 7079-7083.
- Altintas, Z.; Tothill, I. E., DNA-based biosensor platforms for the detection of TP53 mutation. *Sensor Actuat B-Chem* 2012, 169, 188-194.
- Amblard, F.; Cho, J. H.; Schinazi, R. F., Cu(I)-Catalyzed Huisgen Azide–Alkyne 1,3-Dipolar Cycloaddition Reaction in Nucleoside, Nucleotide, and Oligonucleotide Chemistry. *Chemical Reviews* 2009, 109 (9), 4207-4220.
- Aoki, H.; Kitajima, A.; Tao, H., Label-free and ‘signal-on’ DNA detection using a probe DNA terminated with ferrocene and  $\beta$ -cyclodextrin. *Supramolecular Chemistry* 2010, 22 (7-8), 455-460.
- Armour, J. A.; Murphy, D. A.; Yuan, B. X.; MacDonald, S.; Hopkins, D. A., Gross and microscopic anatomy of the human intrinsic cardiac nervous system. *Anat Rec* 1997, 247 (2), 289-298.
- Arroyo-Currás, N.; Somerson, J.; Vieira, P. A.; Ploense, K. L.; Kippin, T. E.; Plaxco, K. W., Real-time measurement of small molecules directly in awake, ambulatory animals. *Proceedings of the National Academy of Sciences* 2017, 114 (4), 645-650.
- Asiello, P. J.; Baeumner, A. J., Miniaturized isothermal nucleic acid amplification, a review. *Lab on a Chip* 2011, 11 (8), 1420-1430.
- Assaf, K. I.; Nau, W. M., Cucurbiturils: from synthesis to high-affinity binding and catalysis. *Chemical Society Reviews* 2015, 44 (2), 394-418.

Atkinson, R. C. J.; Gibson, V. C.; Long, N. J., The syntheses and catalytic applications of unsymmetrical ferrocene ligands. *Chemical Society Reviews* 2004, 33 (5), 313-328.

Baker, B. R.; Lai, R. Y.; Wood, M. S.; Doctor, E. H.; Heeger, A. J.; Plaxco, K. W., An Electronic, Aptamer-Based Small-Molecule Sensor for the Rapid, Label-Free Detection of Cocaine in Adulterated Samples and Biological Fluids. *J Am Chem Soc* 2006, 128 (10), 3138-3139.

Bandodkar, A. J.; Jeerapan, I.; Wang, J., Wearable Chemical Sensors: Present Challenges and Future Prospects. *ACS Sensors* 2016, 1 (5), 464-482.

Bandodkar, A. J.; Wang, J., Non-invasive wearable electrochemical sensors: a review. *Trends in Biotechnology* 2014, 32 (7), 363-371.

Bard, A. J.; Faulkner, L. R., *Electrochemical methods : fundamentals and applications*. 2nd ed.; Wiley: New York, 2001; p xxi.

Batterjee, S. M.; Marzouk, M. I.; Aazab, M. E.; El-Hashash, M. A., The electrochemistry of some ferrocene derivatives: redox potential and substituent effects. *Applied Organometallic Chemistry* 2003, 17 (5), 291-297.

Beaucage, S. L.; Caruthers, M. H., Deoxynucleoside phosphoramidites—A new class of key intermediates for deoxypolynucleotide synthesis. *Tetrahedron Letters* 1981, 22 (20), 1859-1862.

Beaucage, S. L.; Iyer, R. P., Advances in the Synthesis of Oligonucleotides by the Phosphoramidite Approach. *Tetrahedron* 1992, 48 (12), 2223-2311.

Beaucage, S. L.; Iyer, R. P., The synthesis of modified oligonucleotides by the phosphoramidite approach and their applications. *Tetrahedron* 1993, 49 (28), 6123-6194.

Beilstein, A. E.; W. Grinstaff, M., On-column derivatization of oligodeoxynucleotides with ferrocene. *Chemical Communications* 2000, (6), 509-510.

Berg, J. M.; Tymoczko, J. L.; Stryer, L.; Stryer, L., *Biochemistry*. 6th ed.; W. H. Freeman: New York, 2007; p 1 v.

Boczkowska, M.; Guga, P.; Stec, W. J., Stereodefined Phosphorothioate Analogues of DNA: Relative Thermodynamic Stability of the Model PS-DNA/DNA and PS-DNA/RNA Complexes. *Biochemistry* 2002, 41 (41), 12483-12487.

Bonanni, A.; Chua, C. K.; Zhao, G. J.; Sofer, Z.; Pumera, M., Inherently Electroactive Graphene Oxide Nanoplatelets As Labels for Single Nucleotide Polymorphism Detection. *Acs Nano* 2012, 6 (10), 8546-8551.

Bonham, A. J.; Hsieh, K.; Ferguson, B. S.; Vallee-Belisle, A.; Ricci, F.; Soh, H. T.; Plaxco, K. W., Quantification of Transcription Factor Binding in Cell Extracts Using an Electrochemical, Structure-Switching Biosensor. *J Am Chem Soc* 2012, 134 (7), 3346-3348.

Borsenberger, V.; Kukwikila, M.; Howorka, S., Synthesis and enzymatic incorporation of modified deoxyuridine triphosphates. *Organic & Biomolecular Chemistry* 2009, 7 (18), 3826-3835.

Breslauer, K. J.; Frank, R.; Blocker, H.; Marky, L. A., Predicting DNA Duplex Stability from the Base Sequence. *P Natl Acad Sci USA* 1986, 83 (11), 3746-3750.

Bucci, E.; De Napoli, L.; Di Fabio, G.; Messere, A.; Montesarchio, D.; Romanelli, A.; Piccialli, G.; Varra, M., A new ferrocenemethyl-thymidine nucleoside: Synthesis, incorporation into oligonucleotides and optical spectroscopic studies on the resulting single strand, duplex and triplex structures. *Tetrahedron* 1999, 55 (50), 14435-14450.

Burgess, K.; Cook, D., Syntheses of Nucleoside Triphosphates. *Chem Rev* 2000, 100 (6), 2047-2060.

Chen, C. J.; Liu, C. C.; Savinell, R. F., Polymeric redox mediator enzyme electrodes for anaerobic glucose monitoring. *Journal of Electroanalytical Chemistry* 1993, 348 (1), 317-338.

Connelly, N. G.; Geiger, W. E., Chemical Redox Agents for Organometallic Chemistry. *Chem Rev* 1996, 96 (2), 877-910.

Cosnier, S.; Mailley, P., Recent advances in DNA sensors. *Analyst* 2008, 133 (8), 984-991.

Coutouli-Argyropoulou, E.; Kelaidopoulou, A.; Sideris, C.; Kokkinidis, G., Electrochemical studies of ferrocene derivatives and their complexation by  $\beta$ -cyclodextrin. *Journal of Electroanalytical Chemistry* 1999, 477 (2), 130-139.

Cui, L.; Gadde, S.; Li, W.; Kaifer, A. E., Electrochemistry of the Inclusion Complexes Formed Between the Cucurbit[7]uril Host and Several Cationic and Neutral Ferrocene Derivatives†Part of the “Langmuir 25th Year: Molecular and macromolecular self-assemblies” special issue. *Langmuir* 2009, 25 (24), 13763-13769.

Cunningham, A. F., Friedel-Crafts acetylation of bis(trimethylsilyl)- and bis(tributylstannyl)ferrocene: implications on the mechanisms of acylation and proton exchange of ferrocene derivatives. *J Am Chem Soc* 1991, 113 (13), 4864-4870.

Daeneke, T.; Kwon, T.-H.; Holmes, A. B.; Duffy, N. W.; Bach, U.; Spiccia, L., High-efficiency dye-sensitized solar cells with ferrocene-based electrolytes. *Nat Chem* 2011, 3 (3), 211-215.

Daeneke, T.; Mozer, A. J.; Kwon, T.-H.; Duffy, N. W.; Holmes, A. B.; Bach, U.; Spiccia, L., Dye regeneration and charge recombination in dye-sensitized solar cells with ferrocene derivatives as redox mediators. *Energy & Environmental Science* 2012, 5 (5), 7090-7099.

Das, A. K.; Chakraborty, R.; Luisa Cervera, M.; de la Guardia, M., Metal speciation in biological fluids — a review. *Microchimica Acta* 1996, 122 (3), 209-246.

De Crozals, G.; Farre, C.; Sigaud, M.; Fortgang, P.; Sanglar, C.; Chaix, C., Methylene blue phosphoramidite for DNA labelling. *Chemical Communications* 2015, 51 (21), 4458-4461.

Deféver, T.; Druet, M.; Rochelet-Dequaire, M.; Joannes, M.; Grossiord, C.; Limoges, B.; Marchal, D., Real-Time Electrochemical Monitoring of the Polymerase Chain Reaction by Mediated Redox Catalysis. *J Am Chem Soc* 2009, 131 (32), 11433-11441.

Dirks, R. M.; Bois, J. S.; Schaeffer, J. M.; Winfree, E.; Pierce, N. A., Thermodynamic analysis of interacting nucleic acid strands. *Siam Rev* 2007, 49 (1), 65-88.

Drummond, T. G.; Hill, M. G.; Barton, J. K., Electrochemical DNA sensors. *Nat Biotechnol* 2003, 21 (10), 1192-1199.

Du, Y.; Lim, B. J.; Li, B.; Jiang, Y. S.; Sessler, J. L.; Ellington, A. D., Reagentless, Ratiometric Electrochemical DNA Sensors with Improved Robustness and Reproducibility. *Anal Chem* 2014, 86 (15), 8010-8016.

Elghanian, R.; Storhoff, J. J.; Mucic, R. C.; Letsinger, R. L.; Mirkin, C. A., Selective Colorimetric Detection of Polynucleotides Based on the Distance-Dependent Optical Properties of Gold Nanoparticles. *Science* 1997, 277 (5329), 1078-1081.

Ellington, A. D.; Szostak, J. W., In vitro selection of RNA molecules that bind specific ligands. *Nature* 1990, 346 (6287), 818-822.

Fan, C.; Plaxco, K. W.; Heeger, A. J., Electrochemical interrogation of conformational changes as a reagentless method for the sequence-specific detection of DNA. *Proceedings of the National Academy of Sciences* 2003, 100 (16), 9134-9137.

Fang, X.; Jiang, W.; Han, X. W.; Zhang, Y. Z., Molecular beacon based biosensor for the sequence-specific detection of DNA using DNA-capped gold nanoparticles-streptavidin conjugates for signal amplification. *Microchim Acta* 2013, 180 (13-14), 1271-1277.

Fattal, E.; Barratt, G., Nanotechnologies and controlled release systems for the delivery of antisense oligonucleotides and small interfering RNA. *British Journal of Pharmacology* 2009, 157 (2), 179-194.

Fauster, K.; Hartl, M.; Santner, T.; Aigner, M.; Kreutz, C.; Bister, K.; Ennifar, E.; Micura, R., 2'-Azido RNA, a Versatile Tool for Chemical Biology: Synthesis, X-ray Structure, siRNA Applications, Click Labeling. *ACS Chemical Biology* 2012, 7 (3), 581-589.

Ferguson, B. S.; Hoggarth, D. A.; Maliniak, D.; Ploense, K.; White, R. J.; Woodward, N.; Hsieh, K.; Bonham, A. J.; Eisenstein, M.; Kippin, T. E.; Plaxco, K. W.; Soh, H. T., Real-Time, Aptamer-Based Tracking of Circulating Therapeutic Agents in Living Animals. *Science Translational Medicine* 2013, 5 (213), 213ra165.

Fernandez, J. M.; Bilgin, M. D.; Grossweiner, L. I., Singlet oxygen generation by photodynamic agents. *Journal of Photochemistry and Photobiology B: Biology* 1997, 37 (1), 131-140.

Ganbold, E. O.; Kang, T.; Lee, K.; Lee, S. Y.; Joo, S. W., Aggregation effects of gold nanoparticles for single-base mismatch detection in influenza A (H1N1) DNA sequences using fluorescence and Raman measurements. *Colloid Surface B* 2012, 93, 148-153.

Gao, W. C.; Dong, H. F.; Lei, J. P.; Ji, H. X.; Ju, H. X., Signal amplification of streptavidin-horseradish peroxidase functionalized carbon nanotubes for amperometric detection of attomolar DNA. *Chemical Communications* 2011, 47 (18), 5220-5222.

Gao, W.; Emaminejad, S.; Nyein, H. Y. Y.; Challa, S.; Chen, K.; Peck, A.; Fahad, H. M.; Ota, H.; Shiraki, H.; Kiriya, D.; Lien, D.-H.; Brooks, G. A.; Davis, R. W.; Javey, A., Fully integrated wearable sensor arrays for multiplexed in situ perspiration analysis. *Nature* 2016, 529 (7587), 509-514.

Gao, Z.; Agarwal, A.; Trigg, A. D.; Singh, N.; Fang, C.; Tung, C.-H.; Fan, Y.; Buddharaju, K. D.; Kong, J., Silicon Nanowire Arrays for Label-Free Detection of DNA. *Anal Chem* 2007, 79 (9), 3291-3297.

Ge, D.; Levicky, R., A comparison of five bioconjugatable ferrocenes for labeling of biomolecules. *Chemical Communications* 2010, 46 (38), 7190-7192.

Ghosh, S. S.; Kao, P. M.; McCue, A. W.; Chappelle, H. L., Use of maleimide-thiol coupling chemistry for efficient syntheses of oligonucleotide-enzyme conjugate hybridization probes. *Bioconjugate Chemistry* 1990, 1 (1), 71-76.

Gilbert, W., ORIGIN OF LIFE - THE RNA WORLD. *Nature* 1986, 319 (6055), 618-618.

Gilham, P. T.; Khorana, H. G., Studies on Polynucleotides. I. A New and General Method for the Chemical Synthesis of the C5"-C3" Internucleotidic Linkage. Syntheses of Deoxyribo-dinucleotides<sup>1</sup>. *J Am Chem Soc* 1958, 80 (23), 6212-6222.

Gong, H.; Zhong, T. Y.; Gao, L.; Li, X. H.; Bi, L. J.; Kraatz, H. B., Unlabeled Hairpin DNA Probe for Electrochemical Detection of Single-Nucleotide Mismatches Based on MutS-DNA Interactions. *Anal Chem* 2009, 81 (20), 8639-8643.

Gonzalo-Ruiz, J.; Mas, R.; de Haro, C.; Cabruja, E.; Camero, R.; Alonso-Lomillo, M. A.; Muñoz, F. J., Early determination of cystic fibrosis by electrochemical chloride quantification in sweat. *Biosensors and Bioelectronics* 2009, 24 (6), 1788-1791.

Goodchild, J., Conjugates of oligonucleotides and modified oligonucleotides: a review of their synthesis and properties. *Bioconjugate Chemistry* 1990, 1 (3), 165-187.

Gramlich, P. M. E.; Wirges, C. T.; Manetto, A.; Carell, T., Postsynthetic DNA Modification through the Copper-Catalyzed Azide–Alkyne Cycloaddition Reaction. *Angewandte Chemie International Edition* 2008, 47 (44), 8350-8358.

Gritzner, G.; Kuta, J., Recommendations on Reporting Electrode-Potentials in Nonaqueous Solvents (Recommendations 1983). *Pure Appl Chem* 1984, 56 (4), 461-466.

Grubert, H.; Rinehart, K. L., Nitroferrocene. *Tetrahedron Letters* 1959, 1 (12), 16-17.

Hagen, H.; Marzenell, P.; Jentzsch, E.; Wenz, F.; Veldwijk, M. R.; Mokhir, A., Aminoferrocene-Based Prodrugs Activated by Reactive Oxygen Species. *Journal of Medicinal Chemistry* 2012, 55 (2), 924-934.

Hall, D. B.; Barton, J. K., Sensitivity of DNA-Mediated Electron Transfer to the Intervening  $\pi$ -Stack: A Probe for the Integrity of the DNA Base Stack. *J Am Chem Soc* 1997, 119 (21), 5045-5046.

Hammett-Stabler, C. A.; Johns, T., Laboratory guidelines for monitoring of antimicrobial drugs. *Clinical Chemistry* 1998, 44 (5), 1129.

Han, S. W.; Seo, H.; Chung, Y. K.; Kim, K., Electrochemical and Vibrational Spectroscopic Characterization of Self-Assembled Monolayers of 1,1'-Disubstituted Ferrocene Derivatives on Gold. *Langmuir* 2000, 16 (24), 9493-9500.

Hansch, C.; Leo, A.; Taft, R. W., A survey of Hammett substituent constants and resonance and field parameters. *Chemical Reviews* 1991, 91 (2), 165-195.

Harris, D. C., Quantitative chemical analysis. 7th ed.; W.H. Freeman and Co.: New York, NY, 2007; p 1 v.

Hayashi, E.; Takada, T.; Nakamura, M.; Yamana, K., Electronic Aptamer-based Biosensor for Multiprotein Analytes on a Single Platform. *Chem Lett* 2010, 39 (5), 454-455.



Heikenfeld, J., Non-invasive Analyte Access and Sensing through Eccrine Sweat: Challenges and Outlook circa 2016. *Electroanalysis* 2016, 28 (6), 1242-1249.

Herne, T. M.; Tarlov, M. J., Characterization of DNA Probes Immobilized on Gold Surfaces. *J Am Chem Soc* 1997, 119 (38), 8916-8920.

Hiby, N.; Johansen, H. K.; Copenhagen Study Group on Antibiotics in, S.; Jarlv, J. O.; Westh, H.; Prag, J. B.; Bangsberg, J. M.; Moser, C.; Kemp, M.; Hornsleth, A. K.; Hansen, H., Ciprofloxacin in sweat and antibiotic resistance. *The Lancet* 1995, 346 (8984), 1235.

Hili, R.; Niu, J.; Liu, D. R., DNA Ligase-Mediated Translation of DNA Into Densely Functionalized Nucleic Acid Polymers. *J Am Chem Soc* 2013, 135 (1), 98-101.

Hilmer, S. N.; Tran, K.; Rubie, P.; Wright, J.; Gnjjidic, D.; Mitchell, S. J.; Matthews, S.; Carroll, P. R., Gentamicin pharmacokinetics in old age and frailty. *British Journal of Clinical Pharmacology* 2011, 71 (2), 224-231.

Hirao, I.; Kimoto, M.; Mitsui, T.; Fujiwara, T.; Kawai, R.; Sato, A.; Harada, Y.; Yokoyama, S., An unnatural hydrophobic base pair system: site-specific incorporation of nucleotide analogs into DNA and RNA. *Nat Meth* 2006, 3 (9), 729-735.

Hodak, J.; Etchenique, R.; Calvo, E. J.; Singhal, K.; Bartlett, P. N., Layer-by-Layer Self-Assembly of Glucose Oxidase with a Poly(allylamine)ferrocene Redox Mediator. *Langmuir* 1997, 13 (10), 2708-2716.

Hsieh, K. W.; Patterson, A. S.; Ferguson, B. S.; Plaxco, K. W.; Soh, H. T., Rapid, Sensitive, and Quantitative Detection of Pathogenic DNA at the Point of Care through Microfluidic Electrochemical Quantitative Loop-Mediated Isothermal Amplification. *Angew Chem Int Edit* 2012, 51 (20), 4896-4900.

Hsieh, K.; Ferguson, B. S.; Eisenstein, M.; Plaxco, K. W.; Soh, H. T., Integrated Electrochemical Microsystems for Genetic Detection of Pathogens at the Point of Care. *Accounts of Chemical Research* 2015, 48 (4), 911-920.

Hu, X.; Smith, G. D.; Sykora, M.; Lee, S. J.; Grinstaff, M. W., Automated Solid-Phase Synthesis and Photophysical Properties of Oligodeoxynucleotides Labeled at 5'-Aminothymidine with Ru(bpy)<sub>2</sub>(4-m-4'-cam-bpy)<sub>2</sub><sup>+</sup>. *Inorganic Chemistry* 2000, 39 (12), 2500-2504.

Huang, T. J.; Liu, M. S.; Knight, L. D.; Grody, W. W.; Miller, J. F.; Ho, C. M., An electrochemical detection scheme for identification of single nucleotide polymorphisms using hairpin-forming probes. *Nucleic Acids Res* 2002, 30 (12).

Hvastkovs, E. G.; Buttry, D. A., Minor Groove Binding of a Novel Tetracationic Diviologen. *Langmuir* 2006, 22 (25), 10821-10829.

Ihara, T.; Nakayama, M.; Murata, M.; Nakano, K.; Maeda, M., Gene sensor using ferrocenyl oligonucleotide. *Chemical Communications* 1997, (17), 1609-1610.

Iinuma, R.; Ke, Y.; Jungmann, R.; Schlichthaerle, T.; Woehrstein, J. B.; Yin, P., Polyhedra Self-Assembled from DNA Tripods and Characterized with 3D DNA-PAINT. *Science* 2014, 344 (6179), 65-69.

Image from Wikipedia.

Immoos, C. E.; Lee, S. J.; Grinstaff, M. W., Conformationally gated electrochemical gene detection. *Chembiochem* 2004, 5 (8), 1100-1103.

Jadoon, S.; Karim, S.; Akram, M. R.; Kalsoom Khan, A.; Zia, M. A.; Siddiqi, A. R.; Murtaza, G., Recent Developments in Sweat Analysis and Its Applications. *International Journal of Analytical Chemistry* 2015, 2015, 7.

Jäger, S.; Rasched, G.; Kornreich-Leshem, H.; Engeser, M.; Thum, O.; Famulok, M., A Versatile Toolbox for Variable DNA Functionalization at High Density. *J Am Chem Soc* 2005, 127 (43), 15071-15082.

Jenkins, D. M.; Chami, B.; Kreuzer, M.; Presting, G.; Alvarez, A. M.; Liaw, B. Y., Hybridization probe for femtomolar quantification of selected nucleic acid sequences on a disposable electrode. *Anal Chem* 2006, 78 (7), 2314-2318.

Jia, M.; Chew, W. M.; Feinstein, Y.; Skeath, P.; Sternberg, E. M., Quantification of cortisol in human eccrine sweat by liquid chromatography - tandem mass spectrometry. *Analyst* 2016, 141 (6), 2053-2060.

Jia, X.; Dong, S.; Wang, E., Engineering the bioelectrochemical interface using functional nanomaterials and microchip technique toward sensitive and portable electrochemical biosensors. *Biosensors and Bioelectronics* 2016, 76, 80-90.

Jung, C.; Ellington, A. D., A primerless molecular diagnostic: phosphorothioated-terminal hairpin formation and self-priming extension (PS-THSP). *Analytical and Bioanalytical Chemistry* 2016, 1-9.

Kang, D.; Zuo, X.; Yang, R.; Xia, F.; Plaxco, K. W.; White, R. J., Comparing the Properties of Electrochemical-Based DNA Sensors Employing Different Redox Tags. *Anal Chem* 2009, 81 (21), 9109-9113.

Kelley, S. O.; Barton, J. K.; Jackson, N. M.; Hill, M. G., Electrochemistry of Methylene Blue Bound to a DNA-Modified Electrode. *Bioconjugate Chemistry* 1997, 8 (1), 31-37.

Kelley, S. O.; Boon, E. M.; Barton, J. K.; Jackson, N. M.; Hill, M. G., Single-base mismatch detection based on charge transduction through DNA. *Nucleic Acids Res* 1999, 27 (24), 4830-4837.

Khobragade, D. A.; Mahamulkar, S. G.; Pospíšil, L.; Císařová, I.; Rulíšek, L.; Jahn, U., Acceptor-Substituted Ferrocenium Salts as Strong, Single-Electron Oxidants: Synthesis, Electrochemistry, Theoretical Investigations, and Initial Synthetic Application. *Chemistry – A European Journal* 2012, 18 (39), 12267-12277.

Khodagholy, D.; Curto, V. F.; Fraser, K. J.; Gurfinkel, M.; Byrne, R.; Diamond, D.; Malliaras, G. G.; Benito-Lopez, F.; Owens, R. M., Organic electrochemical transistor incorporating an ionogel as a solid state electrolyte for lactate sensing. *Journal of Materials Chemistry* 2012, 22 (10), 4440-4443.

Kidwell, D. A.; Holland, J. C.; Athanaselis, S., Testing for drugs of abuse in saliva and sweat. *Journal of Chromatography B: Biomedical Sciences and Applications* 1998, 713 (1), 111-135.

Kim, D.; Pushkarsky, I.; Tay, A.; Di Carlo, D., Research highlights: aptamers on a chip. *Lab on a Chip* 2015, 15 (7), 1630-1633.

Kim, D.-H.; Lu, N.; Ma, R.; Kim, Y.-S.; Kim, R.-H.; Wang, S.; Wu, J.; Won, S. M.; Tao, H.; Islam, A.; Yu, K. J.; Kim, T.-i.; Chowdhury, R.; Ying, M.; Xu, L.; Li, M.; Chung, H.-J.; Keum, H.; McCormick, M.; Liu, P.; Zhang, Y.-W.; Omenetto, F. G.; Huang, Y.; Coleman, T.; Rogers, J. A., Epidermal Electronics. *Science* 2011, 333 (6044), 838.

Kim, E. E.; Wyckoff, H. W., Reaction mechanism of alkaline phosphatase based on crystal structures. *J Mol Biol* 1991, 218 (2), 449-464.

Kobayashi, Y.; Hoshi, T.; Anzai, J.-i., Glucose and Lactate Biosensors Prepared by a Layer-by-Layer Deposition of Concanavalin A and Mannose-Labeled Enzymes: Electrochemical Response in the Presence of Electron Mediators. *Chemical and Pharmaceutical Bulletin* 2001, 49 (6), 755-757.

Krotz, A. H.; Rentel, C.; Gorman, D.; Olsen, P.; Gaus, H. J.; McArdle, J. V.; Scozzari, A. N., Solution Stability and Degradation Pathway of Deoxyribonucleoside

Phosphoramidites in Acetonitrile. *Nucleosides, Nucleotides and Nucleic Acids* 2004, 23 (5), 767-775.

Lamond, A. I.; Sproat, B. S., Antisense oligonucleotides made of 2'-O-alkylRNA: their properties and applications in RNA biochemistry. *FEBS Letters* 1993, 325 (1-2), 123-127.

Latt, S. A.; Stetten, G., Spectral studies on 33258 Hoechst and related bisbenzimidazole dyes useful for fluorescent detection of deoxyribonucleic acid synthesis. *Journal of Histochemistry & Cytochemistry* 1976, 24 (1), 24-33.

Lee, H.; Choi, T. K.; Lee, Y. B.; Cho, H. R.; Ghaffari, R.; Wang, L.; Choi, H. J.; Chung, T. D.; Lu, N.; Hyeon, T.; Choi, S. H.; Kim, D.-H., A graphene-based electrochemical device with thermoresponsive microneedles for diabetes monitoring and therapy. *Nat Nano* 2016, 11 (6), 566-572.

Lehninger, A. L.; Nelson, D. L.; Cox, M. M., *Lehninger principles of biochemistry*. 4th ed.; W.H. Freeman: New York, 2005; p 1 v.

Lenze, N.; Neumann, B.; Salmon, A.; Stammer, A.; Stammer, H.-G.; Jutzi, P., Multiply trimethylstannyl substituted ferrocenes synthesis, NMR studies, X-ray structural analysis and electrochemistry. *Journal of Organometallic Chemistry* 2001, 619 (1-2), 74-87.

Letsinger, R. L.; Finnan, J. L.; Heavner, G. A.; Lunsford, W. B., Nucleotide chemistry. XX. Phosphite coupling procedure for generating internucleotide links. *J Am Chem Soc* 1975, 97 (11), 3278-3279.

Letsinger, R. L.; Ogilvie, K. K., Nucleotide chemistry. XIII. Synthesis of oligothymidylates via phosphotriester intermediates. *J Am Chem Soc* 1969, 91 (12), 3350-3355.

Li, B.; Ellington, A. D.; Chen, X., Rational, modular adaptation of enzyme-free DNA circuits to multiple detection methods. *Nucleic Acids Res* 2011.

Li, D.; Song, S. P.; Fan, C. H., Target-Responsive Structural Switching for Nucleic Acid-Based Sensors. *Accounts of Chemical Research* 2010, 43 (5), 631-641.

Lin, Y.-J.; Wu, Y.-C.; Mani, V.; Huang, S.-T.; Huang, C.-H.; Hu, Y.-C.; Peter Shan, H.-C., Designing anthraquinone–pyrrole redox intercalating probes for electrochemical gene detection. *Biosensors and Bioelectronics* 2016, 79, 294-299.

Liu, C.; Zeng, G. M.; Tang, L.; Zhang, Y.; Li, Y. P.; Liu, Y. Y.; Li, Z.; Wu, M. S.; Luo, J., Electrochemical detection of *Pseudomonas aeruginosa* 16S rRNA using a biosensor based on immobilized stem-loop structured probe. *Enzyme Microb Tech* 2011, 49 (3), 266-271.

Liu, G.; Wan, Y.; Gau, V.; Zhang, J.; Wang, L. H.; Song, S. P.; Fan, C. H., An enzyme-based E-DNA sensor for sequence-specific detection of femtomolar DNA targets. *J Am Chem Soc* 2008, 130 (21), 6820-6825.

Liu, H.-K.; Sadler, P. J., Metal Complexes as DNA Intercalators. *Accounts of Chemical Research* 2011, 44 (5), 349-359.

Liu, W.; Tang, Y.; Guo, Y.; Sun, B.; Zhu, H.; Xiao, Y.; Dong, D.; Yang, C., Synthesis, characterization and bioactivity determination of ferrocenyl urea derivatives. *Applied Organometallic Chemistry* 2012, 26 (4), 189-193.

Löffler, U.; Wiemhöfer, H. D.; Göpel, W., Amperometric biosensors: characterization of dispersed mediator systems. *Biosensors and Bioelectronics* 1991, 6 (4), 343-352.

Lu, X. C.; Dong, X.; Zhang, K. Y.; Han, X. W.; Fang, X.; Zhang, Y. Z., A gold nanorods-based fluorescent biosensor for the detection of hepatitis B virus DNA based on fluorescence resonance energy transfer. *Analyst* 2013, 138 (2), 642-650.

Lu, Y.; Li, X. C.; Zhang, L. M.; Yu, P.; Su, L.; Mao, L. Q., Aptamer-based electrochemical sensors with aptamer-complementary DNA oligonucleotides as probe. *Anal Chem* 2008, 80 (6), 1883-1890.

Lubin, A. A.; Hunt, B. V. S.; White, R. J.; Plaxco, K. W., Effects of Probe Length, Probe Geometry, and Redox-Tag Placement on the Performance of the Electrochemical E-DNA Sensor. *Anal Chem* 2009, 81 (6), 2150-2158.

Lubin, A. A.; Plaxco, K. W., Folding-Based Electrochemical Biosensors: The Case for Responsive Nucleic Acid Architectures. *Accounts of Chemical Research* 2010, 43 (4), 496-505.

Lucarelli, F.; Marrazza, G.; Turner, A. P. F.; Mascini, M., Carbon and gold electrodes as electrochemical transducers for DNA hybridisation sensors. *Biosensors and Bioelectronics* 2004, 19 (6), 515-530.

Malik, M. A., Water Purification by Plasmas: Which Reactors are Most Energy Efficient? *Plasma Chemistry and Plasma Processing* 2010, 30 (1), 21-31.

Malyshev, D. A.; Dhami, K.; Lavergne, T.; Chen, T.; Dai, N.; Foster, J. M.; Correa, I. R.; Romesberg, F. E., A semi-synthetic organism with an expanded genetic alphabet. *Nature* 2014, 509 (7500), 385-388.

Malyshev, D. A.; Romesberg, F. E., The Expanded Genetic Alphabet. *Angewandte Chemie International Edition* 2015, 54 (41), 11930-11944.

Manoharan, M., 2'-Carbohydrate modifications in antisense oligonucleotide therapy: importance of conformation, configuration and conjugation. *Biochimica et Biophysica Acta (BBA) - Gene Structure and Expression* 1999, 1489 (1), 117-130.

Masaru, S.; Hiromichi, K.; Mikio, S.; Izumi, M.; Kazuo, H., A Simple Modification of Vilsmeier Method for the Preparation of Formylferrocene. *B Chem Soc Jpn* 1968, 41 (1), 252-252.

Matsue, T.; Evans, D. H.; Osa, T.; Kobayashi, N., Electron-transfer reactions associated with host-guest complexation. Oxidation of ferrocenecarboxylic acid in the presence of .beta.-cyclodextrin. *J Am Chem Soc* 1985, 107 (12), 3411-3417.

McCulloch, B.; Ward, D. L.; Woollins, J. D.; Brubaker, C. H., Ferrocenyl sulfides. Preparation and reactivity as bidentate chelating ligands. *Organometallics* 1985, 4 (8), 1425-1432.

Michaelis, L.; Schubert, M. P.; Granick, S., Semiquinone Radicals of the Thiazines. *J Am Chem Soc* 1940, 62 (1), 204-211.

Michelson, A. M.; Todd, A. R., Nucleotides part XXXII. Synthesis of a dithymidine dinucleotide containing a 3': 5'-internucleotidic linkage. *Journal of the Chemical Society* 1955, (0), 2632-2638.

Mills, A.; Lawrie, K.; McFarlane, M., Blue bottle light: lecture demonstrations of homogeneous and heterogeneous photo-induced electron transfer reactions. *Photochemical & Photobiological Sciences* 2009, 8 (3), 421-425.

Mir, M.; Jenkins, A. T. A.; Katakis, I., Ultrasensitive detection based on an aptamer beacon electron transfer chain. *Electrochem Commun* 2008, 10 (10), 1533-1536.

Miranda-Castro, R.; De-Los-Santos-Alvarez, P.; Lobo-Castanon, M. J.; Miranda-Ordieres, A. J.; Tunon-Blanco, P., Hairpin-DNA probe for enzyme-amplified electrochemical detection of *Legionella pneumophila*. *Anal Chem* 2007, 79 (11), 4050-4055.

Nakahata, M.; Takashima, Y.; Hashidzume, A.; Harada, A., Redox-Generated Mechanical Motion of a Supramolecular Polymeric Actuator Based on Host-Guest Interactions. *Angewandte Chemie International Edition* 2013, 52 (22), 5731-5735.

Nakahata, M.; Takashima, Y.; Yamaguchi, H.; Harada, A., Redox-responsive self-healing materials formed from host-guest polymers. *Nature Communications* 2011, 2, 511.



Nelson, B. P.; Grimsrud, T. E.; Liles, M. R.; Goodman, R. M.; Corn, R. M., Surface Plasmon Resonance Imaging Measurements of DNA and RNA Hybridization Adsorption onto DNA Microarrays. *Anal Chem* 2001, 73 (1), 1-7.

Neuhaus-Url, G.; Neuhaus, G., The use of the nonradioactive digoxigenin chemiluminescent technology for plant genomic Southern blot hybridization: A comparison with radioactivity. *Transgenic Research* 1993, 2 (2), 115-120.

Nielsen, P. E., Peptide Nucleic Acids (PNA) in Chemical Biology and Drug Discovery. *Chemistry & Biodiversity* 2010, 7 (4), 786-804.

Nielsen, P. E.; Egholm, M.; Buchardt, O., Peptide nucleic acid (PNA). A DNA mimic with a peptide backbone. *Bioconjugate Chemistry* 1994, 5 (1), 3-7.

Nieto, D.; Bruña, S.; González-Vadillo, A. M.; Perles, J.; Carrillo-Hermosilla, F.; Antiñolo, A.; Padrón, J. M.; Plata, G. B.; Cuadrado, I., Catalytically Generated Ferrocene-Containing Guanidines as Efficient Precursors for New Redox-Active Heterometallic Platinum(II) Complexes with Anticancer Activity. *Organometallics* 2015, 34 (22), 5407-5417.

Obika, S.; Nanbu, D.; Hari, Y.; Morio, K.-i.; In, Y.; Ishida, T.; Imanishi, T., Synthesis of 2'-O,4'-C-methyleneuridine and -cytidine. Novel bicyclic nucleosides having a fixed C3, -endo sugar puckering. *Tetrahedron Letters* 1997, 38 (50), 8735-8738.

Ogilvie, K. K.; Theriault, N.; Sadana, K. L., Synthesis of oligoribonucleotides. *J Am Chem Soc* 1977, 99 (23), 7741-7743.

Oliphant, A. R.; Brandl, C. J.; Struhl, K., Defining the sequence specificity of DNA-binding proteins by selecting binding sites from random-sequence oligonucleotides: analysis of yeast GCN4 protein. *Molecular and Cellular Biology* 1989, 9 (7), 2944-2949.

Ono, A.; Haginoya, N.; Kiyokawa, M.; Minakawa, N.; Matsuda, A., Nucleosides and nucleotides. 127. A novel and convenient post-synthetic modification method for the

synthesis of oligodeoxyribonucleotides carrying amino linkers at the 5-position of 2'-deoxyuridine. *Bioorganic & Medicinal Chemistry Letters* 1994, 4 (2), 361-366.

Osella, D.; Carretta, A.; Nervi, C.; Ravera, M.; Gobetto, R., Inclusion Complexes of Ferrocenes and  $\beta$ -Cyclodextrins. Critical Appraisal of the Electrochemical Evaluation of Formation Constants. *Organometallics* 2000, 19 (14), 2791-2797.

Palecek, E., Adsorptive Transfer Stripping Voltammetry - Determination of Nanogram Quantities of DNA Immobilized at the Electrode Surface. *Analytical Biochemistry* 1988, 170 (2), 421-431.

Papin, J. F.; Floyd, R. A.; Dittmer, D. P., Methylene blue photoinactivation abolishes West Nile virus infectivity in vivo. *Antiviral Research* 2005, 68 (2), 84-87.

Paredes, E.; Evans, M.; Das, S. R., RNA labeling, conjugation and ligation. *Methods* 2011, 54 (2), 251-259.

Pascal, J. M.; O'Brien, P. J.; Tomkinson, A. E.; Ellenberger, T., Human DNA ligase I completely encircles and partially unwinds nicked DNA. *Nature* 2004, 432 (7016), 473-478.

Petersen, M.; Wengel, J., LNA: a versatile tool for therapeutics and genomics. *Trends in Biotechnology* 2003, 21 (2), 74-81.

Pheaney, C. G.; Barton, J. K., DNA Electrochemistry with Tethered Methylene Blue. *Langmuir* 2012, 28 (17), 7063-7070.

Pheaney, C. G.; Barton, J. K., Intraduplex DNA-Mediated Electrochemistry of Covalently Tethered Redox-Active Reporters. *Journal of the American Chemical Society* 2013, 135 (40), 14944-14947.

Piccirilli, J. A.; Benner, S. A.; Krauch, T.; Moroney, S. E.; Benner, S. A., Enzymatic incorporation of a new base pair into DNA and RNA extends the genetic alphabet. *Nature* 1990, 343 (6253), 33-37.

Pinheiro, V. B.; Holliger, P., Towards XNA nanotechnology: new materials from synthetic genetic polymers. *Trends in Biotechnology* 2014, 32 (6), 321-328.

Pitsch, S.; Weiss, P. A.; Xu, X. L.; Ackermann, D.; Honegger, T., Fast and reliable automated synthesis of RNA and partially 2'-O-protected precursors ('caged RNA') based on two novel, orthogonal 2'-O-protecting groups. *Helv Chim Acta* 1999, 82 (10), 1753-1761.

Prakash, T. P.; Johnston, J. F.; Graham, M. J.; Condon, T. P.; Manoharan, M., 2'-O-[2-[(N,N-dimethylamino)oxy]ethyl]-modified oligonucleotides inhibit expression of mRNA in vitro and in vivo. *Nucleic Acids Research* 2004, 32 (2), 828-833.

Prescott, W. A.; Nagel, J. L., Extended-Interval Once-Daily Dosing of Aminoglycosides in Adult and Pediatric Patients with Cystic Fibrosis. *Pharmacotherapy: The Journal of Human Pharmacology and Drug Therapy* 2010, 30 (1), 95-108.

Preston, K. L.; Huestis, M. A.; Wong, C. J.; Umbricht, A.; Goldberger, B. A.; Cone, E. J., Monitoring Cocaine Use in Substance-Abuse-Treatment Patients by Sweat and Urine Testing. *Journal of Analytical Toxicology* 1999, 23 (5), 313-322.

Pretlow, T. P.; Barrow, B. J.; Ashton, W. S.; O'Riordan, M. A.; Pretlow, T. G.; Jurcisek, J. A.; Stellato, T. A., Aberrant Crypts: Putative Preneoplastic Foci in Human Colonic Mucosa. *Cancer Research* 1991, 51 (5), 1564-1567.

Prins, R.; Korswagen, A. R.; Kortbeek, A. G. T. G., Decomposition of the ferricenium cation by nucleophilic reagents. *Journal of Organometallic Chemistry* 1972, 39 (2), 335-344.

Pylae, T. E.; Khanadeev, V. A.; Khlebtsov, B. N.; Dykman, L. A.; Bogatyrev, V. A.; Khlebtsov, N. G., Colorimetric and dynamic light scattering detection of DNA sequences by using positively charged gold nanospheres: a comparative study with gold nanorods. *Nanotechnology* 2011, 22 (28).

Qian, Y.; Tang, D.; Du, L.; Zhang, Y.; Zhang, L.; Gao, F., A novel signal-on electrochemical DNA sensor based on target catalyzed hairpin assembly strategy. *Biosensors and Bioelectronics* 2015, 64, 177-181.

Radi, A. E.; O'Sullivan, C. K., Aptamer conformational switch as sensitive electrochemical biosensor for potassium ion recognition. *Chemical Communications* 2006, (32), 3432-3434.

Rebiere, F.; Samuel, O.; Kagan, H. B., A convenient method for the preparation of monolithioferrocene. *Tetrahedron Letters* 1990, 31 (22), 3121-3124.

Richardson, C. C., Phosphorylation of nucleic acid by an enzyme from T4 bacteriophage-infected *Escherichia coli*. *P Natl Acad Sci USA* 1965, 54 (1), 158-165.

Rinehart, K. L.; Motz, K. L.; Moon, S., Organic Chemistry of Ferrocene. I. The Acetylation of Dialkylferrocenes<sup>1</sup>. *J Am Chem Soc* 1957, 79 (11), 2749-2754.

Rosenblum, M.; Santer, J. O.; Howells, W. G., The Chemistry and Structure of Ferrocene. VIII. Interannular Resonance and the Mechanism of Electrophilic Substitution. *J. Am. Chem. Soc.*, 1963, 85 (10), 1450–1458.

Rosenstein, B. J.; Cutting, G. R., The diagnosis of cystic fibrosis: A consensus statement. *The Journal of Pediatrics* 1998, 132 (4), 589-595.

Rothmund, P. W. K., Folding DNA to create nanoscale shapes and patterns. *Nature* 2006, 440 (7082), 297-302.

Rowe, A. A.; Miller, E. A.; Plaxco, K. W., Reagentless Measurement of Aminoglycoside Antibiotics in Blood Serum via an Electrochemical, Ribonucleic Acid Aptamer-Based Biosensor. *Anal Chem* 2010, 82 (17), 7090-7095.

Rychlik, W.; Spencer, W. J.; Rhoads, R. E., Optimization of the Annealing Temperature for DNA Amplification In vitro. *Nucleic Acids Res* 1990, 18 (21), 6409-6412.

Sadeh, S.; Bhattacharjee, H.; Khozeimeh Sarbisheh, E.; Quail, J. W.; Müller, J., Chiral Bora[1]ferrocenophanes: Syntheses, Mechanistic Insights, and Ring-Opening Polymerizations. *Chemistry – A European Journal* 2014, 20 (49), 16320-16330.

Sági, J.; Szemző, A.; Ébinger, K.; Szabolcs, A.; Sági, G.; Ruff, É.; Ötvös, L., Base-modified oligodeoxynucleotides. I. effect of 5-alkyl, 5-(1-alkenyl) and 5-(1-alkynyl) substitution of the pyrimidines on duplex stability and hydrophobicity. *Tetrahedron Letters* 1993, 34 (13), 2191-2194.

Sanger, F.; Nicklen, S.; Coulson, A. R., DNA sequencing with chain-terminating inhibitors. *Proceedings of the National Academy of Sciences* 1977, 74 (12), 5463-5467.

Sassolas, A.; Leca-Bouvier, B. D.; Blum, L. J., DNA Biosensors and Microarrays. *Chem Rev* 2008, 108 (1), 109-139.

Schazmann, B.; Morris, D.; Slater, C.; Beirne, S.; Fay, C.; Reuveny, R.; Moyna, N.; Diamond, D., A wearable electrochemical sensor for the real-time measurement of sweat sodium concentration. *Analytical Methods* 2010, 2 (4), 342-348.

Schena, M.; Shalon, D.; Davis, R. W.; Brown, P. O., Quantitative Monitoring of Gene Expression Patterns with a Complementary DNA Microarray. *Science* 1995, 270 (5235), 467-470.

Schitteck, B.; Hipfel, R.; Sauer, B.; Bauer, J.; Kalbacher, H.; Stevanovic, S.; Schirle, M.; Schroeder, K.; Blin, N.; Meier, F.; Rassner, G.; Garbe, C., Dermcidin: a novel human antibiotic peptide secreted by sweat glands. *Nat Immunol* 2001, 2 (12), 1133-1137.

Schöning, K.-U.; Scholz, P.; Guntha, S.; Wu, X.; Krishnamurthy, R.; Eschenmoser, A., Chemical Etiology of Nucleic Acid Structure: The  $\alpha$ -Threofuranosyl-(3'→2') Oligonucleotide System. *Science* 2000, 290 (5495), 1347-1351.

Sinkeldam, R. W.; Greco, N. J.; Tor, Y., Fluorescent Analogs of Biomolecular Building Blocks: Design, Properties, and Applications. *Chem Rev* 2010, 110 (5), 2579-2619.

Smith, J. P.; Schrock, A. K.; Schuster, G. B., Chemiluminescence of organic peroxides. Thermal generation of an o-xylylene peroxide. *J Am Chem Soc* 1982, 104 (4), 1041-1047.

Smith, L. M.; Sanders, J. Z.; Kaiser, R. J.; Hughes, P.; Dodd, C.; Connell, C. R.; Heiner, C.; Kent, S. B. H.; Hood, L. E., Fluorescence detection in automated DNA sequence analysis. *Nature* 1986, 321 (6071), 674-679.

Sonner, Z.; Wilder, E.; Heikenfeld, J.; Kasting, G.; Beyette, F.; Swaile, D.; Sherman, F.; Joyce, J.; Hagen, J.; Kelley-Loughnane, N.; Naik, R. The microfluidics of the eccrine sweat gland, including biomarker partitioning, transport, and biosensing implications *Biomicrofluidics*, 2015, p. 031301.

Souza, A. P. R. d.; Lima, A. S.; Salles, M. O.; Nascimento, A. N.; Bertotti, M., The use of a gold disc microelectrode for the determination of copper in human sweat. *Talanta* 2010, 83 (1), 167-170.

Srinivasan, V.; Pamula, V. K.; Fair, R. B., An integrated digital microfluidic lab-on-a-chip for clinical diagnostics on human physiological fluids. *Lab on a Chip* 2004, 4 (4), 310-315.

Stec, W. J.; Zon, G.; Egan, W., Automated solid-phase synthesis, separation, and stereochemistry of phosphorothioate analogs of oligodeoxyribonucleotides. *J Am Chem Soc* 1984, 106 (20), 6077-6079.

Stinner, C.; Wightman, M. D.; Kelley, S. O.; Hill, M. G.; Barton, J. K., Synthesis and Spectroelectrochemistry of Ir(bpy)(phen)(phi)<sup>3+</sup>, a Tris(heteroleptic) Metallointercalator. *Inorg Chem* 2001, 40 (20), 5245-5250.

Stojanovic, M. N.; de Prada, P.; Landry, D. W., Aptamer-Based Folding Fluorescent Sensor for Cocaine. *Journal of the American Chemical Society* 2001, 123 (21), 4928-4931.

Stoltenburg, R.; Reinemann, C.; Strehlitz, B., SELEX—A (r)evolutionary method to generate high-affinity nucleic acid ligands. *Biomolecular Engineering* 2007, 24 (4), 381-403.

Swensen, J. S.; Xiao, Y.; Ferguson, B. S.; Lubin, A. A.; Lai, R. Y.; Heeger, A. J.; Plaxco, K. W.; Soh, H. T., Continuous, Real-Time Monitoring of Cocaine in Undiluted Blood Serum via a Microfluidic, Electrochemical Aptamer-Based Sensor. *Journal of the American Chemical Society* 2009, 131 (12), 4262-4266.

Tataurov, A. V.; You, Y.; Owczarzy, R., Predicting ultraviolet spectrum of single stranded and double stranded deoxyribonucleic acids. *Biophysical Chemistry* 2008, 133 (1–3), 66-70.

Thakur, A.; Adarsh, N. N.; Chakraborty, A.; Devi, M.; Ghosh, S., Synthesis of mono and doubly alkynyl substituted ferrocene and its crystal engineering using  $-C-H\cdots O$  supramolecular synthon. *Journal of Organometallic Chemistry* 2010, 695 (7), 1059-1064.

Thuong, N. T.; Hélène, C., Sequence-Specific Recognition and Modification of Double-Helical DNA by Oligonucleotides. *Angewandte Chemie International Edition in English* 1993, 32 (5), 666-690.

Tierney, M. T.; Grinstaff, M. W., Synthesis and Stability of Oligodeoxynucleotides Containing C8-Labeled 2'-Deoxyadenosine: Novel Redox Nucleobase Probes for DNA-Mediated Charge-Transfer Studies. *Organic Letters* 2000, 2 (22), 3413-3416.

Tolman, C. A., The 16 and 18 electron rule in organometallic chemistry and homogeneous catalysis. *Chemical Society Reviews* 1972, 1 (3), 337-353.

Totsingan, F.; Jain, V.; Bracken, W. C.; Faccini, A.; Tedeschi, T.; Marchelli, R.; Corradini, R.; Kallenbach, N. R.; Green, M. M., Conformational Heterogeneity in PNA:PNA Duplexes. *Macromolecules* 2010, 43 (6), 2692-2703.

Trasatti, S.; Petrii, O. A., Real surface area measurements in electrochemistry. *Journal of Electroanalytical Chemistry* 1992, 327 (1-2), 353-376.

Tuite, E.; Norden, B., Sequence-Specific Interactions of Methylene Blue with Polynucleotides and DNA: A Spectroscopic Study. *J Am Chem Soc* 1994, 116 (17), 7548-7556.

Tyagi, S.; Kramer, F. R., Molecular Beacons: Probes that Fluoresce upon Hybridization. *Nat Biotech* 1996, 14 (3), 303-308.

Tyagi, S.; Landegren, U.; Tazi, M.; Lizardi, P. M.; Kramer, F. R., Extremely sensitive, background-free gene detection using binary probes and Q beta replicase. *P Natl Acad Sci USA* 1996, 93 (11), 5395-5400.

Veedu, R. N.; Vester, B.; Wengel, J., Polymerase directed incorporation studies of LNA-G nucleoside 5[prime or minute]-triphosphate and primer extension involving all four LNA nucleotides. *New Journal of Chemistry* 2010, 34 (5), 877-879.

Velez, A. M. A.; Warfvinge, G.; Herrera, W. L.; Velez, C. E. A.; Montoya, F. M.; Hardy, D. M.; Bollag, W. B.; Hashimoto, K., Detection of mercury and other undetermined materials in skin biopsies of endemic pemphigus foliaceus. *Am J Dermatopath* 2003, 25 (5), 384-391.

Verma, S.; Eckstein, F., Modified oligonucleotides: Synthesis and strategy for users. *Annu. Rev. Biochem.* 1998, 67, 99-134.

Wagner, S. J.; Skripchenko, A.; Pugh, J. C.; Suchmann, D. B.; Ijaz, M. K., Duck hepatitis B photoinactivation by dimethylmethylene blue in RBC suspensions. *Transfusion* 2001, 41 (9), 1154-1158.



Wainwright, M.; Giddens, R. M., Phenothiazinium photosensitisers: choices in synthesis and application. *Dyes and Pigments* 2003, 57 (3), 245-257.

Wang, J., Carbon-Nanotube Based Electrochemical Biosensors: A Review. *Electroanalysis* 2005, 17 (1), 7-14.

Wang, J.; Verbeure, B.; Luyten, I.; Lescrinier, E.; Froeyen, M.; Hendrix, C.; Rosemeyer, H.; Seela, F.; Van Aerschot, A.; Herdewijn, P., Cyclohexene Nucleic Acids (CeNA): Serum Stable Oligonucleotides that Activate RNase H and Increase Duplex Stability with Complementary RNA. *J Am Chem Soc* 2000, 122 (36), 8595-8602.

Wang, M.; Yu, Y.; Liang, C.; Lu, A.; Zhang, G., Recent Advances in Developing Small Molecules Targeting Nucleic Acid. *International Journal of Molecular Sciences* 2016, 17 (6), 779.

Waring, M. J., Complex formation between ethidium bromide and nucleic acids. *J Mol Biol* 1965, 13 (1), 269-282.

Watson, J. D.; Crick, F. H. C., Molecular Structure of Nucleic Acids - a Structure for Deoxyribose Nucleic Acid. *Nature* 1953, 171 (4356), 737-738.

Wedeking, K.; Mu, Z.; Kehr, G.; Cano Sierra, J.; Mück Lichtenfeld, C.; Grimme, S.; Erker, G.; Fröhlich, R.; Chi, L.; Wang, W.; Zhong, D.; Fuchs, H., Oligoethylene Chains Terminated by Ferrocenyl End Groups: Synthesis, Structural Properties, and Two-Dimensional Self-Assembly on Surfaces. *Chemistry – A European Journal* 2006, 12 (6), 1618-1628.

Wilkinson, G.; Rosenblum, M.; Whiting, M. C.; Woodward, R. B., THE STRUCTURE OF IRON BIS-CYCLOPENTADIENYL. *J Am Chem Soc* 1952, 74 (8), 2125-2126.

Wilkinson, G.; Rosenblum, M.; Whiting, M. C.; Woodward, R. B., THE STRUCTURE OF IRON BIS-CYCLOPENTADIENYL. *Journal of the American Chemical Society* 1952, 74 (8), 2125-2126.

Williams, T. T.; Dohno, C.; Stemp, E. D. A.; Barton, J. K., Effects of the Photooxidant on DNA-Mediated Charge Transport. *J Am Chem Soc* 2004, 126 (26), 8148-8158.

Willner, I.; Zayats, M., Electronic aptamer-based sensors. *Angew Chem Int Edit* 2007, 46 (34), 6408-6418.

Wilson, C.; Keefe, A. D., Building oligonucleotide therapeutics using non-natural chemistries. *Current Opinion in Chemical Biology* 2006, 10 (6), 607-614.

Wu, D. H.; Zhang, Q.; Chu, X.; Wang, H. B.; Shen, G. L.; Yu, R. Q., Ultrasensitive electrochemical sensor for mercury (II) based on target-induced structure-switching DNA. *Biosens Bioelectron* 2010, 25 (5), 1025-1031.

Wu, J. K.; Huang, C. H.; Cheng, G. F.; Zhang, F.; He, P. G.; Fang, Y. Z., Electrochemically active-inactive switching molecular beacon for direct detection of DNA in homogenous solution. *Electrochem Commun* 2009, 11 (1), 177-180.

Xiao, Y.; Lai, R. Y.; Plaxco, K. W., Preparation of electrode-immobilized, redox-modified oligonucleotides for electrochemical DNA and aptamer-based sensing. *Nat Protoc* 2007, 2 (11), 2875-2880.

Xiao, Y.; Lubin, A. A.; Baker, B. R.; Plaxco, K. W.; Heeger, A. J., Single-step electronic detection of femtomolar DNA by target-induced strand displacement in an electrode-bound duplex. *P Natl Acad Sci USA* 2006, 103 (45), 16677-16680.

Xiao, Y.; Lubin, A. A.; Heeger, A. J.; Plaxco, K. W., Label-Free Electronic Detection of Thrombin in Blood Serum by Using an Aptamer-Based Sensor. *Angewandte Chemie International Edition* 2005, 44 (34), 5456-5459.

Xuan, F.; Luo, X. T.; Hsing, I. M., Ultrasensitive Solution-Phase Electrochemical Molecular Beacon-Based DNA Detection with Signal Amplification by Exonuclease III-Assisted Target Recycling. *Anal Chem* 2012, 84 (12), 5216-5220.

Xuan, F.; Luo, X.; Hsing, I. M., Sensitive immobilization-free electrochemical DNA sensor based on isothermal circular strand displacement polymerization reaction. *Biosensors and Bioelectronics* 2012, 35 (1), 230-234.

Yamana, K.; Iwase, R.; Furutani, S.; Tsuchida, H.; Zako, H.; Yamaoka, T.; Murakami, A., 2'-Pyrene modified oligonucleotide provides a highly sensitive fluorescent probe of RNA. *Nucleic Acids Res* 1999, 27 (11), 2387-2392.

Yan, Q.; Feng, A.; Zhang, H.; Yin, Y.; Yuan, J., Redox-switchable supramolecular polymers for responsive self-healing nanofibers in water. *Polymer Chemistry* 2013, 4 (4), 1216-1220.

Yang, I. V.; Thorp, H. H., Modification of Indium Tin Oxide Electrodes with Repeat Polynucleotides: Electrochemical Detection of Trinucleotide Repeat Expansion. *Anal Chem* 2001, 73 (21), 5316-5322.

Yang, S.; Chen, Y.-C.; Nicolini, L.; Pasupathy, P.; Sacks, J.; Su, B.; Yang, R.; Sanchez, D.; Chang, Y.-F.; Wang, P.; Schnyer, D.; Neikirk, D.; Lu, N., "Cut-and-Paste" Manufacture of Multiparametric Epidermal Sensor Systems. *Advanced Materials* 2015, 27 (41), 6423-6430.

Yang, X.; Du, Y.; Li, D.; Lv, Z. Z.; Wang, E. K., One-step synthesized silver micro-dendrites used as novel separation mediums and their applications in multi-DNA analysis. *Chemical Communications* 2011, 47 (38), 10581-10583.

Yeh, J. I.; Shivachev, B.; Rapireddy, S.; Crawford, M. J.; Gil, R. R.; Du, S.; Madrid, M.; Ly, D. H., Crystal Structure of Chiral  $\gamma$ PNA with Complementary DNA Strand:

Insights into the Stability and Specificity of Recognition and Conformational Preorganization. *J Am Chem Soc* 2010, 132 (31), 10717-10727.

Yeung, S. S. W.; Lee, T. M. H.; Hsing, I. M., Electrochemical Real-Time Polymerase Chain Reaction. *J Am Chem Soc* 2006, 128 (41), 13374-13375.

Yin, H. S.; Zhou, Y. L.; Zhang, H. X.; Meng, X. M.; Ai, S. Y., Electrochemical determination of microRNA-21 based on graphene, LNA integrated molecular beacon, AuNPs and biotin multifunctional bio bar codes and enzymatic assay system. *Biosens Bioelectron* 2012, 33 (1), 247-253.

Yu, C. J.; Wan, Y.; Yowanto, H.; Li, J.; Tao, C.; James, M. D.; Tan, C. L.; Blackburn, G. F.; Meade, T. J., Electronic Detection of Single-Base Mismatches in DNA with Ferrocene-Modified Probes. *Journal of the American Chemical Society* 2001, 123 (45), 11155-11161.

Yu, C. J.; Yowanto, H.; Wan, Y.; Meade, T. J.; Chong, Y.; Strong, M.; Donilon, L. H.; Kayyem, J. F.; Gozin, M.; Blackburn, G. F., Uridine-Conjugated Ferrocene DNA Oligonucleotides: Unexpected Cyclization Reaction of the Uridine Base. *J Am Chem Soc* 2000, 122 (28), 6767-6768.

Yu, H.; Zhang, S.; Chaput, J. C., Darwinian evolution of an alternative genetic system provides support for TNA as an RNA progenitor. *Nat Chem* 2012, 4 (3), 183-187.

Zatsepin, T.; Stetsenko D. A.; Gait, M. J.; Oretskaya, T. S. Use of Carbonyl Group Addition–Elimination Reactions for Synthesis of Nucleic Acid Conjugates. *Bioconjugate Chem.*, 2005, 16 (3), pp 471–489.

Zhang, D. Y.; Seelig, G., Dynamic DNA nanotechnology using strand-displacement reactions. *Nat Chem* 2011, 3 (2), 103-113.

Zhang, D. Y.; Winfree, E., Control of DNA Strand Displacement Kinetics Using Toehold Exchange. *J Am Chem Soc* 2009, 131 (47), 17303-17314.

Zhang, L.; Peritz, A.; Meggers, E., A Simple Glycol Nucleic Acid. *J Am Chem Soc* 2005, 127 (12), 4174-4175.

Zhang, Y. L.; Huang, Y.; Jiang, J. H.; Shen, G. L.; Yu, R. Q., Electrochemical aptasensor based on proximity-dependent surface hybridization assay for single-step, reusable, sensitive protein detection. *J Am Chem Soc* 2007, 129 (50), 15448-+.

Zhang, Y.; Zhang, K.; Ma, H., Electrochemical DNA biosensor based on silver nanoparticles/poly(3-(3-pyridyl) acrylic acid)/carbon nanotubes modified electrode. *Analytical Biochemistry* 2009, 387 (1), 13-19.

Zuo, X. L.; Song, S. P.; Zhang, J.; Pan, D.; Wang, L. H.; Fan, C. H., A target-responsive electrochemical aptamer switch (TREAS) for reagentless detection of nanomolar ATP. *J Am Chem Soc* 2007, 129 (5), 1042-1043.